POLISH ACADEMY OF SCIENCES
NENCKI INSTITUTE OF EXPERIMENTAL BIOLOGY

ACTA PROTOZOOLOGICA

VOLUME 17

Number 2

W A R S Z A W A 1 9 7 8

POLISH ACADEMY OF SCIENCES
NENCKI INSTITUTE OF EXPERIMENTAL BIOLOGY

ACTA PROTOZOOLOGICA

International Journal of Protozoology

Manuscripts may be submitted to the Editorial Office: Acta Protozoologica, M. Nencki Institute of Experimental Biology, 02-093 Warszawa, 3 Pasteur Street, Poland, or to each member of the Editorial Board.

A subscription order stating the period of time, along with the subscriber's name and address can be sent to your subscription agent or directly to Foreign Trade Enterprise Ars Polona–Ruch, 00-068 Warszawa, 7 Krakowskie Przedmieście, P.O. Box 1001, Poland. Please send payments to the account of Ars–Polona Ruch in Bank Handlowy S.A., 7 Traugutt Street, 00-067 Warszawa, Poland.

ACTA PROTOZOOLOGICA appears quarterly. The indexes of previous volume will appear in No. 1 of the next volume.

Indexed in Current Contents.

ACTA PROTOZOOLOGICA
VOL. 17 (No. 2) WARSZAWA, 30 VI 1978 pp. 215–231

Zoologisches Institut der Universität Salzburg, Akademiestraße 26,
A-5020 Salzburg, Austria

Wilhelm FOISSNER

Das Silberliniensystem und die Infraciliatur der Gattungen *Platyophrya* Kahl, 1926, *Cyrtolophosis* Stokes, 1885 und *Colpoda* O.F.M., 1786: Ein Beitrag zur Systematik der *Colpodida* (*Ciliata, Vestibulifera*)

Synopsis. Eine vergleichende Untersuchung des Silberliniensystems und der Infraciliatur der Gattungen *Platyophrya, Cyrtolophosis* und *Colpoda* zeigte, daß die Familie *Cyrtolophosididae* in die Ordnung der *Colpodida* gestellt werden muß. Das von Grolière (1975) aufgehobene Genus *Woodruffia* wird wieder eingesetzt, da sich die Genera *Platyophrya* und *Woodruffia* hinsichtlich der somatischen Infraciliatur deutlich unterscheiden. Für diese Genera werden aber neue Diagnosen vorgeschlagen. Die Ordnung der *Colpodida* wird in zwei Unterordnungen aufgeteilt. Diese Entscheidung wird ausführlich diskutiert. Die Unterordnung *Cyrtolophosidina* nov. subord. umfaßt die Familien *Woodruffiidae* und *Cyrtolophosididae*. Sie ist durch einen besonderen Bau des Kernapparates (der Mikronucleus liegt im perinuclearen Raum des Makronucleus) und des Silberliniensystems gekennzeichnet. Die Unterordnung *Colpodina* nov. subord. umfaßt die Familien *Colpodidae* und *Marynidae*. Sie ist im wesentlichen durch eine hoch organisierte Vestibularciliatur und das Fehlen von medianen Silberlinien charakterisiert.

Diese Arbeit hat sich in erster Linie das Ziel gesetzt, die systematische Stellung der Gattung *Cyrtolophosis* Stokes, 1885 abzuklären, da hierüber die bisherigen licht- und elektronenmikroskopischen Untersuchungen keine ausreichende Einsicht gebracht haben. Daneben soll auch auf einige andere schwierige Gruppen der von Puytorac et al. (1974) errichteten Ordnung der *Colpodida*, nämlich die Gattungen *Platyophrya* Kahl, 1926 und *Woodruffia* Kahl, 1931 näher eingegangen werden.

Die Gattung *Cyrtolophosis* wurde von Stokes (1888) ohne Angabe von Gründen zu den *Heterotrichina* gestellt. Schewiakoff (1896), Roux (1901) und Penard (1922) ordneten diese Gattung dann den *Pleuronematina* zu, einer Ansicht, der zuerst auch Kahl (1926) gefolgt ist. Später stellte Kahl (1930–35) *Cyrtolophosis* aber zu den *Fronto-*

niidae, ebenfalls ohne nähere Begründung. Corliss (1961) reihte das Genus schließlich in die Gruppe der nicht näher einzuordnenden tetrahymeninen Hymenostomen ein.

Vor kurzem hat nun Mc Coy (1974) die Infraciliatur und Morphogenese von *Cyrtolophosis major* an Hand von Silberpräparaten analysiert. Er errichtete nicht nur die von den früheren Autoren nicht anerkannte Familie *Cyrtolophosididae* Stokes, 1888 wieder, sondern hat sie auch in die *Scuticociliatida* Small, 1967 eingereiht, da während der Morphogenese angeblich ein rudimentärer Richtungsmeridian auftrete und auch eine scuticus- ähnliche Struktur vorhanden wäre. Buitkamp (1975 a), der die Morphologie und Morphogenese von *Cyrtolophosis elongata* studierte, konnte aber weder einen Scuticus noch einen rudimentären Richtungsmeridian feststellen. Daher kann man über die Beobachtungen von McCoy (1974), der übrigens den rudimentären Richtungsmeridian nicht abgebildet hat, nicht sicher sein. Auch die von McCoy (1974) als Scuticus bezeichnete Struktur ist, wie er selbst betont hat, nicht typisch.

In einer bald darauf erschienenen kurzen, aber sehr wichtigen Notiz über die Ultrastruktur der paroralen Membran und des Kernapparates von *Cyrtolophosis mucicola* zitierte Detcheva (1976) eine persönliche Mitteilung von McCoy, nach der dieser Forscher die Familie *Cyrtolophosididae* und die Gattung *Platyophrya* nunmehr als eigene Ordnung in die Überordnung der *Nassulidea* stellen möchte, was nach Detcheva (1976) hinsichtlich der Struktur der paroralen Membran möglich wäre.

Das Studium des Silberliniensystems von *Cyrtolophosis mucicola*, das bisher unbekannt war, sowie ein morphologischer Vergleich mit einigen Gattungen der *Colpodida*, hat mich schon vor längerem zu der Ansicht geführt, daß die bisherigen Einordnungsversuche unrichtig waren und diese Familie gemeinsam mit der Familie *Woodruffiidae* Gelei, 1954 als gesonderte Unterordnung zu den *Colpodida* gestellt werden muß Denselben Gedanken hat offenbar auch Corliss (1977) gehabt, der in seiner neuesten systematischen Revision der *Ciliophora* die *Cyrtolophosididae* ebenfalls in die *Colpodida* eingereiht hat, ohne dies aber zu begründen. Kurz vorher hat Corliss (1976) sie noch zu den *Scuticociliatida* gestellt.

Material und Methoden

Das Untersuchungsmaterial wurde in alpinen Viehweidetümpeln gesammelt und im Standortwasser kultiviert. *Colpoda steini* stammt von einem Laubaufguß aus der Umgebung von Linz.

Zum Studium der Infraciliatur und des Silberliniensystems kamen verschiedene

Silbermethoden (Corliss 1953, Wilbert 1975, Foissner 1976) zur Anwendung. Ich kann die Beobachtung von McCoy (1974) bestätigen, daß *Cyrtolophosis* mit Protargol außerordentlich schwierig zu imprägnieren ist und die zahlreichen Protrichocysten viele Strukturen verdecken. Aber auch mit anderen Silbermethoden erfordert es viel Geduld, gute Präparate zu erhalten.

Ergebnisse

1. Das Silberliniensystem und die Infraciliatur von *Cyrtolophosis mucicola* Stokes, 1885

(a) Interphaseindividuum (Abb. 5, 6, Taf. II, 7, 8, Taf. III, 11): Die von mir hinsichtlich der Infraciliatur festgestellten Verhältnisse stimmen weitgehend mit den Angaben von McCoy (1974) und Buitkamp (1975a) überein. Die 9–11 Wimperreihen setzen sich aus Basalkörperpaaren (Dikineten, s. Lynn 1976 a) zusammen, die im vorderen Teil des Tieres beide bewimpert sind. Im caudalen Abschnitt besitzt jedoch nur der posteriore Basalkörper eines Paares eine Cilie (Abb. 5). Buitkamp (1975a) zeichnete bei *C. elongata* allerdings nur im vorderen Teil des Tieres Dikineten. Die leicht rechtsspiral angeordneten Wimperreihen konvergieren am caudalen Pol, wobei aber die letzten Cilien deutlich von der Polspitze abgesetzt sind, so daß ein wimperfreies Polfeld entsteht, auf dem die Cytopyge ausmündet (Abb. 6, Taf. II 7). Am apikalen Pol konvergiert nur ein Teil der Kineten, während die anderen entlang des rechten und linken Mundrandes enden (Abb. 6, Taf. II 7, 8). Unterhalb des Oralapparates finden sich stets zwei postorale Kineten. Der Aufbau des Oralapparates gleicht ganz der Beschreibung von McCoy (1974): rechts findet sich eine aus zwei Segmenten bestehende parorale Membran, links liegen auf dem etwas eigesenkten Oralfeld vier membranellenartige Strukturen, die beim lebenden Tier als eine Membran erscheinen (Abb. 5).

Das Silberliniensystem läßt sich in vier Abschnitte gliedern. (a) Meridional verlaufende Silberlinien, welche die Dikineten verbinden. Diese Silberlinien teilen sich vor jeder Dikinete in drei Äste auf, von denen der mittlere durch den Basalkörper hindurchzieht, die zwei äußreen aber einen Kreis um die Dikineten bilden, was auch McCoy (1974) bemerkt hat (Abb. 7a). Diese äußere Zirkularfibrille, die auch bei den *Euplotidae* auftritt (Foissner 1978), konnte bei allen Dikineten von *Cyrtolophosis* festgestellt werden. Die meridionalen Silberlinien konvergieren einerseits bei der Cytopyge, andererseits bilden sie im Verein mit den horizontalen Silberlinien ein ziemlich engmaschiges Silberliniensystem im Oralfeld. (b) Horizontal verlaufende Silberlinien, die meist

von den äußeren Zirkularfibrillen der Dikineten ausgehen. Dadurch entsteht ein ziemlich weitmaschiges Silberliniensystem. Der Verlauf der horizontalen Silberlinien ist häufig sehr unregelmäßig, was aber zum Teil sicher auf Präparationsartefakte zurückgeht, da sich die Tiere infolge der Entquellung oft stark verformen. Diese Silberlinien besitzen häufig auch kreisförmige Löcher (Abb. 6), die sicherlich ruhenden Protrichocysten entsprechen, während in ihnen liegende argyrophile Körnchen den Resten gerade ausgestoßener Protrichocysten entsprechen dürften (vgl. Foissner 1977). (c) Semimediane Silberlinien zwischen den postoralen Kineten (Abb. 6, Taf. II 7, 8). Sie sind für *Cyrtolophosis* typisch und teilen durch ihren Verlauf zwischen den Wimperreihen das sonts weitmaschige Silberliniensystem im Gebiet des Oralapparates in ein ziemlich engmaschiges auf. Sie sind nur in sehr guten Präparaten klar erkennbar und ihre Länge erscheint etwas variabel (vgl. Taf. II 7, 8). d) Ein ziemlich engmaschiges Silberliniensystem im Oralfeld, durch welches die paroraole Membran und die Membranellen an das somatische Silberliniensystem angeschlossen werden.

(b) Das Silberliniensystem während der Morphogenese (Abb. 7, 8, Taf. III 9, 10): Infolge der schwierigen Präparation konnte der Verlauf der Morphogenese des Silberliniensystems nicht in allen Einzelheiten verfolgt werden. Die wesentlichen Teilungsveränderungen und deren zeitliche Aufeinanderfolge zeigt die Abb. 7. Bei frühen Teilungsstadien (Abb. 7b, Taf. III 9) erkennt man, daß sich das Silberliniensystem in ganz charakteristischer Weise verändert hat. Rechts der Somakineten hat sich ein engmaschiges Silberliniensystem ausgebildet, dessen äußerer Rand zu einer mehr oder minder geschlossenen Silberlinie verschmilzt, so daß eine durchlaufende mediane Silberlinie entsteht. Von den ursprünglichen horizontalen Silberlinien bleiben sicher nicht alle erhalten. Die verbleibenden verbinden weiterhin die jeweils benachbarten Somakineten. Diese vielen zusätzlichen Maschen im Silberliniensystem stehen ganz offensichtlich im Zusammenhang mit der Neubildung der somatischen Kinetosomen, die ja entlang der Somakineten erfolgt (s. Buitkamp 1975 a). Ein gaz ähnliches Silberliniensystem findet sich beim hinteren Tochtertier auch noch in späteren Morphogenesestadien, wo die Cytogenese bereits ziemlich weit fortgeschritten ist (Taf. III 10). Beim vorderen Tochtertier ist das Silberliniensystem dagegen bereits dem des Interphaseindividuums ziemlich ähnlich. Die zusätzlichen Maschen müssen dahrer resorbiert oder umgeordnet worden sein. Es bildet sich dabei stellenweise recht deutlich ein System heraus, das dem von *Platyophrya* überraschend gleicht (Abb. 7e, Taf. III 10, Pfeil), wo also eine mediane Silberlinie vorliegt, von der Ausläufer rechts und links zu den Dikineten abzweigen.

2. Das Silberliniensystem und die Infraciliatur der Gattung *Platyophrya* (Abb. 1–4, Taf. I 1–3, Taf. II 4–6)

Untersucht wurden mehrere Arten, deren Silberliniensystem und Infraciliatur sich in allen wesentlichen Punkten glich. Hier hauptsächlich auf das Silberliniensystem und die Infraciliatur von *P. vorax* Kahl, 1926 näher eingegangen. Die *Platyophrya* sp. auf den Tafeln II und III ist eine neue Art und wird später beschrieben werden.

Während die Infraciliatur und die Morphogenese bei *Woodruffia* (*Platyophrya*) *spumacola* infolge der Arbeiten von Czapik (1971), Grolière (1975) und Buitkamp (1975) a) bereits gut bekannt ist und auch das Silberliniensystem von *Woodruffia metabolica* bereits beschrieben worden ist (Johnson et al. 1937), lagen über das Silberliniensystem der Gattung *Platyophrya* bisher keine Befunde vor. Die somatische und orale Infraciliatur von *P. vorax* und *Platyophrya* sp. weicht in einigen wesentlichen Punkten von der bei *P. spumacola* be-

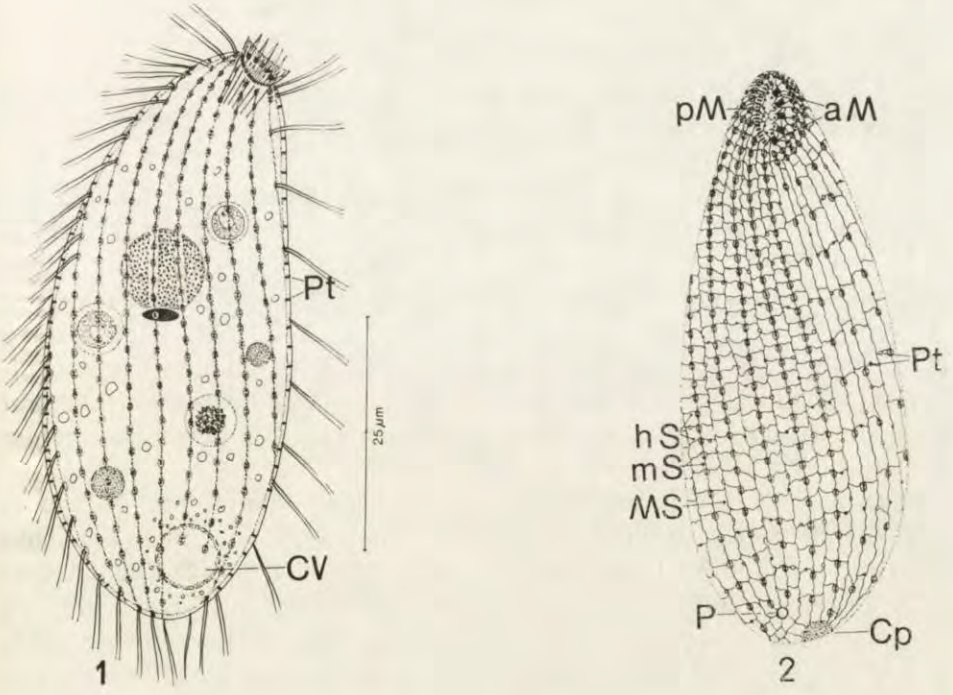

Abb. 1, 2. *Platyophrya vorax* lebend (Abb. 1) und nach trockener Silberimprägnation (Abb. 2). Rechts-laterale bzw. ventrale Ansicht. aM — adorale Membranellen, Cp — Cytopyge, CV — kontraktile Vakuole, hS — horizontale Silberlinien, MS — mediane Silberlinien, mS — meridionale Silberlinien, P — Porus excretorus, pM — parorale Membran, Pt — Protrichocysten

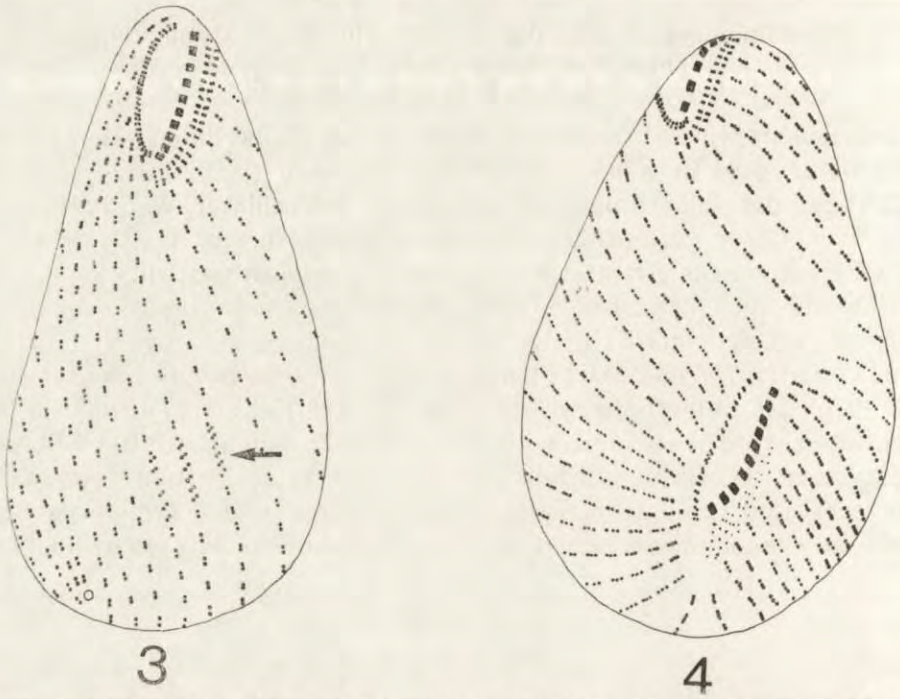

Abb. 3, 4. *Woodruffia* (*Platyophrya*) *spumacola*, frühes (Abb. 3) und spätes Morphogenesestadium (Abb. 4). Der Pfeil weist auf die Anlage des Oralapparates des Tochtertieres. Nach Grolière (1975)

kannten ab. Während bei letzterer der ganze Körper gleichmäßig mit paarig angeordneten Cilien bewimpert ist (vgl. Czapik 1971, Grolière 1975, Buitkamp 1975 a), fand sich bei den von mir untersuchten Species eine dicht bewimperte rechte Körperseite und eine sehr locker bewimperte linke Körperseite (Abb. 2, Taf. I 2). Buitkamp (1975 a) hat bei *P. angusta* eine ganz ähnliche Ausbildung der somatischen Infraciliatur festgestellt. Die Somakineten sind deutlich rechtsspiral angeordnet und im caudalen Körperabschnitt lockerer bewimpert als im apikalen (vgl. Buitkamp 1975 a).

Die orale Infraciliatur setzt sich aus einer, die rechte Mundseite umziehenden doppelreihigen paroralen Membran und nur 4–5 links inserierten Membranellen zusammen (Abb. 1, 2, Taf. I 1, 2). Dicht unterhalb derselben, auf der linken Körperseite, finden sich zwei sehr eng nebeneinander stehende Reihen paarig angeordneter Basalkörper (Abb. 1, 2. Taf. I 1 großer Pfeil, Taf. II 4, 5, 6), die auch bei *W. spumacola* und *P. angustata* festgestellt worden sind (vgl. Grolière 1975, Buitkamp 1975 a). Der Schlund wird von sehr feinen Trichiten ausgekleidet, wodurch die Reuse nicht so auffällig wie bei *W. spumacola* ist.

Das Silberliniensystem der Gattung *Platyophrya* läßt sich ebenfalls

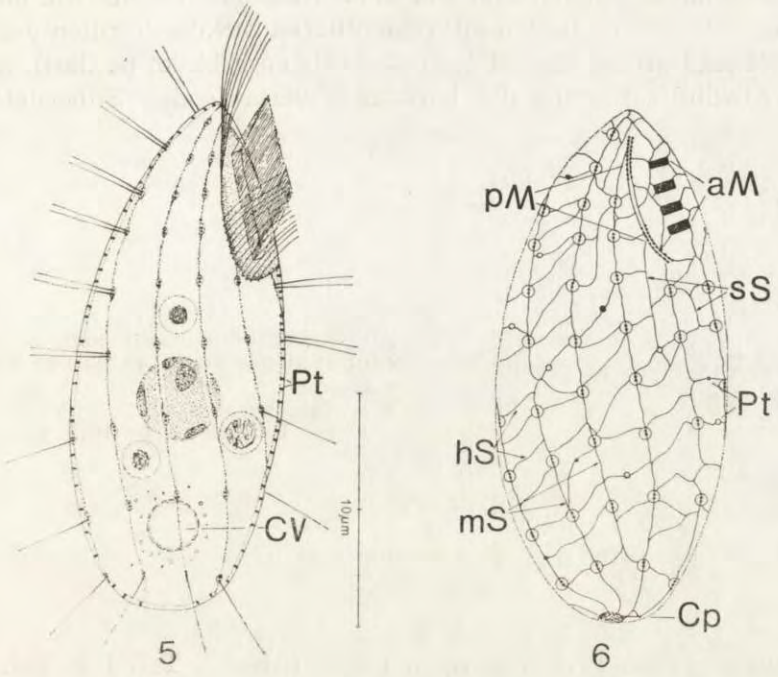

Abb. 5, 6. *Cyrtolophosis mucicola* lebend (Abb. 5) und nach trockener Silberimprägnation (Abb. 6). Rechts-laterale Ansichten. aM — adorale Membranellen, Cp — Cytopyge, CV — kontraktile Vakuole, hS — horizontale Silberlinien, mS — meridionale Silberlinien, pM — parorale Membran, Pt — Protrichocysten, sS — semimediane Silberlinien

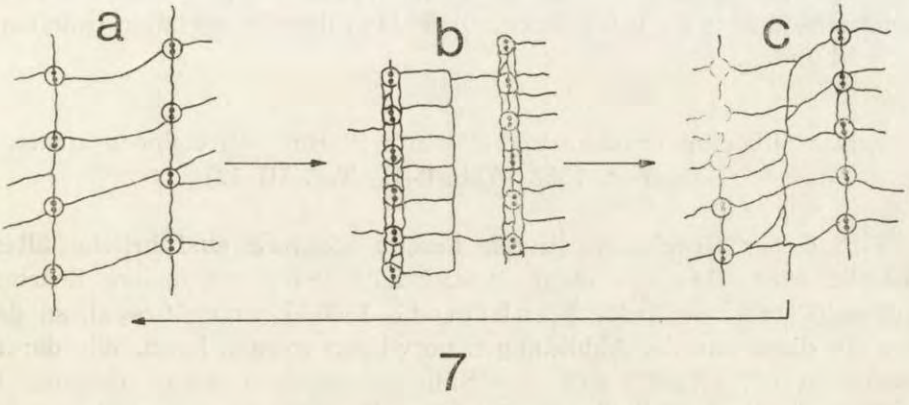

Abb. 7. *Cyrtolophosis mucicola*, Veränderungen des Silberliniensystems während der Morphogenese. Nähere Erklärungen im Text

in vier Abschnitte gliedern. (a) Der erste Abschnitt umfaßt die meridionalen verlaufenden Silberlinien mit den äußeren Zirkularfibrillen der Dikineten. Sie sind genau wie bei *Cyrtolophosis* ausgebildet (s. dort). (b) Der zweite Abschnitt umfaßt die horizontal verlaufenden Silberlinien, in

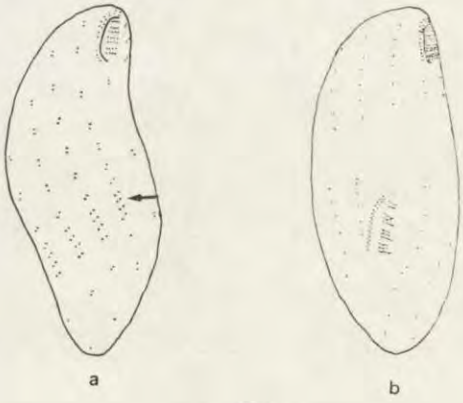

8

Abb. 8. *Cyrtolophosis elongata*, frühes (Abb. 8 a) und spätes (Abb. 8 b) Teilungsstadium. Der Pfeil weist auf die Anlage des Oralapparates des Tochtertieres. Nach Buitkamp (1975 a)

denen wieder viele Protrichocysten liegen (Abb. 2, Taf. I 2, Taf. II 4). (c) Die Silberlinien des zweiten Abschnittes werden — abweichend von anderen *Colpodida* — durch eine median zwischen den Somakineten verlaufende Silberlinie ziemlich genau in der Mitte geteilt, wodurch, auf der rechten Körperseite ein Silberliniensystem mit kleinen quadratischen Maschen auf der linken Körperseite ein solches mit orthogonalen Maschen, entsteht (Abb. 2, Taf. I 2, Taf. II 4). (d) Die meridionalen und medianen Silberlinien setzen sich bis in den Schlund hinein fort, wo sie ein sehr engmaschiges Netzwerk bilden (Taff. II 6). Dadurch werden somatische und orale Infraciliatur über das Silberliniensystem miteinander verbunden.

3. Das Silberliniensystem und die Infraciliatur von *Colpoda steini* Maupas, 1883 (Abb. 9–11, Taf. III 12)

Von dieser Species existieren bereits mehrere ausführliche ältere (Klein 1926, Taylor et al. 1938, Burt 1940) und neuere Bearbeitungen (Tuffrau 1952, Hashimoto 1966, Lynn 1976 a), so daß hier auf diese und die Abbildungen verwiesen werden kann. Wie daraus ersichtlich ist, gliedert sich das Silberliniensystem dieser Gattung in drei Abschnitte, wobei die Abschnitte a, b und d ganz ähnlich wie bei *Cyrtolophosis* ausgebildet sind. Lediglich die horizontalen Silberlinien

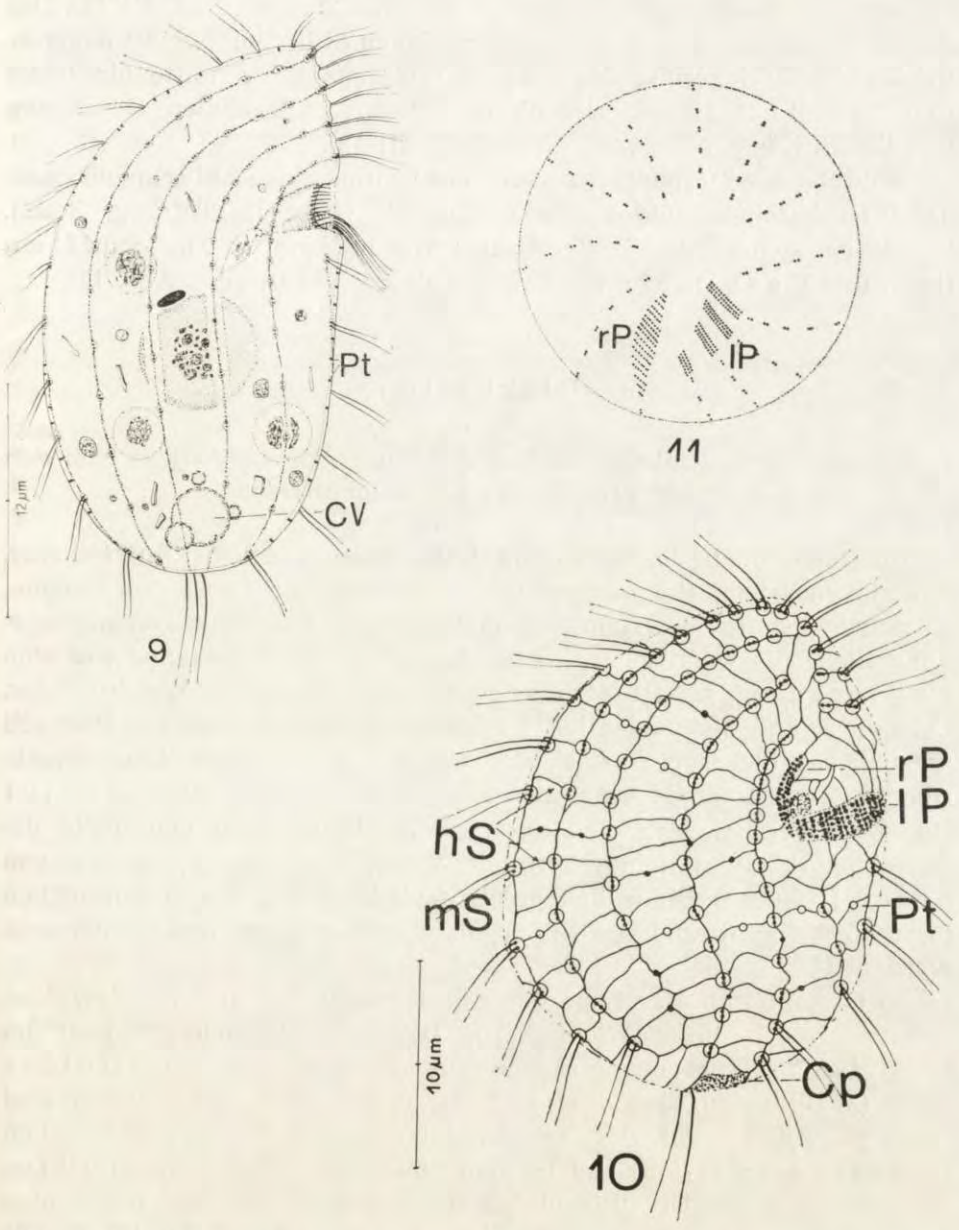

Abb. 9, 10. *Colpoda steini* lebend (Abb. 9) und nach trockener Silberimprägnation (Abb. 10). Rechts-laterale Ansichten. Cp — Cytopyge, CV — kontraktile Vakuole, hS — horizontale Silberlinien, lP — linke Polykinete, mS — meridionale Silberlinien, Pt — Protrichocysten, rP — rechte Polykinete

Abb. 11. *Colpoda steini*, Morphogenese des Oralapparates. lP — linke Polykinete, rP — rechte Polykinete. Kombiniert nach Tuffrau (1952) und Hashimoto (1966)

erscheinen regelmäßiger angeordnet (vgl. Taf. II 7 mit Taf. III 12). Der Abschnitt c, die medianen bzw. semimedianen Silberlinien, fehlt dagegen. Infolge der Verlagerung des Oralapparates zur Körpermitte hin bildet sich ein Kiel aus, an dem sich die meridionalen Silberlinien der rechten und linken Körperseite verflechten (Taf. III 12).

Während der Morphogenese wird das weitmaschige Silberliniensystem des Interphaseindividuums sehr engmaschig (Klein 1926, eig. Beob.). Die Morphogenese des Oralapparates wurde bereits von Tuffrau (1952) und Hashimoto (1966) genau dargestellt (s. auch Abb. 11).

Diskussion

1. Versuch einer phylogenetischen Ableitung der *Colpodidae* von den *Woodruffiidae* und *Cyrtolophosididae*

Überblickt man die bekannten Daten über Cytologie, Infraciliatur, Silberliniensystem, Morphogenese und Ultrastruktur dieser drei Gruppe, so zeigen sich soviele Gemeinsamkeiten, daß ihre nähere stammesgeschichtliche Verwandtschaft kaum bezweifelt werden kann, was von Puytorac et al. (1974) hinsichtlich der Familien *Woodruffiidae*, *Colpodidae* und *Marynidae* bereits früher erkannt worden ist. Hier soll speziell auf die *Cyrtolophosididae* eingegangen werden. Eine direkte Ableitung der *Colpodidae* von den *Woodruffiidae* ist bereits von Stout (1960) versucht worden. Jedoch erscheint diese, wenn man nicht die *Cyrtolophosididae* miteinbezieht, als wenig überzeugend, da die von Stout (1960) als Bindeglied gesetzte Gattung *Bryophrya* hinsichtlich ihrer Infraciliatur und des Silberliniensystems bisher nicht untersucht worden ist.

(a) Gemeinsame Merkmale der *Cyrtolophosididae* und *Woodruffiidae* (geordnet nach ihrer Wichtigkeit): (1) Der Mikronucleus liegt im perinuclearen Raum des Makronucleus (Detcheva 1976, Golder 1976), (2) Dikineten, die von einer äuBeren Zirkularfibrille umgeben sind (Abb. 2,6, Taf. I 3, Taf. II 7), (3) Die Morphogenese ist auffallend ähnlich (s. Buitkamp 1975 a) und ist vom somatischen Typ (Abb. 8), (4) Das Silberliniensystem ist gitterförmig und gleicht sich in bestimmten Morphogenesestadien weitgehend (Abb. 7, Taf. II 4, Taf. III 10), (5) Die parorale Membran ist aus zwei Basalkörperreihen aufgebaut (Taf. I 1, Taf. II 7) (vgl. Griolière 1975, Buitkamp 1975 a, Detcheva 1976). Die eigenartige Unterbrechung der paroralen Membran bei *Cyrtolophosis* betrachte ich als abgeleitetes Merkmal; sie verschwindet übrigens während der Morphogenese (Buitkamp 1975 a), (6) Die

linksseitigen Membranellen sind aus zwei bis drei Basalkörperreihen aufgebaut. Ihre Anzahl ist bei den verschiedenen Gattungen und Arten dagegen unterschiedlich (vgl. Groliere 1975, Buitkamp 1975 a), (7) Leicht rechtsspiraler Kinetenverlauf (Taf. I 1, 2, Taf. II 7, 8), (8) Die Cytopyge liegt am caudalen Körperpol (Abb. 2, 6), (9) Besitz von Protrichocysten (Abb. 2, 6, Taf. I 2, Taf. II 7), (10) Weicher, deutlich metabolischer Körper (vgl. Kahl 1930–35, Johnson et al. 1937, Czapik 1971).

(b) Gemeinsame Merkmale der *Cyrtolophosididae, Colpodidae* und *Marynidae* (geordnet nach ihrer Wichtigkeit): (1) Dikineten, die von einer äußeren Zirkularfibrille umgeben sind (Abb. 6, 10), (2) Morphogenese vom somatischen Typ. Sie erfolgt bei *Colpoda* allerdings ausschließlich in den Teilungscysten (Abb. 8, 11), (3) Das Silberliniensystem ist ein weitmaschiges Gitter (Taf. II 7, 8, Taf. III 12), (4) Der Aufbau der linksseitigen Membranellen (Abb. 8, 11), (5) Kielbildung infolge der Verlagerung des Oralapparates zur Körpermitte hin. Diese Kielbildung ist besonders bei *Cyrtolophosis major* Kahl, 1926 bereits ziemlich ausgeprägt, (6) Leicht rechtsspiraler Kinetenverlauf, der bei den großen *Colpodidae* und den *Marynidae* sehr ausgeprägt wird (s. Stout 1960), (7) Die Cytopyge liegt am caudalen Körperpol (Abb. 6, 10), (8) Besitz von Protrichocysten (Abb. 6, 10), (9) Bau von gelationösen Gehäusen (Dingfelder 1962, McCoy 1974, Buitkamp 1975 a, b), (10) Viele Arten der *Colpodidae, Marynidae* und *Cyrtolophosididae* leben auch edaphisch (vgl. Buitkamp 1975 a).

(c) Gemeinsame Merkmale der *Cyrtolophosidina* und *Colpodina* (geordnet nach ihrer Wichtigkeit): (1) Dikineten, die von einer äußeren Zirkularfibrille umgeben sind, (2) Morphogenese vom somatischen Typ, (3) Das Silberliniensystem ist gitterförmig, (4) Aufbau der linksseitigen Membranellen, zumindest von der Genese her, (5) Rechtsspiraler Kinetenverlauf, (6) Lage der Cytopyge am caudalen Pol. (7) Besitz von Protrichocysten.

Auf Grund dieser vielen gemeinsamen Merkmale fällt es verhältnismäßig leicht, einen phylogenetischen Zusammenhang zwischen den *Woodruffiidae, Cyrtolophosididae* und *Colpodidae* herzustellen. Die ursprünglichste Gruppe sind ohne Zweifel die *Woodruffiidae*, da sie noch eine Reuse, ähnlich wie die primitiven Gymnostomata, besitzen. Eine Tendenz zur Reduktion der Reuse ist bei der Gattung *Platyophrya* zu bemerken (vgl. *P. vorax* mit *W. spumacola*). Die *Cyrtolophosididae* können von den *Woodruffiidae* unter folgenden Annahmen abgeleitet werden: Der Oralapparat wird weiter zur Körpermitte hin verlagert, wodurch ein kleiner Kiel entsteht (Abb. 5). Zugleich wird das Oralfeld etwas eingesenkt. Die parorale Membran erfährt erst im Verlaufe der weiteren

Evolution die für *Cyrtolophosis* typische Ausbildung. Weitgehend aufgegeben wird auch die mediane Silberlinie zwischen den Cilienreihen, was vielleicht mit der Verminderung der Körpergröße und der Basalkörper bei *Cytrolophosis* erklärt werden könnte. Reste der medianen Silberlinien finden sich noch im Gebiet des Oralapparates (Abb. 6, Taf. II 7, 8) und während der Morphogenese (Abb. 7, Taf. III 9, 10). Dadurch findet sich hinsichtlich des Silberliniensystems ein fließender Übergang zu den *Colpodidae*, die unter folgenden Annahmen von den *Cyrtolophosididae* abgeleitet werden können: Der Oralapparat wird noch weiter nach hinten verlagert und stärker eingesenkt, so daß ein deutlicher Kiel und ein ausgeprägtes Vestibulum entstehen. Die linken Membranellen treten ganz zusammen und werden zur linken Polykinete der *Colpodidae*. Schwierig abzuleiten ist dagegen die rechte Polykinete der *Colpodidae*, die entweder eine Neubildung ist oder die besonders modifizierte parorale Membran der *Woodruffidae* bzw. *Cyrtolophosididae*. Die bei manchen *Colpodidae* vorhandene Vestibularkinete (L y n n 1976 b) könnte im ersteren Fall der Rest der paroralen Membran sein.

2. Die Gattungen *Platyophrya* Kahl., 1926 und *Woodruffia* Kahl, 1931

Diese beiden Gattungen, die K a h l (1930–35) auf Grund einer irrigen Auffassung des Aufbaues des Oralapparates einerseits zu den *Holophryidae* andererseits zu den *Colpodidae* gestellt hat, G e l e i (1954) sogar zu den *Heterotrichida*, unterscheiden sich nach neueren Untersuchungen (G r o l i è r e 1975, s. d. weitere Literatur) hinsichtlich der Mundausstattung und der Morphogenese nicht wesentlich, weshalb G r o l i è r e (1975) vorgeschlagen hat, das Genus *Woodruffia* aufzulösen. Diesem Vorschlag ist zuzustimmen, wenn man nur die Oralstrukturen und die Morphogenese in Betracht zieht. Hinsichtlich der somatischen Infraciliatur lassen sich aber zwei klar abgegrenzte Gruppen selektieren, so daß diese beiden Genera unter neuer Diagnose aufrecht erhalten werden sollten. Mehrere Untersuchungen (J o h n s o n et al. 1937, G e l e i 1954, G e l l e r t 1955, C z a p i k 1971, G r o l i è r e 1975, B u i t k a m p 1975 a) zeigten nämlich übereinstimmend, daß es Arten mit gleichmäßiger (z. B. *Woodruffia spumacola*, *Woodruffia metabolica*) und solche mit links reduzierter (*Platyophrya angusta*, s. B u i t k a m p 1975 a, *P. vorax*, *Platyophrya* sp., s. Taf. I 2, Taf. II 4) Körperbewimperung gibt. Dieser Unterschied erscheint mir ausreichend, um damit zwei Genera zu trennen, für die ich folgende neue Diagnosen vorschlage:

Genus *Platyophrya* Kahl, 1926: *Woodruffiidae*, deren Bewimperung auf der linken Körperseite deutlich reduziert ist, so daß das Silberlinien-

system hier ausgeprägt orthogonale Maschen bildet. Auf der rechten Körperseite sind die Maschen des Silberliniensystems dagegen mehr oder minder deutlich quadratisch.

Genotypus: *Platyophrya vorax* Kahl, 1926

Genus *Woodruffia* Kahl 1931: *Woodruffidae*, deren linke und rechte Körperseite gleichmäßig bewimpert ist, so daß das Silberliniensystem einheitlich ist.

Genotypus: Als Typus wird *Woodruffia spumacola* Kahl, 1927 (Syn.: *Platyophrya spumacola*) vorgeschlagen, da die Infraciliatur von *W. rostrata* Kahl, 1931 noch nicht bekannt ist.

3. Vorschlag für eine neue Gliederung der Ordnung *Colpodida* Puytorac et al., 1974

Wie aus der neuesten Publikation von Corliss (1977) hervorgeht, herrscht über die zu der Ordnung *Colpodida* zu stellenden Familien große Unsicherheit. So sind von Corliss (1977) nun die *Cyrtolophosididae* dazugestellt und die *Marynidae*, die er kurze Zeit vorher (Corliss 1975) noch als repräsentative Familie der *Colpodida* betrachtet hat, herausgenommen worden. Zudem führt er noch an (Corliss 1977), daß die Familien *Woodruffiidae* und *Cyrtolophosididae* von einigen Forschern jetzt zu den *Hypostomata* gerechnet werden (s. auch McCoy, Einleitung), so daß in der Ordnung nur mehr die einzige Familie *Colpodidae* verbliebe.

Diese Reduktion halte ich aber in Anbetracht der nicht wenigen gemeinsamen Merkmale dieser vier Familien (s. oben), von denen ich in erster Linie den Besitz von Dikineten erwähne, die von einer äußeren argyrophilen Zirkularfibrille umgeben werden, als unrichtig. Auch gehören die *Marynidae* mit den Genera *Maryna* und *Mycterothrix* (Beschreibung der Infraciliatur bei Buitkamp 1975 b) hinsichtlich ihres Silberliniensystems (Foissner, unveröffentlicht), des Aufbaues des Oralapparates (Gelei 1954, Dingfelder 1962) sowie ihrer sonstigen Organisation mit großer Wahrscheinlichkeit zu den *Colpodida* und sind als deren höchstentwickelter Zweig anzusehen. Ich rechne daher zu dieser Ordnung die folgenden Familien: *Woodruffiidae, Cyrtolophosididae, Colpodidae* und *Marynidae*.

Freilich kann trotz der unzweifelhaft vorhandenen prinzipiellen Gemeinsamkeiten und der gegenseitigen Ableitbarkeit verschiedener Merkmale dieser vier Familien nicht übersehen werden, daß zwischen ihnen auch große Unterschiede existieren, die sicher als Folge einer langen selbständigen Evolution angesehen werden müssen, worauf vor allem die *Colpodidae* mit ihrer großen Formenmannigfaltigkeit hinweisen.

Diese Unterschiede betreffen vor allem den Bau des Kernapparates, der bei den *Woodruffidae* und *Cyrtolophosididae* sehr spezialisiert ist, da der Mikronucleus im perinuclearen Raum des Makronucleus liegt (Detcheva 1976, Golder 1976), sowie den feineren Bau des Silberliniensystems, da den *Colpodidae* und *Marynidae* eine mediane Silberlinie gänzlich fehlt. Auch hinsichtlich des Aufbaues des Oralapparates lassen sich zwanglos zwei Gruppen selektieren: die *Colpodidae* und *Marynidae* mit ausgeprägtem Vestibulum und die *Woodruffiidae* und *Cyrtolophosididae* ohne Vestibulum. Daher schlage ich zwei neue Unterordnungen mit folgenden Diagnosen vor:

(1) U. O. *Cyrtolophosidina* nov. subordo, mit den Familien *Woodruffiidae* und *Cyrtolophosididae*: *Colpodida*, deren Mikronucleus im perinuclearen Raum des Makronucleus liegt und deren Silberliniensystem durch eine mediane Silberlinie, die zwischen den Somakineten verläuft, gekennzeichnet ist. Diese ist allerdings bei den *Cyrtolophosididae* nur mehr rudimentär ausgebildet (postorale semimediane Silberlinien) bzw. tritt nur noch während der Morphogenese deutlicher in Erscheinung.

(2) U. O. *Colpodina* nov. subordo, mit den Familien *Colpodidae* und *Marynidae*: *Colpodida* mit hoch organisierter Vestibularciliatur und gitterförmigem Silberliniensystem ohne mediane Silberlinien.

DANKSAGUNG

Mit dankenswerter Unterstützung des Österreichischen MAB-6 Programmes der UNESCO, des Fonds zur Förderung der wissenschaftlichen Forschung, der Jubiläumsstiftung der Österreichischen Nationalbank, der Gesellschaft zur Förderung der Hochschule für Bodenkultur und der Naturkundlichen Station der Stadt Linz.

SUMMARY

A comparative study of the silverline system and the infraciliature of the genera *Platyophrya, Cyrtolophosis* and *Colpoda* showed that the family *Cyrtolophosididae* must be incorporated into the ordo *Colpodida*. The genus *Woodruffia*, disputed by Grolière (1975), is set up again, because the genera *Platyophrya* and *Woodruffia* are different with regard to their somatic infraciliature. But new diagnoses are suggested for these genera. The ordo *Colpodida* is divided up into two suborders. This decision is largely discussed. The subordo *Cyrtolophosidina* nov. subord. includes the families *Woodruffiidae* and *Cyrtolophosididae*. It is characterized mainly by the special structure of the nuclear apparatus (the micronucleus resides in the perinuclear space of the makronucleus), and the silverline system. The subordo *Colpodina* nov. subord. includes the families *Colpodidae* and *Marynidae*. This subordo is characterized mainly by a highly organized vestibular ciliature and the lack of median silverlines.

LITERATUR

Buitkamp U. 1975 a: Ökologische und taxonomische Untersuchungen an Ciliaten ausgewählter Bodentypen. Diss. Mat.-naturwiss. Fak. Rheinischen Friedrichs-Wilhelms-Universität. Bonn., 102 pp.

Buitkamp U. 1975 b: Eine Neubeschreibung von *Mycterothrix tuamotuens* Balbiani, 1887 (*Ciliophora, Colpodida*). Protistologica, 11, 323–324.

Burt R. L. 1940: Specific analysis of the genus *Colpoda* with special reference to the standardization of experimental material. Trans. Am. Microsc. Soc., 59, 414–432.

Corliss J. O. 1953: Silver impregnation of ciliate protozoa by the Chatton–Lwoff technic. Stain Technol., 28, 97–100.

Corliss J. O. 1961: The Ciliated Protozoa; Characterization, Classification, and Guide to the Literature. Pergamon Press, London and New York, 310 pp.

Corliss J. O. 1975: Taxonomic characterization of the suprafamilial groups in a revision of recently proposed schemes of classification for the phylum ciliophora. Trans. Am. Microsc. Soc., 94, 224–267.

Corliss J. O. 1976: "Bonafide" families and genera assignable to ciliate suprafamilial taxa. Privatdruck, vorläufige Fassung der nächsten Arbeit.

Corliss J. O. 1977: Annotated assignment of families and genera to the orders and classes currently comprising the Corlissian scheme of higher classification for the phylum ciliophora. Trans. Am. Microsc. Soc., 96, 104–140.

Czapik A. 1971: Les observations sur *Platyophrya spumacola*, Kahl. Acta Protozool., 8, 363–366.

Detcheva R. 1976: Particularités ultrastructurales du cilié *Cyrtolophosis mucicola* Stokes, 1885. C.r. Seanc. Soc. Biol., 170, 112–114.

Dingfelder J. H. 1962: Die Ciliaten vorübergehender Gewässer. Arch. Protistenk., 105, 509–658.

Foissner W. 1976: Erfahrungen mit einer trockenen Silberimprägnationsmethode zur Darstellung argyrophiler Strukturen bei Protisten. Verh. Zool.-Bot. Ges. Wien, 115, 68–79.

Foissner W. 1977: Elektronenmikroskopische Untersuchung der argyrophilen Strukturen von *Colpidium campylum* (*Ciliata, Tetrahymenidae*). Acad. Sci. hung., 28, 59–72.

Foissner W. 1978: *Euplotes moebiusi f. quadricirratus* (*Ciliophora, Hypotrichida*). I. Die Feinstruktur des Cortex und der argyrophilen Strukturen. Arch. Protistenk., 120, 86–117.

Gelei J. v. 1954: Über die Lebensgemeinschaft einiger temporärer Tümpel auf einer Bergwiese im Börzönygebirge (Oberungarn) III. Ciliaten. Acta biol. hung., 5, 259–343.

Gellert J. 1955: Die Ciliaten des sich unter der Flechte *Parmelia saxatilis* Mass. gebildeten Humus. Acta biol. hung., 6, 77–111.

Golder T. K. 1976: The macro-miconuclear complex of *Woodruffia metabolica*. J. Ultrastruct. Res., 54, 169–175.

Groliere C.-A. 1975: La stomatogenese du cilié *Platyophrya spumacola* Kahl, 1927; son intérêt pour la compréhension de la diversification buissonnante des *Kinetophragmophora* de Puytorac et coll. C. r. Acad. Sci. Paris, 280, 861–864.

Hashimoto K. 1966: Stomatogenesis in resting cysts of *Colpodidae*. J. Protozool., 13, 383–390.

Johnson W. M. and Larson E. 1937: Studies on the morphology and life history of *Woodruffia metabolica*, nov. sp. Arch. Protistenk., 90, 383–392.

Kahl A. 1926: Neue und wenig bekannte Formen der holotrichen und heterotrichen Ciliaten. Arch. Protistenk., 55, 197–438.

Kahl A. 1927: Neue und ergänzende Beobachtungen holotricher Ciliaten I. Arch. Protistenk., 60, 34–129.

Kahl A. 1930–35: Wimpertiere oder Ciliata. In: Die Tierwelt Deutschlands, (ed. Dahl F.), G. Fischer, Jena.

Klein B. M. 1929: Weitere Beiträge zur Kenntnis des Silberliniensystems der Ciliaten. Arch. Protistenk., 65, 183–258.

Lynn D. H. 1976 a: Comparative ultrastructure and systematics of the *Colpo-*

dida: structural conservatism hypothesis and a description of *Colpoda steinii* Maupas, 1883. J. Protozool., 23, 302–314.
Lynn D. H. 1976 b: Comparative ultrastructure and systematics of the *Colpodida* (*Ciliophora*): Structural differentiation in the cortex of *Colpoda simulans*. Trans. Am. Microsc. Soc., 95, 581–599.
Mc Coy J. W. 1974: Biology and systematics of the ciliate genus *Cyrtolophosis* Stokes, 1885. Acta Protozool., 13, 41–52.
Müller O. F. 1786: Animalcula Infusoria Fluviatilia et Marina. Havniae et Lipsiae. 367 pp.
Penard E. 1922: Études sur les infusoires d'eau douce. Genéve, Georg et Cie, 331 pp.
Puytorac P. de et al. 1974: Proposition d'une classification du phylum *Ciliophora* Doflein, 1901 (réunion de systématique, Clermont-Ferrand). C. r. Acad. Sci. Paris, 278, 2799–2802.
Roux J. 1901: Faune infusorienne des eaux stagnates des environs de Genève. Kündig, Genève. 148 pp.
Schewiakoff W. 1896: The organization and systematics of the infusoria aspirotricha (*Holotricha* auctorum). Mém. Acad. impér. Sci. St. Pétersb. (ser. 8), 4, 1–395 (in Russian).
Small E. B. 1967: The scuticociliatida, a new order of the class ciliatea (Phylum *Protozoa*, subphylum *Ciliophora*). Trans. Am. Microsc. Soc., 86, 345–370.
Stokes A. C. 1885: Some new infusoria. Am. Nat., 19, 433–443.
Stokes A. C. 1888: A preliminary contribution towards a history of the freshwater infusoria of the United States. J. Trenton nat. Hist. Soc., 1, 71–344.
Stout J. D. 1960: Morphogenesis in the ciliate *Bresslaua vorax*, Kahl and the phylogeny of the *Colpodidae*. J. Protozool., 7, 26–35.
Taylor C. V. and Furgason W. H. 1938: Structural analysis of *Colpoda duodenaria* sp. nov. Arch. Protistenk., 90, 320–339.
Tuffrau M. 1952: La morphogenese de division chez les *Colpodidae*. Bull. biol. Fr. Belg., 86, 1–12.
Wilbert N. 1975: Eine verbesserte Technik der Protargolimprägnation für Ciliaten. Mikrokosmos, 6, 171–179.

Received on 24 September 1977

LEGENDEN ZU DEN TAFELN I–III

1: *Platyophrya vorax*, rechts-laterale Ansicht der Infraciliatur. Die zwei kleinen Pfeile weisen auf die zweireihige parorale Membran. Unterhalb der adoralen Membranellen befinden sich zwei dicht stehende Reihen paarig angeordneter Basalkörperreihen (großer Pfeil). Nasse Silberimprägnation
2: *Platyophrya vorax* nach trockener Silberimprägnation. Die unterschiedlich dichte Bewimperung der rechten und linken Körperseite ist klar ersichtlich. Das Silberliniensystem weist auf der rechten Körperseite quadratische, auf der linken Körperseite orthogonale Maschen auf. Die Pfeile weisen auf die adoralen Membranellen. Pt — Protrichocyste
3: *Platyophrya* sp., Teilansicht des Silberliniensystems. Der Pfeil weist auf die parorale Membran. Trockene Silberimprägnation
4: *Platyophrya* sp., Gesamtansicht des Silberliniensystems. Der Pfeil weist auf die parorale Membran, deren Aufbau aus zwei Basalkörperreihen klar erkennbar ist. Auch hier ist die unterschiedlich dichte Bewimperung der rechten und linken Körperseite klar ersichtlich. Pt — Protrichocyste. Trockene Silberimprägnation
5,6: *Platyophrya vorax*, Infraciliatur und Silberliniensystem des Oralapparates. Die Pfeile weisen auf die 4 bzw. 5 adoralen Membranellen, unterhalb derer sich zwei dicht stehende Reihen paarig angeordneter Basalkörperreihen (Abb. 5, große Pfeile) befinden. T — Trichiten. Trockene Silberimprägnation
7, 8: *Cyrtolophosis mucicola*, rechts- und links-laterale Ansichten des Silberliniensystems und der Infraciliatur. Der lange Pfeil weist auf die parorale Membran, die kurzen Pfeile weisen auf die adoralen Membranellen. Die typischen semimedianen Silberlinien (sS), die Cytopyge (Cp) und Protrichocysten (Pt) sind gut erkennbar. Trockene Silberimprägnation
9, 10: *Cyrtolophosis mucicola*, mittleres und spätes Teilungsstadium. Die Pfeile weisen auf mediane Silberlinien. Nähere Erklärungen im Text. Trockene Silberimprägnation
11: *Cyrtolophosis mucicola*, dorsale Ansicht des Silberliniensystems und der Infraciliatur. Trockene Silberimprägnation
12: *Colpoda steini*, rechts-laterale Ansicht der Infraciliatur und des Silberliniensystems. Rechte (rP) und linke (lP) Polykinete des Oralapparates sind gut erkennbar. Trockene Silberimprägnation

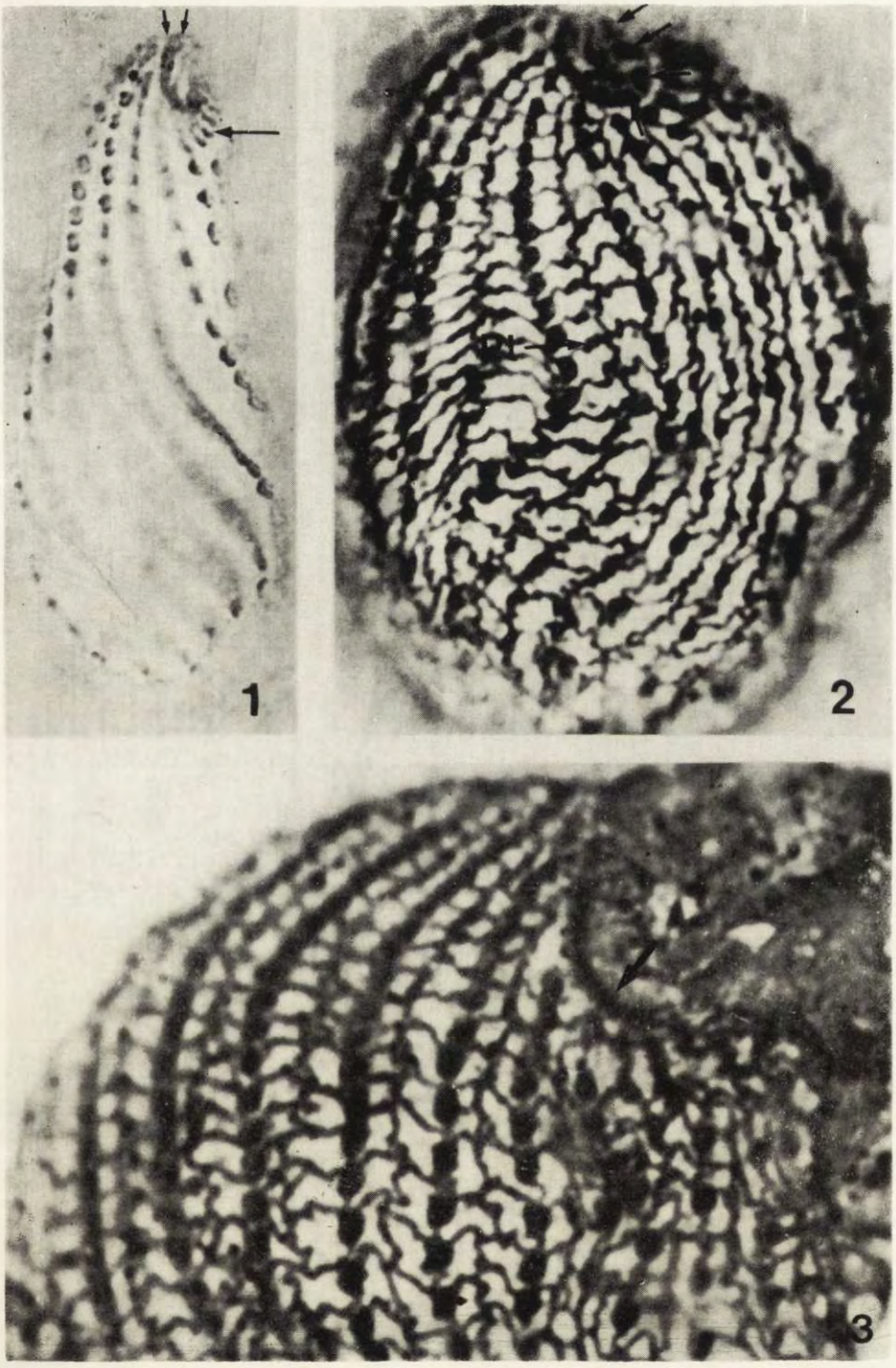

W. Foissner auctor phot.

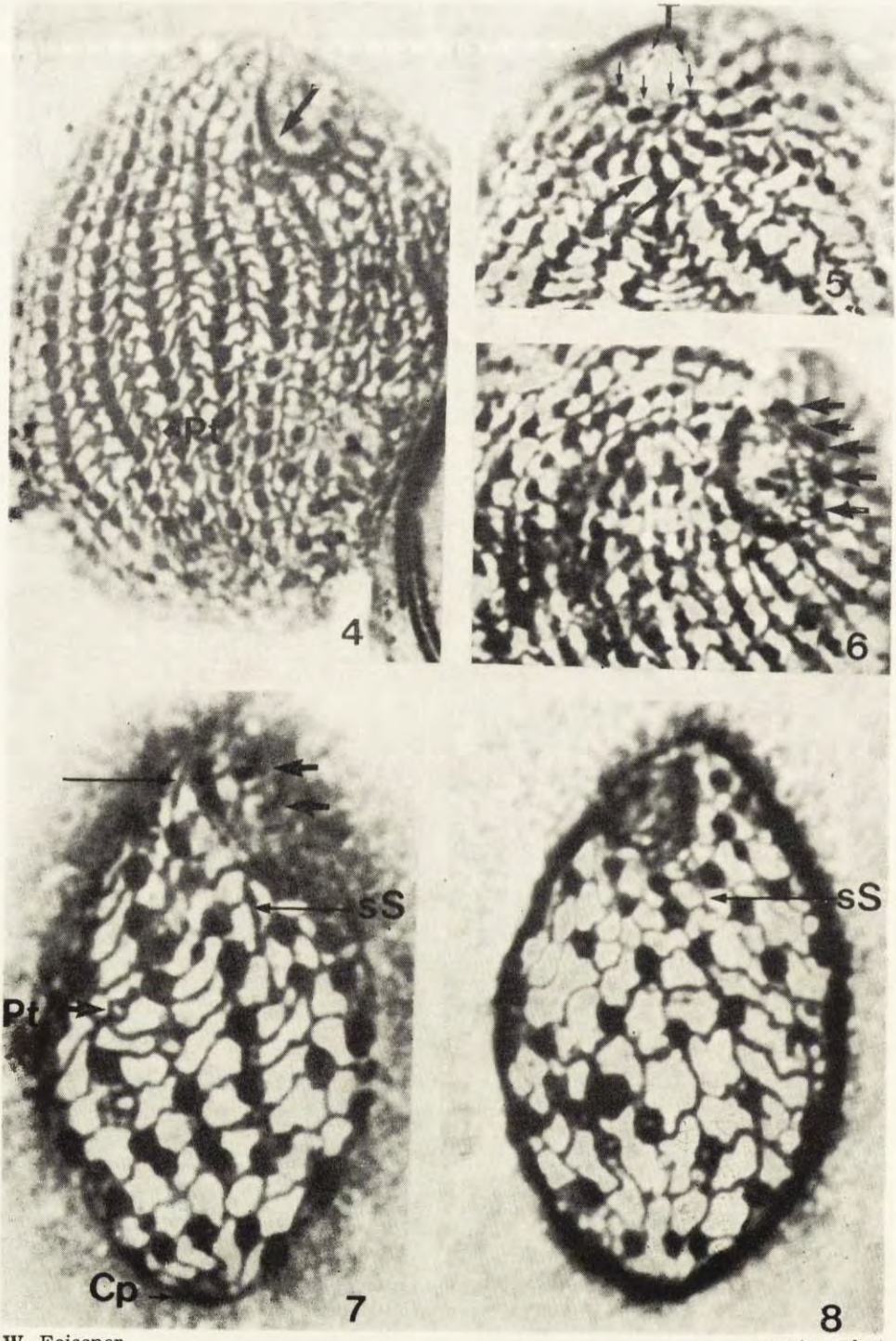

W. Foissner auctor phot.

W. Foissner auctor phot.

ACTA PROTOZOOLOGICA
VOL. 17 (No. 2) WARSZAWA, 30 VI 1978 pp. 233–244

Protozoology Laboratory, Department of Zoology, University of Kalyani, Kalyani 741235, West Bengal, India

D. P. HALDAR and N. CHAKRABORTY

Observations on Three New Species of Cephaline Gregarines (*Protozoa : Sporozoa*) from Insects

Synopsis. The paper contains the descriptions of the morphology and life history of three new species of cephaline gregarines (*Protozoa: Sporozoa*) belonging to the genus *Gregarina* from insects of the order *Coleoptera* collected at Kalyani, West Bengal, India. This are: (1) *Gregarina crescentica* sp. nov. from *Amblyrrhinus* sp.; (2) *G. alcidessi* sp. nov. from *Alcidesii* sp. nr. *leopardus* 01; (3) *G. spraguei* sp. nov. from an unidentified beetle belonging to the family *Curculionidae*, subfamily *Brachyderinae*. The seasonal intensity of these gregarines and the percentage of infection together with informations about the holotype materials are included.

Dufour (1828) established the genus *Gregarina* to include a gregarine, *Gregarina ovata* from the ear wig, *Forficula auricularia*. In their monographs, Watson (1916) and Kamm (1922) revised the generic characters of the genus *Gregarina* Dufour as biassociative sporadins, simple globular epimerite or cylindrical papilla, cyst dehiscence by spore ducts and barrel-shaped or dolioform spores. Since then, a number of species have been described under this genus from different parts of the world. Amoji and Rodgi (1976) have recently presented a chronological list of these gregarine species as well as their hosts and localities.

The present communication records three new species of cephaline gregarines (*Protozoa* : *Sporozoa*) of the genus *Gregarina* Dufor from beetles collected at Kalyani, West Bengal, India. The holotype materials are at present deposited at the Department of Zoology, University of Kalyani, to be submitted later to Zoological Survey of India, Calcutta.

Material and Methods

The host insects were collected from the campuses of Kalyani University and Bidhan Chandra Agricultural University at Kalyani, West Bengal. The methods employed in the present study have been described by Haldar and Kundu

(1977) elsewhere. It has been observed that staining with Heidenhain's haematoxylin of Schaudinn's fluid-fixed materials following overnight mordanting in 3 per cent iron alum gave excellent results. Endogenous stages of the gregarines were studied in 5 μm thick sections stained as above. Cysts were kept in depression slides with 0.5 per cent saline solution inside moist chambers to avoid dessication.

The ratios used in this paper are the ratio of length of protomerite to total length and width of protomerite to width of deutomerite.

Observations

Family *Gregarinidae* Labbé, 1899

Genus *Gregarina* Dufour, 1828

Gregarina crescentica sp. n.

The colepteran, *Amblyrrhinus* sp. is infected with a gregarine belonging to the genus *Gregarina* Dufour which is described here as a new species as it does not resemble any known species of the genus. It is named *Gregarina crescentica.*

Development of the trophozoite

The trophozoite develops intracellularly. The earliest stage within the epithelium of the mid gut is an ovoidal body measuring 9.0 μm. The nucleus is spherical, has a centrally located endosome and lies at one corner of the organism being surrounded by a halo. Subsequent to the appearance of the septum it is characterized by a dome-shaped protomerite, 7.5 × 10.0 μm and the deutomerite, 12.5 × 15.0 μm (Pl. I 1). As it grows further, an epimerite develops in front of the protomerite and it becomes a young intracellular trophozoite. The epimerite at this condition is dome-shaped and 7.0 μm long. The protomerite is rhomboidal and the deutomerite is hemispherical with a spherical nucleus that contains a densely stained endosome.

Trophozoite

The trophozoite (Fig. 1 *1*) remains free within the gut lumen, where the pH varies from 6.2 to 7.0. Very young trophozoites are, however, seen attached to the epithelial cells by means of their epimerites. The body is obase in shape in younger ones but later becomes elongated and cylindrical. In living condition the cytoplasm appears white in colour. The epimerite is usually observed in young forms and it is a knob-like structure situated at the tip of the protomerite. It measures 8.5 μm in the average. The protomerite is subspherical in shape and its width is slightly greater than its length. The deutomerite is elongated with a rounded posterior extremity. It is broadest behind the septum. The

nucleus is spherical in shape and measures 14.3 μm in diameter in the average. The nuclear membrane is well-defined with a definite centrally located endosome and several chromatin dots. The pellicle is uniformly thin throughout its length. Epicyteal striations are wanting.

Sporadin

The sporadin (Fig. 1 *2*, Pl. I 2) has almost the same features as that of the trophozoite although they differ in certain aspects. The protomerite is subspherical and typically greater in breadth than its length. The septum separating it from the deutomerite is thick and characteristically crescentic in appearance. The deutomerite is typically cylindrical and its terminal end is rounded. It is circular in cross-section.

Sporadins in syzygy (Fig. 1 *3*, Pl. I 3) are observed in lesser number

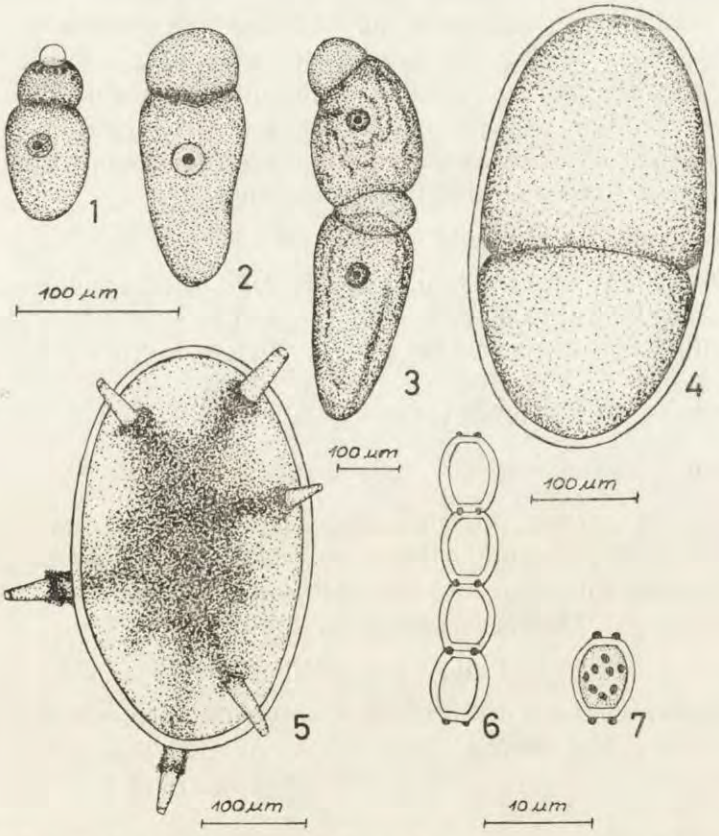

Fig. 1. *1–7*. Camera lucida drawings of *Gregarina crescentica* sp. n. *1* — A trophozoite, *2* — A sporadin; the crescentic septum between protomerite and deutomerite, *3* — Sporadins in association, *4* — A freshly formed gametocyst, *5* — A cyst with sporoducts, *6* — Spores liberated in a chain, *7* — A mature spore

and while in association the primite differs markedly from the satellite in structure. The former is always smaller than the latter. The anterior end of the protomerite of the primite is somewhat cone-shaped and that of the satellite is compressed to receive the posterior end of the primite which is flat.

Gametocyst and spore

The cyst collected from the hind gut of the host has an oval shape. The pair of encysted gamonts at the early condition form an opaque, granular, milky-white sphere with a slight equatorial constriction (Fig. 1 *4*). The cyst measures 340.0 × 210.0 μm. The cyst wall is smooth and moderately thick. At about 24 h of development inside the moist chamber the separating line between the gametocytes disappears and at 48 h six small ducts develop. The ducts later increase in length and their tips gradually narrow to a point (Fig. 1 *5*). The ducts are generally 50.0–60.0 μm in length. Almost at the same time the cysts dehisce through these spore ducts. The spores come out in chains (Fig. 1 *6*).

The spores are characteristically delioform and measure 7.0 × 6.0 μm in the average. There are 4 min knobs, 2 at each pole of the spores, attached to their outer walls. At about 80 h of development eight sporozoites are clearly visible inside the spores (Fig. 1 7).

Measurements (in microns)

Figures within parenthesis indicate average of 20 specimens.

LE 7.5—10.0 (8.4); LP 17.5—62.5 (41.2); LD 42.5—310.0 (109.8); TL 70.0—380.0 (154.2); WP 25.0—150.0 (57.3); WD 30.0—210.0 (70.3); Nucleus 7.5—35.0 (18.5).

LP : TL = 1 : 3.7; WP : WD = 1 : 1.2.

Material

Holotype, trophozoite on slide No. E6/1 prepared from contents of mid gut of the beetle, *Amblyrrhinus* sp., collected at Kalyani University Campus at Kalyani, West Bengal, India on 15 March, 1974. Paratype, many; other particulars are same as for the holotype.

Seasonal intensity and site of infestation

On an average, 20.5 per cent of *Amblyrrhinus* sp. are usually infected with this gregarine from February to August. The seat of infection is the mid gut. The cysts are collected from the hind gut.

Affinities

The gregarine under report belongs to the family *Gregarinidae* Labbé, 1899 and genus *Gregarina* Dufour, 1828 because it has the following

characters: biassociative sporonts, satellite with septum, epimerite is symmetrical and simple, cyst with spore ducts. It somewhat resembles *G. gonocephali* Obata, 1953 during association but differs from it in other characters as well as in the ratios of different body parts. The thick and crescentic septum in the sporont of this gregarine is also very characteristic. The specific trivial name *crescentica* is given to stress this feature.

Gregarina alcidesii sp. n.

The Gregarina species inhabiting the mid gut of the beetle, *Alcides* sp. nr. *leopardus* 01. is described here as a new species as it does not resemble any known species of the genus.

Development of the Trophozoite

This is intracellular and takes place within the epithelial cells of the mid gut (Fig. 2 *8* and *9*, Pl. I 4). The earliest stage of the parasite has an oval body measuring 4.0 × 2.5 μm. It contains a small spherical nucleus. The second intracellular stage is characterized by a subspherical protomerite, 2.5 × 3.0 μm, and a spherical deutomerite, 5.0 × 5.0 μm, containing the nucleus. Later, the parasite grows enormously in size, comes to lie outside the infected cell but remains deeply attached with it for some time. At this stage, the epimerite is characterized by a globular, almost hyaline structure. The protomerite has a long narrow neck and a broad base. The deutomerite is also very much inflated and contains the spherical nucleus.

Trophozoite

This is very seldom observed in smears prepared from contents of the mid gut (pH 6.0–7.0). Out of a total of 329 beetles examined, 111 showed infection with this gregarine, of which only one contained a few trophozoites with small, transparent, knob-like epimerite. The protomerite is hemispherical, broadest near the septum and finely granulated. It is separated from the deutomerite by a thin septum but forming a distinct constriction. The deutomerite is more or less ovoidal in shape, broadest in the middle and has a broadly rounded posterior extremity. This is also the largest segment of the body and is circular in cross-section. The pellicle is thin and epicyteal striations have not been observed. The spherical nucleus lies anywhere within the deutomerite. There is a distinct nuclear membrane and a large central karyosome. The nucleoplasm contains several fine chromatin granules (Fig. 2 *10*, Pl. I 5, 6).

Sporadin

The sporadins are characteristically biassociative but solitary sporadins have also been encountered in smear preparations. In fresh preparations these are observed to move slowly under the microscope and are milky-white in colour. The sporadin has an elongated body with a subspherical protomerite and an elongated deutomerite. It is broadest near the septum and gradually tapers posteriorly and becomes cylindrical near the posterior two-third region. Distinct epicyteal striations are observed (Fig. 2 *11* and *12*).

During association the primite is always smaller than the satellite but

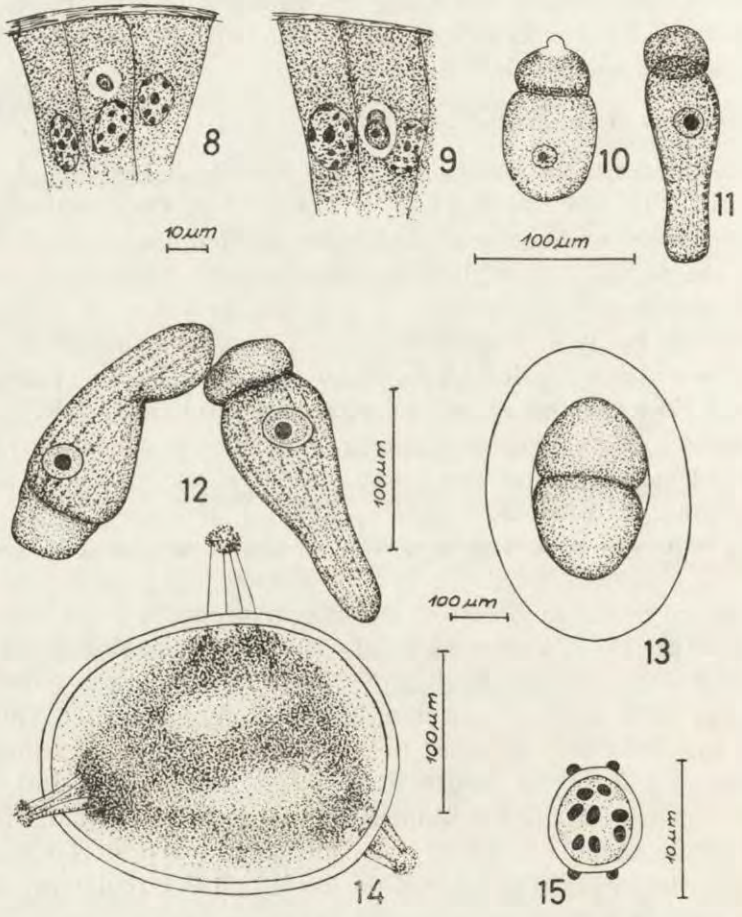

Fig. 2. *8–15.* Camera lucida drawings of *Gregarina alcidesii* sp. n. *8* — First intracellular stage, *9* — Second intracellular stage, *10* — A trophozoite, *11* — A sporadin, *12* — Sporadins in association, *13* — A freshly formed cyst with an ectocyst, *14* — Cyst with sporoducts, *15* — A mature spore

otherwise structurally these are more or less the same. The only difference lies in the shape of the protomerite which is flattened in the primite and subspherical in the satellite. The epicyteal striations are also very distinct in the uniting individuals.

Gametocyst and Spore

The cysts vary much in size. These are almost ovoidal in outline and their size varies from 220.0 × 150.0–320.0 × 170.0 μm. There is a gelatinous transparent ectocyst (Fig. 2 13) varying in thickness from 40–150 μm. The pairs of encysted gamonts are opaque, granular, dull-white bodies at the early condition and there is a deep equatorial constriction between them. They are thick-walled with a smooth outer surface. At about 20 h of development the equatorial constriction disappears and concentration of inner cytoplasm occurs, and at about 36 h three small ducts are formed which come out of the inner sphere (Fig. 2 *14*). The ducts are broad at the base and tapering towards the tip and are 30.0 μm long. At about the same time the cyst dehisces and the spores come out through these ducts. The extrusion of the spores is in chains.

The spores are characteristically oval and measure 6.0 × 5.0 μm. These have two knobs at each pole. Formation of sporozoites is completed within 14 h of development. The sporozoites are small, ovoidal bodies and they are arranged irregularly within the spore (Fig. 2 *15*).

Measurements (in microns)

Figures within parenthesis indicate average of 20 specimens.

LE 5.0, LP 12.5–65.0 (38.0), LD 40.0–300.0 (173.7), TL 52.5–350.0 (212.6), WP 25.0–117.5 (64.8), WD 27.5–152.5 (78.1), Nucleus 12.5–30.0 (22.3).

LP : TL = 1 : 5.5, WP : WD = 1 : 1.2.

Material

Holotype, trophozoite on slide No. F6/1 prepared from contents of mid gut of the beetle, *Alcides* sp. nr *leopardus* 01., collected at Horticulture garden, Bidhan Chandra Agricultural University at Kalyani, West Bengal, India on 24 June, 1974. Paratype, many; other particulars are same as for the holotype.

Seasonal Intensity and Site of Infestation

The host beetle was found infected with this gregarine during June to October, the percentage of infection being 33.7. The seat of infection

is the mid gut. The cysts are collected from the hind gut and these are found in abundance during the month of August. In one case as many as 15 cysts were collected from a single infected host.

Affinities

The parasite somewhat resembles *G. mesomorphi* Devdhar and Deshpande, 1971 in general shape but differs from it in all other characters. Furthermore, the LP : TL and WP : WD ratios do not correspond to any species of the genus *Gregarina* so far described and this is the first time that a gregarine is reported from *Alcides* sp. nr *leopardus* 01. The name *alcidesii* is given after the name of the host.

Gregarina spraguei sp. n.

A beetle belonging to the subfamily *Brachyderinae* under the family *Curculionidae* was found to be infected during the months of February to May with a biassociative gregarine. The host could not be identified beyond the subfamily level. The gregarine is described here as *Gregarina spraguei* as it does not resemble any known species of the genus.

Development of the trophozoite

The earliest stage encountered in sections is a rounded body measuring 6.0 μm in diameter. Its cytoplasm is finely granulated and the nucleus is perfectly spherical. The parasite obviously develops into a two-segmented body, but unfortunately this stage could not be traced in any of our preparations so far. With the formation of the epimerite the parasite develops into a three-segmented individual and comes out of the infected cell but remains firmly anchored with it by the epimerite (Pl. I 7), broad at the base and pointed at the tip; it measures 7.5 μm in length. The protomerite is two times broader than its length and is separated from the deutomerite by a sharp constriction. The nucleus is egg-shaped and contains a spherical karyosome.

Trophozoite

The fully grown trophozoite has an elongated body and appears milkywhite in living condition under the microscope. The epimerite is a simple hyaline knob. The protomerite is hemispherical with round anterior margin. It is slightly broader than long. The deutomerite is broadest slightly below the septum and is marked off from the protomerite by a sharp constriction. It appears circular in cross section. The pellicle is thin and the cytoplasm is finely granulated. The nucleus is spherical in shape and contains a single conspicuous centrally located karyosome. The nucleoplasm possesses several fine chromatin granules (Fig. 3 *16*).

Sporadin

The sporadins are biassociative, although solitary forms are also commonly encountered in smear preparations (Fig. 3 *17*, Pl. I 8). The protomerite of the sporadin is dome-shaped and the septum is somewhat inwardly curved. The deutomerite is obase. The nucleus has the same characters as observed in the trophozoite.

During association (Fig. 3 *18*, Pl. I 9) both the primite and the satellite have cylindrical shape and these exhibit dome-shaped protomerites. Both have blunt posterior extremities and the association is caudofrontal. However, the association is superficial, as even slight disturbance dissociates the uniting individuals.

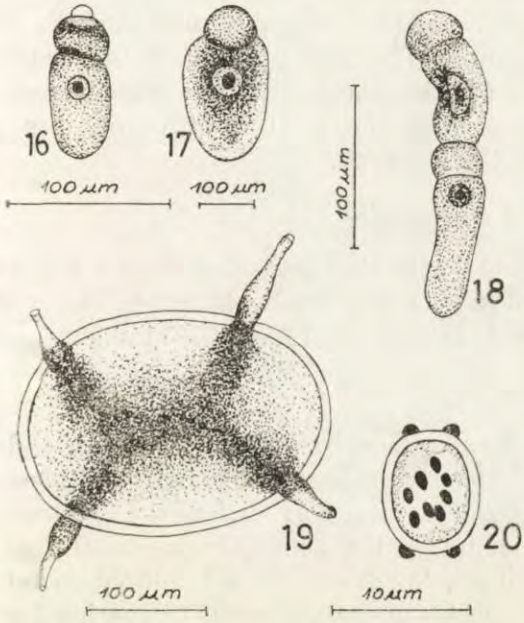

Fig. 3. *16–20*. Camera lucida drawings of *Gregarina spraguei* sp. n. *16* — A trophozoite, *17* — A sporadin, *18* — Sporadins in syzygy, *19* — A cyst with sporoducts, *20* — A mature spore

Gametocyst and Spore

The shape of the cyst does not vary and is always oval. The pair of encysted gametocytes at the early condition forms an opaque granular white structure with a deep equatorial constriction. These are unequal in size. The cysts measure 270.0 × 200 µm–310.0 × 200 µm. The cyst wall is smooth and moderately thick. At about 24 h of development inside the moist chamber four rounded spots are observed on the surface of the cyst. From these spots, four sporoducts are formed at a later stage (Fig. 3 *19*). The sporoducts vary from 70.0–80.0 µm in length. These are broad at the base and gradually taper at the tip. The cyst dehisces through these ducts and the spores always come out in chains.

The spores are ovoidal with four knobs attached to their outer wall and measure 8.0 × 6.0 μm. Formation of sporozoites is completed within 80 h of development inside the moist chamber (Fig. 3 *20*).

Measurements (in microns)

Figures within parenthesis indicate average of 20 specimens.

LE 10.0–15.0 (11.5), LP 30.0–70.0 (52.2), LD 72.5–220.0 (136.1), TL 112.5–280.0 (186.7), WP 42.5–110.0 (61.6), WD 45.9–170.0 (77.1), Nucleus 15.0–50.0 (26.2).

LP : TL = 1 : 3.5, WP : WD = 1 : 1.2.

Material

Holotype, trophozoite on slide No. E7/2 prepared from contents of mid gut of a beetle belonging to subfamily *Brachyderinae* of the family *Curculionidae*, collected at Bidhan Chandra Agricultural University campus at Kalyani, West Bengal, India on 4 March, 1974. Paratype, many; other particulars are same as for the holotype.

Seasonal Intensity and Site of Infestation

The host beetle is found infected with this gregarine during February to May. 33.3 per cent of the insects are usually infected. The seat of infection is the mid gut. The cysts are collected from the hind gut.

Affinities

The parasite belongs to the family *Gregarinidae* Labbé since it is biassociative and the trophozoite possesses a simple symmetrical epimerite. The structure of the sporont and epimerite as well as the dehiscence of the cyst assign its inclusion under the genus *Gregarina* Dufour. After careful comparison with all species described and figured so far, it is proposed to establish a new species under the genus *Gregarina* Dufour for the organism and the name *Gregarina spraguei* is given after the eminent Protozoologist, Dr Victor Sprague.

The comparative characters of the three new species of *Gregarina* described in the paper are presented in Table 1.

Discussion

All the three gregarines described presently undergo their early development within the epithelial cells of the host gut. It is noted that in older classifications as well as that of K u d o (1966), no mention is made

Table 1

Showing the comparative characters of the three new species of cephaline gregarines belonging to the genus *Gregarina* Dufour, 1828

Characters	*G. crescentica* sp. n.	*G. alcidesii* sp. n.	*G. spraguei* sp. n.
Total length	70.0–380.0 μm	52.5–350.0 μm	112.5–280.0 μm
Epimerite	Knob-like; 7.5–10.0 μm long	Knob-like; 5.0 μm long	Hyaline knob; 10.0–15.0 μm long
Protomerite	Subspherical	Hemispherical in trophozoite, subspherical in sporadin	Hemispherical in trophozoite, dome-shaped in sporadin
Sporadin	Biassociative; primite is smaller than satellite	Biassociative; primite is smaller than satellite	Biassociative; primite is smaller than satellite
Gametocyst	Oval; 340.0×210 μm; gametocytes of unequal size; spores issued about 48 h through six sporoducts, 50.0–60.0 μm long	Ovoidal; a gelatinous ectocyst of 40.0–150.0 μm thickness; cyst measures 220.0×150.0–320.0× ×170.0 μm excluding ectocyst; gametocytes of unequal size; spores issued at 36 h through three sporoducts of 30.0 μm length	Oval; 270.0×200.0–310.0 ×200.0 μm; gametocytes of unequal size; spores issued at 48 h through four sporoducts, 70.0–80.0 μm long
Spore	Dolioform; 7.0×6.0 μm; formation of sporozoites 32 h after dehiscence	Oval; 6.0×5.0 μm; formation of sporozoites 8 h after dehiscence	Ovoidal; 8.0×6.0 μm; formation of sporozoites 32 h after dehiscence
LP : TL	1 : 3.7	1 : 5.5	1 : 3.5
WP : WD	1 : 1.2	1 : 1.2	1 : 1.2
Host	*Amblyrrhinus* sp.	*Alcides* sp. nr. *leopardus* 01.	An unidentified beetle of subfamily *Brachyderinae*, family *Curculionidae*

about the development in the definition of the family *Gregarinidae* Labbé. In their systems of classification, Grassé (1953), Chakravarty (1959) and Geus (1969) have, however, described that the members of the family *Gregarinidae* have extracellular development. Recently, Amoji and Rodgi (1976) have described two *Gregarina* species, of which *G. megaspora* develops intracellualarly. Also, *G. cylindrosa described* by Haldar and Kundu (1977) has intracellular development. Since other characters of these gregarines agree with the features of the family as proposed by the authors mentioned above, their inclusion in this family is justified. Possibilities of proposing a new definition of the family *Gregarinidae* in future in the light of these findings, therefore, can not be ruled out.

ACKNOWLEDGEMENTS

The authors are grateful to Prof. G. K. Manna, D. Sc., F.N.A., Head of the Department of Zoology, University of Kalyani, for his interest in this work and for providing laboratory facilities, Grateful acknowledgement is made to the Director, Zoological Survey of India, Calcutta, for identification of the insects and the University Grants Commission, New Delhi, for financial assistance.

RÉSUMÉ

Le travail contient les descriptions de la morphologie et du cycle de développement des trois espéces nouvelles des grégarines (*Protozoa* : *Sporozoa*) du genre Gregarina, parasitaires des coléoptères, provenant de Kalyani (Bengal ouest) aux Indes. Ce son notamment: (1) *Gregarina crescentica* sp. n. de l'*Amblyrrhinus* sp., (2) *G. alcidesti* sp. n. de l'*Alcides* sp. nr. *leopardus* 01, (3) *G. spraguei* sp. n. d'un coléoptère non-identifié appartenant à la famille *Curculionidae* sous-famille *Brachyderinae*. Les données sont inclues concernant l'intensité de l'apparition saisonniaire de ces grégarines, le pourcentage de l'infection, ainsi que les informations sur les holotypes.

REFERENCES

Amoji S. D. and Rodgi S. S. 1976: Two new species of Cephaline Gregarines in the ear Wig, *Forficula ambigua* Burr. Riv. Parassitol., 37, 43–56.

Chakravarty M. 1959: Systematic position of some genera and classification of the suborder *Cephalina* Délage and Herouard. Proc. Zool. Soc., 12, 71–81.

Dufour L. 1828: Note sur le gregarine nouveau genre de ver qui vit en tropeau dans les intestins de divers insectes.Ann. Sci. Nat., 13, 366–368.

Geus A. 1969: Die *Gregarinida*. Die Tierwelt Deutschlands, 57, 1–608.

Grassé P. P. 1953: Traite de Zoologie, 1, Masson et Cie, Paris.

Haldar D. P. and Kundu T. K. 1977: Observations on the Cephaline Gregarine, *Gregarina cylindrosa* n. sp., from *Supella supellectilium*, *Blattidae*, found in India. Vestn. Česk. Spol. Zool., 41, 248–252.

Kamm M. 1922: Studies on gregarines. II. Synopsis of the polycistid gregarines of the world, excluding those from the *Myriapoda*, *Orthoptera* and *Coleoptera*. Ill. Biol. Monogr., 7, 1–104.

Kudo R. R. 1966: Protozoology. Charles C. Thomas, Illinois.

Watson M. E. 1916: Studies on Gregarines. Ill. Biol. Monogr., 2, 211–468.

Received on 7 August 1977

EXPLANATION OF PLATE I

1–3: *Gregarina crescentica* sp. n.

1: Second intracellular stage from a section. × 650
2: A sporadin from a smear. × 250
3: Sporadins in association from a smear. × 68

4–6: *Gregarina alcidesii* sp. n.

4: Second intracellular stage from a section. × 666
5: A trophozoite from a smear, stained with mercury-bromophenol blue. × 133.
6: A trophozoite from a smear, stained with pyronin-methyl green technique. × 300

7–9: *Gregarina spraguei* sp. n.

7: Third intracellular stage from a section. × 700
8: A sporadin from a smear. × 212
9: Sporadins in syzygy from a smear. × 220

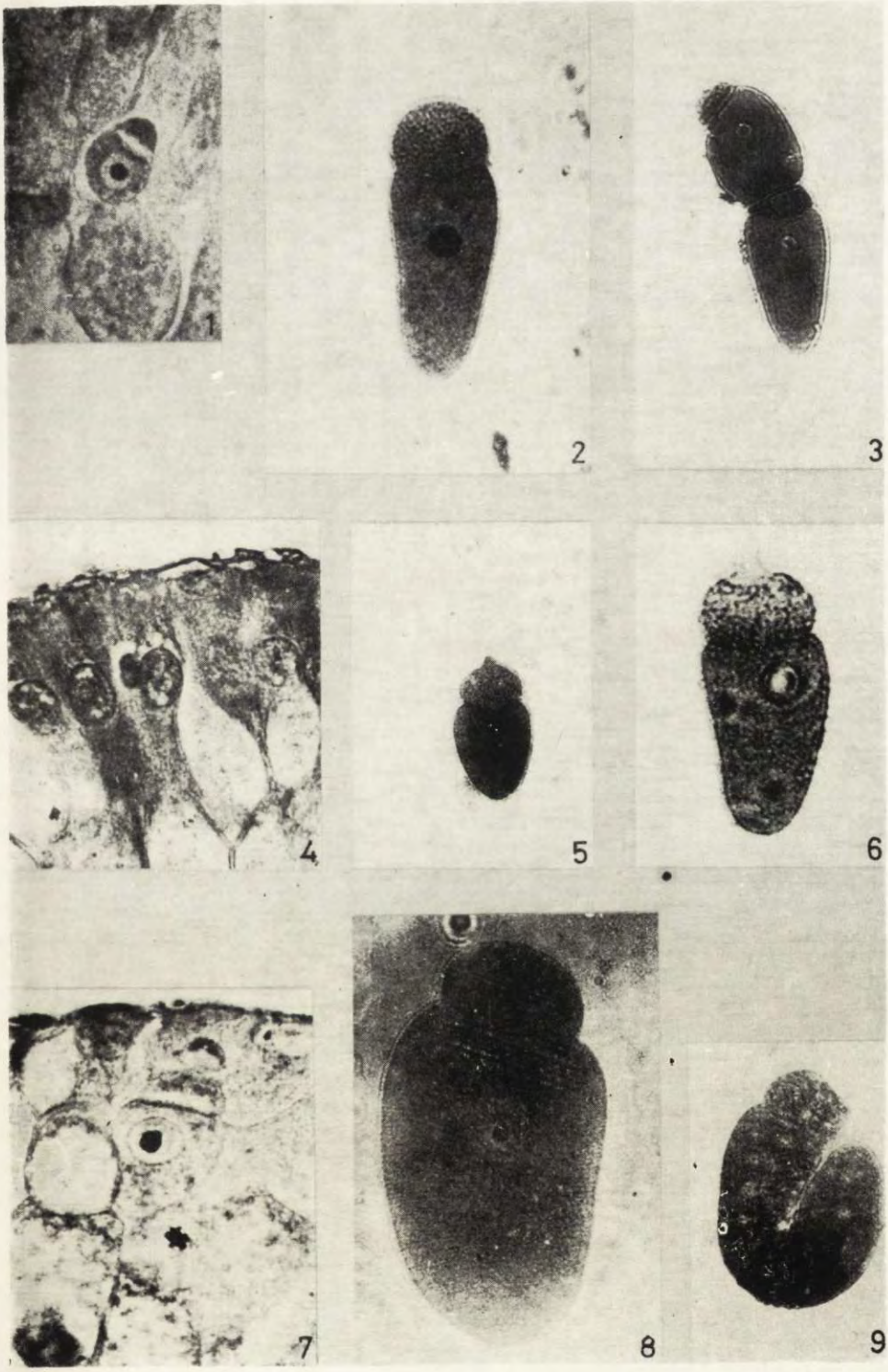

D. P. Haldar et N. Chakraborty auctores phot.

ACTA PROTOZOOLOGICA
VOL. 17 (No. 2) WARSZAWA, 30 VI 1978 pp. 247–253

Department of Zoology, Karnatak Science College, Dharwar 580 001, Karnataka State, India and Department of Microbiology, Post-Graduate Centre, Gulbarga 585 105, Karnataka, State, India

M. J. DEVDHAR and S. D. AMOJI

Sciadiophora gagrellula sp. n. from the Phalangid Arthropod, *Gagrellula saddlana* (Roewer)

Synopsis. Sciadiophora gagrellula sp. n., (*Sporozoa, Eugregarinida*) from the intestine and caeca of the arachnid, *Gagrellula saddlana* (Roewer) collected from the Dharwar and Kumta areas is described in details with special reference to its morphology, life-history stages and taxonomic position.

The genus *Sciadiophora* Labbé, 1899 (Family — *Actinocephalidae* Léger emend Grassé, Subfamily *Actinocephalinae* Labbé) is characterized by "(i) epimerite a large flattened centrally indented papilla with a crenulate periphery and (ii) protomerite with numerous backwardly directed leaf-like processes arranged vertically; each pointed sharply at its extremity" (Kamm 1922). The literature available reveals that only five species of gregarines from phalangid hosts are described under the genus *Sciadiophora* Labbé. These are *S. fissidens, S. caudata, S. goronowitschi, S. phalangii* and *S. claviformis.* The first two gregarines were described earlier by Rössler (1882) under the genera *Actinocephalus* Stein and *Stylorhynchus* Stein respectively. *S. goronowitschi* was also placed in the genus *Actinocephalus* by Johansen (1894). *S. phalangii* was reported by Léger (1897) and was assigned to his newly created genus *Lycosella.* Later, Labbé (1899) after thorough study on the type species (*Lycosella phalangii*) described by Léger (1897) emended the genus and created a new genus *Sciadiophora.* Likewise, he transferred three of the then four known species to this new genus. Subsequently, Minchin (1903), Wellmer (1911), Ellis (1913) and Geus (1969) redescribed *Sciadiophora phalangii.* Kamm (1922) shited *Stylorhynchus caudata* (Rössler) to the genus *Sciadiophora* Labbé. Recently, Ormières and Budoin (1973) have described *S. claviformis.*

The present report deals with the description of a new eugregarine parasite of the genus *Sciadiophora* Labbé infecting the intestine and the intestinal caeca of the phalangid arthropod, *Gagrellula saddlana* collected from Dharwar and Kumta areas.

Materials and Methods

The arachnids were collected from the various fields near Dharwar and Kumta areas of the Karnataka State, India. The smears of the intestine and caeca were prepared and stained following the method described by Devdhar and Amoji (1976). Cysts were isolated from the intestinal and caecal contents and subjected to a moist chamber for their further development. Observations of live specimens of the gregarine in its various developmental stages were also made using intra vital stains such as Lugol's iodine, neutral red and safranin in dilute concentrations.

Permanent preparations of the smear slides were screened at different magnifications and measurements were made by a calibrated ocular micrometer. India ink figures illustrated in this report were made with the help of camera lucida. Photomicrographs were also made of some of the important stages in the life-cycle of the gregarine.

Results

Sciadiophora gagrellula sp. n.

Sporonts

Sporonts are solitary, elongate, cylindrical and taper gradually posteriorly (Fig. 1 *1*, Pl. I 10). They measure from 2000 μm to 3000 μm in length and 115 μm to 204 μm in breadth. The average ratio of the protomerite length (PL) to total length (TL) of the body is 1 : 19.7 and the protomerite width (PW) to the deutomerite width (DW) is 1 : 1.05. The epimerite is absent in sporont stage.

The protomerite is broadly dome-shaped, widest at or a little above the septum and tapers anteriorly to a flattened end (Fig. 1 *1*, *8*, Pl. I 12). It has a stumpy stalk connecting with the deutomerite. In many cases, when this stalk is hidden by the surrounding lamellae, the protomerite appears sessile. Nine lamellar plates run backwards from the apex of the protomerite. All these plates are uniformly thickened and bifurcated into two short cones at their terminal ends (Fig. 1 *8*). When viewed from the above the protomerite looks like an ephyra larva of *Aurelia* (Fig. 1 *9*, Pl. I 14). From the sides the protomerite resembles an open umbrella (Fig. 1 *8*). The ectoplasm is thin and is not clearly distinguishable from

the endoplasm. The latter is composed of fine granules and is dense except at the tips of the lamellar plates. On an average the protomerite measures 140 μm in length and 175 μm in breadth. The septum separating the protomerite from the deutomerite is convex.

The deutomerite is elongated and cylindrical. It is broader in the anterior half and gently tapers posteriorly. The thin ectoplasm is not clearly distinguishable from the endoplasm as in the protomerite. The endoplasm is finely granular and dense, more so at the anterior end in mature sporonts. On account of the dense nature of the endoplasm, the

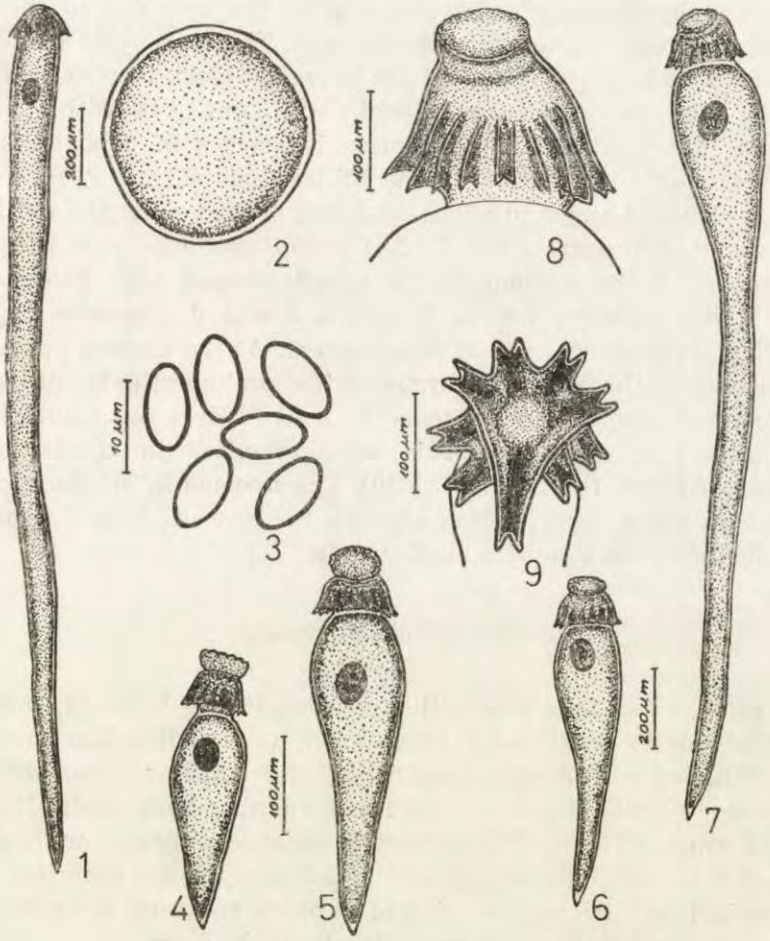

Fig. 1. 1–9. *Sciadiophora gagrellula* sp. n. are camera lucida drawings. *1* — Solitary sporont, *2* — Gametocysts in which the line of association is obscured, *3* — Biconical sporocysts, 4–7 — Cephalonts in successive stages of development, *8* — Anterior region of Fig. 7 englarged to show the lamellar plates on the protomerite and the shape of the epimerite, *9* — Protomerite as seen from the above showing the bifurcations of the lamellar plates

nucleus is not often visible. The endoplasm appears greyish in colour in the living condition. The nucleus is oval and is often situated in the anterior half of the deutomerite. On an average the nucleus measures 81 μm in length and 47 μm in breadth. The nuclear membrane is distinct and a single karyosome is seen in the clear nucleoplasm.

Life-cycle stages: The mature sporont lie sluggish in the intestinal caeca and soon oppose each other to form a gametocyst. Though the cephalonts and trophozoites are common in the intestine and intestinal caeca, the cysts were rarely met with. The cysts are large and spherical in shape (Fig. 1 *2*). They measure about 500 μm in diameter. In a moist chamber, cysts sporulated after the 10th day of their development by simple rupture of the cyst wall. The sporocysts are biconical, rounded off at both the ends and are brownish-black in colour (Figs. 1 *3*, Pl. I 15). They measure 8 μm in length and 5 μm in breadth.

Figure 1 4–7 illustrate four successive stages of cephalonts in the development of the parasite. In the initial stage (Fig. 1 *4*, Pl. I 13) the cephalont is short and stout. The epimerite is saucer-shaped and its margin is surrated uniformly (Pl. I 12, 13). The protomerite is roughly dome-shaped and the deutomerite is spindle-shaped with the maximum width in the shoulder region. Figure 1 *5* and *6* represent cephalonts in a slightly advanced stage of development. As the growth proceeds, the deutomerite of the parasite surpasses the protomerite in size and the latter becomes dome-shaped. Figure 1 7 and Pl. I *11* represent cephalont which is as long as sporont. This cephalont after the epimerite is lost becomes a sporont (Fig. 1 *1*, Pl. I 10). The nucleus in all these development stages has a fixed position which is far forward from the mid-point of the deutomerite along its median axis.

Taxonomic Summary

Diagnosis: Sporonts solitary, elongate, cylindrical, measuring 2000–3000 μm in length and 115–204 μm in breadth. The protomerite is dome-shaped with a corona consisting of 9 lamellar plates with bifurcated ends; starting from the apex and running backwards. Nucleus is oval (81 μm × 47 μm). The epimerite is saucer-shaped with surrated edge and it persists only in cephalonts. Gametocysts are spherical (500 μm in diameter) and dehisce by simple rupture releasing biconical sporocysts with rounded off ends measuring 8 μm × 5 μm.

Host: *Gagrellula saddlana* (Roewer).
Site of infection: Intestine and intestinal caeca.
Host locality: Dharwar and Kumta, Karnataka State, India.

Table 1

Comparative characters of species of *Sciadiophora*

Comparative characters	*S. fissidens* (Rössler) Labbé	*S. caudata* (Rossler) Kamm	*S. goronowitschi* (Johansen) Labbé	*S. phalangii* (Léger) Labbé	*S. claviformis* (Ormières and Baudoin)	*S. gagrellula* sp. n.
Body Shape and size	Elongate, 2000–3000 μm long	Elongate, 2000–2500 μm long with a 2000–3000 μm long tail process	Elongate, 5000 μm long	Elongate, widest at shoulder, tapering to a very long slender extremity, 2500 μm long	Elongate, 800 μm long	Elongate, cylindrical and tapers posteriorly gradually, 2000–3000 μm long
Epimerite	?	?	?	Large, sessile papilla, indented in middle and crenulate on periphery	?	Sessile, saucer-shaped with a surrated margin
Protomerite	Broadly dome-shaped and corona consisting of 12 lamellar plates each bifurcated at their end	Dome-shaped, situated on a short neck and corona consisting of 12 digitiform processes in two rows	?	Broadly conical with 15–16 lamellar plates terminating in sharp hooks	Boadly dome-shaped, at the mid region is folded inside all over its circumference like mashroom	Dome-shaped set on a stumpy stalk. 9 lamellar plates with bifurcated ends
Nucleus	Small and spherical	Spherical	Oval or ellipsoidal	Ovoidal or spherical with many karyosomes	Ovoidal	Oval, 81 μm × 47 μm, with a karyosomes
PL : TL Ratio	1 :8	?	?	1 : 12	?	1 : 19.7
PW : DW Ratio	1 : 1.5	?	?	1.3 : 1	?	1 : 1.05
Cysts	?	?	?	Spherical, 500 μm in diameter	?	Spherical, 500 μm in diameter
Sporocysts	?	?	?	Bionical with rounded off at poles, 9 μm × 5 μm	?	Bionical with both poles rounded off, 8 μm × 5 μm
Host(s)	*Phalangidae* sp.	*Phalangidae* sp.	*Phalangium opilio*	*Phalangium crossum P. cornutum* and *Opillio grossipes*	*Mitopus* sp.	*Gagrellula saddlana*
Locality	Germany	Germany	Soviet Union	France, Poland and Soviet Union	France	India

Repository: The holotype specimens (sporonts, cephalonts and sporocysts) of this species, stained (iron haematoxylin) and mounted (euperol) on glass slides, are deposited in British Museum (Natural History), Cromwell Road, London S. W. 7.

Discussion

The structural features of this gregarine such as the large sessile saucer-shaped epimerite, dehiscence of the gametocysts by simple rupture and the biconical sporocysts, indicate that it belongs to the family *Actinocephalidae* Léger emend Grassé.

The complex epimerite and the biconical sporocysts indicate the position of this gregarine in subfamily *Actinocephalinae* Labbé.

Of the five known species of *Sciadiophora*, the present species resembles, in some respects, *S. phalangii* (Léger) Labbé and *S. fissidens* (Rössler) Labbé. Nevertheless, it differs from them in the following points:

(1) The PL : TL ratio of the new form is 1 : 19.7, while the same in *S. phalangii* is 1 : 12 and in *S. fissidens* is 1 : 8.

(2) The number of lamellar plates in one row is 9; in *S. phalangii* there are 16 and in *S. fissidens* there are about 12 (with 12 spines in an upper row).

(3) The lamellar plates in *S. phalangii* are not bifurcated at their tips, while in the present form they are bifurcated.

(4) The deutomerite of *S. phalangii* is widest at the shoulder and tapers to a very long, slender, acuminate extremity. The deutomerite of the new gregarine is elongate, cylindrical and slightly wider in the anterior third and gradually tapers posteriorly. The deutomerite of *S. fissidens* is widest at the shoulder and tapers gently backwards. Its posterior third, however, is very much narrowed to form a sort of posterior tail and thus differs from the presently described species.

Table 1 of comparative characters makes clear that the species under investigation differs radically from all the known species of *Sciadiophora*. It is therefore considered new and is named *Sciadiophora gagrellula* sp. n., after the generic name of its host, *Gagrellula saddlana* (Roewer). This appears to be the first record of a *Sciadiophora* species from a phalangid host in India.

RÉSUMÉ

Sciadiophora gagrellula sp. n. (*Sporozoa, Eugregarinida*) de l'intestin et du caecum de l'araignée *Gagrellula saddlana* (Roever), provenant de régions Dharwar et Kumta, est décrite sous les aspects détaillés de sa morphologie, de son cycle de développement, et de sa position taxonomique.

REFERENCES

Devdhar M. J. and Amoji S. D. 1976: *Stylocephalus* gregarines found in tenebrionid beetle, *Gonocephalum hoffmannseggi* Stev. Arch. Protistenk., 118, (in press).

Ellis M. M. 1913: A descriptive list of the cephaline gregarines of the New World. Trans. Am. Microsc. Soc., 32, 259–296.

Geus A. 1969: Die Gregarinida der Land und susswasserbewohnenden Arthropoden Mitteleuropas. Die Tierw. Deutsch , 57, 1–608.

Johansen H. 1894: *Actinocephalus goronowitschi,* eine anscheinend neue Gregarineform. Zool. Anz., 17, 140–145.

Kamm M. W. 1922: Studies on Gregarines II. Synopsis of the polycystid gregarines of the World, excluding those from the *Myriapoda, Orthoptera* and *Coleoptera.* Ill. Biol. Monogr., 7, 1–104.

Labbé A. 1899: *Sporozoa,* in Das Tierreich. Friedlander, Berlin Lief, 5, 1–180.

Léger L. 1897: Nouvelles recherches sur les polycystides parasites des arthropodes terrestres. Ann. Fac. Sci. Mars., 6, 54.

Minchin E. A. 1903: Introduction and *Protozoa,* In: A Treatise on Zoology, (ed. Lankester E. R.), 1, London, 451.

Ormières R. and Baudoin J. 1973: Eugregarines parasites d'Opilions de la region de Besse. Ann. Stn. Biol. Besse-en-Chandesse, 7, 199–208.

Rössler R. 1882: Beiträge zur Anatomie der Phalangiden. Z. Wiss. Zool., 36, 671–702.

Wellmer L. 1911: Sporozoen ostprüssischer Arthropoden. Schr. Physik-Oken. Gessellsch. Konigsb., 52, 103–164.

Received on 21 October 1977

EXPLANATIONS OF PLATE I

Sciadiophora gagrellula sp. n.

10: Photomicrographs of sporont. × 75
11: Cephalont in advanced stage of development. × 85
12: Anterior region of Fig. 11 enlarge. × 270
13: Youngest cephalont. × 330
14: Protomerite as seen from the above. × 285
15: Sporocysts in clumps. × 1600

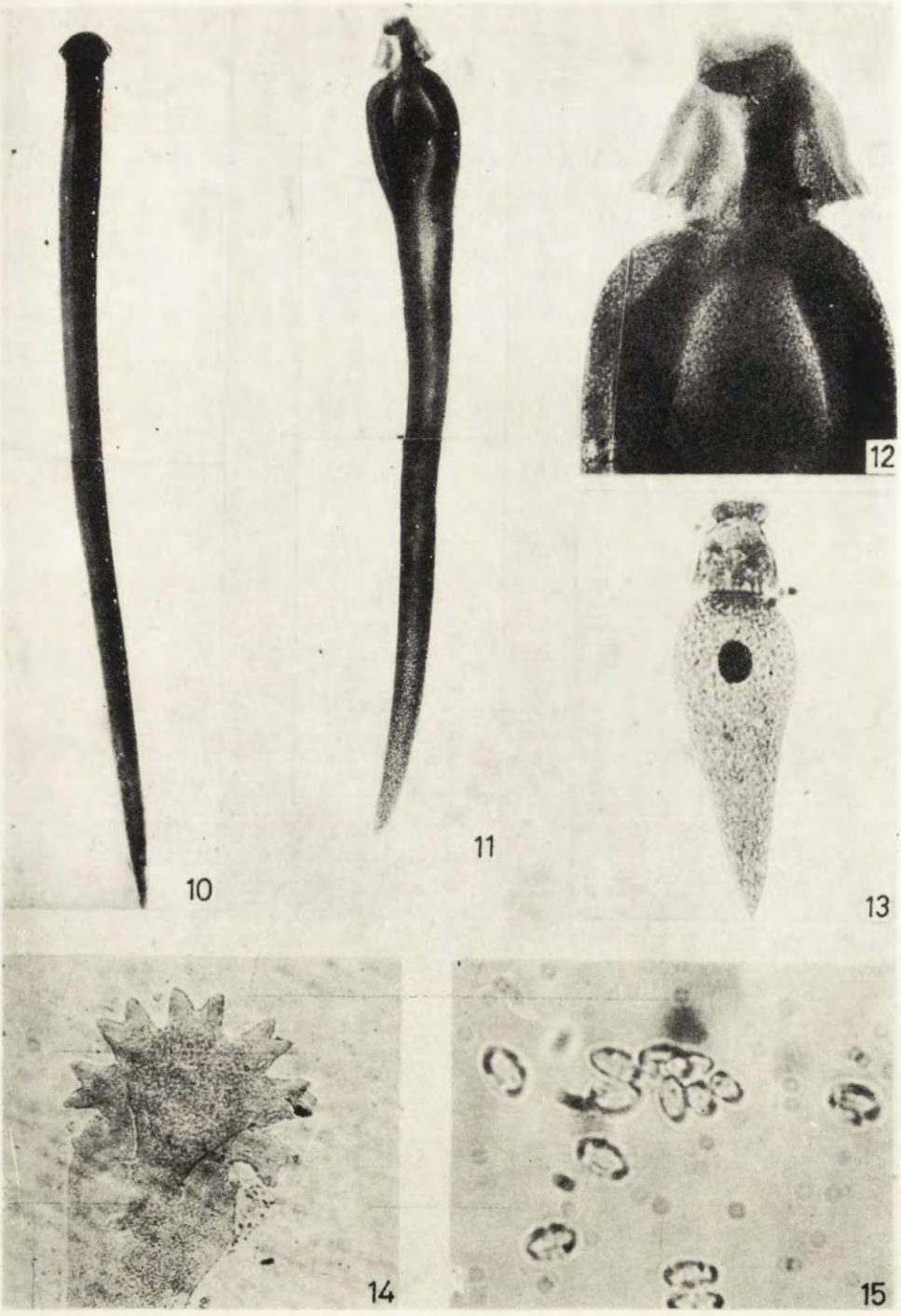

M. J. Devdhar et S. D. Amoji auctores phot.

ACTA PROTOZOOLOGICA
VOL. 17 (No. 2) WARSZAWA, 30 VI 1978 pp. 255–259

Department of Insect Pathology, Institute of Entomology, Czechoslovak Academy of Sciences, Flemingovo 2, 166-09 Prague 6, Czechoslovakia

Z. ŽIŽKA

Fine Structure of the Neogregarine *Farinocystis tribolii* Weiser, 1953. Free Gametocytes

Synopsis. A description is given of the fine structure of gametocytes of the neogregarine *Farinocystis tribolii* Weiser and their developmental stages in the fat body of larvae of *Tribolium castaneum*. Joined gametocytes form spherical syzygies which harbour differentiating gametes.

The fine structure of free gametocytes is similar to the inner structure of merozoites except for differences in the number and size of mitochondria and dark bodies.

The fine structure of schizonts and merozoites (asexual stages of the life cycle of the neogregarine *Farinocystis tribolii* Weiser) has been described in an earlier paper. The present report is concerned with the part of sexual phase of development of this parasite, i.e., with the fine structure of free gametocytes.

Material and Methods

The neogregarine *Farinocystis tribolii* Weiser, 1953 was maintained in infected larvae of *Tribolium castaneum* Hbst. which were grown on a mixture of maize and corn flour at 25°C in darkness.

For light microscopy, parasites were inspected in 0.6% (w/v) NaCl, in paraffin sections and moist smears stained with Heidenhain's haematoxylin.

For electron microscopy, small pieces of fat body of *T. castaneum* larvae were used. These were fixed with glutaraldehyde and/or OsO_4 in Millonig's (1962), Sabatini's et al. (1962) and Caulfield's (1957) phosphate-, cacodylate- or veronal buffers. The fixed material was rinsed in buffer-solutions, embedded in 2% agar Difco, dehydrated in an alcohol series (30%, 50%, 70%, 96%, 100%), placed in pure acetone or propylenoxyde and saturated with Vestopal W or Durcupan ACM. The material was polymerized in gelatine capsules at 70°C and cut with a glass knife on the ultramicrotome Tesla BS 490. The sections were stained with lead

citrate according to Reynolds's (1963) method or in a saturated solution of uranyl acetate and examined in the electron microscopes Tesla BS 613 and Tesla BS 242.

Results

After the division of the schizont we observed the appearance of spindle-shaped, pregamogonial, uninucleate merozoites (8.2–9.5 × 2.5–4 μm) with slightly ovoid nuclei. These develop in young motile gametocytes which, by head-to-head-conjunction, produce spherical syzygies.

The fine structure of a young gametocyte (Pl. I 1) is similar to that of a macronucleate merozoite except for bodily measurements (11 × × 3.3 μm). Morphologic differentiation into males and females was not observed.

The surface of the gametocyte is lined with a bilayered membrane (breath 15 nm). After lead staining we distinguished a thicker, darker, inner layer and a thinner, lighter outer layer, which is analogous to our finding in merozoite. Typical of the anterior extremity is a conoidal complex composed of a conoid, a polar ring with microtubules identical to those described for the merozoite. In the front part of the body of the young gametocyte were also found rhoptries and micronemes. Differences were found mainly in the number and size of mitochondria and dark bodies. Numerous mitochondria, generally of the vesicular type, were spherical to moderately ovoid (0.7 × 0.4 μm). Dark bodies, however, although analogous in maximum size to those of merozoites differed in that their number in the individual gametocytes was bigger than that in the merozoites.

The nucleus of the gametocyte is spherical to feebly ovoid (Pl. I 2), of either an analogous or slightly bigger size (2.3 μm) to that of the nucleus of macronucleate merozoites (2–2.2 μm). The karyolymph harbours more granules and mainly the granular component of its nucleolus is particularly well-visible. The nuclear membrane (17–30 nm in width) possesses pores of a simple structure with a diameter of roughly 100 nm.

Discussion

The fine structure of a young gametocyte of neogregarines is similar to that of merozoites from which they develop. This fact indicates that no remarkable structural changes occur in gamogony. Differences were found mainly in the number and size of mitochondria and dark bodies (Žižka 1971). Although sexual dimorphism is common by coccidians

(Scholtyseck et al. 1971, Scholtyseck et al. 1972, Žižka 1969) this was not observed in an electron microscopic examination of studied gametocytes and in those of other neogregarines (Canning and Sinden 1974, Canning and Sinden 1975, Liu et al. 1974, Vávra and McLaughlin 1970, Žižka 1971). Members of the genus *Schizocystis* (Léger 1900) may be exception, but the fine structure of this genus has not been studied as yet.

Eugregarines differ from neogregarines in that the epicyte on their surface forms regular folds without organelles except for micropores (Beams et al. 1959, Korn and Rühl 1972, Vávra 1969, Vivier 1968). A polysaccharide "cell-coat" consisting of a dark, filamentous layer, was found on their surface (Schrével 1972). No such "coat" has ever been found in gametocytes of *F. tribolii*.

The continuity of the cytoplasmic membrane of various sporozoans is disturbed in one or several sites of the micropores (Vávra and McLaughlin 1970, Vivier 1968, Vivier and Schrével 1964, Žižka 1969). Vávra and McLaughlin (1970) reported the presence of micropores for *Mattesia grandis*, but I failed to discern similar organelles in *F. tribolii*.

As in neogregarines, a polar arrangement of the body with a clear differentiation of its anterior and posterior portion has been recorded for both archi- and eugregarines. On the other hand, archi- and eugregarines differ from neogregarines in a concentric differentiation of their cytoplasm into an ectoplasm which does not contain amylopectin, and an endoplasm which is occupied mainly by amylopectin (Korn and Rühl 1972, Sanders and Poinar 1973, Schrével 1970, Vávra 1969, Vivier 1968, Vivier and Schrével 1966). In studies on reserve substances, Vivier et al. (1969) found minute granules of amylopectin (150 × 300 nm) in gregarines; these are five times as big in coccidians (Scholtyseck et al 1971, Žižka 1969). Although amylopectin granules are present only exceptionally in the neogregarine *F. tribolii*, lipoid bodies are quite common for it.

One more problem referred to in the discussion will have to be clarified, namely the absence of distinct micropores in the superficial cytoplasmic membrane of the gametocyte of *F. tribolii*. Vávra and McLaughlin (1970) reported the presence of micropores in the cytoplasmic membrane of *M. grandis*, which we did not observe in our material.

ACKNOWLEDGEMENTS

I wish to thank Dz. J. Weiser for his careful revision of my paper and his valuable comments.

РЕЗЮМЕ

Было показано тонкое строение гаметоцитов неогрегарины *Farinocystis tribolii* Weiser при помощи электронного микроскопа и развитие этих стадий в жировом теле личинок жуков *Tribolium castaneum* Hbst. Соединеные гаметоциты формируют шаровидные сизигии с гаметами.

Ультраструктура свсбодных гаметоцитов похсжа на тонкое строение мерозоитов. Дифференции можно найти только в числе и в размеров митохондрий и темных тел.

REFERENCES

Beams H. N., Tahmisian T. N., Devine R. K. and Anderson E. 1959: Studies on fine structure of gregarine parasitic in the gut of the grasshopper *Melanoplus differentialis*. J. Protozool., 6, 136–146.

Canning E. U. and Sinden R. E. 1974: The fine structure of *Farinocystis tribolii* (*Schizogregarinida*) in *Palembus ocularis*. 3rd Int. Congr. Parasitol. Münich, 1974. Facta Publications H. Egermann, Vienna, 1, 35–36.

Canning E. U. and Sinden R. E. 1975: Development of *Farinocystis triboli* Weiser (*Sporozoa, Neogregarinida*) in *Palembus ocularis* Casey (*Coleoptera, Tenebrionidae*) and some observations on its fine structure. Protistologica, 11, 221–231.

Caulfield J. B. 1957: Effects of varying the vehicle of OsO_4 in tissue fixation. J. Biophys. Biochem., 3, 827.

Korn H. and Rühl H. 1972: Vergleich der Ultrastrukturen von *Gregarina polymorpha* und *Gregarina cuneata* (*Sporozoa, Gregarinida*). Z. Parasitenkd., 39, 285–301.

Léger L. 1900: Sur un nouveau sporozaire des larves de Diptères (*Schizocystis*). C. r. Acad. Sci. Paris, 131, 722–724.

Liu H. J., McFarlane R. P. and Pengelly D. H. 1974: *Mattesia bombi* n. sp. (*Neogregarinida, Ophryocystidae*) a parasite of *Bombus* (*Hymenoptera: Apidae*). J. Invertebr. Pathol., 23, 225–231.

Millonig G. 1962: Further observations on a phosphate buffer for osmium solutions in fixation. 5th Internat. Congr. Elec. Micr. Philodelphia, 2, 1–8.

Reynolds E. S. 1963: The use of lead citrate at hight pH as an electronopaque stain in electron microscopy. J. Cell Biol., 17, 208–212.

Sabatini D. D., Bensch K. G. and Barnett R. J. 1962: New means of fixation for electron microscopy and histochemistry. Anat. Rec., 142, 274.

Sanders R. D. and Poinar G. O. J. 1973: Fine structure and life cycle of *Lankesteria clarki* sp. n. (*Sporozoa, Eugregarinida*) parasitic in the mosquito *Aedes sierrensis* (Ludlow). J. Protozool., 20, 594–602.

Scholtyseck E., Mehlhorn H. and Hammond D. M. 1971: Fine structure of macrogametes and oocysts of *Coccidia* and related organisms. Z. Parasitenkd., 37, 1–43.

Scholtyseck E., Mehlhorn H. and Hammond D. M. 1972: Electron microscope studies of microgametogenesis in *Coccidia* and related groups. Z. Parasitenkd., 38, 95–131.

Schrével J. 1970: Recherches ultrastructurales et cytochimiques sur le paraglycogène, réserve glucidique des Grégarines et Coccidies. J. Microsc., 9, 593–610.

Schrével J. 1971: Observations biologiques et ultrastructurales sur la systématique des *Grégarinomorphes*. J. Protozool., 18, 448–470.

Schrével J. 1972: Les polysaccharides associés a la surface cellulaire des grégarines (Protozoaires parasites). I. Ultrastructure et cytochimie. J. Microsc., 15, 21–40.

Vávra J. 1969: *Lankesteria barretti* n. sp. (*Eugregarinida, Diplocystidae*), a para-

site of the mosquito *Aedes triseriatus* (Say) and a review of the genus *Lankesteria mingazzini*. J. Protozool., 16, 546–570.

Vávra J. and McLaughlin R. E. 1970: The fine structure of some developmental stage of *Mattesia grandis* McLaughlin (*Sporozoa, Neogregarinida*), a parasite of the bool weevil *Anthonomus grandis* Boheman. J. Protozool., 17, 483–496.

Vivier E. 1968: L'organisation ultrastructurale corticale de la grégarine *Lecudina pellucida*; ses rapports avec l'alimentation et la locomotion. J. Protozool., 15, 230–246.

Vivier E. and Petitprez A. 1968: Les ultrastructures superficielles et leur évolution au niveau de la jonction chez des comtes de *Diplauxis hatti*, Grégarine parasite de *Perinereis cultrifera*. C. r. Acad. Sci. Paris, 266, 491–493.

Vivier E., Petitprez A. and Prensier G. 1969: Recherches sur les polysaccharides et les lipides chez la Grégarines *Diplauxis hatti*; observations en microscopie électronique. C. r. Acad. Sci. Paris, 268, 1197–1199.

Vivier E. and Schrével J. 1964: Etude, au microscope électronique, d'une grégarine du genre *Selenidium*, parasite de *Sabellaria alveolata* L. J. Microsc., 3, 651–670.

Vivier E. and Schrével J. 1966: Les ultrastructures cytoplasmigues de *Selenidium hollandei*, n. sp. Grégarine parasite de *Sabellaria alveolata* L. J. Microsc., 5, 213–228.

Žižka Z. 1969: The fine structure of the macrogametocytes of *Adelina tribolii* Bhatia, 1937 (*Eucoccidia, Telosporea*) from the fat body of the beetle *Tribolium castaneum* Hbst. J. Protozool., 16, 111–120.

Žižka Z. 1971: The fine structure of some developmental stages of *Farinocystis tribolii* Weiser (*Sporozoa, Neogregarinida*) from the fat body of the beetle *Tribolium castaneum* Hbst. J. Protozool., 17 Suppl.), 46.

Received on 15 August 1977

EXPLANATIONS OF PLATE I

Farinocystis tribolii Weiser.
Explanation of both figures: cm – superficial cytoplasmic membrane, db – dark bodies, er – endoplasmic reticulum, mi – mitochondria, mn – nuclear membrane, nl – nucleolus, nu – nucleus, ri – ribosomes, rp – rhoptries
1: Motile young gametocyte. × 29 800
2: Nucleus (nu) with a large nucleolus (nl) in a mature gametocyte. × 49 000

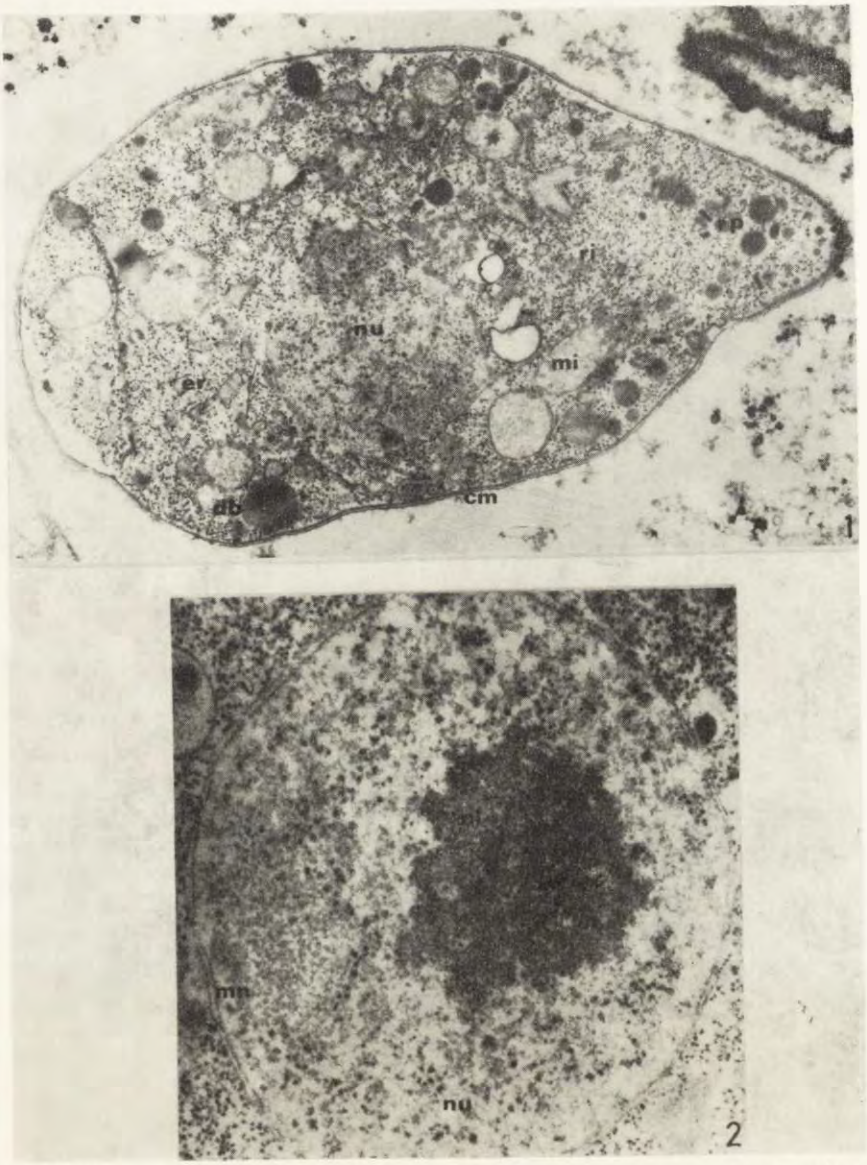

Z. Žižka auctor phot.

ACTA PROTOZOOLOGICA
VOL. 17 (No. 2) WARSZAWA, 30 VI 1978 pp. 261–270

Institut de Zoologie, boul. Rouski 1, 1000 Sofia, Bulgarie

VASSIL GOLEMANSKY

Description de neuf nouvelles espèces de Coccidies (*Coccidia: Eimeriidae*), parasites de Micromammifères en Bulgarie

Synopsis. Dans le présent travail sont décrites neuf nouvelles espèces de coccidies, parasites de micromammifères en Bulgarie, à savoir: *Eimeria flexilis* sp. n. (Hôte: *Talpa europaea* L.), *E. ropotamae* sp. n. (Hôte: *Crocidura leucodon leucodon* Hermann), *E. neomyi* sp. n. (Hôte: *Neomys anomalus* Cabrera and *N. fodiens* Penant), *E. micromydis* sp. n. (Hôte: *Micromys minutus* Pall.), *E. guentheri* sp. n. (Hôte: *Microtus guentheri* Danford et Alston), *E. arcutinae* sp. n. (Hôte: *Apodemus sylvaticus* L., *A. flavicollis* Milch. and *A. agrarius* Pall.), *Isospora tapae* sp. n. (Hôte: *Talpa europaea* L.), *I. neomyi* sp. n. (Hôte: *Neomys anomalus* Cabrera and *N. fodiens* Penant) and *I. aranea* sp. n. (Hôte: *Sorex araneus* L.).

Dans le cadre d'une étude sur les Coccidies des Mammifères en Bulgarie, effectuée de 1971 à 1977, nous avons eu la possibilité de recolter et examiner un grand nombre des Micromamifères, appartenant aux ordres *Insectivora* et *Rodentia*. Parmi les Coccidies déjà connues de la littérature parasitologique nous avons également trouvé quelques espèces inconnues jusqu'à présent, dont la description est présentée ci-dessous.

Malgré leur large répartition géographique et leur importance économique et sanitaire très grande, les Micromammifères ne sont pas encore suffisemment étudiés de point de vue parasitologique. Les derniers travaux de Ryšavy (1954), Pellerdy (1954, 1965), Svanbaev (1956), Černa et Daniel (1956), Levine et al. (1959), Saxe et al. (1960), Černa (1962), Moussaev et Veissov (1961), Moussaev (1967), Ernst et al. (1971) etc. et surtout les monographies spéciales de Levine et Ivens (1965), Moussaev et Veissov (1963) et Pellerdy (1965, 1974) ont montré que les Micromammifères sont invasés par une faune coccidienne assez riche, mais encore très peu connue de point de vue taxonomique et biologique.

Aux fins de la présente étude est recoltée une partie du gros intestin des animaux attrappés, conservée en 3% de $K_2Cr_2O_7$. Au laboratoire est utilisée la méthode de Fülleborn. La sporulation est poursuivie au t° — 23°C ± 2°C.

Eimeria flexilis sp. n. Fig. 1 a, b

Description: Les oocystes sont ronds et incolores. L'enveloppe unique est mince et flexible: elle est souvent déformée par les spores volumineuses, qui remplissent complètement l'oocyste. Micropyle n'est pas observé. Le diamètre varie de 20 à 24 μm. Il manque dans les oocystes mûrs un reliquat cytoplasmique ou des granules polaires.

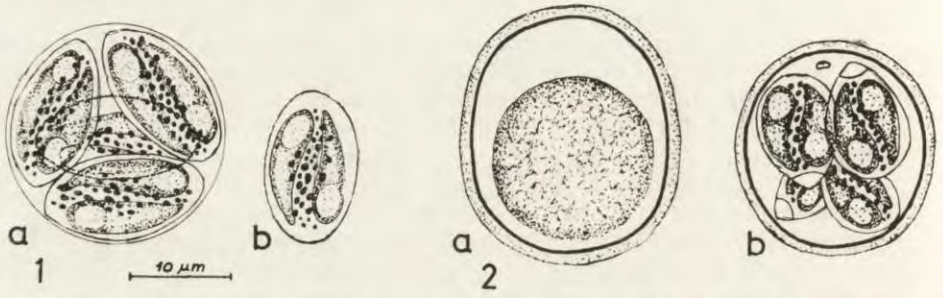

Fig. 1–2. 1 — *Eimeria flexilis* sp. n. a — oocyste mûr; b — spore, 2 — *Eimeria ropotamae* sp. n. a — oocyste frais; b — oocyste mûr

Les spores sont ovales et relativement grandes, sans pôle marqué. Leurs dimensions varient en longueur de 14 à 16 μm. et en largeur de 10 à 12.5 μm. Entre les deux sporosoïtes, dont les dimensions moyennes sont 12 × 4.5 μm, sont observées les granules diffusées du reliquat cytoplasmique.

Hôte: *Talpa europaea* L.
Localité: Montagne de Strandja, Sud-est de Bulgarie.
Extension de l'invasion: Oocystes trouvés dans 1 sur 10 exemplaires étudiés.

Discussion: *E. flexilis* sp. n. diffère de *E. goussevi* Yakimoff, décrite du même hôte de la partie européenne de l'USSR, par la forme ronde des oocystes et la présence d'une enveloppe unique et flexible, le plus souvent déformée par les spores ovales.

Eimeria ropotamae sp. n. Fig. 2 a, b

Description: Les oocystes sont ovales ou subsphériques et incolores. La surface de l'exocyste est légèrement sculptée. Les dimensions des oocystes sont: 22–25 × 20–22.5 μm.

Les spores sont ovales et rétrécies à l'un des pôles, où un bouchon hyalin est observé. Stieda body typique n'est pas observé. Les dimensions moyennes des spores sont: 12 × 7.6 μm. Un reliquat cytoplasmique existe uniquement dans les spores et est difusé entre les sporozoïtes. Parfois dans les oocystes se forment 1 à 2 granules polaires.

La sporulation dure environs 56 heures à t° = 24°C.

Hôte: *Crocidura leucodon leucodon* Hermann.
Localité: Les environs de la rivière de Ropotamo, Sud-est de Bulgarie.
Extension de l'invasion: Oocystes trouvés dans 1 sur 2 exemplaires étudiés.

Discussion: Jusqu'à présent sont décrites quatre espèce du genre *Eimeria*, parasites des Insectivores du genre *Crocidura*: *E. firestonei* Bray et *E. milleri* Bray, de *Crocidura schweitzeri* de Liberia (Bray 1958), *E. corcidurae* Galli-Valerio de *Crocidura aranea* de Suisse (Galli-Valerio, 1927) et *E. leucodontis* Moussaev et Veissov de *Crocidura leucodon* de Azerbaidjan (Moussaev et Veissov 1961). *E. ropotamae* sp. n. diffère nettement de *E. firestonei*, *E. milleri* et *E. crocidurae* par les dimension plus grandes des oocystes, la forme des spores et la structure de l'exocyste. *E. ropotamae* n. sp. diffère aussi de *E. leucodontis* par la forme des oocystes, la présence de l'exocyste sculpté et l'existence de 1 à 2 granules polaires dans les oocystes sporulés. Les spores de *E. ropotamae* n. sp. comparées aux spores de l'espèce *E. leucodontis*, illustrées par Moussaev et Veissov, (1961), sont plus allongées et rétrécies à l'un des poles.

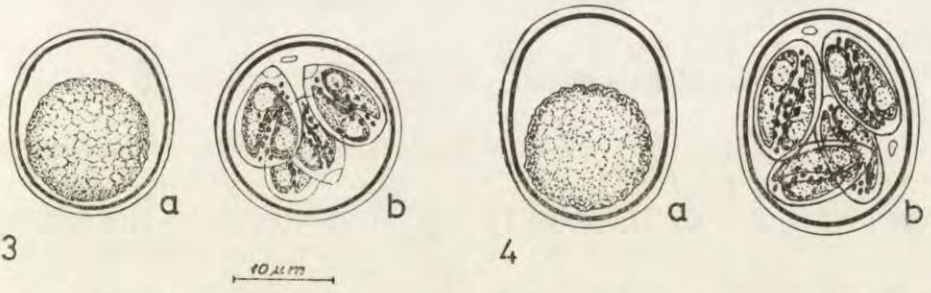

Fig. 3–4. 3 — *Eimeria neomyi* sp. n. a — oocyste frais; b — oocyste mûr, 4 — *Eimeria micromydis* sp. n. a — oocyste frais; b — oocyste mûr

Eimeria neomyi sp. n. Fig. 3 a, b

Eimeria komareki Černa et Daniel. Černa, 1961: 181–183 (pro parte).

Description: Les oocystes sont ronds ou subsphérique et incolores. L'enveloppe est lisse et double. Le diamètre des oocystes ronds varie de 18 à 20 μm. Les oocystes subsphériques ont les dimensions

suivantes: 16–20.5 × 15.2 × 17.8 μm. Les dimensions moyennes sont: 18.3 × 16.5 μm.

Les spores sont allongées rétrécies à l'un des pôles. Stieda body tipique absent, mais à sa place est observé un bouchon hyalin. Il manque chez les oocystes sporulés un reliquat cytoplasmique, mais prèsque toujours est constaté un granule polaire. Le reliquat cytoplasmique dans les spores est difusé entre les sporozoïtes. Les dimensions moyennes des spores sont: 12 × 7.5 μm.

Hôte: *Neomys anomalus* Cabrera.
Localité: Montagne de Rila, Sud-ouest de Bulgarie.
Extensité de l'invasion: Oocystes trouvés dans 5 sur 8 exemplaires examinés.
Autres hôtes: *Neomys fodiens.* Pennant.
Localité: Montagne de Rila, Sud-ouest de Bulgarie.
Extensité de l'invasion: Dans 1 sur 3 exemplaires examinés.

Discussion: Černa (1961) note pour la première fois, qu'elle a trouvé l'espèce *E. komareki* Černa et Daniel, décrite de *Sorex araneus,* également dans l'intestin de *Neomys fodiens* de Tchécoslovaquie. Plus tard Pellerdy (1965, 1974) doute que l'espèce *E. komareki* de *Sorex araneus* soit également parasite de *Neomys fodiens* et suppose que le dernier hote est invasé probablement d'une autre espèce. Les oocystes de *E. neomyi* sp. n. ont une forme subsphérique et parfois ronde, tandis que ceux de *E. komareki* sont ovales. De plus, les spores de *E. neomyi* sp. n. sont allongées et rétrécies à l'un des pôles, où un bouchon hyalin est également observé. D'après l'illustration de Černa et Daniel (1956) les spores de *E. komareki* sont ovales et sans pôle marqué.

Eimeria micromydis sp. n. Fig. 4 a, b

Description: Les oocystes sont ovales et incolores. L'enveloppe est double, environ 2 μm. Les dimensions des oocystes varient en longueur de 20 à 24 μm et en largeur de 17 à 19 μm. Il manque dans les oocystes un reliquat cytoplasmique. Après la sporulation sont observées 1 à 2 granules polaires.

Les spores sont ovales, sans Stieda body. Dimensions moyennes: 12 × 8 μm. Le reliquat cytoplasmique est difuse parmi les sporozoi'tes.

Hôte: *Micromys minutus* Pall.
Localité: La réserve de Srebarna, Nord-est de Bulagarie.
Extensité de l'invasion: L'espèce est trouvée chez 1 sur 3 exemplaires examinés.

E. *micromydis* sp. n. est la première espèce du genre *Eimeria,* décrite jusqu'à présent de *Micromys minutus* Pall.

Eimeria guentherii sp. n. Fig. 5 a, b

Description: Les oocystes sont ovales et incolores, avec une enveloppe lisse et mince (environ 1 μm). Les dimensions des oocystes varient en longueur de 19 à 23 μm et en largeur de 13 à 15.5 μm. Il manque dans les oocystes sporulés un reliquat cytoplasmique, mais sont observées de 1 à 4 granules polaires.

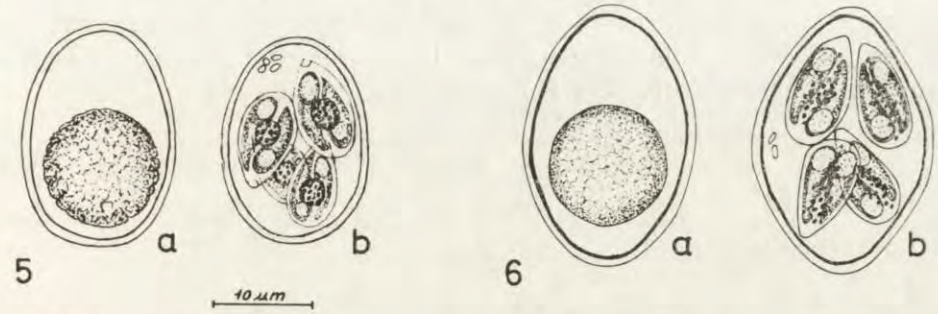

Fig. 5–6. 5 — *Eimeria guentheri* sp. n. a — oocyste frais, b — oocyste mûr. 6 — *Eimeria arkutinae* sp. n. a — oocyste frais, b — oocyste mûr

Les spores allongées et rétrécies à l'un des pôles, sont munies d'un bouchon hyalin. Dimensions moyennes: 11 × 6 μm. Le reliquat cytoplasmique dans les spores est compact, avec un diamètre de 3 à 4 μm.

Hôte: *Microtus guentheri* Danford et Alston.

Localité: Arkoutino, Sud-est de Bulgarie.

Extensité de l'invasion: L'espèce est trouvée dans 3 sur 11 exemplaires examinés.

Discussion: *E. guentheri* sp. n. est la première espèce du genre *Eimeria*, trouvée en *Microtus guentheri*. Les oocystes de la nouvelle espèce ont certaines ressemblances morphologiques avec les oocystes de *E. arvicolae* (Galli-Valerio, 1905) Reichenow, 1921 (H.: *Microtus arvalis* Pall.), *E. chudatica* Moussaev, Veissov et Alieva, 1963 (H.: *Microtus socialis* Pall.) et *E. majorici* Veissov, 1962 (H.: *Microtus majori* Thom.). *E. guentheri* sp. n. diffère des espéces citées par la forme et la structure des spores, la présence d'un reliquat cytoplasmique compact dans les spores et l'existence de plusieurs granules polaires dans les oocystes.

Eimeria arkutinae sp. n. Fig. 6 a, b

Eimeria keilini Yakimoff et Gousseff sensu Ryšavy, 1954: 131–174; Černa et Daniel, 1956: 19–23; Černa, 1962: 1–13.

[non] *Eimeria keilini* Yakimoff et Gousseff, 1938: 1–3.

Extensité de l'invasion: Dans 5 sur 127 exemplaires examinés.
Eimeria sp. Golemansky et Yankova, 1973: 17–19.

Description: Les oocystes sont ellipsoidaux, souvent asymétriques et rétrécis aux pôles, incolores ou jaune pâles. Leurs dimensions varient en longueur de 22 à 32 μm et en largeur de 15 à 21 μm. La plupart des oocystes ont des dimensions moyennes de 27 × 18 μm. L'enveloppe est double, environs 1.8 μm. Micropyle absent.

Les spores sont aussi ellipsoidales et rétrécies à l'un des pôles. Stieda body absent. Dimensions moyennes: 12 × 6.5 μm. Un reliquat cytoplasmique existe uniquement dans les spores. Dans les oocystes sporulés sont observées parfois 1 à 2 granules polaires.

Hôte: *Apodemus sylvaticus* L.
Localités: Arkoutino, Sud-est de Bulgarie; Montagne de Rila, Sud-ouest de Bulgarie.
Extensité de l'invasion: *E. arkutinae* sp. n. est trouvée dans 8 sur 126 exemplaires examinés.
Autres hôtes: (a) *Apodemus flavicollis* Milch.
Localité: Montagne de Rila, Sud-ouest de Bulgarie.
Extensité de l'invasion: Dans 5 sur 127 exemplaires examinés.
(b) *Apodemus agrarius* Pall.
Localité: La réserve de Srebarna, Nord-est de Bulgarie.
Extensité de l'invasion: Dans 1 sur 19 exemplaires examinés.

Discussion: Ryšavy (1954) signale d'avoir trouvé dans le rongeur *Apodemus sylvaticus* de Tchécoslovaquie quelques oocystes ellipsoidaux ou asymétriques, qu'il identifie comme *E. keilini* Yakimoff et Gousseff. Les dimensions des oocystes, d'après Ryšavy, varient de 24–29 × 16–20 μm. Plus tard Černa et Daniel (1956) et Černa (1962) ont aussi trouvé des oocystes pareils dans l'intestin de *A. flavicollis*, qu'ils indentifient aussi comme *E. keilini*. Les dimensions des oocystes, d'après les derniers auteurs, sont 25–28 × 16–20 μm.

L'espèce *E. keilini* est décrite par Yakimoff et Goussey (1938) de *Mus musculus* de la partie européenne de l'USSR. Les dimensions des oocystes, d'après la descripsions originale sont: 24–32 × 18–21 μm. (En moyenne: 28.8 × 19.4 μm).

Ayant en vue les resultats negativs de Pellerdy (1954) pour une infestation experimentale des rongeurs avec des oocystes des coccidies, provenant d'autres hôtes du même ordre, Levine et Ivens (1965) pensent que les oocystes trouvés par Ryšavy (1954) et Černa et Daniel (1956) ne peuvent pas etre identifiés comme *E. keilini* et les indiquent comme *Eimeria* sp. (Ryšavy 1954).

Golemansky et Yankova (1973) ont trouvé des oocystes pareilles chez *A. sylvaticus* et *A. flavicollis* de Bulgarie, qu'ils identifient également comme *Eimeria* sp.

Au cours de la présente étude nous avons eu la possibilité d'étudier un matérial plus rich, recolté de 3 espèces du genre *Apodemus* et de nous persuader, que dans ce cas il s'agit d'un nouveau taxon, parasite de tous les trois rongeurs examinés: *A. sylvaticus*, *A. flavicollis* et *A. agrarius*.

Les oocystes de *E. arkutinae* sp. n. diffèrent des oocystes de l'espèce *E. apionodes* Pellerdy, décrite de *A. flavicollis* de Hongrie par ses dimensions plus grandes, la couleur jaune pâle de l'enveloppe et la morphologie des spores. La présence des granules polaires, la couleur des oocystes, la forme et les dimensions des spores distinguent la nouvelle espèce également de l'espèce proche *E. divichinica* Moussaev et Veissov, décrite de *A. sylvaticus* de Azerbaidjan (Moussaev et Veissov 1963).

Isospora talpae sp. n. Fig. 7a, b

Description: Les oocystes sont ronds, rarement subsphériques et incolores. L'enveloppe double est relativement mince et se déforme facilement. Le cytoplasme occupe complètement les oocystes. Le dia-

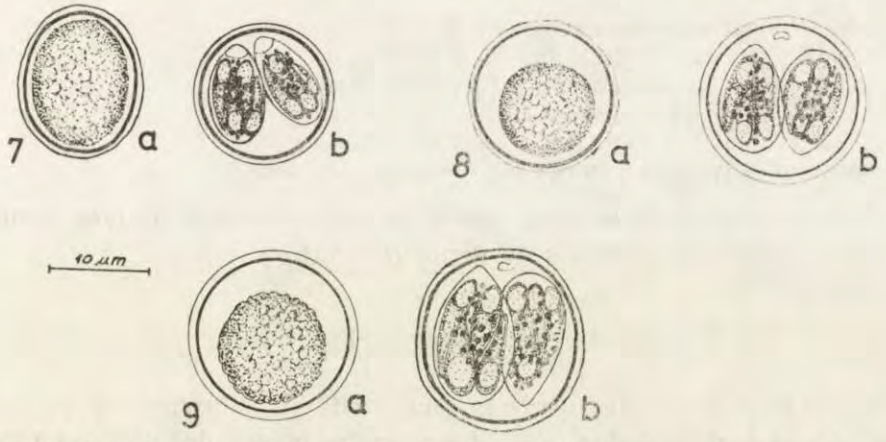

Fig. 7–9. 7 — *Isospora talpae* sp. n. a — oocyste frais, b — oocyste mûr, 8 — *Isospora neomyi* sp. n. a — oocyste, frais, b — oocyste mûr, 9 — *Isospora araneae* sp. n. a — oocyste frais, b — oocyste mûr

mètre des oocystes ronds est environ 12.5 µm. Les dimensions des oocystes subsphériques varient en longueur de 12.5 à 14 µm et en largeur de 10 à 13 µm.

Les spores sont ovales. Stieda body manque mais à l'un des pôles est observée une matière plus claire et hyaline. Les dimensions des

spores sont: 10–13 × 5.4–7.6 μm. Un reliquat cytoplasmique difusé n'est observé que dans les spores.

La sporulation des oocystes dure environs 48 à une t° = 23°C±1°C.

Hôte: *Talpa europaea* L.

Localités: Les environs de Sofia et la réserve de Srebarna, Nord-est du Bulgarie.

Extensité de l'invasion: Oocystes trouvés dans 3 sur 10 exemplaires examinés.

I. talpae sp. n. est la secule espèce du genre *Isospora*, trouvée jusqu'à présent en *Talpa europaea*.

Isospora neomyi sp. n. Fig. 8 a, b

Description: Les oocystes sont ronds et incolores. L'endocyste est foncé. Le diamètre des oocystes varie de 12 à 16 μm.

Les spores sont ovoides, sans Stieda body. Leurs dimensions varient de 8–10.6 × 5–6.5 μm. Dans les oocystes sporulés manque un reliquat cytoplasmique, mais souvent un granule palaire est observé. Le reliquat cytoplasmique dans les spores est granulé et diffusé entre les sporozoites.

Hôte: *Neomys anomalus* Cabrera.
Localité: Montagne de Rila, Sud-ouest de Bulgarie.
Extensité de l'invasion: Dans 1 sur 6 exemplaires examinés.
Autre hôte: *Neomys fodiens* Pennant.
Localité: Montagne de Rila, Sud-ouest de Bulgarie.
Extensité de l'invasion: Dans 1 sur 3 exemplaires examinés.

I. neomyi sp. n. est la seule espèce du genre *Isospora*, trouvée jusqu'à présent dans les Insectivores du genre *Neomys*.

Isospora araneae sp. n. Fig. 9a, b

Description: Les oocystes sont ronds ou subsphérique et incolores. L'endocyste est plus foncé. Le diamètre moyen des oocystes ronds est 17 μm. Les dimensions des oocystes subsphériques varient en logueur de 16 à 18.5 μm et en largeur de 15 à 18 μm. Parfois dans les oocystes sporulés existent 1 à 2 granules polaires. Le granule polaire se forme après la première division du cytoplasme.

Les spores allongées et rétrécies a l'un des pôles, avec des dimensions moyennes: 12.5 × 9.5 μm. Le reliquat cytoplasmique est difusé entre les sprozoïtes.

La sporulation dure environ 48 h à une temperature de 24°C.

Hôte: *Sorex araneus* L.
Localité: Montagne de Rila, Sud-ouest de Bulgarie.
Extensité de l'invasion: Oocystes trouvés dans 2 sur 52 exemplaires examinés.

Discussion: Golemansky et Yankova (1973) ont décrit la premiére espéce du genre *Isospora*, parasite de *Sorex araneus* — *I. soricis*. Les oocystes de *I. soricis* sont ellipsoidaux et leurs dimensions sont plus grandes: 24 × 17 μm. *I. araneae* sp. n. différe de *I. soricis* par la forme et les dimensions des spores également, qui sont allongée-ovoides chez la nouvelle espèce.

REMERCIEMENTS

Je remercie sincèrement mes collègues Doz. Dr. T. Guenov et M. M. Manassiev du Laboratoire Central d'Helminthologie (Sofia), Dr. E. Gančovsky et Mme V. Mitzeva de l'Institut de zoologie, Sofia), qui m'ont aidé pour la recolte du matériel et au cours de mes recherches.

SUMMARY

This report gives the description of nine new coccidian species of the genus *Eimeria* and *Isopsora*, found in Micromammalians from Bulgaria: *E. flexilis* sp. n. (Host: *Talpa europaea* L.), *E. ropotamae* sp. n. (Host: *Crocidura leucodon leucodon* Hermann), *E. neomyi* sp. n. (Hosts: *Neomys anomalus* Cabrera and *Neomys fodiens* Penant), *E. micromydis* sp. n. (Host: *Micromys minutus* Pall.), *E. guentheri* sp. n. (Host: *Microtus guentheri* Danford et Alston), *E. arkutinae* sp. n. (Hosts: *Apodemus sylvaticus* L., *A. flavicollis* Milch. and *A. agrarius* Pall.), *I. talpae* sp. n. (Host: *Talpa europaea* L.), *I. neomyi* sp. n. (Hosts: *Neomys anomalus* Cabrera and *N. fodiens* Penant) and *I. aranaea* sp. n. (Host: *Sorex aranus* L.). A morphometric characteristic and date concerning the sporulation time of the oocysts as well as the locality of the host, the prevalence of the parasite etc. are presented.

BIBLIOGRAPHIE

Bray R. S. 1958: On the parasitic *Protozoa* of Liberia. I. Coccidia of some small mammals. J. Protozool., 5, 81–83.
Černa Z. 1961. The development of the Coccidia *Eimeria komareki* Černa-Daniel 1956 from *Sorex araneus*. Vestn. Cesk. Spol. Zool., 25, 2, 181–183.
Černa Z. 1962: Contribution to the knowledge of Coccidia parasitic in *Muridae*. Acta Soc. Zool. Boh., 26, 1–13.
Černa Z. et Daniel M. 1956: K poznáni kokcidii volne zijcich drobnych ssavcu. Cesk. Parasitol., 3, 19–23.
Ernst I. V. Chobotar B. and Hammond D. M. 1971: The oocysts of *Eimeria vermiformis* sp. n. and *E. papilata* sp. n. (*Protozoa*: *Eimeriidae*) from the mouse *Mus musculus*. J. Protozool., 18, 2, 221–223.

Golemansky V. and Yankova P. 1973: Studies on the species composition and occurrence of *Coccidia* (*Sporozoa, Coccidia*) in some small mammals in Bulgaria. Bull. Inst. Zool. Sofia, 37, 5–31. (in bulg.).
Levine N. D., Bray R. S., Ivens V. and Gunders A. E. 1959: On the parasitic protozoa from Liberia. V. *Coccidia* of Liberian rodents. J. Protozool., 6, 215–222.
Levine N. D. and Ivens V. 1965: The coccidian parasites (*Protozoa, Sporozoa*) of rodents. Ill. Biol. Monogr., 33, Urbana, 365 pp.
Moussaev M. A. 1967: A new species of *Eimeria* from *Microtus* (*Pitymys*) *schelkovnikovi* Satunin. Izv. AN Azerb. SSR, 1, 44–46, (in russ.).
Moussaev M. A. and Veissov A. M. 1961: A new coccidian species from *Crocidura leucodon* Herm. DAN Azerb. SSR, 17, 10, 967–969. (in russ.).
Moussaev M. A. and Veissov A. M. 1963: Coccidia of *Apodemus sylvaticus* from Azerbaidjan. Izv. AN Azerb. SSR., 5, 3–14. (in russ.).
Moussaev M. A. and Veissov A. M. 1965: The *Coccidia* of rodents in USSR. AN Azerb. SSR, Baku, 154 pp. (in russ.).
Pellerdy L. 1954: Zur Kenntnis der Coccidien aus *Apodemus flavicollis*. Acta Vet. Hung., 4, 187–191.
Pellerdy L. 1965: *Coccidia* and Coccidiosis. Ed. Kiado, Budapest, 656 pp.
Pellerdy L. 1974: *Coccidia* and *Coccidiosis*. Ed. Kiado, Budapest, 959 pp.
Ryšavy B. 1954: Přispěvek k poznáné kokcidii našich i dovezených obratlovcu. Cesk. Parasitol., 1, 131–174.
Saxe L. H., Levine N. D. and Ivens V. 1960: New species of *Coccidia* from the meadow mouse *Microtus pennsylvanicus*. J. Protozool., 7, 61–63.
Svanbaev S. K. 1956: Matériaux à la faune des coccidies des mammifères sauvages de Kasahstan de l'ouest. Tr. Inst. Zool. Akad. Nauk. Kaz. SSR, 5, 180–191 (in russ.).
Yakimoff W. L. and Gousseff M. 1938: The coccidia of mice (*Mus musculus*). Parasitology, 30, 1–3.

Received on 15 September 1977

ACTA PROTOZOOLOGICA
VOL. 17 (No. 2) WARSZAWA, 30 VI 1978 pp. 271–278

Department of Entomology and Nematology, University of Florida, Gainesville, Florida 32611, USA

J. D. KNELL and G. E. ALLEN

Morphology and Ultrastructure of *Unikaryon minutum* sp. n. (*Microsporida : Protozoa*), a Parasite of the Southern Pine Beetle, *Dendroctonus frontalis* [1]

Synopsis. A new species of *Microsporida, Unikaryon minutum,* is described from the southern pine beetle, *Dendroctonus frontalis.* Spores are uninucleate and arise, in isolation, from sporonts through binary fission. The absence of a cyst, xenoma, and parasitophorous vesicle is characteristic of the microsporidium. The microsporidium infects muscle, malphigian tubule, fat body, and midgut tissue.

Weiser (1955) described the first microsporidium from a scolytid *Nosema typographi,* from the fat body of *Ips typographus.* Two additional microsporidia, *Nosema curvidens* Weiser, 1961 from *Pityokteines curvidens,* and *Pleistophora scolyti* Weiser, 1968 from *Scolytus scolytus,* were described in Czechoslovakia. Lipa (1968) transferred *P. scolyti* to the genus *Stempellia* on the basis of material collected in Poland, the Soviet Union, and the German Democratic Republic. *Nosema scolyti* Lipa, 1968 was described in mixed infections with *Stempellia scolyti* in 4 hosts, *Scolytus scolytus, S. ensifer, S. multistriatus,* and *S. pygmaeus.* Finally, Weiser (1970) described *Nosema dendroctoni* from *Dendroctonus pseudotsugae* collected in British Columbia, Canada.

During an extensive survey of major pathogens associated with the southern pine beetle (SPB), *Dendroctonus frontalis,* in the southeastern United States, the most common organisms found were the nematode *Contortylenchus brevicomi* and a minute microsporidium. A description of this microsporidium is presented in this report.

Material and Methods

Southern pine beetles used in this study were obtained from a heavily infected population in Meadville, Mississippi.

[1] Florida Agriculture Experiment Station Journal Series Number 670.

Light Microscopy

Vegetative stages of the microsporidium were detected by Giemsa stained smears. Air dried smears of larval, pupal, and adult SPB were fixed in 100% methanol for 5 min stained with 10% Giemsa (made with $NaPO_4$ buffer, pH 7.41) for 11 min and differentiated with tap water.

Heidenhain wet mounts were prepared by smearing infected adult SPB on cover slips, fixing for 6 h in aqueous Bouin's solution, and holding overnight in 70% ethanol. The smears were mordanted for 4 h in iron alum, stained overnight in aqueous Heidenhain's hematoxylin, and destained to the desired intensity.

Fresh spores were measured under phase contrast microscopy using an E. I. Cook splitting image micrometer at 1000 ×. Giemsa stained material was measured with an AO optical micrometer at 1000 ×.

Paraffin sections were prepared by cutting infected adult SPB in half and fixing overnight in aqueous Bouin's solution. Excess picric acid was removed by several successive washes in 70% ethanol, followed by dehydration in increasing concentrations of tertiary butanol. The tissue was infiltrated in Tissuemat in tertiary butanol. Sections were cut 5 μm thick and were stained with Delafield's hematoxylin and eosin.

Electron Microscopy

Southern pine beetle abdomens were cut into small (1 mm^3) pieces and fixed in 4% gluteraldehyde in 0.1 M sodium cacodylate buffer (pH 7.2) at 8°C for 24 h. The tissues were rinsed in cacodylate buffer (pH 7.2), post-fixed in 1% OsO_4, dehydrated in ethanol, infiltrated using an extended schedule (Endo, personal communication) and embedded in Spurr's low viscosity medium (Spurr 1969). Thin sections (60–90 nm) were cut on a Sorvall MT-2 ultramicrotome with a diamond knife and stained with uranyl acetate and lead citrate (Venable and Coggeshall 1965). Sections were examined and photographed with a Hitachi 125-E electron microscope at an accelerated voltage of 50 kv.

Results

Light Microscopy

Merogony cycle: The first meronts visible in Giemsa stain preparations are uninucleate cells which measure 2.2 μm in diameter and stain intensely (Fig. 1 a, b). The nucleus, which is 1.0 μm in diameter, has no definite location in the cell. Karyogamy results in binucleate meronts 3.0 μm in diameter with nuclei measuring 0.7 μm in diameter. The cytoplasm and nuclei of binucleate meronts also stain intensely with Giemsa (Fig. 1 c, d). Subsequent merogony cycles are represented by lightly staining cells (3.4 μm–4.2 μm) having 1 or 2 nuclei measuring 1.3 μm. Due to a light spot in the center, these nuclei appear as a dark ring often surrounded by a clear zone in the cytoplasm (Fig. 1 e, f, g).

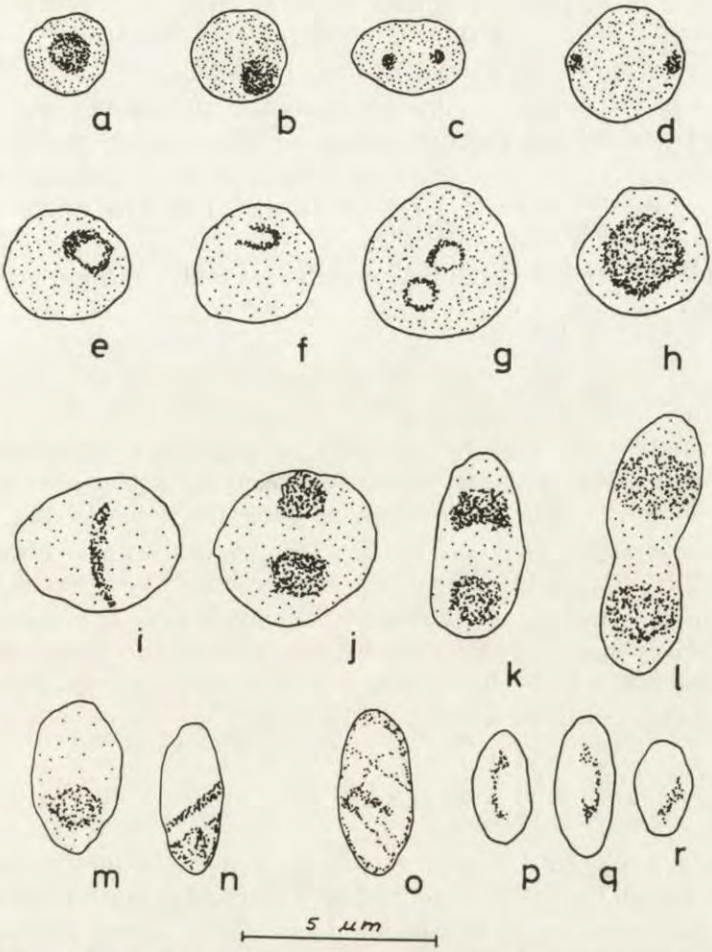

Fig. 1. Vegetative stages of *Unikaryon minutum*. a, b — uninucleate meront, c — binucleate meront, d — binucleate meront starting to divide, e, f — meront with 1 nucleus in form of ring, g — meront with 2 ring-shaped nuclei, h — uninucleate sporont, i — sporont with nucleus in process of division, j — binucleate sporont, k, l — binucleate sporont in process of division, m — early sporoblast, n — intermediate sporoblast still clearly showing nucleus, o — late sporoblast with poorly staining nucleus near middle of cell, p, q, r — mature spores. All from giemsa stained smears observed under oil immersion. 1000 ×

Sporogony sequence: The majority of sporonts are 3.2 µm in diameter and have a single nucleus in the center of the cell, which measures 2.1 µm (Fig. 1 h). Both the cytoplasm and nucleus stain faintly with Giemsa. The nuclei of a small percentage of uninucleate sporonts were seen dividing (Fig. 1 i) to form a binucleate sporont (Fig. 1 j) 4.1 µm in diameter with the nuclei averaging 1.6 µm. After karyokinesis, the cell elongates (Fig. 1 k, l) and divides to form two sporo-

blasts (Fig. 1 m). Early sporoblasts stain much like sporonts, but have a characteristic oval shape (Fig. 1 n). Mature sporoblasts have unstained areas and an irregularly stained nucleus (Fig. 1 o).

Spores: In Giemsa stain preparations, the spores are partially stained and the nucleus remains unstained (Fig. 1 p, q, r). Under phase contrast spores are refractile, are elongate-oval to cylindrical in shape, and measure 0.9 ± 0.1 μm × 2.3 ± 0.3 μm (Pl. I 2). The range of widths is 0.8 μm to 1.0 μm and lengths range from 1.9 μm to 3.3 μm. Spores were found in Malpighian tubules, muscle, fat body, and midgut.

Electron Microscopy

Small groups of spores were scattered throughout the tissue. Spore development occurs in isolation with no parasitophorous vesicle, xenoma, or cyst formation (Pl. I 3). Spore walls have a thin electron dense exospore layer (Pl. I 4, EX) and a thicker electron transparent endospore layer (Pl. I 4, EN). The polar filament coils six times in the posterior portion of the spore (Pl. I 4, F). The single, centrally-located nucleus (Pl. I 4, N) is bordered on the sides and posterior by several layers of ribosomes (Pl. I 4, R). The polaroplast is composed of tightly compressed lamellae which are oriented at a 45° angle from the longitudinal axis of the spore (Pl. I 4, P). The polar cap is attached eccentrically at the anterior end of the spore (Pl. I 4, PC).

Discussion

Canning et. al. (1974) erected the genus *Unikaryon* to include microsporidia which produce uninucleate spores by the binary fission of the sporonts. Members of this genus do not form xenoma tumors as do the microsporidia of the genus *Glugea* found in fish. Unlike the mammalian parasite *Encephalitozoon*, spores of the genus *Unikaryon* do not develop attached to the wall of a parasitophorous vesicle (Sprague and Vernick 1971). The microsporidium under consideration meets the criteria for this genus. Merogony and the sporulation sequence occur in direct contact with the host cytoplasm and there is no xenoma formation.

At present there are two described species of *Unikaryon* which are hyperparasites of trematodes. *Unikaryon piriformis* (Canning et al. 1974), the type species, infects the rediae and cercariae of *Enchinoparyphium dunni* and *Echinostoma audyi*, parasites of the snail *Lymnaea rubiginosa* in West Malaysia. The spores of *U. piriformis* are pyriform in shape and measure 3.8 × 2.7 μm. *Unikaryon legeri* (Dollfus, 1912) infects the metacercariae of *Meigymnophylus minutus* in the snail *Cardium*

edule. The oval spores of this species measure 3.03 × 1.76 μm. *Unikaryon minutum* sp. n. infects the southern pine beetle, *Dendroctonus frontalis*, and has cylindrical spores measuring 2.3 × 0.9 μm. Members of the genus *Unikaryon* are easily distinguished on the basis of spore size, shape, host, and geographic distribution.

Canning and Nicholas (1974) studied the development of *U. legeri* using electron microscopy. The spore of this species has an eccentrically located polar cap, a polar filament which coils 6 or 6.5 times, a single nucleus, and abundant ribosomal material in the region of the nucleus. *Unikaryon minutum* spores are ultrastructurally similar, having an eccentrically placed polar cap, 6 polar filament coils, and a single nucleus surrounded by ribosomes (Pl. II 4).

On the basis of morphology, *U. minutum* is similar to *Nosema dendroctoni* Weiser, 1970. *Nosema dendroctoni* infects the malpighian tubules and to a lesser extent the adjacent fat body, gut, and skeletal musculature of the douglas fir beetle, *Dendroctonus pseudotsugae*. Vegetative stages have 1 or 2 single nuclei and the uninucleate spores are oval to kidney-shaped, range from 2–3 μm wide, and average 2.7 × 1.4 μm. Although the sporulation sequence has not been described, it seems likely that *N. dendroctoni* also belongs to the genus *Unikaryon* since no mention of diplokarya is made. The average spore of *U. minutum* is slightly smaller than the published value for *N. dendroctoni*. This difference may be due to individual idiosyncrasies. Until ultrastructural studies are made on *N. dendroctoni*, the two species may be distinguished by the widely separated geographic locations and the different host species.

Unikaryon minutum may easily be separated from the various European species on the basis of morphology. Both *Nosema typographi* and *N. curvidentis* have binucleate spores and thus meet criteria erected by Cali (1970) and Ishihara (1970) for the genus *Nosema*. The spores of both species are larger than *U. minutum* (3.6–5.3 × 2–3.5 μm for *N. typographi* and 2.5–3.6 × 1.2–2 μm for *N. curvidentis*) and the infections occur only in the fat body of the host. *Stempellia scolyti* produces sporonts with 2, 4, 8, 16 or more nuclei which give rise to similar numbers of spores enclosed in a pansporoblast membrane. The meronts have 1, 2, 4 or more nuclei; and the spores, although only slightly larger than those of *U. minutum* (2.7–4 μm × 1.2–2 um), are ellipsoidal rather than cylindrical.

Nosema scolyti was described as being frequently found in mixed infections with *Stempellia scolyti* Lipa, 1968 and could correspond to the "major strain" of spores reported by Weiser (1968) for *Pleistophora scolyti*. *N. scolyti* may thus represent one form of a dimorphic micro-

sporidium such as *Vairimorpha necatrix* (Kramer, 1965), Pilley, 1976. The spore of *N. scolyti,* measuring 3.6–6.2 μm, × 1.5–.0 μm, is oval or ellipsoidal in shape and much larger than the spore of *U. minutum.*

The exact effect of *U. minutum* on its host is not known at present. The heavily infected population in Meadville, Mississippi, from which material for this study was taken, has dramatically declined in size over the past three years. Spores are rarely found in larvae and only a few dead larvae are found in trees which have yielded heavily infected adults. Attacking adults containing 3×10^5 or more spores have been recovered from newly-attacked trees. Thus, there appears to be little larval or adult mortality. This may indicate that the microsporidium causes a reduction in fecundity and longevity which would radically decrease the beetle population. Large numbers of attacking females are required to penetrate a tree successfully since smaller numbers are overcome by the flow of resin produced by the trees in response to an attack.

The mode of transmission of *U. minutum* is not clear. Sikorowski (1976, personal communication) has been able to infect late instar larvae by feeding them spores, indicating that transmission is *per os.* Southern pine beetle eggs are laid in niches cut off the main galleries by the attacking females. The larvae feed as they burrow through the cambium and have little opportunity to encounter spores. Weiser (1961) stated that *Nosema curvidentis* is spread through adult galleries by mites and staphylinids. Larvae of the host *Pityokteines curvidens* become infected only when they accidentally cross such galleries. Weiser (1976, personal communication) also suggested that if the ovaries of females are infected, spores may adhere to the surface of the eggs to be consumed by hatching larvae. In addition, females may cement eggs into niches using contaminated saliva or detritus from the galleries.

Considering the cryptic habits of the southern pine beetle, it is unlikely that *Unikaryon minutum* offers any potential other than natural control. Since populations of heavily infected beetles tend to decline, the exact effect of the microsporidium should be determined in order to produce an accurate population model.

Unikaryon minutum sp. n.

Host:	The southern pine beetle *Dendroctonus frontalis.*
Type locality:	Meadville, Mississippi.
Site of infection:	Muscle, midgut, malpighian tubules, and fat body.
Derivation of name:	The small size of the spores.
Vegetative stages:	Two types of meronts have been seen: small dark staining cells having 1 or 2 small dark staining single nuclei, and meronts, have light staining cytoplasm and 1 or 2 light

shape of a ring. Meronts principally occur in larvae and pupae.

Sporulation stages: Sporonts occur in late pupae and adults, are larger than meronts, have light staining cytoplasm and 1 or 2 light staining single nuclei. Binucleate sporonts give rise to sporoblasts through binary fission.

Spores: The spores are small, measuring 0.9 × 2.3 μm, oval to cylindrical in shape, and refractile under phase contrast. No vacuole, cyst or xenoma is formed and spores are produced in isolation without a membrane.

Type material: Holotype slides have been sent to the United States National Museum, Washington, D. C.

RÉSUMÉ

Une nouvelle espèce de Microsporidie est décrite: *Unikaryon minutum*, provenent du coléoptère *Dendroctonus frontalis*. Les spores sont mononucléaires et ils se développent des sporonts par le division binaire. Le kyste, xenoma, est absent et le vésicule parasitophore est typique pour ce microsporidien. Il infècte les muscles, les tubes de Malpighi, le corps adipeux, et les tissus de l'intestin.

REFERENCES

Cali A. 1970: Morphogenesis in the genus *Nosema*. Proc. 4th Int. Colloq. Insect Pathol., Maryland, 431–438.

Canning E. U., Lai P. F. and Lie K. J. 1974: Microsporidian parasites of trematode larvae from aquatic snails in West Malaysia. J. Protozool., 21, 19–25.

Canning E. U. and Nicholas J. P. 1974: Light and electron microscope observations on *Unikaryon legeri* (*Microsporidia, Nosematidae*), a parasite of the metacercaria of *Meigymnophallus minutus* in *Cardium edule*. J. Invertebr. Pathol., 23, 92–100.

Dollfus R. Ph. 1912: Contribution à l'étude des trématodes marins des côtes du Boulonnais. Une méta-cercaire margaritigène parasite de *Donax vittatus* Da Costa. Mém. Soc. Zool. France, 25, 85–144.

Ishihara R. 1970: Fine structure of *Nosema bombycis* (*Microsporidia, Nosematidae*), developing in the silkworm (*Bombyx mori*) — I. Bull. Coll. Agric. Vet. Med. Nihon Univ., 27, 84–91. (in Japan.).

Kramer J. P. 1965: *Nosema necatrix* sp. n. and *Thelohania diazoma* sp. n. microsporidians from armyworm *Pseudaletia unipuncta* (Haworth). J. Invertebr. Pathol., 7, 117–121.

Lipa J. J. 1968: *Stempellia scolyti* (Weiser) comb. nov. and *Nosema scolyti* sp. n. microsporidian parasites of four species of *Scolytus* (*Coleoptera*). Acta Protozool., 6, 69–86.

Pilley B. 1976: A new genus, *Vairimorpha* (*Protozoa*: *Microsporidia*), for *Nosema necatrix* Kramer 1965 — Pathogenicity and life cycles in *Spodoptera exempta* (*Lepidoptera: Noctuidae*). J. Invertebr. Pathol., 28, 177–183.

Sprague V. and Vernick S. H. 1971: The ultrastructure of *Encephalitozoon cuniculi* (*Microsporida, Nosematidae*) and its taxonomic significance. J. Protozool., 18, 560–569.

Spurr A. R. 1969: A low viscosity epoxy resin embedding medium for electron microscopy. J. Ultrastruct. Res., 26, 31–43.

Venable J. H. and Coggeshall R. 1965: A simplified lead citrate stain for use in electron microscopy. J. Cell. Biol., 25, 407–408.
Weiser J. 1955: Příspěvek k znalosti cizopasníků kůrovce *Ips typographus*, II. Vestn. Cesk. Spol. Zool., 19, 374–380.
Weiser J. 1961: A new microsporidian from the bark beetle *Piktyokteines curvidens* Germar (*Coleoptera, Scolytidae*) in Czechoslovakia. J. Insect. Path., 3, 324–329.
Weiser J. 1968: *Plistophora scolyti* sp. n. (*Protozoa, Microsporidia*), a new parasite of *Scolytus scolytus* F. (*Col., Scolytidae*). Folia Parasit. (Praha), 15, 11–14.
Weiser J. 1970: Three new pathogens of the douglas fir beetle, *Dendroctonus pseudotsugae*: *Nosema dendroctoni* sp. n., *Ophrycistis dendroctoni* sp. n. and *Chytridiopsis typographi* n. comb. J. Invertebr. Pathol., 16, 436–441.

Received on 20 June 1977

EXPLANATION OF PLATE I

2: Fresh mount of *Unikaryon minutum* spores. Phase contrast, 1000 ×
3: Electron micrograph of field of spores, 7000 ×
4: Electron micrograph of *U. minutum* spore. EX — exospore layer, EN — endospore layer, F — polar filament, N — nucleus, P — polaroplast, PC — polar cap, R — ribosomes. 20,000 ×

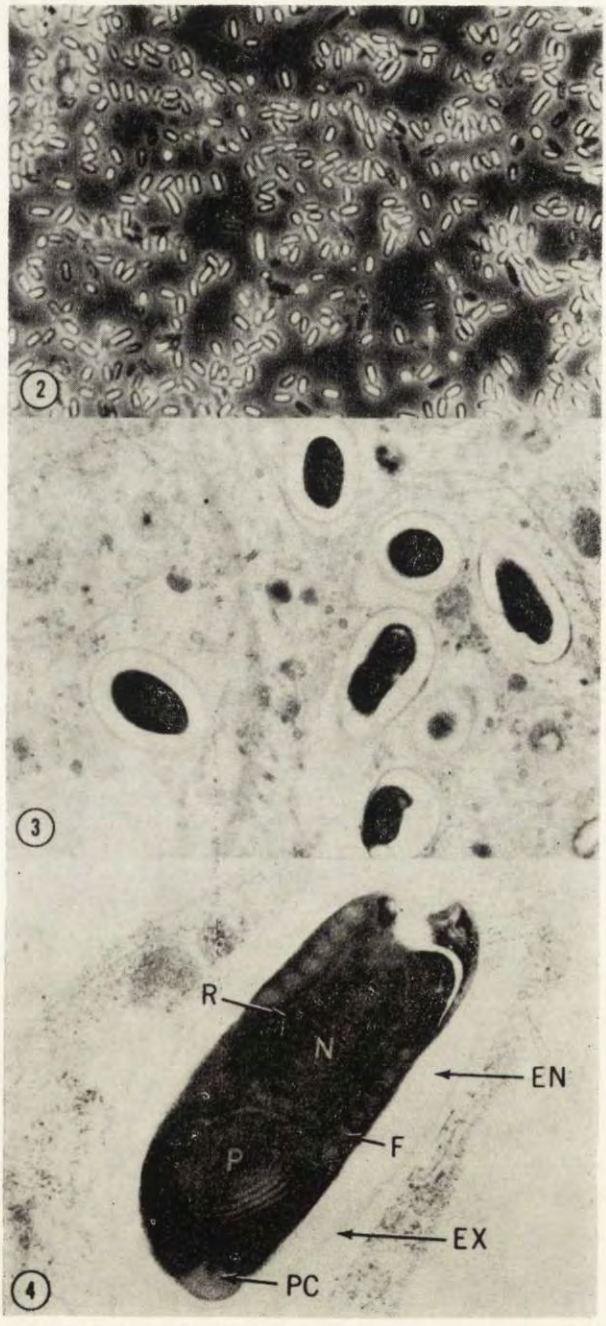

J. D. Knell et G. E. Allen auctores phot.

ACTA PROTOZOOLOGICA
VOL. 17 (No. 2) WARSZAWA, 30 VI 1978 pp. 279–283

Department of Zoology, Andhra University, Waltair 530003, India

C. KALAVATI and C. C. NARASIMHAMURTI

A New Microsporidian Parasite, *Toxoglugea tillargi* sp. n. from an Odonate, *Tholymis tillarga* [1]

Synopsis. The morphology and life history of a new microsporidian parasite, *Toxoglugea tillargi* sp. n. from an odonate, *Tholymis tillarga* is described. The parasite is host specific.

While examining the odonate larvae occurring in a stream near the dairy farm at Visakhapatnam (Andhra Pradesh, India) we came across a microsporidian parasite belonging to the genus *Toxoglugea* Léger and Hesse, 1924 infecting the oenocytes of *Tholymis tillarga* Hagen. The

Table 1

List of microsporidians described from Odonate hosts

Parasite and Author	Host	Locality	Description
Nosema aeschnae	*Aeschaena grandis* L. (Fat body)	Canada	Spores oval, 5.9–7.4×3.4–4.6 μm. Length of polar filament 80 μm
Gurleya aeschnae	*Aeschaena grandis* L. (Oenocytes on the surface of the fat body of nymphs)	Canada	Spores ovoid or pyriform 5.5–6.6×3.0–4.1. Schizonts round with granulated cytoplasm with 2-many nuclei. Pansporoblasts oval, 12.9–14.4×8.5–10.4 μm with 4 spores
Stempellia calopterygiae (Weiser) Weiser, 1951	*Calopteryx virgo* and *Calopteryx* sp. (Larval fat body)	Czechoslovakia and Yugoslavia	Spores oval and are of 2 sizes. Microspores 3.9×1.7 μm; Macrospores 5.0–6.0×3.0–3.5 μm. Plasmodia with 4 and 8 nuclei. Occasionally bigger plasmodia with irregular number of nuclei are also seen
Toxoglugea tillargi sp. n.	*Tholymis tillarga* (Oenocytes present on the surface of the larval gut)	India	Spore kidney- or bean-shaped. Spores of 2 sizes. Microspores 3.5–4.0×1.8–2.0; Macrospores 4.8–5.4×1.8–2.0. Pansporoblasts 5.0–5.4×5.4–6.2 μm. 8 spores

[1] Abstract of the paper presented at the I National Congress of Parasitology held in Baroda (India) from 24th Feb–27th Feb., 1977.

larvae of another odonate, *Tramea limbata* also occur in the same locality but they did not show any infection with the microsporidian parasite.

A perusal of the available literature showed that three microsporidians, *Nosema aeschnae* (Fantham et al., 1941, Weiser, 1958) and *Gurleya aeschnae* (Fantham et al., 1941) form *Aeschena grandis L.* and *Stempellia aeschnae* Weiser, 1951 from *Calopteryx virgo* and *C.* sp. two of which are from Canada and one from Czechoslovakia have so far been reported from Odonate hosts (Table 1). For reasons mentioned below the present form is described as a new species and the name *Toxoglugea tillargi* sp. n. after the host has been proposed.

Material and Methods

Odonate larvae occur in large numbers underneath the *Hydrilla* plants in the stream near the dairy farm at Visakhapatnam. They were collected during the period August–October in 1975 and 1976. They were maintained in the laboratory in glass vials (Temp. 28–30°C). The larvae remained alive for a week with daily chage of water. Heavily infected larvae could be distinguished externally but to obtain earlier stages of development of the parasite all the larvae had to be dissected and examined under a compound microscope.

Observations on the fresh material were made by using a light microscope and dark-ground illumination. Smears were air-dried, fixed in methyl alcohol and stained with Giemsa. Smears were also fixed in Schaudinn's fluid and stained with iron haematoxylin or according to PAS technique. Initial hydrolysis in 1 N HCl at 60°C for 10 min prior to staining with Giemsa or iron haematoxylin gave better results. Material fixed in alcoholic Bouin's fluid was sectioned at 8 μm thickness and stained with iron haematoxylin. Various conventional methods were used for the release of the polar filaments.

Observations

Toxoglugea tillargi sp. n. (Fig. 1 1–13)

Host: *Tholymis tillarga* Hagen
Locality: Stream near Dairy farm, Viskhapatnam (Andhra Pradesh, India).
Site of infection: Oenocytes in the body cavity.

The material for the present study was collected during the mansoon period. August–October during 1975 and 1976. The larvae occur in large numbers but the percentage infection was low (1%). Heavily infected larvae have a yellowish brown colour and have an enlarged abdomen (Fig. 2 *15*). The haemocoel is filled with numerous pansporoblasts. In light infections the parasites are found within the oenocytes. The infected host cells are hypertrophied and the host cell nucleus is pushed to a side. In a heavily infected cell the spores are seen surrounded by a thick layer

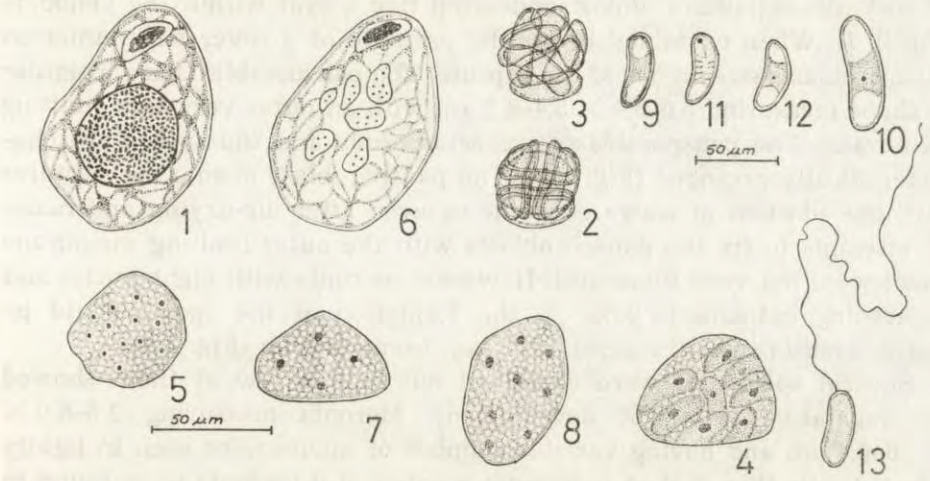

Fig. 1. *1* — Oenocyte showing spores: Note that the host cell nucleus is pushed to a side, *2* — A fresh pansporoblast, *3* — A pansporoblast stained with Giemsa, *4* — A sporent showing 8 fully formed daughter cells, *5* — A meront showing 13 nuclei, *6* — A oenocuyte with meronts, *7, 8* — Sporogonial plasmodia, *9* — A fresh spore, *10* — A macrospore, *11* — Spore stained according to PAS technique: Note the polar cap and polar filament, *12* — A spore stained with Giemsa, *13* — A spore with extruded polar filament

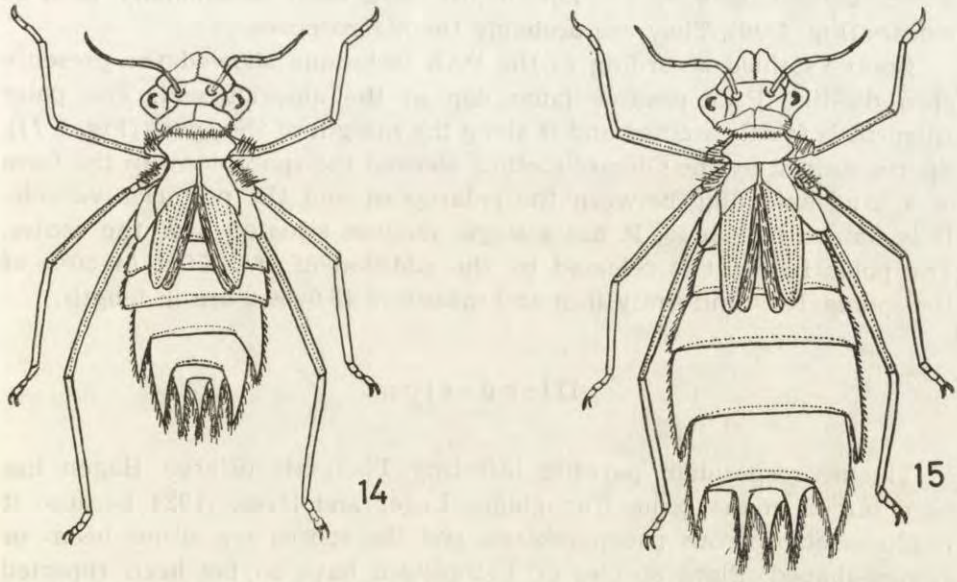

Fig. 2. *14* — An uninfected larva of *Tholymis tillarga*, *15* — An infected larva. Note enlarged abdomen

of host cell cytoplasm almost appearing like a cyst within the oenocyte (Fig. 1 *1*). When examined under the pressure of a cover slip numerous pansporoblasts stream out of the capsule. The pansporoblasts are irregular in shape measuring 5.0–5.4 × 5.4–6.2 μm with an outer very thin limiting membrane. The pansporoblasts are octosporous and the spores are characteristically arranged (Fig. 1 *2*). The pansporoblast membrane ruptures with the addition of water or saline or even after air-drying and hence all attempts to fix the pansporoblasts with the outer limiting membrane intact were not very successful. However, sporonts with eight nuclei and undergoing cytokinesis prior to the formation of the spores could be clearly seen in smears stained with iron haematoxylin (Fig. 1 *4*).

Several specimens were examined but only a few of them showed the vegatative stages of development. Meronts measuring 2.8–6.0 × × 1.6–5.4 μm and having variable number of nuclei were seen in lightly infected cells (Fig. 1 *5*). A maximum number of 6 meronts were found in a single oenocyte (Fig. 1 *6*). Sporogonial plasmodia measuring 3.6–5.0 × × 4.2–6.0 μm and containing 4–8 nuclei were seen in smears stained with Giemsa. The cytoplasm is hyaline and the nuclei are deeply stained and there are no inclusions (Fig. 1 *7*, *8*).

Spores in the fresh condition are kidney or bean-shaped. They measure 3.5–4.0 × 1.0–1.6 μm. The spore wall is refractive and thick. A polaroplast at the anterior end and a vacuole at the posterior end are seen clearly in haematoxylin stained preparations (Fig. 1 *9*). Abnormal spores measuring 4.8–5.4 × 1.8–2.0 μm have been occasionally seen in smears (Fig. 1 *10*). They are probably the macrospores.

Spores stained according to the PAS technique showed the presence of a dot-like PAS positive polar cap at the anterior end. The polar filament is faintly stained and is along the margin of the spore (Fig. 1 *11*). Spores stained by the Giemsa method showed the sporoplasm in the form of a band extending between the polaroplast and the posterior vacuole. It is stained pale blue. It has a single nucleus situated near the centre. The polar filament is released by the addition of 1% KOH in 50% of the spores. It is uniformly thin and measures 45.0–50.0 μm in length.

Discussion

The microsporidian parasite infecting *Tholymis tillarga* Hagen has been placed in the genus Toxoglugea Léger and Hesse, 1924 because it produces octosporous pansporoblasts and the spores are either bean- or kidney-shaped. Eight species of *Toxoglugea* have so far been reported from Insects (Four from *Diptera*, three from *Hemiptera* and one from

Plecoptera) but in none of them have all the stages in the life-history been described. As stated by Sprague (1974) this is a poorly defined genus and he retained it in the family *Cougourellidae* where it was originally placed by Poisson (1953) although its affinities are not very clear. This is the first report of a microsporidian parasite belonging to the genus *Toxoglugea* from an odonate host. It does not agree in all its features with any of the species of *Toxoglugea* so far described from insect hosts. Hence it is described as a new species for which the name *Toxoglugea tillargi* sp. n. after the host has been proposed.

ACKNOWLEDGMENTS

Our thanks are due to Prof. K. Hanumantha Rao, Head of the Department of Zoology for the facilities provided to carry out this work.

RÉSUMÉ

La morphologie et le cycle d'evolutions sont decrites d'une espece nouvelle de microsporidie *Toxoglugea tillargi* sp. n. de l'Odonate, *Tholymis tillarga*. Le parasite est specifique par rapport a l'hote.

REFERENCES

Fantham H. B., Porter A. and Richardson L. R. 1941: Some microsporidia found in certain fishes and insects of eastern Canada. Parasitology, 33, 186–208.

Léger L. and Hesse E. 1924: Microsporidies nouvelles Parasites des animaux d'eau douce. II. Microsporidies bacteriformes et essai de systematique du groupe. Trav. Lab. Hydrobiol. Pisc. Univ. Grenoble. 14.

Poisson R. 1953: Order des Microsporidies In: Traite de Zoology. (ed. P. P. Grasse) Masson et Cie, Paris, pp. 1042–1070.

Sprague V. 1974: Classification and phylogeny of the *Microsporidia*. Publ. University of Maryland; Chesapeake Biol. Lab. Maryland. 1–63.

Weiser J. 1951: Studie o microsporidiích z larev hmyzu hašich Vod. II. Česk. Parasitol., 3, 193–202.

Weiser J. 1958: Unterlagen der Taxonomie der Microsporidien. Trans. First Intern. Congr. Insect. Pathol. Biol. Control., Prague, 277–285.

Received on 24 September 1977

ACTA PROTOZOOLOGICA
VOL. 17 (No. 2) WARSZAWA, 30 VI 1978 pp. 285–301

Department of Biology, Nencki Institute of Experimental Biology, Pasteura 3, 02-093 Warszawa, Poland

Julita BĄKOWSKA and Maria JERKA-DZIADOSZ

Ultrastructural Analysis of the Infraciliature of the Oral Apparatus in *Paraurostyla weissei* (*Hypotricha*)

Synopsis. The oral ciliature of *Paraurostyla weissei* comprises adoral membranelles: frontal and ventral and preoral membranelles: outer and inner ones. All adoral membranelles (AZMs) consist of four rows of basal bodies. The frontal and ventral AZM membranelles differ in respect of their spatial orientation and the distribution of basal bodies within ciliary rows. The outer preoral membranelle consists of 4–5 rows of cilia. The inner preoral membranelle possesses only one row of basal bodies which proximal ends are directed toward the ventral side of the cell. The connections between kinetosomes within membranelles and between membranelles are described as well as the microfilamentous and microtubular systems integrating the oral apparatus.

The oral apparatus of *Hypotrichida* is a complex system of ciliary aggregates forming membranelles. The general topographic and structural features of the oral ciliatures are similar in most hypotrichous ciliates. Differences in disposition and structure support their division into adoral and preoral ones. The ventral adoral membranelles surround the left side of the cytostome and peristomal groove whereas the frontal membranelles are situated alongside the anterior margin of the cell. The structure of the ventral membranelles has been carefully described in only few species: *Gastrostyla steini* by Grim (1972), in *Oxytricha fallax* by Grimes (1972) and *Stylonychia mytilus* by de Puytorac et al. (1976). There are no data concerning the ultrastructure of the frontal membranelles.

Two preoral membranelles surround the oral groove on the right side. Among hypotrichs the outer preoral membranelle show much greater structural variability than the adoral membranelles. It can be formed by only one kinetosomal row (as in *O. fallax* Grimes, 1972) or by several (four rows in *G. steini* Grim, 1972) ciliary rows. The inner preoral membranelles in all so far studied hypotrichs consist of only one

Supported by grant MR II. 1.3.6.

longitudinal row of ciliated kinetosomes. There are very few data concerning the structure of the inner preoral membranelle, those available are not complete.

Basic features of the oral ciliature in *Paraurostyla weissei* have been described previously (Jerka-Dziadosz 1965, Jerka-Dziadosz and Frankel 1969). This study has been undertaken in order to analyse the ultrastructure of the oral apparatus and is meant as a base for further study on the regulation of the size of the oral apparatus and changes in the ultrastructure after experimental miniaturization of cells.

A preliminary report of this study has been published elsewhere (Bąkowska and Jerka-Dziadosz 1977).

Material and Methods

Cells used in observations were a clone of *Paraurostyla weissei* line Z-6 isolated after total conjugation. They were kept in sterile Pringsheim solution and fed on green algae *Chlorogonium* grown on earth medium after Heckmann (1963).

Observations were performed on interphasal cells as well as on miniaturized by starvation or repetitive operations. Operations were performed by hand using a glas microneedle. For light microscopy cells were stained with Protargol after Jerka-Dziadosz and Frankel (1969). For electron miscrosopy the ciliates were fixed in the mixture of 2% glutaraldehyde (1V) and 2% osmium tetroxide (2V) buffered with 0,05 M cacodylate buffer with pH = 7.2. Cells were fixed for 1 h in 0°C and then dehydrated. Single cells were oriented flat and embeded in Epon 812. Sections were stained with uranyl acetate for one hour and for several dozen seconds with lead citrate. Sections were examined with electron microscope JEM 100B. For scanning electron microscopy ciliates were fixed in the mixture of saturated mercuric chloride and 2% aqueous solution of osmic acid (1 : 1). Next they were washed in water, dehydrated and dried with the method of Small and Marschalek (1969) and Ruffalo (1974) and observed in the scanning electron microscope JSM-S1.

Results

The Anatomy of the Oral Apparatus

The oral apparatus of *Paraurostyla weissei* consists of a buccal cavity surrounded by ciliary membranelles and subpellicular system of microtubular fibers which integrates all elements of the oral ciliature (Bąkowska and Jerka-Dziadosz 1977). The adoral zone of membranelles (AZM) begins in the oral groove on its left side and runs anteriad alongside the left side of the ventral surface. In the anterior part

of the cell AZM shifts toward dorsal side and returns to the ventral side on the right anterior margin. The two parts of AZM differing with respect of their structure and orientation are called respectively: the antero-dorsal part as "frontal" and the buccal part as "ventral". Both parts of the AZM are sometimes called "collar" and "lapel" (Yocum 1918, Hammersmith 1976) respectively.

The two types of membranelles are characterized by different orientation against the long axis of the cell (Pl. I 1, II 3, 4). The ventral membranelles are perpendicular to this axis, and only the distal ventral membranelles change a bit this orientation. Membranelles of the part of the frontal membranelles which are situated on the dorsal side of the cell are parallel to the long axis. The right part of the frontal membranelles are again perpendicular but rotated about 180° against the ventral membranelles. In well fed ciliates the number of AZM membranelles is about 64 (Jerka-Dziadosz 1976). The ventral membranelles in the middle of the zone are the longest. The shortest are those on the right frontal part. Membranelles among each other are separated by cytoplasmic folds (Pl. I 2, III 9).

The right side of the peristome is bordered by two ciliary membranelles: the outer preoral membranelle (Pl. I 1, 2) and inner preoral membranelle (Pl. II 5). They are separated by a cytoplasmic fold. A similar fold is situated on the right side of the outer membranelle (Pl. I 2).

The oral ciliature is accompanied by a system of microtubular fibers (Pl. I 1, Fig. 1). The strongest part of that system is formed by fibers derived from AZM membranelles. Between adjacent membranelles there are fibers running toward the left side of the cell. On the left side of the zone these fibers turn posteriad. The intermembranellar fibers (IMF) fuse along the margin of the AZM and form longitudinal postmembranellar fiber (PMF) which runs toward the cytostome, surrounds the posterior margin of the oral opening and passes toward the preoral membranelles (Pl. I 1, II 4). Under the ventral AZM membranelles there is a longitudinal submembranellar fiber (SMF) running posteriad parallel to the longitudinal axis of the cell. The part of the SMF connected with the proximal part of the ventral zone is located closer to the left margin of the cell. In the middle part of the ventral AZM this fiber runs under the middle of the membranelles and in the distal part it is shifted toward the right side of the membranelles. The part of the SMF connected with the "collar" part of the AZM is located closer to the ventral surface of the cell and is connected with microtubular fibers originating at the base of frontal cirri (Pl. I 1).

The preoral membranelles, outer and inner ones are connected among

each other by fibers running in oblique fashion and forming a sort of network (Pl. I 1, IV 10). The microtubular fibers originating from preoral membranelles run also toward the peristome underlying its walls and also join the postmembranellar fiber originating in AZM. The outer membranelle is also connected with the frontal cirrus from the second row of frontal ciri.

All described above microtubular systems connected with the oral ciliature integrate the ciliature securing the stability of the whole system and efficiency of its functioning.

Structure of the Oral Kinetosome and its Derivatives

All oral kinetosomes show the same basic structure (Pl. III 6, Fig. 1). The kinetosomal wall is formed by nine mocrotubular triplets. The proximal part is surrounded by an amorphic matter. At the bottom there is so called cartwheel. In the proximal part of the cartwheel the connection between adjacent microtubular triplets joining microtubule C from one triplet with microtubule A with the adjacent triplet originate (Pl. III 7, 8, Figs 1, 2). This connections are seen on the whole length of the kinetosome. In the distal part of the cartwheel its spokes are connected not only centrally but also peripherically (Fig. 2). In the lumen of the kinetosome there are 4 to 7 granules disposed helically. Approximately in the middle of the kinetosome there is a dark ring which possesses links with A-microtubules from all triplets. Above this ring there are another connections between the triplets running from A-microtubule to A-microtubule. The triplets are interconnected in this way up to the distal end of the basal body. The distal part is closed by the septum and by located above axosome (Pl. III 6, Fig. 1).

The amorphic substance surrounding and closing the proximal end of the kinetosomes gives rise to projections which connect the adjacent kinetosomes in the adoral membranelles. The oral kinetosomes are accompanied by several types of microtubular derivatives. The postciliary and transverse fibers originate at the proximal end of the kinetosome and root fibers originate at the base. The oral kinetosomes of *P. weissei* do not have kinetodesmal fibers. Details of the microtubular derivatives will be described below.

Ultrastructure of the Adoral Membranelles

The membranelles of the adoral zone are composed of four rows of kinetosomes (Pl. II 3, 4, Pl. III 7, 8, 9, Fig. 1, 2). We introduce here a numeration of rows counting as the first one the most posterior row

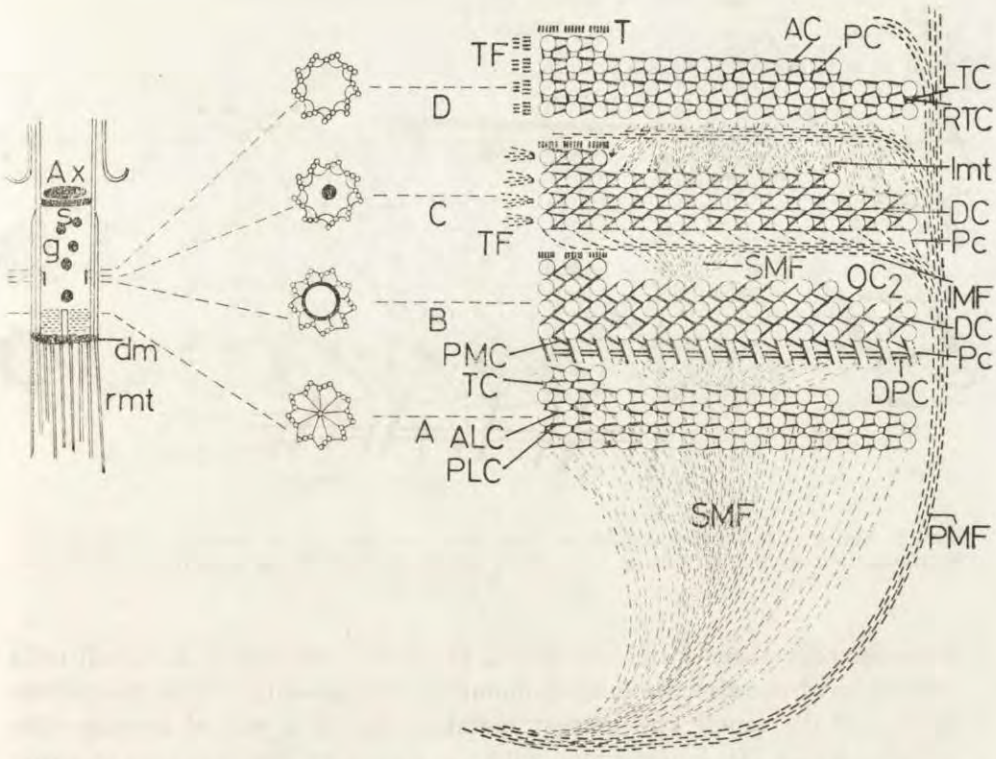

Fig. 1. Schematic reconstruction of the adoral membranelles of *Paraurostyla weissei*. The left side of the drawing: a longitudinal section through oral kinetosome. In the middle of the drawing a schematic cross section through the kinetosome at different levels. On the right side of the drawing a scheme of microfibrillar and microtubular connectives of kinetosomes in membranelle. Large circles are kinetosomes, a continuous line represent amorphous connection, dashed lines represent microtubular ribbons. Abbreviation: A, B, C, D — levels of section through kinetosome. AC — anterior connection, ALC — anterior longitudinal connection, AMC — anterior marginal connection, Ax — axosome, DC — diagonal connection, dm — dense matter, DPC — double posterior connection, g — axial granules, IMF — intermembranellar fiber, Imt — microtubules connecting membranelles, LTC — left transverse connection, OC_1 — first oblique connection, OC_2 — second oblique connection, Pc — postciliary fibers, PC — posterior connection, PLC — posterior longitudinal connection, PMC — postmembranellar connection, rmt — root microtubules, PMF — postmembranellar fiber, ps — parasomal sac, RTC — right transverse connection, S — septum, SMF — submembranellar fiber, T — transverse fiber, TC — transverse connection, TF — terminal fiber

(the longest). Such succession is in agreement with the sequence of differentiation of the membranelle during development of the oral primordium (Grimes 1972, Jerka-Dziadosz, unpublished).

The first and second rows of kinetosomes in ventral membranelles are equally long and are the longest ones, the third row is slightly shorter, the fourth row is the shortest and on ventral part of the AZM

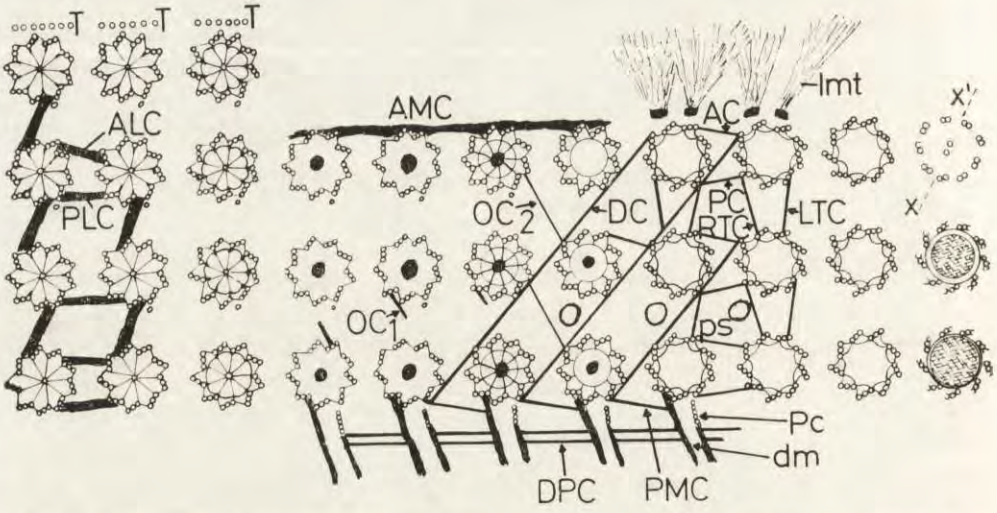

Fig. 2. Schematic representation of the cross section of a ventral membranelle. Abbreviations as in Fig. 1. x–x′ — a plane perpendicular to the direction of effective stroke of a cilium

possesses only three kinetosomes (Pl. II, III 4, 7, 8, Fig. 1, 2). In all cells regardless of the size the longest membranelles are situated in the middle portion of the lapel. The longest membranelle in a cell of average size contains about 110 kinetosomes with the following distributions in rows: first and second — each 39 kinetosomes, third row — 29 kinetosomes and fourth row — 3 kinetosomes. The membranelles become shorter when approaching the distal and proximal ends of the zone. The number of kinetosomes in each row in corresponding membranelles in cells of similar size is the same.

The frontal — collar membranelles — differ in certain respects from ventral ones. The first two rows are much shorter than in ventral membranelles. The difference between second and third row is much smaller. The fourth row is shifted toward the middle of the membranelle (Pl. II 3). The first kinetosome of the fourth row is located next to 4 kinetosome of the third row. The fourth row is composed of 4, rarely 5 kinetosomes. The cilia of these kinetosomes are much shorter than in the rest of the membranelles, they also appear more rigid and are slightly bended toward the right side of the cell. This can be seen both on protargol preparations (Pl. I 1) and on EM sections (Pl. II 3). In average cell there is about 16–19 frontal membranelles, they constitute about 36% percent of all membranelles (Bąkowska nad Jerka-Dziadosz in preparation).

The basal bodies within each adoral membranelle are connected among

themselves on two levels. The bases of all kinetosomes are surrounded by dense amorphic matter. This gives rise to projections binding kinetosomes along the same row and adjacent rows. (Fig. 1 A, Fig. 2). Between kinetosomes of the same row there are double connections originating: the first from triplet No. 9 and running toward a region between triplet 7 and 8 (PLC) and second: from region between triplet No. 2 and 3 terminating at triplet No. 5 (ALC) of adjacent kinetosome situated toward the left side of the membranelle (right side of the drawing on Fig. 2). At the same level (proximal) kinetosomes of adjacent rows are joined by single connective (TC) originating between triplets No. 4 and 5 of kinetosomes in one row and running toward triplets No. 8 and 9 of kinetosome in the next row (according to the numeration from posterior to anterior rows).

At the level of the distal part of cartwheel originates an oblique connection integrating both levels of junctions (Fig. 2). It starts at triplets No. 3 in kinetosomes of odd rows at the cartwheel level and terminates at triplet No. 7 at the level of the middle of kinetosome in even rows (OC_1). The second oblique connection (OC_2) is seen in the level of middle of kinetosomes and connects kinetosomes of adjacent rows. It joins triplet No. 5 from odd rows with the region between triplets No. 1 and 9 of kinetosomes from even rows. The diagonal connective (DC) integrates three rows of kinetosomes. It originates at a region between triplet No. 1 and 9 of kinetosomes from the first row then touches the triplet No. 5 of an adjacent kinetosome from the same row. Next it runs toward the second row and to the following one joining respectively pairs of kinetosomes. It terminates at triplet No. 5 of kinetosomes of the last row.

On the same level, that is at the middle of kinetosome, adjacent kinetosomes possess a second double connectives within a row (Fig. 1 C and D, Fig. 2). First of those starts from triplet No. 9 (PC) and triplet No. 3 (AC) of one kinetosome and join respectively triplets No. 7 and 5 of adjacent kinetosome situated leftward. The second double connection (Fig. 1 D, Fig. 2) occurs between neighbouring rows connecting triplets: 7 (RTC) and 3 (LTC) from one kinetosome with respectively triplets 7 and 9. Beside above described connections, the basal bodies from the anterior-most rows and in part of the third and second rows are connected alongside the anterior margins of the row (Fig. 2) (AMC). The kinetosomes from the posterior-most row have connections attached to the triplet No. 9 and running posteriorly and to the left. They join a strand of amorphic matter attached to the 7th and 8th triplets of adjacent kinetosome (PMC) (Fig. 1 B, Fig. 2). The distal portions of kinetosomes are not interconnected.

The internal asymmetry of kinetosome and its cilium determines the

direction of the stroke of cilium. A line drawn across the section of the two central microtubules of a cilium (Fig. 2) forms an acute angle with the antero-posterior axis (short axis) of a membranelle.

The kinetosomes of adoral membranelles are accompanied by microtubular derivatives of several types. At the level of cartwheel from the kinetosomes of the first row the postciliary microtubules originate (Pl. III 7, Fig. 3). There is 4–5 microtubules in this ribbon which run first toward the cell surface then it turns to the left and continues along the cytoplasmic fold which separates two adjacent membranelles. Single postciliary ribbons join together and form the intramembranellar fiber (IMF) (Fig. 1, Pl. III 7). As has been observed on protargol preparations those fibers after leaving the membranelle turn to the posterior of the cell, join similar fiber from adjacent membranelles and form a strong postmembranellar fiber (PMF) (Pl. II 4, 4a, Fig. 1). On cross section through this fiber the microtubular character of this fiber is well seen. The microtubules are connected by links. Each microtubule is connected with 5 to 7 neighbouring microtubules. This on cross section appears as more or less regular hexagonal network.

Kinetosomes located in rows 2–4 of the adoral membranelle have a "remnant" of the postciliary ribbon in the form of single short microtubule located at the triplet No. 9.

The transverse microtubular fiber is observed only adjacent to the anterior margin of the kinetosomes of the fourth (anterior-most) row (Pl. III 7, 8, Fig. 1, 2). The transverse fiber is composed of 6 microtubules located in one row. They run parallely to the surface of the cytoplasmic fold separating the membranelles. They intertwine with the postciliary fibers originating from the first row of the adjacent membranelle.

Two adjacent membranelles are also connected by microtubules originating along the anterior part of a membranelle. The first two kinetosomes (counting from right to left of the cell) of the fourth row lack this type of microtubular connections. From the third and fourth kinetosome at the triplet No. 2 there is a clump of a dense matter from which originate several microtubules running tangentially toward the anteriorly located membranelle (Fig. 2 Imt). Starting with the fourth kinetosome of the third row all kinetosomes in this row as well as the "free" kinetosomes of the second row possess two such clumps of the dense matter. They are located between the triplets No. 3 and 4 and between triplets No. 4 and 5 respectively. As previously from this clupms anteriorly directed microtubules originate (Pl. III 7).

Two types of microtubular derivatives remain to be described. The first are the terminal fibers (TF) originating at the dense matter located between the triplet No. 5 and 6 on the right marginal kinetosomes of all

four kinetosomal rows on a given membranelle (Pl. III 8, Fig. 1). They run toward the right side of the cell and toward the cytostome, underlining most probably its left dorsal side (Pl. IV 10).

The last type of microtubular derivatives are the root fibers which are attached to all kinetosome of a membranelle. They run deep into the cytoplasm where they intertwine and turn posteriorly forming a submembranellar fiber (SMF) (Fig. 1, Pl. III 9).

In the distal part of the AZM the membranelles are much shorter and the spaces between adjacent membranelles are larger than between the ventral membranelles (Pl. I 1). A change in the orientation against the longitudinal axis of the cell causes also change in the orientation of the microtubular derivatives. The postciliary fibers which in the lapel part run posteriorward in the collar part run toward the left of the cell, and in the most distal frontal membranelles they run toward the anterior of the cell (Pl. I 1, II 3). The change of direction of the postciliary fibers follows that of the inversion of the membranelles. It should be stressed, however, that within a given membranelle irrespective of the location in the cell the distribution of microtubules is constant and in agreement with the intrinsic polarization of the membranelle.

Under the adoral membranelles in the ventral part a large number of mitochondria can be seen (Pl. II 4). Along the left margin of the AZM there is an irregular row of mucocysts.

Ultrastructure of Preoral Membranelles

The outer preoral membranelle is composed of 4–5 rows of kinetosomes arranged longitudinally with respect to the antero-posterior axis of the ciliate. All kinetosomes are ciliated (Fig 3, Pl. II 5, Pl. IV 10, Pl. V 11, 12, 13).

The two right rows are the longest ones, the left-most is the shortest and often does not reach the proximal and distal ends of the membranelle. The kinetosomes within longitudinal rows are not connected among each other. Kinetosomes in adjacent rows are arranged alternatively and not in transverse rows as it can be observed in adoral membranelles. They form a zig-zag pattern. The kinetosomes from the inner rows are connected with four adjacent kinetosomes by double connectives (Pl. V 12, 13, Fig. 3).

The outer preoral membranelle is equipped with microtubular derivatives. The kinetosomes from the left most row are accompanied by transverse fibers. There are about 6–7 microtubules in each fiber. They run under the surface toward the cytoplasmic fold separating the two preoral membranelles (Pl. II 5). Kinetosomes from the right most row

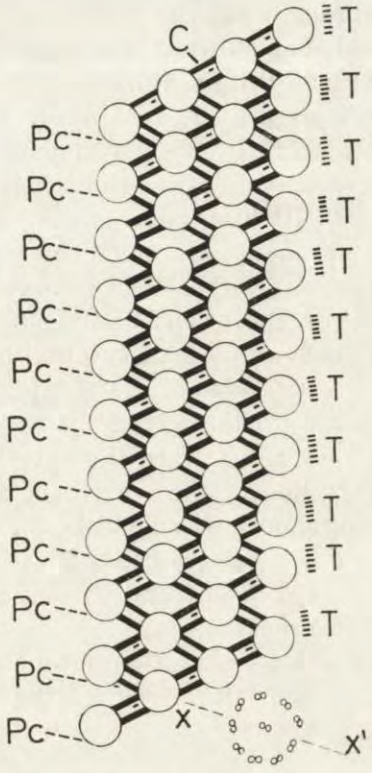

Fig. 3. Schematic representation of the cross section through the outer preoral membranelle. c — connections between kinetosomes, Pc — postciliary microtubules, T — transverse microtubules, x–x′ — a plane perpendicular to the effective stroke of membranellar cilia

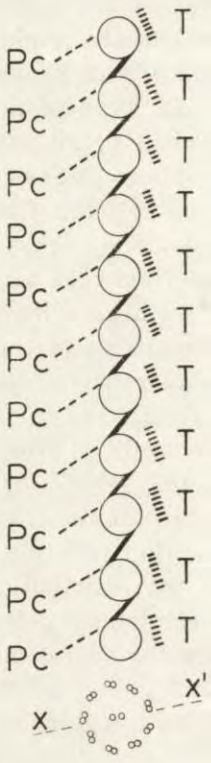

Fig. 4. Schematic representation of a cross section through the inner preoral membranelle. Abbreviations as in Fig. 3

are equipped with postciliary fibers. There are about 2–3 microtubules in each ribbon which runs to the right and slightly anterior (Pl. V 11). At corresponding locations other kinetosomes from the inner rows possess one microtubule. From the bases of kinetosomes originate root microtubules which run deep into the cytoplasm and join the inner preoral membranelle (Cmt) (Pl. V 16) and the SMF from adoral membranelles.

The orientation of the central pair of ciliary microtubules is such that a line drawn through cross section of those microtubules forms an acute angle with the longitudinal axis of the membranelle.

The inner preoral membranelle is composed of single longitudinal row of ciliated kinetosomes (Pl. II 5, Pl. V 14, 15, 16, Fig. 4). Adjacent kinetosomes are linked by amorphic connectives with joins the triplet No. 9 of one kinetosome with a region between triplets No. 4 and 5 of

an anterior kinetosome. Below this runs another connection oriented in the opposite fashion. On the right side of the row there are postciliary fibers. There are usually 4–5 microtubules arranged in convergent fashion (Pl. V 14, 15 a). They run toward the cytostome and underline its walls (Pl. IV 10). On the other side of the ciliary row a transverse fiber can be seen, they are, however, less conspicious. Numerous root microtubules are attached to the kinetosomes. They run in mainly two directions: anterior-right and posterior-right, joining the root fibers from the outer preoral membranelle and the submembranellar fiber (Pl. V 15, 16).

The kinetosomes of the inner membranelle are inversed in the dorso-ventral plane in such a way that their proximal ends are facing the ventral side of the cell (Pl. V 16). This is due to the location of this membranelle under a cytoplasmic fold inside the buccal cavity. Therefore the triplets in kinetosomes at the level of the cartwheel "turn" in opposite direction with respect to the kinetosomes of the rest of oral membranelles seen from the some side (Pl. V 15 a). Moreover, the kinetosomes of the inner preoral membranelle are rotated with respect to the orientation of the outer membranelle kinetosomes in the ventral plane of about 90°. This causes that the transverse fibers from both membranelles run toward the cytoplasmic fold separating the membranelles.

The cytostome is located inside the buccal cavity. The walls of the oral funnel are lined by microtubules originating from postciliary and terminal fibers of oral membranelles (Pl. IV 10). Among the microtubular ribbons there are groups of tightly packed membraneous structures.

The analysis of the ultrastructure of the oral apparatus of *Paraurostyla weissei* has been performed on sections obtained from normal growing cells as well as from cells miniaturized by double operation or starvation. No qualitative differences in the ultrastructure between those cells have been found. In miniaturized cells the number of oral membranelles diminishes (Jerka-Dziadosz 1976), also the number of constituent kinetosomes decreases. The basic structure of the oral kinetosome as well as the microtubular and microfilamentous connectives is the same in membranelles from normal and miniaturized cells. Therefore both kinds of cells were used for illustrations (Pl. II–V).

Discussion

The results described in the present paper deal with the ultrastructure of the oral apparatus of *Paraurostyla weissei*. It is a necessary introduction into a study on the regulation of the oral ciliature related to changes of the cell size.

The structure of the oral apparatus of *P. weissei* appears very similar to that in *Gastrostyla steini* described by Grim 1972, in *Oxytricha fallax* described by Grimes (1972) and in *Stylonychia mytilus* described by Puytorac et al. (1976). A comparison of the main features in several hypotrichous species are illustrated in Table 1. The adoral membranelles and the inner preoral membranelles are very similar in all studied species. The outer preoral membranelles show a great deal of variability. It is interesting to point out that the number of ciliary rows in the outer membranelle does not correspond with the average size of a given species but rather it is correlated with the extent of specialization (or evolutionary differentiation).

Table 1

Species studied	References	Preoral membranelles number of rows		AZM number of rows	
		Inner	Outer	Lapel	Collar
Paraurostyla weissei	present paper	1	4–5	4	4
Pseudourostyla cristata	Jerka-Dziadosz (unpublished)	1	4–5	4	
Keronopsis rubra	,,	1	4–5	4	
Gastrostyla steinii	Grim, 1972	1	2–4	4	
Oxytricha fallax	Grimes, 1972	1	1	4	
Stylonychia mytilus	Puytorac et al., 1976	1	1	4	

The AZM of *P. weissei* similarly to previously mentioned species can be differentiated into two parts: the ventral (lapel) and frontal (collar). Differences between those two parts concern their orientation with respect to the long axis of the cell, their structure as well as differences in developmental fates in various processes of the life cycle.

All ventral membranelles are oriented more or less perpendicularly to the longitudinal axis of the cell, whereas most of the frontal membranelles are oriented parallel to this axis. The collar membranelles are also shorter, the fourth row of kinetosomes contains four or even five kinetosomes. The fourth row is definitely different from the rest, the cilia are shorter and appear more stiff. There are no detailed ultrastructural data concerning collar membranelles in other hypotrichs.

The ventral membranelles have been carefully described in several species such as *O. fallax, S. mytilus, G. steini.* The connective system of amorphic and microfilamentous projections between kinetosomes in membranelles as well as the microtubular derivatives are similar in all described representants of lower hypotrichs. The transverse fibers are

present in front of the fourth row of kinetosomes in ventral AZM membranelles in *P. weissei, O. fallax, G. steini* and *S. mytilus.* The kinetosomes from the third and second rows do not have transverse fibers in *O. fallax, G. steini* as well as in *P. weissei* (except in late stages of morphogenesis — Jerka-Dziadosz, unpubl.) whereas they are present in *S. mytilus* (Puytorac et al. 1976).The terminal microtubules have been described also in *G. steini.*

The differentiation of the AZM into two parts is manifested also during conjugation, regeneration and reorganization. During division as first the frontal membranelles differentiate (Jerka-Dziadosz and Frankel 1969, Ruffalo 1976). Both parts behave differently in conjugating mates of *P. weissei* (Jerka-Dziadosz and Janus 1974) and in *O. falax* (Hammersmith 1976).

All so far studied ultrastructurally hypotrichs possess two preoral membranelles (Table 1). The outer preoral membranelle in *P. weissei* as well as in *Pseudourostyla cristata* and *Keronopsis rubra* (Jerka-Dziadosz, unpublished) consists of 4–5 longitudinal kinetosomal rows. In. *G. steini* it is formed by 2–3 rows, whereas in *O. fallax* and *S. mytilus* it is formed by only one row of kinetosomes. The kinetosomes of the left most row in outer membranelle of *P. weissei* are equipped with the transverse fiber. Puytorac et al. (1976) showed pictures of the outer membranelle of *Stylonychia* where in the single rowed membranelle every second kinetosome has a transverse fiber. The kinetosomes lacking the fiber are slightly retracted. It appears as a "stretched" double kinetosomal row. The alternative distribution of kinetosomes in adjacent rows in the outer preoral membranelle of *P. weissei* is characteristic also for *P. cristata, Urostyla grandis, K. rubra* (Jerka-Dziadosz, unpublished) and *G. steini* (Grim 1972). A similar zig-zag pattern is formed in the pairs of kinetosomes in preoral membranelles of many ciliates, to mention only *Ancistruma mytili* and *Boveria subcilindrica* described by Lom et al. (1968), in *Chilodonella cucullulus* described by Sołtyńska (1971) and *Dileptus cygnus* described by Grain and Golińska (1969). The orientation of kinetosomes in the outer preoral membranelle of *P. weissei* corresponds with the scheme of the formation of the buccal kinety in *C. cucullulus* proposed by Peck (1977) (see Fig. 30 c in Peck's paper). Further proliferation next to so oriented pairs of kinetosomes would lead to the formation of triplets and quadruplets of kinetosomes, that is to the formation of additional longitudinal rows of kinetosomes, as it is in *P. weissei.* In this way the original zig-zag pattern is maintained.

The inner preoral membranelle in all so far studied hypotrichs is formed by single ciliated row of kinetosomes. The kinetosomes of that

row are inverted in the dorso-ventral plane of about 180° with respect to the kinetosomes of the outer preoral membranelle and adoral membranelles.

The morphogenesis of the preoral membranelles at the ultrastructural level is not known. Preliminary observations (Jerka-Dziadosz, unpubl.) showed that the primordium of the preoral membranelles is formed adjacent to the AZM primordium. The postciliary fiber of the inner membranelle is from the very beginning located on the "wrong" side of the kinetosomes and is directed toward the AZM. The inversion of the kinetosomes in the dorso-ventral plane is caused by the formation of the intermembranellar longitudinal fold which causes a shift of the membranelle inside the oral apparatus. As a result in adult ciliates the postciliary fibers run toward the right side of the cytostome. As a final result of the inversion appears such an orientation of the inner membranelle where the transverse microtubules of both inner and outer membranelles are directed toward the cytoplasmic fold.

An alternate arrangement of ciliature in oral apparatuses is not rare in ciliates (Puytorac et Grain 1976). The kinetosomes of the oral ciliature on the left and right side of *Dileptus* are rotated against each other in the ventral plane of about 180° (Grain and Golińska 1969). Also in *Chilodonella* (Sołtyńska 1971) and *Chilodochona* (Grain et Batisse 1974) the kinetosomes from the right circumoral kinety have inverted orientation with respect to the somatic kineties.

The analysis of the structure of the oral ciliature of representatives of ciliates indicates, that irrespectively of whether the cytostomal walls are equipped with postciliary microtubules (*Oligohymenophora*) or transverse microtubules (*Kinetophragmophora*) there is a change in orientation of the ciliature on one side of the cystome. In effect a cystomal wall is lined by one kind of microtubular derivatives of oral kinetosomes.

The spatial orientation of kinetosomes within adoral and preoral membranelles determines a definite orientation of the central microtubule pair for each membranelle. Different spatial orientation of central microtubules causes that the effective stroke of membranelles form a water currents directed toward the cytostome (Hiramoto 1974, Machemer 1974).

ACKNOWLEDGEMENTS

The authors wish to express their sincere appreciation to dr Krystyna Golińska for teaching the difficult protozoan EM technique and for helpful discussions at interpretation of the electromicrographs. The technical assistance of the staff of the Laboratory of Electron Microscopy is also acknowledged.

RÉSUMÉ

Le ciliature orale de *Paraurostyla weissei* est composée des membranelles adorales frontales et ventrales, et des membranelles preorales intérieures et extérieures. Chaque membranelle adorale contient 4 rangées des cinétosomes. Les différences entre les membranelles frontales et ventrales concernent leur orientation géométrique, leur nombre, et la répartition des cinétosomes dans les rangées. La membranelle preorale extérieure est constituée par 4–5 rangées des cinétosomes. La membranelle preorale intérieure comporte une seule rangée des cinétosomes dont les extrémités proximales sont orientées vers le côté ventral de la céllule. On a décrit le caractère des jonctions entre les cinétosomes dans membranelles et entre les membranelles, ainsi que le système des microtubules lié avec l'appareil oral.

REFERENCES

Bąkowska J. and Jerka-Dziadosz M. 1977: Ultrastructural observations on the infraciliature of the oral apparatus in *Paraurostyla weissei*. J. Protozool., 24 (Suppl.) abstr. 145, 26A.

Grain J. et Batisse A. 1974: Etude ultrastructurale du cilie chonotriche *Chilodochona quennerstedti* Wallengren, 1895. I. Cortex et structures buccales. J. Protozool., 21, 95–111.

Grain J. et Golińska K. 1969: Structure et ultrastructure de *Dileptus cygnus* Claperéde et Lachmen, 1859, Cilie Holotriche, *Gymnostome*. Protistologica, 5, 269–291.

Grim J. W. 1972: Fine structure of the surface and infraciliature of *Gastrostyla steinii*. J. Protozool., 19, 113–126.

Grimes G. W. 1972: Cortical structure in non-dividing and cortical morphogenesis in dividing *Oxytricha fallax*. J. Protozool., 19, 428–445.

Hammersmith R. 1976: Differential cortical degradation in the two members of early conjugant pairs of *Oxytricha fallax*. J. Exp. Zool., 196, 45–70.

Heckmann K. 1963: Paarungssystem genabhängige Paarungstypdifferenzierrung bei den hypotrichen Ciliaten *Euplotes vannus* O. F. Müller. Arch. Protistentk., 106, 393–421.

Hiramoto Y. 1974: Mechanics of ciliary movement. In: Cilia and Flagella (ed. M. A. Sleigh) Academic Press, London, 199–286.

Jerka-Dziadosz M. 1965: Morphogenesis of ciliature in division of *Urostyla weissei* Stein. Acta Protozool., 3, 345–353.

Jerka-Dziadosz M. 1976: The proportional regulation of cortical structures in a hypotrich ciliate *Paraurostyla weissei*. J. Exp. Zool., 195, 1–14.

Jerka-Dziadosz M. and Frankel J. 1969: An analysis of the formation of ciliary primordia in hypotrich ciliate *Urostyla weissei*. J. Protozool., 16, 612–637.

Jerka-Dziadosz M. and Golińska K. 1977: Regulation of ciliary pattern in ciliates. J. Protozool., 24, 19–26.

Jerka-Dziadosz M. and Janus I. 1974: Discontinuity of cortical pattern during total conjugation of hypotrich ciliate *Paraurostyla weissei*. Acta Protozool., 13, 1–28.

Lom J., Corliss J. O. and Noirot-Timothee C. 1968: Observations on the ultrastructure of the buccal apparatus in thigmotrich ciliates and their bearing on thigmotrich-peritrich affinities. J. Protozool., 15, 824–840.

Machemer H. 1974: Ciliary activity and metachronism in Protozoa. In: Cilia and Flagella (ed. M. A. Sleigh), Academic Press, London, 199–286.

Peck R. K. 1977: Cortical ultrastructure of the scuticociliates *Dexiotricha media* and *Dexiotricha colpidiopsis* (*Hymenostomata*). J. Protozool., 24, 122–134.

Puytorac P. de et Grain J. 1976: Ultrastructure du cortex buccal et evolution chez cilie. Protistologica, 12, 49–67.

Puytorac de P., Grain J. et Redrigues de Santa Rosa 1976: À propos de l'ultrastructure corticaïe du cilié hypotriche *Stylonychia mytilus* Ehrbg., 1838: Les caracteristiques du cortex buccal adoral et paroral des *Pylyhymenophora* Jankowski, 1967. Trans. Am. Microsc. Soc., 95, 327–345.

Ruffalo J. J., Jr. 1974: Critical point drying of protozoan cells and other biological specimen for scanning electron microscopy: apparatus and methods of specimen preparation. Trans. Am. Microsc. Soc., 93, 124–131.

Ruffalo J. J. Jr. 1976: Cortical morphogenesis during the cell division cycle in *Euplotes*: An integrated study using light optical scanning electron and transmission electron microscopy. J. Morph., 148, 489–528.

Small E. B. and Marschalek D. S. 1969: Scanning electron microscopy of fixed, frozen and dried Protozoa. Science, 163, 1964–1965.

Sołtyńska M. 1971: Morphology and fine structure of *Chilodonella cucullulus* (O.F.M.). Cortex and cytopharyngeal apparatus. Acta Protozool., 9, 49–82.

Yocum H. B. 1918: The neuromotor apparatus of *Euplotes pattela*. Univ. Calif. Publ. Zool., 18, 337–396.

Received on 4 November 1977

EXPLANATION OF PLATES I–V

Plate I. Oral apparatus of *Paraurostyla weissei*

1: A combined photograph of the frontal part of the cell stained with Protargol. The anterior of the cell is up. F — frontal adoral membranelles, V — ventral adoral membranelles. The dashed line represents the border between the frontal and ventral membranelles. Abbreviations: IMF — intermembranellar fiber, IPM — inner preoral membranelle, Cmt — microtubular connections between the preoral membranelles, OPM — outer preoral membranelle, PFM — postmembranellar fiber, SMF — submembranellar fiber. Tre arrows indicate short cilia from the fourth row of kinetosomes in frontal membranelles. 3600 ×
2: Oral ciliature as seen on scanning electron microscope. Fd_1 — outer cytoplasmic fold, Fd_2 — inner cytoplasmic fold. OPM — outer preoral membranelle, AZM — ventral adoral membranelles 3488 ×

Plates II–V. Photographs taken from sections observed in the transmission electron microscope. All photographs are oriented in such a way (except 6 and 9) that the anterior of the cell is up

3: The right most frontal adoral membranelle. mt — microtubules running toward the SMF (compare with Fig. 2). 1–4 numeration of the subsequent rows of kinetosomes in membranelle. Cell was fixed 5 h after two successive operations. 6462 ×
4: The ventral adoral membranelles. m — mitochondria, mu — mucocysts, PMF — postmembranellar fiber, SMF — submembranellar fiber. The cell was fixed after four days of starvation. 5279 ×
4 a: A cross section through postmembranellar fiber, mt — microtubules, 1 — links between microtubules. 68 460 ×
5: A cross section through the preoral membranelles. IPM — inner preoral membranelle, OPM — outer preoral membranelle, 1–4 numeration of successive rows of cilia. Small cell after two successive operations. 9600 ×
6: Longitudinal section through oral kinetosome. Ax — axosome, g — axial granules, dm — dense matter, s — septum. 29 328 ×
7: Cross section through ventral membranelles. Abbreviations as on Fig. 1 and 2. The cell was starved before fixation for four days. 24 000 ×
8: Cross section through the right side of the ventral membranelle. 1–4 — numeration of the subsequent rows of kinetosomes. Abbreviations as on Fig. 1. 24 000 ×
9: Sagital sections through the ventral membranelle. The anterior of the cell is on the right side of the photograph. Imf — intermembranellar fold. 15 692 ×
10: Section through the anterior part of a cell fixed several hours after two successive operations. Cmt — microtubular connections between preoral membranelles, IPM — inner preoral membranelle, OPM — outer preoral membranelle. T — transverse microtubules, Tf — terminal microtubules, Pc — postciliary microtubules. 5257 ×
11–13: Cross section through outer preoral membranelle, c — connection between kinetosomes, Pc — postciliary microtubules, T — transverse microtubules. 3237 ×
14: Cross section through inner preoral membranelle in cell subjected to two successive operations. c — connection between kinetosomes, Pc — postciliary microtubules. 24 000 ×
15: Longitudinal section through the inner preoral membranelle. Cmt — microtubular connection between preoral membranelles. 24 000 ×
15 a: Cross section through a kinetosome from the inner preoral membranelle. Pc — postciliary microtubules, T — transverse microtubules. 68 300 ×
16: Cross section through both preoral membranelles. Cmt — connections between membranelles. IPM — inner preoral membranelle, OPM — outer preoral membranelle. 12 000 ×

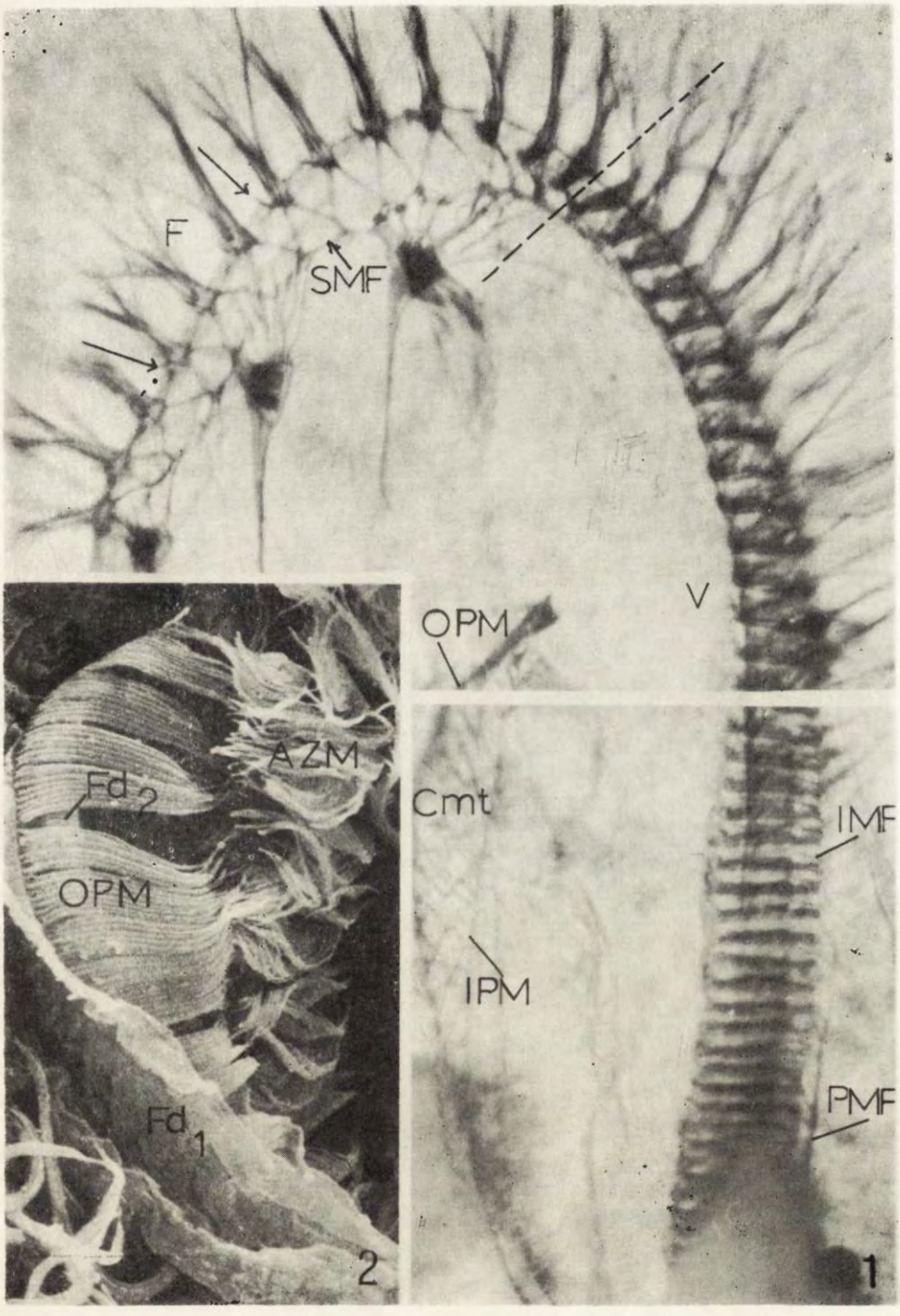

J. Bąkowska et M. Jerka-Dziadosz auctores phot.

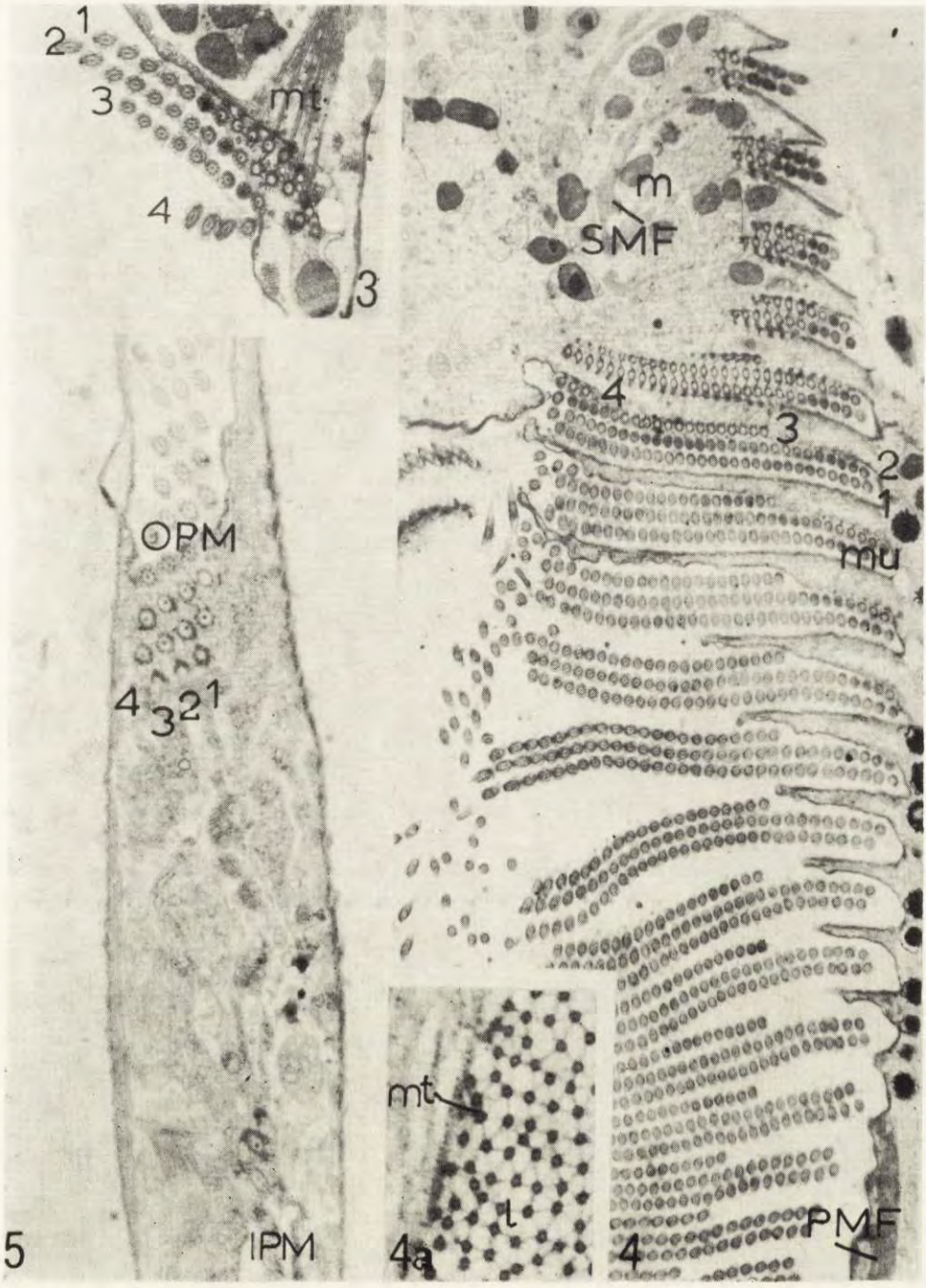

J. Bąkowska et M. Jerka-Dziadosz auctores phot.

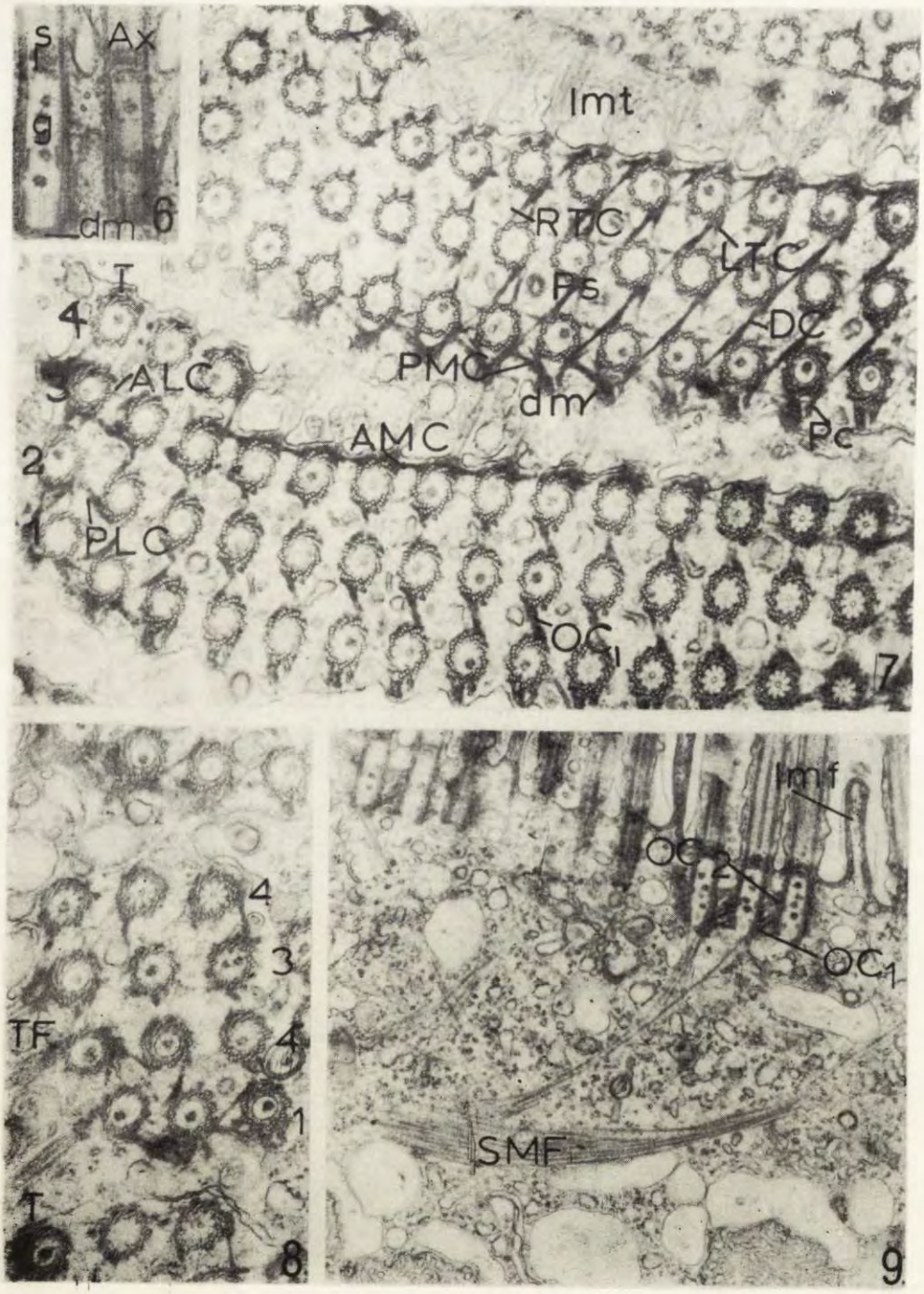

J. Bąkowska et M. Jerka-Dziadosz auctores phot.

J. Bąkowska et M. Jerka-Dziadosz auctores phot.

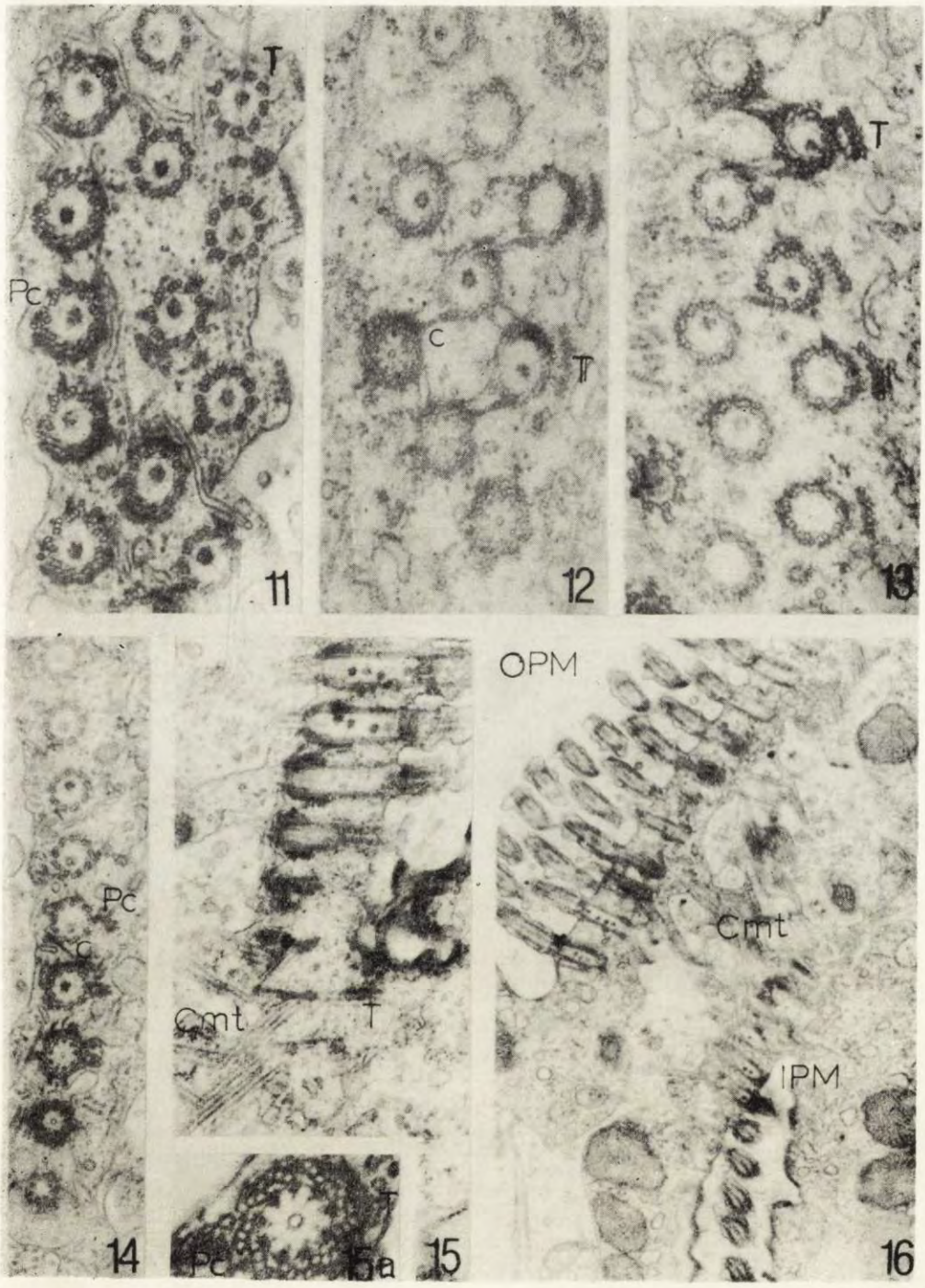

J. Bąkowska et M. Jerka-Dziadosz auctores phot.

ACTA PROTOZOOLOGICA
VOL. 17 (No. 2) WARSZAWA, 30 VI 1978 pp. 303–319

Institute of Zoology, Department of Cytology, Warsaw University, Krakowskie Przedmieście, 00-927/1 Warszawa, Poland

Janina KACZANOWSKA

Shape Transformation, Contractility and Endocytose/Exocytose Cycle in *Paramecium* Genically Deprived of Excitability

Synopsis. In *Paramecium tetraurelia* mutants named "pawns" — the voltage-dependent Ca^{++} gating through cell membrane into the cell is blocked (Kung 1975). This kind of membrane lesion has no effect on cortical morphology and morphogenesis and on endo/exocytose system of cell. Spontaneous shape change occurring in starved pawns comprises a posterior displacement of the cytoplasm with an increase of its optic density at the posterior cell end. This process is different from chemically induced contraction of the cell. It represents the pleiotropic effect of pawn mutation which is experimentally dissected from the effect of mutation on the active electrogenesis.

In *Paramecium* cell is possible to study many cellular function as a cortical differentiation during divisional morphogenesis, mating, endo/exocytotic cycle, electrogenesis and others. In general, the metazoan high excitable cell is specialized and lost some functions.

The isolation in *Paramecium tetraurelia* of "pawn" mutants deprived of excitability (Kung 1971 a, b) has created an opportunity to test the effects of this lesion on other physiological processes performed by the cell. As far as is known this lesion in pawns concerns their inability to perform the voltage-dependent gating of Ca^{++} across the membrane to the inside of the cell and downwards to the existing electrochemical gradient resulting in an action potential (Kung 1975). Excitable *Paramecium* cell reacts on different stimuli by the reversion of the ciliary beating resulting in a backward swimming of entire cell (avoiding reaction). Ciliary reversal occurs in close association with a membrane depolarization which is mediated by an influx of Ca^{++} in a response to a transient increase in the calcium conductance of the membrane (Eckert and Naitoh 1972). This is readily visualized by swimming

backwards of the cell. Pawn cells are not able to perform a ciliary reversal after stimulation (Kung and Eckert 1972). Pawns used here display normal resting potential and delayed rectification (Schein et al. 1976) and a normal sensitivity of ciliary system to Ca^{++} concentration (Kung and Naitoh 1973).

It is known that Ca^{++} concentration controls an assembling of microtubules and their depolimerization (Kirschner at al. 1974). One may ask whether transient Ca^{++} influx after stimulation affects fibrillogenesis of microtubules in the cortical layer of *Paramecium*. Pawns were used to test this relation.

Processes of electrogenesis, endocytose and contraction shares some common features. These three phenomena are coupled with depolarization of cell membrane and often with Ca^{++} controlled change of the cell membrane conductance (Allison et al. 1971, Eckert and Naitoh 1972, and Joseffson 1975). Studies on pawns may throw light on their interrelations. In the present studies the rate of food vacuole formation and the contractility of pawn cells were compared with those in wild type cells.

Recent studies on exocytosis (secretion) of some glandular cells revealed the coupling of this phenomenon with the calcium potential after stimulation. (Kidokoro 1975, Davis and Hadley 1976). On the other hand, coupling of endocytosis and exocytosis (Allen 1974) and the effects of Ca^{++} influx on triochocysts exocytosis are known in *Paramecium* (Plattner 1976). Pawn mutants were used here to find out whether the blocking of voltage-dependent Ca^{++} conductance influences exocytosis of digested food vacuoles.

While the most pawn cells are morphologically normal, some of them display morphological abnormalities (Kung 1971 a). The character of this transformation and the conditions necessary for its expression are studied here. As it was suggested by Kung (1971 a) and by the present studies behave like the pleiotropic effect of mutation. However, a phenocopy of this effect was received in wild type cells with no loss of excitability.

The character of shape transformation and the recovery of the normal shape were studied here.

Materials and Methods

Paramecium Stocks and Cultures

Three strains used were of species *Paramecium tetraurelia*. They are: the wild type stock 51S and stocks d_4-94 referred here as "pawn A" with the genotype

pw A/pw A and stock d_4-95 referred as "pawn B1" of the genotype *pw B/pw B*. The mutant stocks were derived by Kung (1971 a) from mutagenized strain 51. They are the single-gene recessive mutants with the mutations unlinked each to other (Chang et al. 1974). Cells were cultured in baked lettuce medium inoculated with *Klebsiella pneumoniae* and alkalized with Ca $(OH)_2$ to pH 6.5–7.5 (Sonneborn 1970). This medium is referred to here as "Culture medium". Culture and handling of paramecia followed the methods of Sonneborn (1950, 1970).

In some experiments phosphate buffered Cerophyl medium (Sonneborn 1970) containing 3.6 mM potassium and about 9 mM of sodium and less than 3×10^{-6} M of free calcium ions was used and referred as "Calcium-poor medium" (Cronkite 1974). Lettuce medium supplemented with 2 mM EDTA was used as "Ca^{++}-chelating medium". Culture medium supplemented with 0.2 M glucose was used as "hypertonic solution". Culture medium supplemented with 20 mK KCl was used as "K^+ — rich medium". "Exhausted medium" was prepared by filtering out cells from a culture that had been inoculated 5 days earlier (1 part inoculum from a log phase culture to 8 parts culture medium) and kept at 27°C.

For the crosses mutants of mating O were mated to wild type cells of mating type E. Exconjugants were isolated and in F2 was derived through autogamy, which reults in complete homozygosity of all genes (Sonneborn 1970). Autogamous cells were isolated and their progeny were tested both for "pawn" behavior and transformed phenotypes after about 12–15 cell generations. Virtually all exautogamonts survived. No other genic marker was introduced to test whether true conjugation occurred. Therefore the only pairs used for studies were those in which both exconjugants 24 h after separation demonstrated "wild type" behavior in the pawn test media and in which the progeny of both exconjugants demonstrated segregation of the pawn and wild behaviors after autogamy (Berger 1976). Cytological examination for autogamy was done using Dippell's (1955) stain. The above requirements were fulfilled in very few cases: many cases of pairs which had not crossfertilized were recorded and eliminated.

Test Solutions for Study of Cell Behavior

The standard adaptation medium was used as prescribed by Kung et al. (1975) as a bath for about 20 min before introducing the cells into the test media, or for 60 min before introduction of cells into labelled food. "Ba^{++}/Ca^{++} solution" contained 8 mM $BaCl_2$, 1 mM $CaCl_2$ and 1 mM tris (pH 7.2). "K^+/Ca^{++} solution" contained 20 mM KCl, 1 mM $CaCl_2$ and 1 mM tris (pH 7.2). "Na^+/Ca^{++} solution" was as prescribed by Dryl (1959).

Tests for Recovery of the Transformed Phenotypes

Conspicously invaginated pawn cells were isolated for 24 h in the following media: (1) a fresh portion of culture medium, (2) a 1% vol/vol solution of dimethylsulfoxide (DMSO) in culture medium, (3) the above DMSO solution supplemented with 16 μg/ml Cytochalasin B (CB) (grade B Aldridge Comp., England), and (4) exhausted medium.

Tests for the Rate of Food Vacuole Formation and Release

Cells isolated for 1 h in the adaptation medium were next introduced for 5 min into culture medium containing latex beads (PLP 0.76 μm diam. Serva Comp.) in a final concentration of 10^5 beads per ml. The cells were then fixed and the number of food vacuoles per cell was counted after Preer's method (1975). Release of food vacuoles was tested after cells labelled with PLP latex for 5 min were twice

washed and reisolated into plain culture medium. The number of food vacuoles filled with latex was counted after the lapse of 30 and 60 min. Experiments were done twice at each indicated temperature.

Tests for Effects of Starvation, Centrifugation and Ca++ Depletion on Penetrance of the Invaginated Phenotype

Samples of rapidly growing cells of all stocks were inoculated into test tubes and fed with plain culture medium, or with culture medium containing 2 mM EDTA (one part of cell culture to 8 parts of media). On each of five successive days two portions of the cultures were removed from every sample: one of them was centrifuged 5 min at 5000 RPM (rotor 12 cm). Both portions were fixed with Bouin fixative and the numbers of late dividers (in cytokinesis) and of invaginated cells were counted among at least 200 cells. Experiments were done twice. The cells were kept at 22°C throughout the experiments.

Tests for Contractility and Shrinkage of Cells

Two methods for inducing contraction of cells were used: (1) Glycerinated models of cells were made exactly following the method of Rinaldi et al. (1975). In some preparations many cells preserved their original shape and could be tested with 0.5 mM $CaCl_2$, 0.5 mM $MgCl_2$ and 0.5 mM Na_2ATP under phase microscope. (2) Cells were introduced into culture medium supplemented with 0.15 mg/ml of dibucaine (Dibucaine hydrochloride, Amer. Chem. Co.) either in the presence or in the absence of 20 mM KCl. Cells were followed until their death and changes of shape were noted.

Shrinkage of the cells was observed after very slow dropping of hypertonic medium or K+ rich medium to the samples. After about 1 h cells were replaced either in plain hypertonic solution or to K+ rich medium. The shape of the cell was recorded after a few hours and after 24 h.

Studies on Cell Morphology and Morphometry

Silver impregnation: The Chatton–Lwoff silver impregnation technique as modified by Frankel and Heckmann (1968) was used. These preparations were used to study of cortical pattern and for morphometrical analysis. Although this method primarily reveals cortical structures, the position of the macronucleus was also visible in some cells. The distance from the posterior edge of the macronucleus to the posterior end of the cell was measured on such cells.

Transmission electron microscope study: wild type cells (as control), pawn A normal and pawn A invaginated cells were either immediately fixed or after hour preincubation in 1 mM $CaCl_2$ and 1 mM KCl bath (following Allen's 1971 method) with 0.5% vol/vol glutaraldehyde (Biological Grade), followed in 2% osmium tetraoxide. Material was embedded in Epon 812 and sections were made with an LKB-880 microtome and stained with uranyl acetate and lead citrate in the standard way. Sections were examined in a TESLA B S-500 EM and recorded on AGFA-Geveart film.

Measurements of Dry Mass of the Cell

PZO MPI-5 interference microscope with a polarizing unit (Wollastone type) was used. Dry mass measurements of the cells were made on wild type and on pawn B1 normal and invaginated cells flattened in a microcompression chamber (Rotocompressor) sealed in a ring of liquid parafine. Cells were flattened to

a standard thickness (about 32 μm). For measurements cells were chosen which maniefested: a proper immobilization (indispensable for measurements), with actively working contractile vacuoles (CV) turned toward the observer (i.e., cells immobilized with dorsal surface up). In the case of invaginated cells, cells were chosen with an invagination shallow enough not to extend as far back as the level of the anterior CV.

Measurements were made of the shift of two successive bright pictures of the same maximally filled CV after rotation of polarizing unit. From the difference of the optic paths the dry mass of the total layer per one μm^2 was calculated (Ostrowski et al. 1963). The mean value and statistics were based on measurements of at least 12 individuals in each category all measured at the levels of the anterior (CV-1) and posterior (CV-2) contractile vacuoles. The diameters of filled CVs were also measured.

Estimation of the Difference between the Volumes of Invaginated and Normal Pawn A Cells

In this study only one slide of silvered pawn A cells was used. Outlines of properly embedded invaginated and normal cells were made at the same magnification on the same sheet of photographic paper. On the outlines of the invaginated cells the depth of the anterior invagination was marked and added to the observed length of the cell to give the total length of the specimens. For comparison the outlines of normal specimens and invaginated cells of the same total length were chosen. Thus 25 paired cells (invaginated and invaginated) were used for further study. These outlines were cut out of the paper. Their length, width and weight were tabulated the statistics were calculated and the correlation between lengths and width in invaginated and normal cells was graphed.

Two or three outlines of invaginated and normal cells closely fitting to received mean values for length, width and weight were chosen to make standard outlines of two types of cells. The standards were used for construction of plastic models of half cells. The bases of the models were fitted to the standard outlines. These models were simplified in two respects: (a) the oral invagination was omitted (b) the shape of the cell was regular in the sense that any transverse section of the model was a half circle. A standard size invagination was substracted at the anterior end of the invaginated cell. Both models were weighed and the percentage of the difference between their weights was calculated. It is assumed that this difference represents the percentage difference between the volumes of the two models.

Results

Genetic Analysis of the Abnormal Phenotype of Pawn Cells

Table 1 summerizes the genetic results. It follows from this Table that the behavioural reaction is coupled with the ability to form invaginated cells spontaneously. The fact that this coupling characterized homozygotes for each of the two unlinked pawn genes indicates that a single basic lesion leads to both aspects of phenotype. So far as known, no pawn mutant fails to yield invaginated cells spontaneously.

Table 1

F2 segregation of lines derived by autogamy from (a) *pw* A/+ and from (b) *pw* B1/ +

	Pawn behaviour (no backward swimming)	Normal behaviour (backing in the test media)
invaginated cells present	(a) 17 lines (b) 77 lines	0 lines 0 lines
ivaginated cels absent	(a) 0 lines (b) 0 lines	22 lines 83 lines

Cells were tested for their behavioural reaction by immersion in test media and for the existence at least one clearly invaginated cell among about 700 cells of a given clone in a depression slide. Tests were performed 12—15 generations after autogamy on cells in stationary phase.

Studies on Phenotypes of Pawn Cells

Normal Phenotype

Analysis of silvered specimens of well fed cells of pawn A and pawn B1 revealed that these cells manifest normal morphology both in morphostatic (Pl. I 1) and morphogenetic stages. Their normality was also confirmed by the morphometrical studies (Table 2) and by studies of their ultrastructure, duration of cell generation and duration of cytokinesis.

Abnormal Phenotype

During starvation of the pawn cultures some cells with more or less deep and with more or less symmetrical invagination at the anterior end appeared among the morphologically normal cells. This effect was observed at various temperatures (13, 19, 22, 27 and 35°C) with a frequency of about 1–5%.

The invaginated cells has a normal cortical pattern including an invaginated part. The oral apparatus anatomy and topography of CV's pores are not altered in these cells (Table 2 and Pl. I 2). Transversal sections of the anterior part of invaginated cells (Pl. I 3) revealed that the invagination is bounded by cortex containing all normal cortical structures including unexploded trichocysts, alveoles, cilia, striated fibrills and infraciliary lattice. Between this invaginated cortex and the normally positioned outer cortex is a narrow ring of endoplasm containing normal endoplasmic constituents including parts of the excretory system (Pl. II 4). The cortical and subcortical layer bounding the invagination were thrown into folds (Pl. I 3). Thus there was more cortex and subcortical material than needed to line the invagination.

Table 2

Morphometrical data of wild type and *pw* A and *pw* B1 cells. (From silver impregnated specimens)

(1) stock	right (2) kineties	left (3) kineties	(4) total length (in μm)	maximal (5) width (in μm)	CVP-1 to (6) CVP-2 (in μm)	CVP-2 to (7) post. end (in μm)	macronucleus to (8) post. end (in μm)
wild, fed, normal	31.2±1.2	44.0±1.1	122.0±2.5	42.1±0.8	50.0±4.2	25.0±3.0	48.5±7.0
wild, starved, normal	32.4±2.6	43.8±1.6	111.0±8.6	38.8±4.5	49.9±7.7	23.1±3.7	45.0±6.2
pw A, fed, normal	30.3±1.6	44.0±2.4	108.3±6.2	38.8±4.0	47.9±7.5	23.0±2.4	45.1±6.1
pw A, starved, normal	29.8±1.2	43.2±2.3	105.0±6.8	36.8±4.5	44.9±7.0	24.5±3.7	45,1±8.5
pw A, invaginated	29.3±1.0	42.7±1.7	101.5±7.8 (74.5±7.8 plus 27.0±7.8)	35.6±4.3	43.6±7.2	23.3±2.3	25.8±8.5
pw B1, fed, normal	32.6±2.4	43.4±3.3	116.1±8.7	40.1±3.4	46.1±5.4	25.1±5.1	49.6±9.5
pw B1, starved, normal	32.3±2.4	42.1±3.6	116.0±12.4	38,3±5.7	45.4±6.9	23.4±3.9	36.1±7.4
pw B1, invaginated	31.6±3.1	43.7±2.6	106.5±12.1 (82.3±15.3 plus 23.2±9.2)	39.1±8.2	42.9±7.0	23.5±3.0	28.6±6.2

All cells measured at the interdivisional stage (as described by Kaneda and Hanson 1974). Each entry represents a mean and standard deviation of 20 measurements.

Explanation of the column legends: (1) description of the feeding conditions and morphology of a given strain, (2) number of right kineties scored from the anterior contractile vacuole pore (CVP-1) to the oral opening including right vestibular kineties, (3) number of left kineties scored from CVP-1 to the oral opening including left vestibular kineties, (4) total length of the specimens (in invaginated cells-the total length of the cell body plus the length of the invaginated pocket), (5) maximal width measured on unflattened specimens well-embedded in gelatin, (6) distance between the anterior and posterior contractile vacuole pores, (7) distance from the posterior contractile vacuole pore (CVP-2) to the posterior end of cell, (8) distance from the posterior edge of the macronucleus to the posterior cell end.

This excludes the interpretation that invagination is due to a deficiency of cortical material or to the contraction of subcortical layer. No indication of autophagy or resorption of structures could be found, nor could any evidence be found for organelles such as additional fibrillar material that could be implicated in pulling inward the anterior part of the cell. Transverse sections at the level of the oral apparatus and more posterior parts of the cell showed no difference between invaginated and wild type cells and agreed with the descriptions and photos by other observers (Schneider 1960, Jurand and Selman 1969, Allen 1971, Ehret and Mc Ardle 1974). Interconnections between adjacent alveoles in a form of intervlveolar pores were also found in invaginated pawn A cells (Pl. II 5).

Morphometrical data (Table 2) show no significant differences among the various classes of cells, but starved invaginated pawn B1 cells are shorter than normal controls while their width was normal.

The invaginated phenotype is positively correlated with a posterior shift in the position of the macronucleus. Some cells with a deep invagination still posses a centrally located macronucleus, but 80% of the invaginated cells have the macronucleus in the posterior part of the cell but still anterior to CV-2. Posterior replacement of macronucleus accompanies invaginated phenotype but evidently is not indispensable for it.

Indirect estimation of difference in volume between invaginated and normal pawn A cells revealed that standard invaginated cell is broader than normal cell of the same length, with a deccrease of the total volume not higher than of about 2%.

Comparison of Dry Mass in Wild Type and Normal and Invaginated Pawn B1 Cells

Results of these measurements are tabulated (Table 3). From this Table it is seen that dry mass per μm^2 at the level of CV-1 does not

Table 3

Dry mass (in $m\mu g/\mu m^2$) beneath the contour of the maximally filled anterior contractile vacuole (CV-1), and posterior contractile vacuole of the same specimens of wild, *pw* B1 normal and *pw* B1 invaginated cells. Diameters of maximally filled contractile vacuoles are also tabulated. Data calculated from 12–16 measurements. sd–standard deviation

Stock	Dry mass at level of CV-1	Diameter of CV-1	Dry mass at level of CV-2	Diameter of CV-2
wild	0.0093±0.0006	15.7±1.77	0.0084±0.0005	12.9±0.86
pw B1, normal	0.0090±0.0007	15.7±1.79	0.0079±0.0019	12.9±1.24
pw B1 invaginated	0.0086±0.0007	14.4±1.07	0.0107±0.0003	11.9±0.77

significantly differ in all categories of cells. Dry mass at the CV-2 level is significantly greater in invaginated pawn B1 cells than in either normal or pawn B1 normal cells, and also than at the CV-1 level in invaginated pawn B1 cells. This is not due to the presence of the macronucleus at this level; the macronucleus was anterior to the CV-2 level in all of the cells. Nor were there any perceptible differences among three groups of cells in the amount of crystals or food vacuoles at the CV-2 level.

Studies on Penetrance of the Invaginated Phenotype and on a Phenocopy of this Mutant Trait Resulting from Centrifugation

Studies were performed on the effects of centrifugation, starvation and external Ca^{++} depletion on the penetrance of the invaginated phenotype in all three stocks. Hinrickson (personal com.) has observed invaginated cells in wild type after centrifugation. Results are presented in Table 4. Centrifugation increases the frequency of invaginated cells in

Table 4

The effects of starvation, Ca^{++} chelating medium, and centrifugation on the penetrance of the invaginated phenotype

Stock	Days	% of dividers	% of invaginated cells			
			C	C+ Centrif.	EDTA	EDTA + Centrif.
wild	2	3.2	0.0	1.3	0.0	0.0
	3	1.1	0.0	2.2	0.1	0.0
	4	0.2	0.0	0.4	0.0	0.0
	5	0.1	0.0	0.3	0.0	0.0
pw A	2	1.4	1.0	5.7	0.0	0.0
	3	2.9	1.4	4.2	0.0	0.0
	4	2.0	2.3	5.1	0.7	0.8
	5	0.2	4.8	6.9	0.5	0.7
pw B1	2	0.9	0.6	3.1	0.0	0.0
	3	1.3	0.6	2.5	0.0	1.0
	4	1.0	4.5	7.5	1.1	1.2
	5	0.9	4.0	6.0	1.0	1.0

Days = number of days since last fed, div = percentage of cells in cytokinesis, percentage of invaginated cells in a sample of at least 400 specimens among: C = untreated control cells, C + Centrif. = observations after centrifugation, EDTA = cells in Ca++ chelating medium, EDTA = Centrif. = the same after centrifugation

all stocks, but to higher levels in the pawns than in wild type. Invaginated wild type cells display the normal excitation after stimulation. EDTA decreases the frequency of invaginated phenotype in pawns, but

has no effect on wild type since invaginated cells do not occur in untreated wild type. Centrifugation of EDTA-treated cells has little or no effect. More invaginated cells occur in the untreated pawn cultures during later days of the experiment i. e., the longer since last feeding. This is correlated with a decrease in the frequency of dividing cells.

Effects of Various Media on Maintenance of Invagination and Recovery of Shape

Naturally occurring invaginated pawn B1 cells and those induced after centrifugation were used for this study (Table 5). Invaginated cells of pawn B1 were isolated singly in various media and observed 24 h later.

Table 5

The effects of 24 h incubation in various media on individually isolated *pw* B1 invaginated cells induced by centrifugation (Centrif), or spontaneously occurring in starved cultures (S)

Invagination induced by:	Medium used for incubation	n	No division in 24 h (phenotypes in %)		Division(s) in 24 h (phenotypes in %)	
			normal	invaginated	normal	invaginated proter
(1) Centrif.	F	40	5	5	87.5	2.5
(2) S	F	43	4,6	55.8	13.9	25.6
(3) S	F+DMSO	54	16.6	57,4	0	25.9
(4) S	F+DMSO+CB	49	12.2	83,7	0	4.1
(5) S	E	38	10.5	81,5	0	7.9

Media: E = exhausted medium, F = fresh culture medium, F + DMSO = fresh culture medium supplemented with 1% vol./vol dimethyldulfoxide, F + DMSO + CB = the same supplemented with 16 μ g/ml cytochalasin B. n = number of isolates. Other values expressed as the percentage of the total number of isolates in a given experiment

In fresh culture medium 81% of the spontaneously invaginated isolates remained invaginated and 60% of the isolates failed to divide; but among normal cells induced to invaginate by centrifugation, only 8% remained invaginated and only 10% failed to divide. Thus the invagination induced by centrifugation is much more readily reversed and interferes much less with growth and cell division. The other media were used only with spontaneously invaginated cells. Both cytochalasin B and exhausted media greatly inhibited their recovery of shape and cell division. Cytochalasin B does not induce shape transformation.

In vivo observation and examination of silvered specimens reveal that during cell division the invagination either evaginates or becomes shallower (Pl. II 6, 7). Morphogenesis seems to proceed quite normally.

No invagination persisted through two cell divisions in the progeny of 100 isolates. In some cases some slowing down of the process of cytokinesis was recorded in dividing invaginated cells.

Attempts to Change the Shape of Wild Type, normal and Invaginated Pawn B1 Cells by Agents that Induce Shrinkage or Contraction of the Normal Cells

The aim of this study was to induce shape transformation of the cell either by inducing anterior invagination in cells of normal morphology, or by inducing normal shape in invaginated cells (Table 6). In no case

Table 6

The effects of various procedures on cell shape

Stock	Hyper	K^+ medium	Dibuc	Dibuc+ K^+	Extr.	Extr.+Contr.
wild, normal	shrunken, no invagination	shrunken, no invagination	posterior contraction	posterior contraction	no change	posterior contraction
pw B1, normal	shrunken, no invagination	shrunken, no invagination	posterior contraction	posterior contraction	no change	posterior contraction
pw B1 invaginated	shrunken, sometimes evaginated	shrunken, sometimes evaginated	posterior contraction evaginated	posterior contraction invagination maintained	no change sometimes evaginated	posterior contraction and evagination

Explanation of columns: Hyper. = hypertonic medium, K+ = K+ rich medium, Dibuc. = dibucaine solution Dibuca + K+ medium = dibucaine solution in presence of 20 mM KCl, all media described in methods. Extr. and Extr. + Contr. = extraction medium and next followed by contraction medium according to Rinaldi et al. (1975) procedure. In rows: short characteristic of cell shape

could invagination be induced in morphologically normal cells of wild type or pawn B1 types by shrinkage or contraction procedures. In some of these procedures the invagination was maintained inspite of contraction of the posterior end or shrinkage of the cell.

Studies on the Rate of Endocytose and Exocytose of the Wild Type, Normal and Invaginated Pawn B1 cells

The statistical analysis of the data presented in Table 7 shows that there is a decrease in the number of ingested food vacuoles in invaginated pawn B1 cells at 35°C in comparison with the other groups. However,

Table 7

The number of food vacuoles formed during 5 min of feeding at various temperatures, and retained at 22°C after elapse of 30 and 60 min. Comparison of wild type with normal and invaginated pawn B1 cells. Number of tested cells is given in parentheses. L-0.95 confidence internal for each entry

Stock	Number of food vacuoles formed at temperature:			Number of food vacuoles remaining after:	
	35° L	27°C L	22° L	30 L	60 L
wild	4.2 0.4 (44)	6.0 0.2 (70)	4.9 0.2 (51)	2.0 0.5 (40)	0.2 0.2 (40)
pw B1, normal	3.2 0.5 (50)	5.0 0.3 (67)	4.6 0.6 (67)	2.3 0.4 (54)	0.8 0.4 (40)
pw B1, invaginated	1.6 0.8 (20)	4.9 0.5 (20)	4.9 0.5 (40)	3.1 0.5 (40)	2.4 0.5 (40)

these cells are able to perform phagocytosis at the normal rate at 22°C but they are slowed down in their defecation. It was observed at 22°C that some food vacuoles in the invaginated cells are trapped at the anterior end in the vicinity of the invagination; they are not released for a long time.

However, normal pawn B1 cells show the same rate of phagocytosis and exocytosis as control cells in all experiments. Electronograms of the invaginated pawn A cells demonstrated that their oral apparatus is unaffected. At the bottom of the cytopharynx disk-like bodies, microtubules and microfilaments show normal arrangement (Pl. II 8). All fibrillar structures of the oral apparatus as described by Allen (1974) were seen in the invaginated pawn cells.

Discussion and Conclusions

The pawn used here are unconditional: they are deprived of excitability under all tested conditions. Schein et al. 1976 suggested that gene *pw A* plays a role in depolarization sensitivity while gene *pw B* plays a role affecting either wall of the channel itself or the total number of channels. Despite of these differences both pawns, if well fed, manifest the normal general morphology, fine structure and development.

It is known that Ca^{++} flux affects an assembly of microtubules (Gallin and Rosenthal 1974). However, on the base of presented data it is assumed that ions flux after stimulation do not control fibrillogenesis, insertion of organelles and pattern formation in cortex of *Paramecium*.

Obviously pawns are capable of endocytose/exocytose cycle for they are able to survive. But the present studies establish that pawns are able for food vacuole formation at the normal rate. Hence capacity to reverse ciliary beat and voltage-dependent Ca^{++} entry are not involved in the control of this function. If one considers that pawn cells cilia are able to reverse if the concentration of the Ca^{++} is higher than 10^{-6} M (Kung and Naitoh 1973) it is suggested that the concentration of Ca^{++} beneath the cytostome membrane necessary to maintain the food vacuole formation is below this treshold value.

The normal rate of defecation observed in pawns proves that calcium action potential is irrelevant for the control of this kind of exocytosis of *Paramecium*.

Studies on pawns osmotically induced to shrink, relaxed with cytochalasin B and contracted during cytokinesis or after glycerination revealed that morphologically normal cells behave like wild type cells.

Irrelavance of the excitability for maintaining of the normal shape, ultrastructure and for duration of cytokinesis and for the rate of exocytosis are challenged by the spontaneously occurence of the sickle shaped cells among the pawn cells. Shape transformation of pawns represents a pleiotropic effect of *pw* mutation expressed only under some physiological conditions namely among the nondividing cells during starvation in the absence of chelating agent. This shape transformation is enhanced by centrifugation of cells. A phenocopy of this effect was received after centrifugation of wild type cells with no loss of their excitability. It follows from the above that there is a possibility of experimental dissection of the effect of block of excitability from the shape transformation.

Shape transformation is a transient phenomenon and is reversed under good culture conditions. As far as it was tested, transformed cells are not changed either in cortical pattern or in fine structures of organelles. Invaginated cortical layer and the infraciliary lattice do not reveal any contraction. The subsequent divisional morphogenesis of invaginated cell does not deviate from the normal its course even if in anterior daughter cell some slight invagination might still persist.

The change of the shape of *Paramecium* that occurs after contraction of the cell is characterized by (1) requirement of Ca^{++} in the external medium (Czarska 1965), (2) increase of the cell circumference (Miller et al. 1968), (3) preferential contraction of the posterior end of the cell (Miller et al. 1968, Browning and Nelson 1976) due to contraction of the ectoplasmic tube (Czarska 1965) possibly localized in the infraciliary lattice filaments (Sibley and Hanson 1974), (4) contraction of the contractile vacuoles (Miller et al. 1968), (5) extrusion of trichocysts (Plattner and Fuchs 1975).

Change of shape by anterior invagination shares two common features with these for contraction: cell diameter slightly increase and the shape change is inhibited by the chelating agent and by calcium poor medium, but differs in other respects. Anterior invagination is not a simple effect of decrease in cell volume because osmotically shrunken cells do not fold their cortex like pawn cells.

Invaginated cells in comparison to the morphologically normal pawns differ in: (1) displacement of the cell cytoplasm retracted from the anterior end of the cell, (2) slight increase of cell diameter, (3) possible decrease in the cell volume, and (4) high optic density of posterior part of the cell, probably by increase of optic density of the cytoplasm itself. This results rather from change of the state of the cytoplasm than from the new kind of synthesis during transformation since the shape transformation may occur after brief centrifugation of wild type cells.

Invaginated glycerinated model evaginates. This might result from an expansion of the glycerinated model (O p a s 1976). *In vivo* cell may retain both the invaginated anterior end and contracted its posterior part. The shape transformation does not result from ATP induced contraction of the glycerinated model of a normal pawn B1 cell. The mechanism(s) of this phenomenon and its polarity are not known. A polar effect does not involve the compartmentalization of alveoles supposed (A l l e n and E c k e r t 1969) to store Ca^{++}.

Shape transformation occurs in some only pawn cells (1–5%) even under proper culture conditions. Therefore it is suggested that some internal prerequisites which renders transformation possible are not permanently present in a given cell.

Spontaneous shape transformation of pawns is the first case of predictable change of shape of *Paramecium* due to directional changes inside the cytoplasm and not under the morphogenetic control of the cortex.

ACKNOWLEDGMENTS

I acknowledge my debt to Doctor Tracy M. Sonneborn, especially for his encouragement, patience and many corrections of manuscript and for generous hospitality during my stay in USA.

I thank Doctor Joseph Frankel for his comments and suggestions and corrections of manuscript. I thank people from EM Unit of Department of Cytology at Warsaw University and Mister Adamiec for help in making EM studies and dry mass measurements.

Grateful acknowledgment is expressed to Doctor Ching Kung for permission to use his mutants for the present studies. This work was supported in part by U.S.N.S.C. grant No 2440 to Doctor Sonneborn and by grant of Polish Academy of Sciences MR II.1.3.7.

RÉSUMÉ

Chez les mutants de *Paramecium tetraurelia* appelés "pawns" il y a un blocus du passage de Ca++ par la membrane céllulaire en fonction du voltage (Kung 1975). Ce défaut de la membrane n'a pas d'effet sur la morphologie corticale, sur la morphogénèse, ni sur le système de l'endocytose et de l'exocytose.

Les changements spontanés de forme observés chez les "pawns" privés de nourriture concernent le déplacement du cytoplasme vers l'extrémité postérieure de la céllule et l'augmentation de la densité optique de cette région. Le phénomène est différent d'une contraction de la céllule provoguée par les facteurs chimiques. Il présente un effet pléiotropique de la mutation "pawn" dont la distinction de son effet sur l'électrogénese active est mis en évidence de manière expérimentale.

REFERENCES

Allison A. C., Davies P. and de Petris S. 1971: Role of contractile microfilaments in movement and endocytosis. Nat. New Biol., 232, 153–155.

Allen R. D. 1971: Fine structure of membraneous and microfibrillar systems in the cortex of *Paramecium caudatum*. J. Cell Biol., 49, 1–20.

Allen R. D. 1974: Food vacuole membrane growth with microtubule associate membrane transport in *Paramecium*. J. Cell Biol., 63, 904–922.

Allen R. D. and Eckert R. 1969: A morphological system in ciliates comparable to the sarcoplasmic reticulum transverse tubular system in striated muscle. J. Cell Sci., 43, 4a.

Berger J. D. 1976: Gene expression and phenotypic change in *Paramecium tetraurelia* exconjugants. Genet. Res., 27, 123–134.

Browning J. L. and Nelson D. L. 1976: Amphipathic amines effect membrane excitability in *Paramecium*: Role for bilayer couple. Proc. Nat. Acad. Sci. USA, 73, 452–456.

Chang S. Y., Van Houten J., Guyer L. R., Lui S. S. and Kung C. 1974: An extensive behavioural and genetic analysis of the pawn mutants in *Paramecium aurelia*. Genet. Res., 23, 165–173.

Czarska L. 1965: Cytoplasmic streaming in *Paramecium caudatum* exposed to electric field. Acta Protozool., 3, 69–75.

Cronkite D. L. 1974: Genetics of chemical induction of conjugation in *Paramecium aurelia*. Genetics, 76, 703–714.

Davis M. D. and Hadley M. E. 1976: Spontaneous electrical potentials and pituitary hormone (MSH) secretion. Nature, 261, 422–423.

Dippell R. V. 1955: A temporary stain for paramecium and other ciliate protozoa. Stain Technol., 30, 69–71.

Dryl S. 1959: Antigenic transformation in *Paramecium aurelia* after homologous antiserum treatment during conjugation or autogamy. J. Protozool., 6, 25.

Ehret C. F. and Mc Ardle E. W. 1974: The structure of *Paramecium* as viewed from its constituents levels of organization. In: *Paramecium*-A current survey (ed. V. J. van Wagtendonk), Elsevier Publ. Co., Amsterdam, pp. 263–338.

Eckert R. and Naitoh Y. 1972: Bioelectric control of locomotion in ciliates. J. Protozool., 19, 237–243.

Frankel J. and Heckmann K. 1968: A simplified Chatton–Lwoff silver impregnation procedure for use in experimental studies with ciliates. Trans. Microsc. Soc., 87, 317–321.

Gallin J. I. and Rosenthal A. S. 1974: The regulatory role of divalent cations in human granulocyte chemotaxis. Evidence for an association between calcium exchanges and microtubule assembly. J. Cell Biol., 62, 594–609.

Joseffson J. O. 1975: Studies on the mechanism of induction of pinocytosis in *Amoeba proteus*. Acta physiol. scand. Suppl., 432, 1–65.

Jurand A. and Selman G. G. 1969: The anatomy of *Paramecium aurelia*. Macmillan, London and St. Martin's Press, New York.

Kaneda M. and Hanson E. D. 1974: Growth patterns and morphogenetic events in the cell cycle of *Paramecium aurelia*. In: *Paramecium*-A current survey (ed. V. J. van Wagtendonk), Elsevier Publ. Co., Amsterdam, pp. 219–262.

Kidokoro Y. 1975: Spontaneous calcium action potentials in a clonal pituitary cell line and their relationship to prolactin secretion. Nature, 258, 741–742.

Kirschner M. W., Williams R. C., Weingarten M. and Gerhardt J. C. 1974: Microtubules from mammaliam brain: some properties of their depolimerization products and a proposed mechanism of assembly and dusassembly. Proc. Nat. Acad. Sci. USA, 71, 1159–1163.

Kung C. 1971 a: Genic mutations with altered system of excitation in *Paramecium aurelia*. II. Mutagenesis, screening and genetic analysis of the mutants. Genetics, 69, 29–45.

Kung C. 1971 a: Genic mutations with altered system of excitation in *Paramecium aurelia*. I. Phenotypes of the behavioural mutants. Z. Vgl. Physiol., 71, 142–164.

Kung C. 1975: Genetic dissection of the excitable membrane of *Paramecium*. Genetics, 79, 413–423.

Kung C. and Eckert R. 1972: Genetic modifications of electric properties in an excitable membrane. Proc. Nat. Acad. Sci. USA, 69, 93–97.

Kung C. and Naitoh Y. 1973: Calcium induced ciliary reversal in the extracted models of "Pawn" a behavioural mutant of *Paramecium*. Science, 179, 195–196.

Miller D. M., Jahn, T. L. and Fonseca, J. R. 1968: Anodal contraction of *Paramecium* protoplasm. J. Protozool., 15, 493—497.

Ostrowski K., Darżynkiewicz Z., Sawicki W. and Stocka Z. 1963: The possibilities of application of the new model of interference microscope (MPI) in biological research. Folia Histochem. Cytochem., 1, 553–557.

Opas M. 1976: Course of glycerination of *Amoeba proteus* and contraction of glycerinated models. Acta Protozool., 15, 485–499.

Plattner H. 1976: Membrane disruption, fusion and resealing in the course of exocytosis in *Paramecium* cells. Exp. Cell Res., 163, 431–435.

Plattner H. and Fuchs S. 1975: X ray microanalysis of a calcium binding sites in *Paramecium* with special reference to exocytosis. Histochem., 45, 23–49.

Preer J. R. 1975: The hereditary symbionts of *Paramecium aurelia*. Soc. Exp. Biol., 29, 125–144.

Rinaldi R., Opas M. and Hrebenda B. 1975: Contractility of glycerinated *Amoeba proteus* and *Chaos chaos*. J. Protozool., 22, 286–292.

Schein S. J., Bennett M. V. L. and Katz G. M. 1976: Altered calcium conductance in pawns behavioural mutants of *Paramecium aurelia*. J. Exp. Biol., 65, 699–724.

Schneider L. 1960: Elektronenmikroskopische Untersuchungen ueber das Nephridialsystem von *Paramecium*. J. Protozool., 7, 75–90.

Sibley J. T. and Hanson E. D. 1974: Identity and function of a subcortical cytoskeleton in *Paramecium*. Arch. Protistenk., 116, 221–235.

Sonneborn T. M. 1950: Methods in the general biology and genetics of *Paramecium aurelia*. J. Exp. Zool., 113, 87–148.

Sonneborn T. M. 1970: Methods in *Paramecium* research. In: Methods in Cell Physiology 4 (ed. D. M. Prescott), Academic Press N. Y. and London, pp. 241–339.

EXPLANATIONS OF PLATES I–II

1: Silvered specimen of *Paramecium tetraurelia* pawn A. A normal well fed cell
2: Silvered specimen of pawn A. A starved invaginated cell. An invagination of the anterior part of the cell is clearly seen
3: A transverse section through an invaginated pawn A cell. This section extends through an engulfed pocket (IP). The external cortical layer and engulfed folded cortical layer (ICL) leaves little space between for the remaining cytoplasm with its constituents. Fragment of section through a folded bottom of the pocket (BIP) is also seen. (EM 3000 ×)
4: The fragment of a transverse section through an invaginated pawn A cell, showing an invagination (IP) made at the level of the anterior contractile vacuole pore (CVP-1). The narrow space between the external cortical layer and the engulfed part of the cortex (ICL) is occupied by exretory system (CV). (EM 15 000 ×)
5: A section through the cortical layer of a pawn A cell fixed after preincubation (Allen 1971). Between two adjacent alveoli (A_1 and A_2) a septum (arrow) with a narrow interalveolar pore in its upper part is visible. This pore, however, is slightly shadowed with some electron dense material (EM 44 000 ×)
6: Silvered specimen of an invaginated pawn A cell. An advanced divider with the engulfed anterior part
7: Silvered specimen of an invaginated pawn A cell. Specimen fixed in early cytokinesis, probably during recovery of the normal shape. The shallow anterior invagination is clearly asymmetric
8: Fragment of the bottom of the oral apparatus of pawn A cell. A normal appearance of the sectioned cilia (C), disk-bodies (DB) involved in food vacuole formation, bundles of microtubules (MT) and microfilaments (MF). (EM 33 000×)

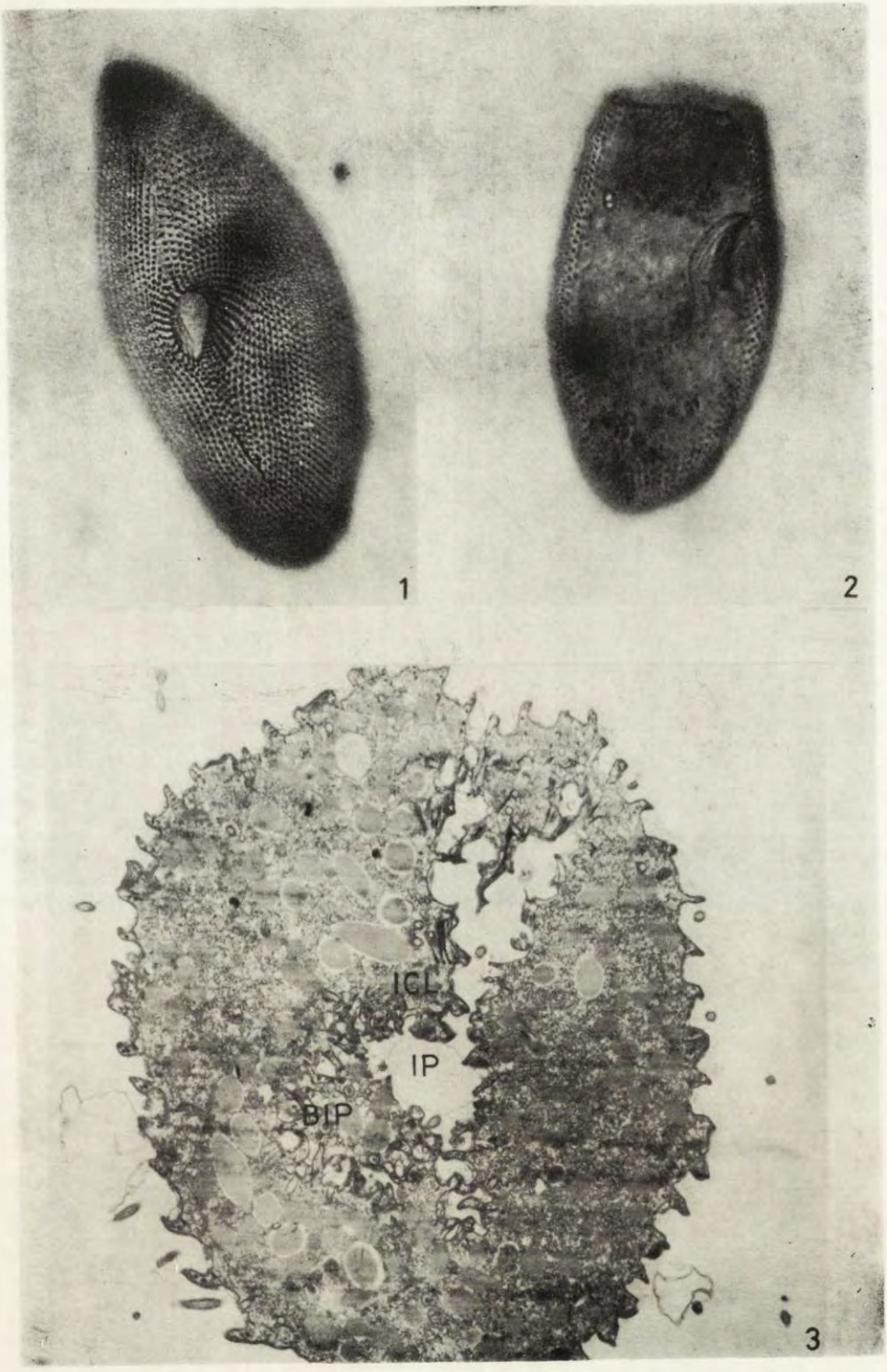

J. Kaczanowska auctor phot.

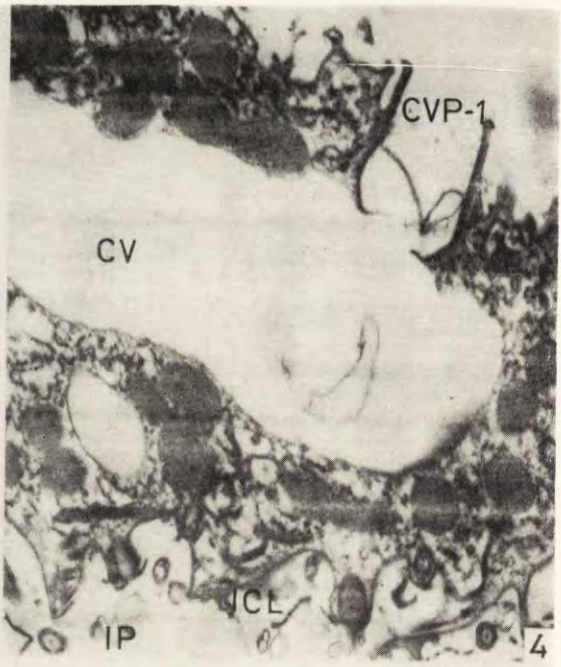

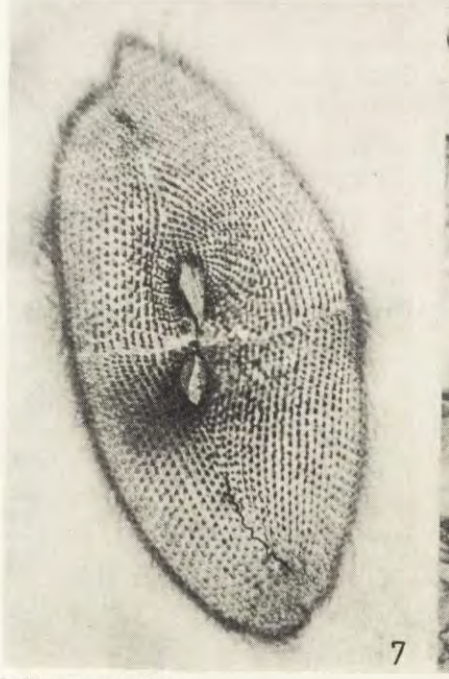

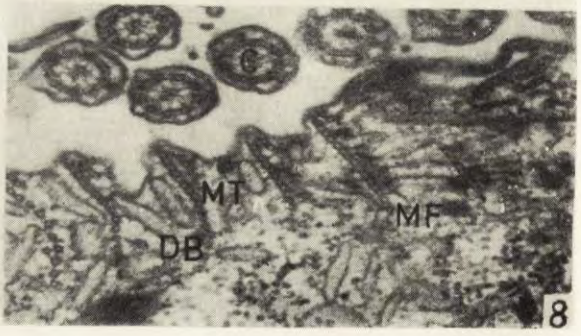

J. Kaczanowska auctor phot.

ACTA PROTOZOOLOGICA
VOL. 17 (No. 2) WARSZAWA, 30 VI 1978 pp. 321–330

Биологический институт Ленинградского Государственного Университета, Даборатория Зоологии беспозвоночных, Старый Петергоф Ленинградской области, Ораниенбаумское шоссе 2, СССР
Laboratory of Inverterbrate Zoology, Biological Research Institute, Leningrad State University, Leningrad 164, USSR

И. И. СКОБЛО, М. С. РАУТИАН и Д. В. ОСИПОВ
I. I. SKOBLO, M. S. RAUTIAN and D. V. OSSIPOV

Потеря генеративных ядер у инфузории *Paramecium caudatum* вызываемая на ранних стадиях инфекции их симбиотическими бактериями

The Loss of the Generative Nuclei in *Paramecium caudatum* during Early Stages of Infection by Symbiotic Bacteria

Синопсис. В работе экспериментально исследуется вопрос о возможности получения Ми$^-$ клеток инфузории *Paramecium caudatum* в результате заражения Ми симбиотическими бактериями — омега-частицами, характеризующимися строго специфичной локализацией в Ми. Опыты по заражению „чистых" парамеций 4-х клонов гомогенатом, приготовленным из инфицированных клеток, показали, что при высоких концентрациях частиц, кроме зараженных клеток, появляются Ми$^-$ клетки, доля которых в культуре может достигать 100%. Получены экспериментальные доказательства истинной амикронуклеарности таких клеток. Таким образом, заражение омега-частицами можно использовать как эффективный способ получения Ми$^-$ клеток из любого нормального клона *P. caudatum*, что важно для проведения исследований морфо-функциональной дифференцировки ядер инфузорий. Обсуждается обнаруженное явление снижения жизнеспособности у Ми$^-$ клеток и, как следствие, низкая частота (1,25%) получения Ми$^-$ клонов с помощью предложенного метода.

В последнее десятилетие в протозоологической литературе широко обсуждается вопрос об активности генеративного ядра инфузорий микронуклеуса (Gorovsky 1973, Борхсениус 1975). Этот вопрос выходит за рамки чисто протозоологических проблем, поскольку исследователи все шире начинают использовать простейших как модельные объекты при изучении механизмов, регулирующих активность ядра (Allen and Gibson 1972, Gorovsky et al. 1973, Prescott et al. 1973, Lipps et al. 1974, Yao and Gorovsky 1974, Yao et al. 1974). Особый интерес к инфузориям в этом отношении вызван тем, что у этих организмов в цитоплазме одной клетки присутствуют ядра двух

типов: активно синтезирующий РНК высокополиплоидный Ма и полностью неактивный, или активный в очень малой степени, Ми. Совершенно очевидно, что все данные, касающиеся функциональной активности Ми приобретают чрезвычайный интерес. При исследовании этого вопроса используется несколько подходов: (1) методы количественной цитохимии, биохимии и авторадиографии, позволяющие определять интенсивность синтеза РНК в Ми (Gorovsky 1973); (2) сравнительные электронномикроскопические исследования ультраструктуры Ма и Ми (Винникова 1974); (3) создание клеточных линий — гетерокарионов инфузорий, у которых Ма и Ми различаются по какому-то гену, фенотипическое проявление которого можно контролировать (Sonneborn 1966); и (4) получение Ми⁻ инфузорий и анализ изменений клеточных функций, которыми сопровождается утрата Ми (Wells 1961, Ammermann 1970).

В данной работе обсуждается вопрос о возможности получения Ми⁻ клонов инфузорий *Paramecium caudatum* в результате заражения Ми симбиотическими бактериями — омега-частицами. Эти симбионты ядерного аппарата инфузорий были описаны нами ранее (Осипов и Ивахнюк 1972). Омега-частицы — грамотрицательные бактерии, способные жить и размножаться только в Ми *P. caudatum*. Ни цитоплазма, ни Ма зараженных парамеций не содержат омега-частиц. Добавления к инфузориям „чистого" клона неочищенного гомогената зараженных клеток достаточно, чтобы заразить его Ми омега-частицами. Более подробное изучение начальных стадий инфекции показало, что помимо зараженных, появляются клетки с различными изменениями числа и размеров Ми, а у части клеток Ми вообще не удается цитологически обнаружить (Раутиан и др. 1975). Невозможность выявить Ми при ядерных окрасках еще нельзя считать надежным доказательством отсутствия Ми в этих клетках. Во-первых, можно допустить существование неизвестной стадии заражения омега-частицами, когда Ми цитологически не выявляется специфическими ядерными красителями; во-вторых, не исключено, что в результате заражения Ми происходит элиминация значительной части ДНК, в результате чего может резко снизиться способность зараженных ядер окрашиваться по Фельгену. Опыты по заражению чистых клеток гомогенатом, содержащим определенную концентрацию спиралевидных омега-частиц (Раутиан и др. в печати), показали, что при концентрациях выше $1 \cdot 10^6$ частиц/см^3 более 90% инфицированных клеток становятся Ми⁻, тогда как при концентрациях ниже $1 \cdot 10^3$ — $1 \cdot 10^4$ частиц/см^3 образуются лишь единичные Ми⁻ клетки, а основная масса парамеций инфицированной культуры проходит обычные стадии развития инфекциии (Раутиан и др. 1975).

Таким образом, в любом клоне *P. caudatum* оказалось возможным получать клетки, лишенные нормального Ми, однако вопрос об истинной амикронуклеарности таких инфузорий пока оставался открытым. В настоящей

работе несколькими способами получены экспериментальные доказательства того, что инфекция омега-частицами при определенных концентрациях действительно приводит к утрате Ми.

Материал и методы

В работе использованы 4 клона *P. caudatum*: М-201; М-209; М-319 и М-339, относящиеся к двум типам спаривания одного сингена. Все эти клоны имеют Ми дикого типа. В качестве клона, содержащего омега-частицы, использовали культуру М-209-3-омега, полученную в результате экспериментального заражения и последующего клонирования клона М-209.

Все манипуляции с клетками — культивирование в пробирках, клонирование, скрещивание клонов комплементарных типов спаривания — проводили общепринятыми для парамеций способами (Sonneborn 1970).

Заражение омега-частицами культур парамеций с нормальными Ми проводили следующим образом: к 2 мл суспензии клеток „чистого" клона добавляли 1 мл гомогената клеток М-209-3-омега, приготовленного по методу Прир (Preer 1969). Предварительно в камере Горяева определяли концентрацию омега-частиц инфекционной стадии в данной порции гомогената. Опыты проведены с 3 независимо приготовленными порциями гомогената, концентрация частиц в них была от $1 \cdot 10^6$ до $3 \cdot 10^6$ омега-частиц/см^3. Клон М-339 заражали симбионтами в 3-х повторностях, три другие клона — по одному разу.

Выведение симбионтов из зараженных Ми достигалось обработкой раствором пенициллина. В пробирку с культурой зараженных клеток добавляли равный объем раствора пенициллина в концентрации 20 мкг/мл, т.е. окончательная концентрация антибиотика в культуральной среде оказывалась 10 мкг/мл. Эту процедуру повторяли ежедневно в течение 10 дней.

Для определения соотношения числа клеток, с определенными особенностями ядерного аппарата, в инфицированной культуре производили подсчет клеток на тотальных препаратах, окрашенных по Фельгену. Препараты парамеций просматривали на микроскопе Amplival при увеличении объектива 40× и 100× и окуляра — 10×. При этом клетки, в которых Ми не выявлялся, относили в класс Ми$^-$, клетки с Ми морфологически не отличимыми от дикого типа, считали не зараженными, те же, в которых Ми находился на любой стадии заражения омега-частицами (Раутиан и др. 1975), попадали в класс Ми-омега.

Результаты и обсуждение

В работе изучены последствия заражения 4-х клонов *Paramecium caudatum* омега-частицами в концентрации 1.10^6 — 3.10^6 частиц/см^3. Через сутки после заражения в большинстве клеток всех исследованных клонов Ми цитологически не выявлялись (Табл. 1). Как видно из приведенных результатов, относительное количество Ми$^-$ клеток очень велико, хотя во всех случаях (кроме одного варианта заражения клона М-209) в некоторой части популяции клеток Ми хорошо виден, т.е. культура оказывается смешанной. Стремясь получить чистую линию Ми$^-$ клеток, мы проклонировали некоторые из полученных после заражения омега-частицами культуры; полученные результаты представлены в Табл. 2.

Таблица 1

Table 1

Доля амикронуклеарных клеток *Paramecium caudatum* через сутки после момента заражения „чистых" клонов омега-частицами

Frequency of amicronuclear *Paramecium caudatum* cells 24 h after beginning of infection of „free" clones by omega-particles

Индекс клона Index of clone	Число клеток с нормальными Ми Number of cells with normal Mi	Число Ми⁻клеток Number of amicronuclear cells	Доля Ми⁻ клеток в процентах Frequency of amicronuclear cells (%)
М-339*	37	163	81
„ „	51	49	49
„ „	34	66	66
М-319	58	142	71
М-201	39	161	80
М-209	0	400	100

* Для клона М-339 приведены результаты трех повторностей опыта.
* The data of three experimental repetitions for clone M-339.

Таблица 2

Table 2

Результаты клонирования смешанных культур, полученных в результате заражения „чистых" клонов *Paramecium caudatum* омега-частицами

The data of cloning of mixed cultures, resulted from infection of "free" *Paramecium caudatum* clones by omega-particles

Индекс клона Index of clone	Число проклонированных клеток Number of cloned cells	Число полученных субклонов Number of obtained sub-clones			Доля нежизнеспособных клеток в скобках в процентах Part of nonviable cells (%)
		с нормальными Ми with normal micronuclei	с зараженными Ми with infected micronuclei	Ми⁻ without micronuclei	
М-339*	80	0	5	0	75 (95.5%)
„ „	40	4	10	1	25 (62.5%)
„ „	40	10	5	1	24 (60.0%)
М-319	80	2	12	0	66 (82.5%)
М-201	80	2	5	4	69 (86.0%)
М-209	160	0	0	0	160 (100%)

* Для клона М-339 приведены результаты трех повторностей опыта.
* The data of three experimental repetitions for clone M-339.

Обращает на себя внимание крайне низкая эффективность клонирования смешанных культур: от 60 до 100% клеток не могли дать жизнеспособный клон. Из 480 зараженных и клонируемых клеток удалось получить только 61 жизнеспособный субклон (12.71%), из них: с нормальными Ми — 18, с инфицированными омега-частицами ядрами — 37 и только 6 (1.25%) — Ми⁻ субклонов. Таким образом, от всех жизнеспособных субклонов (61) доля Ми⁻ составляет всего 9.84%. Все полученные Ми⁻ субклоны имели низкий темп деления и при культивировании их в пробирках плотность клеточной популяции была очень невысокой. В большинстве случаев, через некоторое время Ми⁻ клоны погибали. Все это делало невозможным проведение с ними дальнейшей экспериментальной работы. Поэтому последующие опыты были проделаны на неклонированной культуре Ми⁻ клеток, полученной после заражения омега-частицами клона М-209 (Табл. 1), которая в дальнейшем будет называться М-209-Ми⁻.

В течение 2–3 месяцев после заражения омега-частицами культура М-209-Ми⁻ имела заметно сниженную жизнеспособность. Однако через 3–4 месяца темп деления клеток восстановился, количество уродливых делений клеток уменьшилось, оказалось возможным получить высокую плотность культуры, необходимую для последующих опытов. Несмотря на такие физиологические изменения с клетками М-209-Ми⁻, на препаратах которые приготовлялись ежемесячно в течение года, никогда не встречались клетки с чистым или зараженным Ми. Помимо повторных визуальных исследований препаратов клеток М-209-Ми⁻, были предприняты три типа опытов, преследовавших цель доказать, что клетки этой культуры лишены микронуклеуса.

(1) Поведение клеток культуры М-209-Ми⁻ при конъюгации. Ранее нами было показано, что зараженные омега-частицами клетки не способны вступать в половой процесс (Осипов и др. 1974). На этом основании мы ожидали, что если клетки М-209-Ми⁻ будут конъюгировать с парамециями комплементарного типа спаривания, следовательно, они не содержат симбионтов и либо лишены Ми, либо имеют „чистый" Ми, который не выявляется по Фельгену вследствие малого содержания ДНК. Решить, какая из двух названных возможностей имеет место, можно по характеру фрагментации Ма. Известно, что при конъюгации двух Ми⁻ партнеров, распадающийся старый Ма при фрагментации не образует вытянутых лент, как в норме, а сразу распадается на фрагменты, сильно различающиеся по величине, и потомство от такого скрещивания не жизнеспособно (Скобло 1969). Если же хотя бы один из партнеров имеет Ми, и в конъюгирующих парах происходит миграция пронуклеуса, то наблюдается нормальная фрагментация старого Ма, и эксконъюганты обычно дают начало жизнеспособным клонам (Осипов и Скобло 1973).

Исходя из этих посылок был проведен следующий опыт. В один микроаквариум сливали культуру парамеций М-209-Ми⁻ и комплементарную по

типу спаривания — М-201, имеющую нормальный Ми. Наблюдалась активная реакция агглютинации и образовывались конъюгирующие пары. Это доказывает, что клетки М-209-Ми⁻ не инфицированы омега-частицами. В другом варианте, клетки М-201 заражали омега-частицами в концентрации $1 \cdot 10^6$ омега-частиц/см³. Через 30 часов после заражения в 98% клеток Ми цитологически не выявлялся. Эту культуру использовали в качества Ми⁻ партнера в скрещивании с М-209-Ми⁻. Точно так же, как в предыдущем случае, наблюдалась реакция агглютинации и образование пар. Через восемь часов после начала конъюгации 60 пар были отловлены и рассажены по одной в микроаквариумы. То же было проделано с 40 парами в контрольном скрещивании исходных клонов М-201 х М-209. Через 20 часов, когда партнеры разошлись, но еще не успели поделиться, их рассадили в отдельные микроаквариумы, В контроле 61 из 80 экскоңъюгантов дали жизнеспособные клоны, тогда как в опыте гибель экскоңъюгантов была 100%.

Цитологические наблюдения на стадии 36 и 48 часов конъюгации показали, что в скрещивании М-209-Ми⁻ х М-201-Ми⁻ фрагментация Ма происходила ненормально — по амикронуклеарному типу. Таким образом, изучение способности клеток М-209-Ми⁻ вступать в конъюгацию и анализ особенностей ядерной реорганизации доказывают, что клетки М-209-Ми⁻, действительно, лишены Ми.

(2) Повторное заражение омега-частицами клеток культуры М-209-Ми⁻. Характерной особенностью омега-частиц является их строго специфическая локализация в Ми. Проведенные ранее эксперименты показали, что Ми⁻ клоны никогда не заражаются омега-частицами, тогда как клоны, содержащие Ми, могут быть заражены, независимо от количества ДНК в Ми (Осипов 1975). В частности, даже клоны с крайне малым содержанием ДНК в Ми (в 13 раз меньше, чем в Ми дикого типа) заражаются омега-частицами. В таких клонах парамеций Ми, бедные ДНК, с большим трудом выявляются при окраске по Фельгену, и видны только в небольшом числе клеток клона. Однако, после заражения симбионтами, Ми значительно увеличиваются в объеме и хорошо заметны благодаря присутствию большого количества сильно преломляющих свет омега-частиц (Осипов и Ивахнюк 1972), поэтому способность клона *P. caudatum* к заражению омега-частицами может служить весьма чувствительным тестом на присутствие в его клетках Ми.

Нами было проведено 4 повторных опыта по заражению культуры М-209-Ми⁻ омега-частицами в концентрации $1 \cdot 10^4$ омега-частиц/см³. Эта концентрация в контроле — при заражении „чистого" клона М-209 — неизменно вызывала обычную картину инфекции; в то же время в культуре М-209-Ми⁻ зараженные клетки никогда не появлялись.

(3) Действие пенициллина на клетки культуры М-209-Ми⁻. Ранее установлено, что омега-частицы чувствительны к ряду антибиотиков, в частности к пенициллину: в широком диапазоне концентраций (от 0.1 мкг/мл до 200 мкг/мл) пенициллин приводит к потере симбионтов из зараженной

клетки, не оказывая видимого действия на инфузорию (Ивахнюк 1976). После потери омега-частиц, в освободившихся клетках начинают выявляться „чистые" Ми, морфологически резко отличные от исходных ядер: они вытянуты по продольной оси, слабо окрашиваются по Фельгену (Осипов и др. 1975, Ивахнюк 1976).

В наших опытах парамеций трех клонов *P. caudatum*: М-209, М-209-3-омега, М-209-Ми⁻ обрабатывали пенициллином. Антибиотик не оказывал никакого заметного действия на клетки клона М-209: парамеции нормально делились, и не изменялись ни форма, ни размер Ми. В клетках М-209-3-омега под действием пенициллина происходила потеря симбионтов, и через 10 суток после начала обработки в 94% клеток не было характерных зараженных Ми. Цитологически в 52% клеток можно было обнаружить „чистый" Ми, как правило, ланцетовидной формы и бледно окрашенный по Фельгену. В противоположность этому, обработка пенициллином не вызывала изменений в культуре М-209-Ми⁻ — в клетках не появлялось никаких структур, которые можно было бы отождествлять с „чистыми" Ми. Это является еще одним доказательством отсутствия Ми в клетках культуры М-209-Ми⁻.

Приведенные эксперименты показывают, что в результате заражения *P. caudatum* омега-частицами (при высокой концентрации их в гомогенате) возникают клетки, утратившие Ми. Об этом свидетельствуют все полученные результаты:

(1) В таких клетках невозможно выявить Ми цитологически на фельгеновских препаратах.

(2) Возникшие Ми⁻ клетки способны вступать в конъюгацию, и в эксконъюгантах происходит типичная для Ми⁻ клеток аномальная фрагментация Ма, потомство таких клеток нежизнеспособно.

(3) Клетки Ми⁻ не способны поддерживать омега-частицы при повторной инфекции.

(4) Обработка Ми⁻ клеток пенициллином не вызывает таких изменений, как у инфицированных омега-частицами клеток.

Каков механизм утраты генеративного ядра — блок митотической активности, ненормальное распределение делящихся ядер по дочерним клеткам, асинхронность деления Ми и клетки, деструкция его в момент проникновения симбионтов или в результате их жизнедеятельности в ядре — пока остается неизученным. Однако, каким бы путем ни происходила потеря генеративного ядра, и, тем самым, образование Ми⁻ клеток, крайне заманчиво использовать этот метод для получения Ми⁻ клеточных линий от любого клона *P. caudatum*.

К настоящему времени известен ряд способов получения жизнеспособных Ми⁻ клонов инфузорий:

(1) выделение из природных популяций;

(2) выделение из лабораторных культур от спонтанно возникающих Ми⁻ клеток;

(3) получение эксконъюгантных Ми⁻ клеточных линий в результате аномального полового процесса;

(4) при микрургическом удалении Ми;

(5) после тотальной обработки Х-лучами или жестким ультрафиолетовым светом (Фокин и Осипов 1975);

(6) в результате локального УФ микрооблучения генеративного ядра;

(7) после обработки клеток некоторыми веществами, например, растворами мочевины (см. обзор: Борхсениус 1975).

Каждый из этих способов, имея свои преимущества, обладает теми или иными недостатками. Например, выделение спонтанно возникающих Ми⁻ клеток из природных популяций или лабораторных культур, как процесс случайный, затрудняет направленное получение Ми⁻ клеточных линий от заранее выбранных клонов. В ходе полового процесса происходит перестройка всего ядерного аппарата, в том числе и Ма, что лишает возможности получать пары клонов, различающиеся только наличием-отсутствием Ми. Тотальная обработка клеток Х-лучами или УФ вызывает глубокие изменения во всех клеточных органеллах и особенно в Ма. Более мягким является локальное УФ облучение, однако недостаток метода состоит в трудоемкости, т.к. приходится работать с индивидуальными клетками на специальных установках. Микрургическое удаление может быть применимо только для ограниченного числа видов инфузорий с особыми механическими свойствами клеточной оболочки и цитоплазмы.

Получение Ми⁻ клеток в результате инфекции омега-частицами „чистого" Ми, методически крайне просто и удается со всеми проверенными клонами, однако, благодаря видовой инфекционной специфичности симбионтов (Осипов 1973) — только на одном виде инфузорий — *P. caudatum*. Каков характер действия симбионтов на хозяина, на какие органеллы или функции клетки влияют омега-частицы? В настоящее время по этому поводу можно высказывать только спекулятивные соображения, т.к. конкретные взаимоотношения симбионта и хозяина изучены совершенно недостаточно. Тем не менее следует учитывать строгую избирательность омега-частиц по отношению к Ми. В случае инфекции, когда симбионты активно развиваются в ядре, их взаимоотношения с клеткой, безусловно, многоплановы. Например, присутствие симбионтов в Ми блокирует способность парамеции вступать в половой процесс, а известно, что вещества спаривания, ответственные за эту реакцию, синтезируются под контролем генов Ма (Осипов и др. 1974). Но после спонтанной или индуцированной потери симбионтов способность к конъюгации восстанавливается, следовательно, возникающее нарушение обратимо. В случае же потери Ми в результате заражения омега-частицами мы склонны считать, что Ми является единственной мишенью, на которую действуют симбионты, не вызывая необратимых изменений в других структурах клетки-хозяина.

Кажется, что сделанный вывод противоречит данным о низкой жизнеспособности получающихся Ми⁻ клеток. Однако при обсуждении этого вопроса необходимо учитывать, что потеря Ми очень часто ведет к снижению жизнеспособности инфузорий. Многие авторы, пытавшиеся получить Ми⁻ клоны самыми разными методами, приводят данные о резком снижении у них темпа деления, увеличении числа аберраций клеточных делений и, в конечном счете, снижении жизнеспособности (Wells 1961, Ammermann 1970, Осипов 1966, Борхсениус 1975, Борхсениус и Осипов 1978).

SUMMARY

In the present study attempts have been made to obtain experimentally amicronucleate (Mi⁻) cells of *Paramecium caudatum* as a result of infection of the micronuclei (Mi) of "pure" clones by symbiotic bacteria — omega-particles. The latters characterize rigorously specific localization — only in Mi. "Pure" paramecia of four clones were infected with cell homogenate containing $1 \cdot 10^6 - 3 \cdot 10^6$ "spores"/ml. One day after beginning of experiment the portion of infected Mi— cells in culture attained 100% in single cases. Experimental evidences of real amicronucleation of cell have been given by three means in such paramecium cultures. Thus, the infection by omega-particles may be used as an effective method for obtaining Mi— cells from any one normal clone of *P. caudatum*. This phenomenon is a promising mean for research of morpho-functional nuclear differentiation in ciliates. The fact of decreased vitality in Mi— cells and, in consequence, too low frequency (1.25%) of obtaining vigorous Mi— clones by means of proposed method is discussed.

ЛИТЕРАТУРА

Allen S. and Gibson I. 1972: Genome amplification and gene expression in the ciliate macronucleus. Biochem. Genet., 6, 293–313.

Ammermann D. 1970: The micronucleus of the ciliate *Stylonychia mytilus*: its nucleic acid synthesis and its function. Expl. Cell Res., 61, 6–12.

Борхсениус О. Н. 1975: К вопросу об активности генеративного ядра инфузорий. Вестн. ЛГУ, сер. биол., 21,7–16.

Борхсениус О. Н. и Осипов Д. В. 1978: Влияние избирательной инактивации генеративного ядра инфузории *Paramecium caudatum* на жизнеспособность клеток. Acta Protozool., 15, 331–345.

Фокин С. Н. и Осипов Д. В. 1975: Влияние локального УФ микрооблучения на ядерный аппарат и цитоплазму инфузорий *Paramecium caudatum*. Цитология, 17, 9, 1073–1080.

Gorovsky M. A. 1973: Macro- and micronuclei of *Tetrahymena pyriformis*: a model system for studing the structure and function of eukaryotic nuclei. J. Protozool., 20, 19–25.

Gorovsky M. A., Hattman S. and Pleger G. L. 1973: [^{6}N]-methyl adenine in the nuclear DNA of a eukaryote *Tetrahymena pyriformis*. J. Cell. Biol., 56, 697–701.

Ивахнюк И. С. 1976: Освобождение инфузорий *Paramecium caudatum* от эндосимбионтов — омега-частиц — с помощью пенициллина и хлорамфеникола. Вестн. ЛГУ (в печати).

Lipps H. I., Sapra G. R. and Ammermann D. 1974: The histones of the ciliated *Protozoan Stylonychia mytilus*. Chromosoma (Berl.), 45, 273–280.

Осипов Д. В. 1966: Методы получения гомозиготных клонов *Paramecium caudatum*. Генетика, 2, 41–48.

Осипов Д. В. 1973: Видовая инфекционная специфичность омега-частиц, симбиотических бактерий микронуклеуса инфузорий *Paramecium caudatum*. Цитология, 15, 2, 211–217.

Ossipov D. V. 1975: The specificity of localization of omega particles, the intranuclear symbiotic bacteria in *Paramecium caudatum*. Acta Protozool., 14, 43–57.

Осипов Д. В. и Ивахнюк И. С. 1972: Омега-частицы, симбиотические бактерии микронуклеуса инфузорий *Paramecium caudatum* клона MI-48. Цитология, 14, 11, 1414–1419.

Осипов Д. В., Раутиан М. С. и Борхсениус О. Н. 1975: Полиморфизм микронуклеусов *Paramecium caudatum*. VI. Влияние инфекции омега-частицами — внутриядерными симбиотическими бактериями. Вестн. ЛГУ, сер. биол., 1, 17–27.

Осипов Д. В., Раутиан М. С., и Скобло И. И. 1974: Потеря способности к половому процессу у клеток *Paramecium caudatum* инфицированных внутриядерными симбиотическими бактериями. Генетика, 10, 7, 62–70.

Ossipov D. V. and Skoblo I. I. 1973: Morphogenetic activity of generative nucleus in the sexual cell reorganization of ciliates. Acta Protozool., 12, 151–164.

Preer L. B. 1969: Alpha, an infections macronuclear symbiont of *Paramecium aurelia*. J. Protozool., 16, 570–578.

Prescot D. M., Murti K. G. and Bostock C. J. 1973: Genetic apparatus of *Stylonychia* sp. Nature, 242, 576, 597–600.

Раутиан М. С., Осипов Д. В. и Скобло И. И. 1975: Изменение хроматина микронуклеуса инфузорий *Paramecium caudatum* при заражении омега-частицами. Цитология, 17, 10, 1200–1207.

Раутиан М. С., Скобло И. И., и Осипов Д. В. Инфекционная стадия в жизненном цикле омега-частиц симбиотических бактерий инфузории *Paramecium caudatum* и концентрационный эффект инфекции. Цитология (в печати).

Скобло И. И. 1969. Поведение амикронуклеарных *Paramecium caudatum* в половом процессе. Успехи протозоологии, Тезисы докладов III Межд. Конгресса Пторозоологов, Ленинград 1969, Изд. „Наука", Ленинград, 40–41.

Соннеборн Т. М. 1966: Генетика простейших и ее отношение к общей генетике. Генетика, 11, 31–41.

Sonneborn T. M. 1970: Methods in *Paramecium* research. In: Methods in cell physiology. Academic Press, New York, 4, 241–339.

Wells C. 1961: Evidence for micronuclear function during vegetative growth and reproduction of the Ciliate, *Tetrahymena pyriformis*. J. Protozool., 8, 284–290.

Винникова Н. В. 1974: Ультраструктура микронуклеусов инфузории *Dileptus anser* в интерфазе и митозе. Цитология, 16, 4, 504–508.

Yao M.-Ch. and Gorovsky M. A. 1974: Comparison of the sequences of macro- and micronuclear DNA of *Tetrahymena pyriformis*. Chromosoma (Berl.), 48, 1–18.

Yao M.-Ch., Kimmel A. R. and Gorovsky M. A. 1974: A small number of cistrons for ribosomal RNA in the germinal nucleus of a eukaryote, *Tetrahymena pyriformis*. Proc. natn. Acad. Sci. USA, 71, 3082–3086.

Received on 27 July 1977

ACTA PROTOZOOLOGICA
VOL. 17 (No. 2) WARSZAWA, 30 VI 1978 pp. 331–345

Биологический институт Ленинградского Государственного Университета Лаборатория зоологии беспозвоночных, Старый Петергоф Ленинградской обл., Ораниенбаумское шоссе 2, СССР
Laboratory of Invertebrate Zoology, Biological Research Institute, Leningrad State University, Leningrad 164, USSR

О. Н. БОРХСЕНИУС и Д. В. ОСИПОВ
O. N. BORCHSENIUS and D. V. OSSIPOV

Влияние избирательной инактивации генеративных ядер инфузории *Paramecium caudatum* на вегетативные функции клеток

Influence of Selective Inactivation of Generative Nuclei on the Vegetative Cell Functions in *Paramecium caudatum (Ciliata, Protozoa)*

Синопсис. Изучено влияние микронуклеуса (Ми) на жизнеспособность и темп клеточного деления у двух клонов *Paramecium caudatum*. Избирательная функциональная инактивация (денуклеация) Ми у исходно нормальных клеток достигалась двумя способами: локальным УФ микрооблучением Ми и в результате инфекции парамеций симбиотическими бактериями — омега-частицами. После УФ облучения Ми 217 парамеций было получено жизнеспособное потомство от 27 клеток. Все они дали начало линиям, содержащим Ми, последние в ряде случаев были морфологически отличны от Ми „дикого" типа. Сравнение результатов клонирования с данными по анализу распределения Ми у потомков I и II пострадиационных клеточных делений показало, что возникающие амикронуклеарные ($Ми^-$) клетки оказываются нежизнеспособными. Аналогичная закономерность наблюдалась и в опытах по инфекции Ми омега-частицами. Через сутки после начала опыта 96—98% клеток инфицированных культур становились $Ми^-$. Ни одна из 280 клеток, подвергнутых клонированию, не дала начало жизнеспособному клону — их потомство вымирало на 3–4 сутки. Полученные результаты доказывают функциональную значимость генеративного ядра в вегетативной жизни клеток. Обсуждается возможное биологическое значение наличия вегетативных функций у Ми инфузорий.

В последние годы наблюдается повышенный интерес к явлению ядерного дуализма у инфузорий. В пределах одной клетки у инфузорий имеют место соматическое ядро — макронуклеус (Ма) и генеративное — микронуклеус (Ми). Эти ядра весьма контрастно различаются в морфо-функциональном отноше-

нии и представляют удобные модельные объекты при изучении механизмов регуляции генной активности (см., обзор: Gorovsky 1973). До недавнего времени принято было считать Ми инертным, аналогично ядру спермального типа, поскольку оно, в отличие от Ма, проявляет полное отсутствие или крайне низкую степень синтеза РНК. Однако стали появляться не укладывающиеся в обычные представления данные о том, что Ми, по крайней мере у ряда видов инфузорий, в период вегетативной части жизненного цикла, может контролировать отдельные клеточные функции (см., обзор: Борхсениус 1975). Биологический смысл этого явления ждет своего объяснения. Одним из подходов к решению поставленного вопроса может оказаться сравнительное изучение клеточных функций у амикронуклеарных (Ми$^-$) и исходных — нормальных клонов инфузорий (Wells 1961, Скобло 1969, Ammermann 1970). К сожалению, до сих пор не были проведены с помощью адекватных методов прямые исследования корреляции избирательной инактивации (утраты) Ми и изменения активности конкретных клеточных функций. Таким образом, полученные ранее результаты настоятельно требуют переисследования.

Настоящая работа предпринята с целью изучения эффекта избирательной инактивации Ми у инфузории *P. caudatum*. О нарушении вегетативных клеточных функций судили по темпу клеточного деления и жизнеспособности клеток. Функциональная инактивация Ми нормальных клеток достигалась двумя способами: локальным УФ микрооблучением (см., обзор: Сахаров 1972) и инфекцией парамеций симбиотическими бактериями — омега-частицами, которые локализуются только в Ми (Осипов и др. 1976). Методом УФ микрооблучения (УФ укол) можно вызвать направленные локальные повреждения отдельных органелл живой клетки. При определенных условиях УФ укол может быть использован для выявления функциональной значимости облученной клеточной органеллы, в наших опытах — Ми. Ранее для этих целей метод был отработан на инфузории *P. caudatum* (Фокин и Осипов 1975). Возможность использования омега-частиц для подобных целей была также доказана ранее (Скобло и др. 1978). В последнем случае избирательность повреждения Ми основана на следующем явлении. При использовании относительно высоких концентраций споровых форм омега-частиц (от $1 \cdot 10^6$ частиц/см^3 и выше), через несколько часов от момента инфекции „чистых" клеток *P. caudatum*, с очень высокой частотой (иногда до 100%) возникают Ми$^-$ клетки.

Материал и методика

Работа выполнена на двух клонах *Paramecium caudatum* (Бе-1-4 и Бе-5), выделенных из одной природной популяции. Инфузорий поддерживали по общепринятой методике при 25°С на салатной забуференной среде, зараженной предварительно *Aerobacter aerogenes*.

Облучение Ми инфузорий *P. caudatum* производили на установке, изготовленной фирмой Carl Zeiss, Jena на базе микроскопа Nf. Для обездвиживания парамеций в момент УФ укола использован прибор — ротокомпрессор, разработанный в лаборатории зоологии беспозвоночных БиНИИ (Фокин и Осипов 1975). Облучение проводили УФ светом длиной волны 240–280 nm (максимум 260 nm). Продолжительность облучения в разных вариантах опыта была 1 или 5 мин. Площадь УФ микролуча квадратного сечения составляла 100 μm^2 в плоскости фокусировки, что составляет около 0,05% площади сдавленной в ротокомпрессоре парамеции. Во избежание фотореактивации операция осуществлялась в темной комнате (с подсветкой объекта видимым светом — красный фильтр КС-10, толщина 3 mm), а дальнейшие манипуляции и наблюдения за облученной клеткой и ее непосредственными потомками (в течение 2 суток) производили при красном свете. Облучали интерфазные Ми парамеций из несинхронной популяции. В контрольных опытах облучали участки Ма и цитоплазмы парамеций, не содержащие глотки и сократительных вакуолей, УФ микролучом той же площади (100 μm^2).

Облученные клетки переносили из ротокомпрессора микропипеткой в микроаквариумы (многолунковые стекла) с небольшим количеством инкубированной культуральной среды. В зависимости от схемы опыта анализ ядерного аппарата потомства оперированных клеток производили либо после культивирования на многолунковых стеклах (потомки I и II пострадиационных делений парамеций), либо после 4–5 дневной инкубации инфузорий на многолунковых стеклах и последующего переноса в 12 ml пробирки.

У всех полученных жизнеспособных субклонов определяли темп клеточного деления с помощью метода ведения индивидуальных культур. Обычно 10 клеток от каждого субклона отсаживали по одной клетке в микроаквариум; в течение 7 суток после подсчета числа поделившихся клеток оставляли в каждой лунке по одной клетке, изолируя ее от остального потомства. Темп деления парамеций в каждой индивидуальной культуре определяли по формуле: $R = \frac{\log B - \log A}{\log 2}$, где A — число парамеций в 1-е сутки, B — число парамеций в данной индивидуальной культуре на вторые сутки. Одновременно учитывали эффективность клонирования, которая определялась как процент жизнеспособных индивидуальных культур от числа клеток, подвергнутых клонированию. Средний темп клеточного деления пострадиационных субклонов подсчитывали с учетом только жизнеспособных индивидуальных линий.

Для заражения омега-частицами чистых клонов *P. caudatum* использовали неочищенный гомогенат клеток клона М-209-омега. Гомогенат содержал $3 \cdot 10^6$ спиралевидных инфекционных форм омега-частиц/cm^3. Подсчет инфекционных частиц производили в камере Горяева. Заражение исходных клонов омега-частицами осуществлено М. С. Раутиан, за что авторы статьи приносят глубокую благодарность.

Ядерный аппарат парамеций изучали на тотальных препаратах, окрашенных по Фельгену с модификацией Де-Ламатер.

Результаты и обсуждение

В опытах по инактивации Ми с помощью УФ укола было облучено 217 парамеций, и от каждой оперированной клетки начата клеточная линия. Однако жизнеспособное потомство удалось получить только от 27 клеток, и все они дали начало линиям, содержащим Ми, которые в ряде случаев были

Таблица 1

Table 1

Темп клеточного деления, эффективность клонирования и морфологический тип микронуклеуса у клонов, полученных после локального УФ микрооблучения микронуклеуса и цитоплазмы клеток двух клонов *Paramecium caudatum*

The fission-rate, efficiency of cloning and morphological type of micronuclei in sub-clones resulted from local ultraviolet microbeam irradiation of micronucleus and cytoplasm of cells in two clones of *Paramecium caudatum*

Индексы культур Indexes of sub-clones	Длительность УФ облучения (мин) Time of UV-irradiation (min)	Эффективность клонирования (%), в скобках число исследованных индивидуальных линий Efficiency of cloning (%), in brackets the number of individual lines	Средний темп клеточного деления (делений/сутки) Average fission-rate (divisions/days)	Морфологический тип Ми Morphological type of micronucleus
1	2	3	4	5
Бе-1-4 Be-1-4	0	100 (18)	2.2±0.03	дикий тип wild type
Бе-1-4-60УФМи Be-1-4-60UVMi	1	90 (10)	2.3±0.06	,, ,,
Бе-1-4-61УФМи Be-1-4-61UVMi	1	40 (10)	1.9±0.8	,, ,,
Бе-1-4-62УФМи Be-1-4-62UVMi	1	60 (10)	1.8±0.14	,, ,,
Бе-1-4-63УФМи Be-1-4-63UVMi	1	80 (10)	1.9±0.03	,, ,,
Бе-1-4-64УФМи Be-1-4-64UVMi	1	60 (10)	2.1±0.25	,, ,,
Бе-1-4-67УФМи Be-1-4-67UVMi	1	80 (10)	2.1±0.04	,, ,,
Бе-1-4-39УФцит Be-1-4-39UVcyt	1	80 (10)	2.0±0.13	,, ,,
Бе-1-4-59УФцит Be-1-4-59UVcyt	1	45 (20)	2.0±0.19	,, ,,
Бе-1-4-6УФМи Be-1-4-6UVMi	5	44 (9)	1.2±0.11*	удлиненное ядро elongated nucleus
Бе-1-4-8УФМи Be-1-4-8UVMi	5	33 (9)	1.9±0.13	,, ,,

1	2	3	4	5
Бе-1-4-41УФМи Be-1-4-41UVMi	5	30 (10)	1.2±0.13*	идлиненное ядро elongated nucleus
Бе-1-4-18УФМи Be-1-4-18UVMi	5	88 (8)	2.0±0.17	,, ,,
Бе-1-4-10УФМи Be-1-4-10UVMi	5	70 (10)	1.7±0.12	,, ,,
Бе-5 Be-5	0	80 (10)	1.7±0.05	дикий тип wild type
Бе-5-16УФМи Be-5-16UVMi	1	90 (10)	2.1±0.12	,, ,,
Бе-5-17УФМи Be-5-17UVMi	1	90 (10)	2.0±0.07	,, ,,
Бе-5-18УФМи Be-5-18UVMi	1	100 (10)	1.7±0.04	,, ,,
Бе-5-20УФМи Be-5-20UVMi	1	100 (10)	1.8±0.03	,, ,,
Бе-5-21УФМи Be-5-21UVMi	1	100 (10)	2.1±0.06	,, ,,
Бе-5-24УФМи Be-5-24UVMi	1	100 (10)	2.1±0.11	,, ,,
Бе-5-25УФМи Be-5-25UVMi	1	80 (10)	1.4±0.05*	,, ,,
Бе-5-27УФМи Be-5-27UVMi	1	100 (10)	1.9±0.04	,, ,,
Бе-5-30УФМи Be-5-30UVMi	1	70 (10)	1.5±0.11*	,, ,,
Бе-5-31УФМи Be-5-31UVMi	1	100 (10)	1.9±0.02	,, ,,
Бе-5-22УФцит Be-5-22UVcyt	1	100 (10)	1.8±0.04	,, ,,
Бе-5-26УФцит Be-5-26UVcyt	1	80 (10)	1.1±0.09*	,, ,,
Бе-5-6УФМи Be-5-6UVMi	5	80 (10)	1.8±0.11	,, ,,
Бе-5-8УФМи Be-5-8UVMi	5	100 (10)	2.2±0.04	,, ,,
Бе-5-1УФМи Be-5-1UVMi	5	50 (10)	1.5±0.09*	удлиненное ядро elongated nucleus
Бе-5-3УФМи Be-5-3UVMi	5	70 (10)	1.6±0.13	,, ,,
Бе-5-5УФМи Be-5-5UVMi	5	90 (10)	2.1±0.07	,, ,,
Бе-5-9УФМи Be-5-9UVMi	5	70 (10)	1.6±0.13*	,, ,,

Примечание: В индексе полученного субклона вводятся обозначения: УФМи, если у исходной клетки облучался микронуклеус, и УФцит, если облучался участок цитоплазмы. Звездочкой отмечены линии, характеризующиеся достоверно сниженным темпом клеточного деления (при $p<0.01$).

Footnote: Designations of clones: UVMi irradiated micronucleus in the original cell, UVcyt irradiated cytoplasm. The lines showing decreased fission-rate (with $p<0.01$) are marked with asterisks.

морфологически отличны от Ми „дикого" типа (Табл. 1). Потомство остальных облученных клеток вымирало спустя несколько суток либо так и не претерпев ни одного клеточного деления, либо после резкого снижения его темпа.

После одноминутного облучения Ми 59 клеток клона Бе-1-4 образовалось 7 жизнеспособных субклонов (11.8%); 21 клетка клона Бе-5 с облученными Ми дала начало 10 субклонам (47.6%). Среди потомства 111 клеток клона Бе-1-4, Ми которых облучали 5 мин., жизнеспособными оказались потомки только 4 клеток (3,6%), а из 26 клеток клона Бе-5 — 6 клеток (23.1%). Обращают на себя внимание существенные различия между двумя изученными клонами (Бе-1-4 и Бе-5) по проценту жизнеспособных клеточных линий, полученных от клеток с облученными Ми. Однако обсуждать причины этих различий на основании имеющихся данных преждевременно.

Все 11 субклонов, полученные от облученных клеток Бе-1-4, оказались способными к половому процессу с необлученными клонами комплементарного типа спаривания. Изучение особенностей ядерной реорганизации при конъюгации потомков клеток с облученными Ми (что является показателем сохранения собственно генеративных функций Ми) послужит темой отдельного исследования. Важно отметить что 5 мин. УФ микрооблучение Ми часто приводит к образованию измененных морфологических форм Ми: в 8 из 11 (72.7%) полученных жизнеспособных субклонов; при 1 мин. воздействии подобное явление не было обнаружено.

В контрольных опытах, когда у парамеций облучали участок цитоплазмы, равный по величине облучаемой площади Ми, из 10 облученных получено 9 жизнеспособных клеточных линий. Все они содержали Ми „дикого" типа. Темп клеточного деления, однако, в одном из 4-х исследованных случаев (субклон Бе-5-26 УФ цит) был ниже, чем у исходного клона.

Каков характер нарушений, возникающих в результате УФ укола Ми? Хорошо известно, что УФ укол быстро и эффективно подавляет синтез РНК в облученном ядре многоклеточных (Сахаров 1972) и приводит к почти полному прекращению транспорта РНК из ядра в цитоплазму, обеспечивая избирательную функциональную инактивацию ядра, в наших опытах — Ми. С другой стороны, кроме функциональной инактивации Ми в результате УФ укола может произойти физическая утрата этого ядра из клетки или его морфологическое изменение. Кроме результатов, представленных в Табл. 1, это подтверждается характером распределения дочерних ядер облученного Ми по клеткам-потомкам I и II пострадиационных делений (Табл. 2).

Из потомков I пострадиационного деления 14 облученных клеток клона Бе-1-4 каждая пара дочерних клеток от 12-и образовала $Ми^-$ и нормальные (с Ми) клетки, тогда как потомки 2-х облученных клеток имели исключительно $Ми^-$ потомство. Важно отметить, что Ми в 12 дочерних клетках представляли бледноокрашенные по Фельгену ядра, вытянутые по продольной оси, в отличие от ярко окрашенных Ми „дикого" типа, имеющих боченковидную форму.

Таблица 2

Table 2

Ядерный аппарат клеток — потомков I и II пострадиационных делений клона Бе-1-4 *Paramecium caudatum*. (Продолжительность локального УФ микрооблучения микронуклеусов — 5 мин.)

The nuclear apparatus of cells — descendants of I and II post- irradiated divisions in clone Be-1-4 *Paramecium caudatum* (Time of UV-irradiation of micronuclei — 5 min)

Потомки I пострадиационного деления Descendants of I post-irradiated divisicn		Потомки II пострадиационного деления Descendants of II post-irradiated division	
Характеристика двух потомков Character of two descendants Ми⁻ : Ми⁺	Количество пар Number of pairs	Характеристика „тетрад" потомков Character of „tetrads" of descendants Ми⁻ : Ми⁺	Количество „тетрад" Number of „tetrads"
0:2	0	0:4	1
1:1	12	1:3	1
2:0	2	2:2	6
		3:1	6
	всего пар 14	3:1 (2 Ми⁺)	2
	total number of pairs 14	4:0	0
			всего „тетрад" 16 total number of „tetrads" 16

Примечание: Ми⁻ — амикронуклеарные клетки, Ми⁺ — клетки, содержащие микронуклеус, 2Ми⁺ — клетки содер,ащиежда микронуклеуса.
Footnote: Mi⁻ — amicronuclear cels, Mi⁺ — cells with micronucleus, 2Mi⁺ — cells with two micronuclei.

„Тетрады" дочерних клеток, полученные после II пострадиационного деления, характеризуются почти всеми возможными сочетаниями Ми⁻ и нормальных клеток. Причем, в 15 из 16 проанализированных „тетрад" возникали клетки, утратившие Ми. По-видимому, УФ укол вызывает, с одной стороны, временную асинхронность клеточного и ядерного (Ми) делений, в результате чего образуются Ми⁻ и клетки, содержащие по два Ми, что и наблюдалось нами в 12.5% исследованных „тетрад". С другой стороны, УФ микрооблучение приводит к временной или даже необратимой деструкции веретена деления и повреждению кинетохоров хромосом при последующем митозе облученного ядра, аналогично тому, как это показано для самых разнообразных типов растительных и животных клеток (Сахаров 1972). И, наконец, нельзя исключить, что локальное УФ облучение ядра может приводить к угнетению синтеза ДНК и к появлению у облученных участков хромосом в митозе свойства „клейкости"; слипаясь они могут создавать

в анафазе мосты. Эти явления позволяют объяснить, почему уже после I и II пострадиационных делений облученного Ми возникают бледноокрашенные по Фельгену генеративные ядра, утратившие большую часть ДНК. Как уже отмечалось, 5 мин. УФ микрооблучение Ми вызывает появление отклонений от обычного морфологического типа Ми в 72.7% жизнеспособных клеточных линий.

В контрольных вариантах опыта (в Табл. 2 они не представлены) у потомков 5 парамеций (исследовано 18 дочерних клеток), цитоплазма которых подвергалась УФ уколу, и у потомков 5 парамеций (исследовано 20 дочерних клеток) с облученным Ма не наблюдалось ни видимых морфологических изменений ядерного аппарата клеток, ни подавления клеточных делений. В обоих случаях экспозиция УФ луча была 5 мин. Таким образом, снижение жизнеспособности и последующая гибель Ми⁻ клеток, возникающие в наших экспериментальных условиях, доказывают функциональную значимость генеративного ядра *P. caudatum* в вегетативном периоде жизни инфузорий.

Аналогичная закономерность отмечена нами и при избирательной инактивации Ми у исходно нормальных клеток с помощью другого способа денуклеации — в результате инфекции Ми омега-частицами. После заражения клеток двух исходно „чистых" клонов: Бе-1-4 и Бе-5 через сутки были получены культуры парамеций, состоящие практически целиком из Ми⁻ клеток. Так, для клона Бе-1-4 доля Ми⁻ клеток в культуре составляла 96%, а для клона Бе-5 — 98%. С целью определения жизнеспособности клеток, у которых синхронно произошла деструкция Ми, в результате инфекции ядра большим количеством омега-частиц, было проведено клонирование клеток инфицированной культуры и определение темпа клеточного деления методом индивидуальных культур: 160 клеток из инфицированной культуры Бе-1-4 и 120 клеток из инфицированной культуры Бе-5. Ни одна из 280 клеток не дала начало жизнеспособному клону — полное вымирание клеток происходило на 3–4 сутки от момента субклонирования. Тогда как эффективность клонирования и темп клеточного деления этих двух клонов в контроле составляли соответственно: 100%, 2.2 ± 0.03 дел./сутки и 80%, 1.7 ± 0.05 дел./сутки (Табл. 1). Учитывая высокую специфичность внутриклеточной локализации омега-частиц и особенности ультраструктурной организации зараженных клеток (Осипов и др. 1976), мы склонны считать, что Ми является единственной мишенью, на которую действуют симбионты, не вызывая необратимых изменений в других органеллах парамеций. Таким образом, гибель Ми⁻ клеток, возникающих в результате заражения омега-частицами, происходит не вследствие общего воздействия симбиотических бактерий на парамеций, а в результате потери клеткой Ми.

В известном противоречии с нашими выводами стоят данные ряда авторов о генетической инертности Ми. Один из основных доводов в пользу мнения о функциональной инертности Ми состоит в том, что, по крайней мере для

некоторых видов инфузорий, известно большое число Ми⁻ жизнеспособных линий (см., обзор: Борхсениус 1975). Так например, для *Tetrahymena pyriformis* доля Ми⁻ штаммов, выделенных из природных популяций, составляет до 65% в районах Тихого Океана, и 33–39% для США и Европы. Более того, в экспериментальных исследованиях на этом, ставшем излюбленным, объекте большая часть работ, возможно до 80% по оценке Юдина (1976), выполнена на Ми⁻ штаммах. В этой же связи нельзя не упомянуть работы по цитологии конъюгации клеток вполне жизнеспособных Ми⁻ линий *Paramecium bursaria* (Chen 1940); *P. aurelia* (Sonneborn 1954); *P. multimicronucleatum* (Diller 1961, 1965); *P. caudatum* (Wichterman 1959, Осипов и Тавровская 1969, Скобло 1969, Ossipov and Skoblo 1973).

С другой стороны, результаты наших опытов и многие литературные данные (в том числе и на видах, перечисленных выше) свидетельствуют либо о снижении жизнеспособности клеток и увеличении продолжительности генерационного периода после потери в клеточных линиях Ми, либо о полной нежизнеспособности возникших Ми⁻ клеток. Как правило, в таких случаях утрата Ми была вызвана старением культуры или индуцирована какими-либо воздействиями или агентами: Х-лучами, митотическими ядами, инфекционными агентами, микрургической операцией и др. (Miyake 1956, Wichterman 1959, Wells 1961, Осипов 1966, Бомфорд 1967, Ammermann 1970). Итак, представляется вполне вероятным, что разные пути утраты Ми: деструкция ядра в результате действия каких-либо агентов, спонтанная или индуцированная асинхронность ядерного и клеточного делений, ненормальное распределение дочерних ядер, хромосомные и геномные нарушения и др., могут приводить к существенно отличающимся последствиям. Как уже отмечалось выше, пока не были проведены прямые исследования влияния избирательной инактивации и утраты Ми с помощью адекватных и идентичных методик одновременно на нескольких видах инфузорий. Эти вопросы до сих пор ждут своего объяснения и анализа с рассмотренных позиций. Мы считаем, что особенно важно в качестве объектов привлекать виды инфузорий, широко используемые в настоящее время в молекулярно-генетических исследованиях, такие как *T. pyriformis*, *P. aurelia*, *Stylonychia mytilus*.

Наконец, следует учитывать одно из ранее высказанных соображений, согласно которому при некоторых условиях функцию утраченного Ми может „брать на себя" Ма клетки, что и обеспечивает жизнеспособность Ми⁻ линий (Ammermann 1970). К сожалению, мы не знаем как экспериментально возможно проверить это предположение. Вместе с тем, нельзя не упомянуть имеющиеся в литературе данные по возникновению в клетках Ми⁻ линий некоторых видов инфузорий структур, напоминающих по ряду признаков дефектные Ми, названные поэтому „псевдомикронуклеусами" (Schwartz 1947, Ammermann 1970, Голикова 1972). По-видимому, „псевдомикронуклеусы" возникают из Ма в результате отпочковывания фрагментов ядер-

ного материала. Однако вопросы о способе образования „псевдомикронуклеусов", их природе и функции настоятельно требуют переисследования.

Для решения поставленного вопроса о функциональной активности Ми помимо метода, основанного на необратимой утрате Ми, мог бы быть использован анализ клеточных линий с морфологически различными Ми, характеризующимися градуальной потерей части ДНК в результате гапло- или анеуплоидии (см., обзор Осипов и Борхсениус 1973). Известные примеры полиплоидии генеративных ядер инфузорий в данном случае не изменили бы существа дела. Полиморфизм Ми отмечен для многих видов инфузорий, однако в этих исследованиях, к сожалению, уделялось недостаточно внимания изучению корреляции количества ДНК в Ми с жизнеспособностью, темпом клеточного деления или какими-либо другими вегетативными функциями клетки. Как правило, в таких работах сравниваемые линии с полиморфными Ми имеют разный возраст, происхождение и, следовательно, генотип и другие характеристики, что не позволяет определить вклад собственно Ми в наблюдаемые физиологические различия линий. В немногих работах, где изучались генетически идентичные (по Ма) линии с морфологически разными Ми, не отмечено существенных различий по жизнеспособности и темпу клеточных делений (см., например: Осипов и др. 1976).

В наших опытах полученные после УФ укола жизнеспособные субклоны от каждого из двух исходных клонов можно считать генетически идентичными (по Ма). Существенно, что в 9 жизнеспособных субклонах Ми оказались морфологически отличными от ядер „дикого" типа, они имели вытянутую вдоль продольной оси форму и содержали меньшее по визуальной оценке количество ДНК (Табл. 1). В опытах с клоном Бе-5 не удалось установить достоверных отличий по темпу клеточных делений между линиями с нормальным и удлиненным Ми: контроль — 1.7 ± 0.05, субклоны с Ми „дикого" типа — 1.8; субклоны с Ми удлиненного типа — 1.7 дел./сутки. Для 9 субклонов, полученных от облученных клеток клона Бе-1-4 и характеризующихся Ми нормального „дикого" типа, средняя скорость клеточного деления (2.0 дел./сутки) достоверно не отличалась от контрольного клона (2.2 дел./сутки), тогда как среди 4-х субклонов с удлиненными Ми два имели значительно сниженный темп клеточного деления (1.2 дел./сутки). Следует отметить, что в контрольных опытах с облучением участка цитоплазмы парамеций один из полученных субклонов (Бе-5-26 УФ цит) также имел резко сниженный темп клеточного деления (1.1 дел./сутки). Последнее, по-видимому, может свидетельствовать о воздействии УФ укола на какие-то цитоплазматические структуры или участки кортекса клетки, влияющие на темп деления клетки (см., например: Hanson 1962).

Таким образом, имеющийся в настоящее время материал не позволяет сделать вывод о влиянии утраты части ДНК из Ми на снижение жизнеспособ-

ности клеток. Можно думать, что Ми, имеющие сниженное количество ДНК, обеспечивают выполнение тех же вегетативных клеточных функций, что и Ми „дикого" типа. В данном случае основой этого явления у *P. caudatum* несомненно является полиплоидия Ми (Осипов и Борхсениус 1973).

Итак, у инфузорий, по-видимому, нет абсолютно строгого разграничения соматической и вегетативной функции между Ма и Ми. Полученные нами и некоторые литературные данные показывают, что для нормальной жизнедеятельности клеток в период вегетативной жизни существенна незначительная метаболическая активность Ми, помимо исключительно высокой транскрибирующей активности Ма. Методами количественной радиоавтографии, однако с некоторыми условными допущениями, это показано для ряда видов инфузорий, в том числе и для *P. caudatum* (Rao and Prescott 1966, Pasternak 1967). В то же время генетическими методами на гетерокарионах инфузории *P. aurelia* и *T. pyriformis* с различными аллелями в Ма и Ми не удалось обнаружить активность Ми по нескольким изученным генам (Sonneborn 1947, 1966, Allen 1971).

Обсуждая трудности, связанные с доказательством относительной инертности генеративных ядер, не следует забывать, что у некоторых видов инфузорий установлены различия между нуклеотидным составом геномов Ма и Ми (см., обзор: Райков и Аммерманн 1976). Так, у *Stylonychia mytilus* геном дефинитивного Ма составляет лишь 1.6% от генома Ми, тогда как у *T. pyriformis* — до 80–90%. Таким образом, согласно общим принципам организации и функционирования генома эукариот макронуклеусу для обеспечения вегетативной функции клетки достаточно только часть генома Ми. Функция нуклеотидных последовательностей, не представленных в геноме Ма инфузорий, к сожалению не ясны. Можно думать, что наряду с обычно приписываемой им ролью (по аналогии с другими эукариотами) в структурной организации и поведении хромосом в период половой реорганизации, некоторые из них значимы в агамной части жизненного цикла. В противном случае, трудно объяснить, почему избирательная инактивация Ми, согласно нашим экспериментальным данным, так существенно влияет на нормальную жизнедеятельность вегетативных клеток.

В чем же состоит биологический смысл значимости генеративного ядра в вегетативной жизни инфузорий? Мы считаем, что основной акцент в ответе на поставленный вопрос следует перенести не на то, какие именно вегетативные функции клетки контролируются геномом Ми, а на то, что такие функции все же имеются. Благодаря наличию вегетативных функций у Ми, возникшие Ми⁻ клетки приобретают сниженную селективную ценность или даже оказываются совсем нежизнеспособными. В противном случае при абсолютной инертности Ми, Ми⁻ клеточные линии характеризовались бы нормальной жизнеспособностью и, будучи „генетически мертвыми" (стерильными) линия-

ми, могли бы составить определенную часть естественных популяций и, следовательно, структуры вида. Последнее, по общепринятым положениям, следовало бы признать эволюционно неоправданным.

Если наши соображения верны, то биологический смысл функциональной активности Ми следует рассматривать как эффективный механизм, гарантирующий поддержание генеративной линии ядер в сложном жизненном цикле инфузорий. Напомним, что у инфузорий ядра соматического и зачаткового (генеративного) пути репродуцируются при каждом клеточном делении, хотя продолжительность вегетативного периода исчисляется многими сотнями, а нередко даже и тысячами бинарных делений. Если к тому же добавить, что синтез ДНК и контроль за делениями ядер осуществляется независимо в Ма и Ми (Райков 1967, Jerka-Dziadosz and Frankel 1970, Frankel et al. 1975), а также учесть пространственные соотношения размеров Ми и размеров клетки, то сохранение ядер зачаткового пути в течение агамной части жизненного цикла инфузорий следует признать крайне острой задачей.

Вместе с тем, рассмотренный нами гипотетический механизм, направленный на повышение надежности поддержания Ми в клеточных линиях, по-видимому, является не единственным фактором и его следует рассматривать наряду с другими, основанными на следующих хорошо известных морфо-функциональных особенностях ядер инфузорий (Райков 1967). Кратко отметим некоторые из них. Для видов инфузорий с одним Ми при митозе характерно образование веретена деления необычно больших размеров (относительно размеров клетки), благодаря чему дочерние ядра распределяются в противоположные концы делящейся инфузории. С другой стороны, для видов инфузорий с крупными размерами клетки обычно характерна множественность генеративных ядер, иногда до нескольких десятков, что резко снижает вероятность появления Ми⁻ клеток. Наконец, из работ, выполненных на световом и электронномикроскопическом уровне, известны различного рода морфологические контакты между ядерными оболочками Ма и Ми, что также способствует правильному распределению генеративных ядер между дочерними клетками (см., например: Tucker 1967, Райков и Аммерманн 1976, Golder, 1976). Разумеется, в дальнейшем предстоит еще выяснить для конкретных видов инфузорий, характеризующихся определенными особенностями ядерного аппарата, насколько названные выше факторы дополняют или, напротив, исключают друг друга. Весьма вероятно, что разрешение этого вопроса позволит понять причину многочисленных противоречий в имеющихся данных о функциональной активности Ми. Наконец, межвидовые различия инфузорий, наблюдающиеся в отношении „склонности" образовывать жизнеспособные Ми⁻ линии, несомненно, связаны с особенностями структуры жизненного цикла конкретных видов и внутривидовых групп инфузорий и, в первую очередь, с продолжительностью периода старения. Так, например, у *T. pyriformis* период старения крайне продолжителен и, как уже

упоминалось выше, наряду с этим отмечена исключительно высокая частота возникновения Ми⁻ штаммов. Напротив, у сингенов *P. aurelia*, имеющих короткий период старения, Ми⁻ линии практически не известны (Sonneborn 1957). У *P. multimicronucleatum* период старения сопровождается уменьшением числа Ми в клетках от 4–7, обычного для молодых клонов, до 1–2 у стареющих клонов, и Ми⁻ клетки возникают только в старых клонах.

SUMMARY

Influence of generative nucleus — micronucleus (Mi) — on vitality and fission-rate in two clones of *Paramecium caudatum* was studied. The selective functional inactivation (denucleation) of Mi in originally normal cells was caused by two different methods: local ultraviolet microbeam irradiation and infection of the paramecia by symbiotic bacteria (omega-particles) in defined conditions. After UV irradiation of 217 paramecia the viable posterity was received only from 27 cells. All of them gave raise to normal cell lines with Mi being in several cases distinct from Mi of "wild" type. The comparison of cloning results with the data of analysis of Mi segregation in descendants of I and II post-irradiated cell divisions demonstrated the mortality of arising amicronucleate cells. The analogical regularity was observed also in the experiments on Mi infection by omega-particles. One day after the beginning of the experiment 96–98% of cells in infected cultures became amicronucleate. None of 280 cells, which were cloned, gave raise to viable clone — their descendants died after 3–4 days. Experimental data point to functional importance of the generative nucleus during the vegetative life of paramecia. Possible biological importance of this phenomenon is discussed.

ЛИТЕРАТУРА

Allen S. L. and Weremiuk S. L. 1971: Defective micronuclei and genomic exclusion in selected C* subclones of *Tetrahymena*, J. Protozool., 18, 509–515.

Ammermann D. 1970: The micronucleus of the ciliate *Stylonychia mytilus*: its nucleic acid synthesis and its function. Expl. Cell Res., 6–12.

Бомфорд Р. 1967: Ядерные изменения у *Paramecium bursaria* после абортивной конъюгации. Цитология, 9, 589–594.

Борхсениус О. Н. 1975: К вопросу об активности генеративного ядра инфузории. Вестник ЛГУ, 21, 7–16.

Chen T. T. 1940: Conjugation between *Paramecia* with and without micronuclei. J. Hered., 31, 185–196.

Diller W. F. 1961: Nuclear activity crosses of micronucleate and amicronucleate strains of *Paramecium multimicronucleatum*. In: Progress in Protozoology, Proc. First int. Congr. Prozotool., Prague 1961, Publ. House Czechosl. Acad. Sci., Prague, 105–110.

Diller W. F. 1965: The relation of amicronuclearity to stomatogenic activity during conjugation in several ciliates. J. Morphol., 116, 51–64.

Фокин С. И. и Осипов Д. В. 1975: Использование ультрафиолетового микрооблучения в исследованиях ядерного дуализма инфузорий. Цитология, 17, 1073–1080.

Frankel J., Doerder F. P., Jenkins L. M., Nelsen E. M. and Debault

L. E. 1975: Nucleocytoplasmic relations in mutants affecting cell division and cell shape in *Tetrahymena pyriformis*. In: Molecular Biology of Nucleocytoplasmic Relationships. Netherlands, 285–289.

Golder I. K. 1976: The macromicronuclear complex of *Woodruffi metabolica*. J. Ultrastruct. Res., 54, 169–175.

Голикова М. Н. 1972: Полиморфизм микронуклеуса *Paramecium bursaria* Focke. Цитология, 14, 637–645.

Gorovsky M. A. 1973: Macro- and micronuclei of *Tetrahymena pyriformis*: a model system for studying the structure and function of eukariotic nuclei. J. Protozool., 20, 19–25.

Hanson E. D. 1962: Morphogenesis and regeneration of oral structures in *Paramecium aurelia*: an analysis of intracellular development. J. Exp. Zool., 150, 45–67.

Jerka-Dziadosz M. and Frankel J. 1970: The control of DNA synthesis in macronuclei and micronuclei of a Hypotricha ciliate; a comparison of normal and regenerating cells. J. Exp. Zool., 173, 1–22.

Юдин А. Л. 1976: О возможностях генетического исследования агамно размножающихся простейших. В сб.: Кариология и генетика простейших. Изд. „Наука", Ленинград, 19–32.

Miyake A. 1956: Artifically induced micronuclear variation in *Paramecium caudatum*. J. Inst. Polytechn. Osaka City Univ., ser. D, biology, 7, 147–161.

Осипов Д. В. 1966: Методы получения гомозиготных клонов *Paramecium caudatum*. Генетика, 2, 41–48.

Осипов Д. В. и Борхсениус О. Н. 1973: Особенности полиплоидии микронуклеусов у инфузорий. Цитология, 15, 243–253.

Осипов Д. В., Громов Б. В., Мамкаева К. А., Раутиан М. С., Скобло И. И. и Борхсениус О. Н. 1976: Использование симбиотических бактерий для анализа структуры и функции ядерного аппарата инфузории. В сб.: Кариология и генетика простейших. Изд. „Наука", Ленинград, 101–139.

Ossipov D. V. and Skoblo I. I. 1973: Morphogenetic activity of generative nucleus in the sexual cell reorganization of ciliates. Acta Protozool., 12, 151–164.

Осипов Д. В. и Тавровская М. В. 1969: Микронуклеус и морфогенез кортекса у *Paramecium caudatum*. В сб.: Успехи протозоологии, Тезисы докладов III Межд. Конгресса Протозоологов, Ленинград 1969, Изд. „Наука", Ленинград, 103.

Pasternak I. I. 1967: Differential genic activity in *Paramecium aurelia*. J. Exp. Zool., 165, 395–418.

Райков И. Б. 1967: Кариология простейших. Изд. „Наука", Ленинград, 260.

Райков И. Б. и Аммерманн Д. 1976: Новые успехи в изучении макронуклеуса инфузорий. В сб.: Кариология и генетика простейших. Изд. „Наука", Ленинград, 64–90.

Rao M. V. N. and Prescott D. M. 1966: Micronuclear RNA synthesis in *Paramecium caudatum*. J. Cell Biol., 33, 281–285.

Сахаров В. Н. 1972: Исследование живой клетки методом ультрафиолетового и лазерного облучения. Усп. соврем. биол., 73, 231–249.

Schwartz V. L. 1947: Über die Physiologie des Kerndimorphismus bei *Paramecium bursaria*. Z. Naturforsch., 26, 369–381.

Скобло И. И. 1969: Поведение амикронуклеарных *Paramecium caudatum* в половом процессе, В сб.: Успехи протозоологии, Тезисы докладов III Межд. Конгресса Протозоологов. Ленинград 1969, Изд. „Наука", Ленинград, 24–25.

Скобло И. И., Раутиан М. С. и Осипов Д. В. 1978: Потеря генеративных ядер у инфузории *Paramecium caudatum*, вызываемая на ранних стадиях инфекции их симбиотическими бактериями. Acta Protozool., 17, 321-330.

Sonneborn T. M. 1947: Recent advances in the genetics of *Paramecium* and *Euplotes*. Adv. Genet., 1, 263–358.

Sonneborn T. M. 1954: Pattern of nucleocytoplasmic integration in *Paramecium*. Caryologia, 6, 307–325.

Sonneborn T. M. 1957: Breeding systems, reproductive methods and species problems in *Protozoa:* In: The Species Problem. AAAS, Washington, 50, 155–324.

Соннеборн Т. М. 1966: Генетика простейших и ее отношение к общей генетике. Генетика, 11, 31–41.

Tucker J. B. 1967: Changes in nuclear structure during binary fission in the ciliate *Nassula*. J. Cell Sci., 2, 481–498.
Винникова Н. В. 1974: Ультраструктура микронуклеусов инфузории *Dileptus anser* в интерфазе и митозе. Цитология, 16, 504–508.
Wells C. 1961: Evidence for micronuclear function during vegetative growth and reproduction of the Ciliate, *Tetrahymena pyriformis*. J. Protozool., 8, 284–290.
Wichterman R. 1959: Mutation in the protozoan *Paramecium multimicronucleatum* as a result of x-irradiation. Science, 129, 207–208.

Paramecium caudatum.

ACTA PROTOZOOLOGICA
VOL. 17 (No. 2) WARSZAWA, 30 VI 1978 pp. 347–352

Department of Cell Biology, M. Nencki Institute of Experimental Biology, Pasteura 3, 02-093 Warszawa, Poland

Grażyna NOWAKOWSKA

Twisting of Suspended Monotactic Specimens of *Amoeba proteus*

Synopsis. The monotactic specimens of *Amoeba proteus* attached with their tails to the lower surface of the horizontal glass shelf and hanging vertically down, were observed. Under such experimental conditions twisting of the amoebae was recorded. Two components of this motion were seen: gyration and torsion.

In this report the behaviour of *Amoeba proteus* is described under such conditions, when its contraction activity is not affected by the cyclic changes of attachment to the substrate and detachment. The monotactic forms of *A. proteus* with the vesicular frontal cap (according to the terminology proposed by Grębecki and Grębecka 1978) were studied. This particular form of amoeba, probably because of its simplicity, manifested a rotational component of movement in regular manner.

Material and Methods

The monotactic forms of *Amoeba proteus* were used for experiments. They originated from the cultures maintained in Pringsheim medium. Colpidia grown in yolk cultures were added as food. All the experiments were performed in room temperature. The behaviour of individual amoebae was recorded by means of the time-lapse cinematography (1 frame per second), through the differential interference contrast optics.

Amoebae were placed on the glass shelf inside the glass test-chamber filled with Pringsheim solution. When amoebae attached to the substrate, the chamber was carefully turned upside-down. In this way amoebae were made walk on "the ceiling" (Fig. 1).

Two kinds of observations were made. For the first group of amoebae the side-view was recorded by using the horizontally mounted microscope (observations of this type were made first by Dellinger 1906). For the amoebae of the second group, the upside-view through the ordinary microscope was recorded. In this way the body projection upon the horizontal plane was recorded.

Supported by grant MR II. 1.3.1.1.

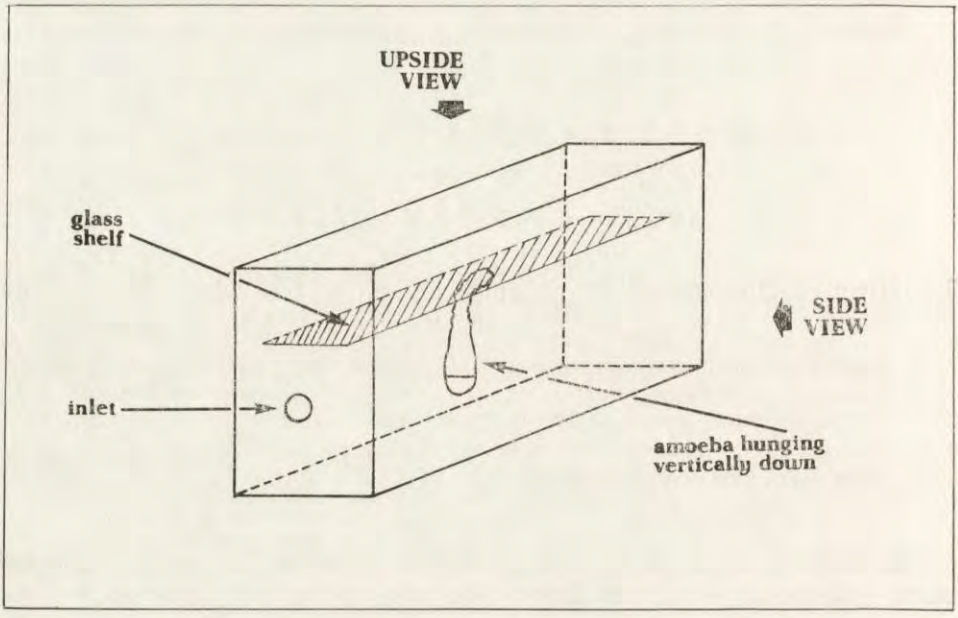

Fig. 1. The principle of the test chamber used in experiments

Results

When a monotactic individual of *A. proteus* is temporarily attached only by the posterior body end, it manifests a tendency to "stand up" on its uroid (Pl. I 1) and, sometimes to perform rotational movements. If such a movement is sustained for enough long time, it may result in a screw-like conformation of the uroid region (Pl. I 2). This behaviour, which is seen under normal conditions occasionally, becames a rule when amoeba is put in the upside-down position.

It was found that the attachment of amoebae to the substrate was so strong, that most of the specimens remained fastened to the "ceiling" after inversion of the chamber. The were hanging vertically down, being attached to the substrate only by the uroid. Their frontal caps were directed downwards. The endoplasm streamed downwards and the ectoplasmic tube was flowing upwards. Small lateral pseudopodia which were formed occasionally, were seen to move upwards together with the ectoplasmic tube.

In the posterior region of trunk, near the uroid, bendings of the body were observed. These bendings took place in the zone distant by about 2/3 of the body length from the front of amoeba. Sometimes they were so intense, that the frontal part of amoeba touched to the "ceiling", and if the place of contact became the new region of attachement, the previous attachment was broken. However, the bendings strong enough to

allow the amoeba to form the new point of attachment were rather exceptional. Usually the experimental conditions restricted the attachment to the uroid only and allowed to observe, for the long time, the contractions of amoebae not affected by the attachment changes which take place during normal movement. It turned out, that these contractions cause the motion consisting of two components: gyration of the anterior body part around the vertical axis and torsion of the body around its own longitudinal axis.

The observations in the horizontal plane showed, that in isolated cases the motion of suspended amoebae may be irregular, but the large majority of specimens recorded for time longer than one hour, gyrated in the clockwise direction (when seen from above). Sometimes, for a short period of time, the counter-clockwise motion was observed, but after the recession by a few degrees, the previous clockwise gyration was restored. The succesive positions of the body projection upon the horizontal plane are shown on the Plate II. To describe the gyration of amoebae the angle (Θ) was measured between the projection of the longitudinal body axis on the horizontal plane at the successive stages of gyration, and its projection corresponding to the initial position of amoeba at the begining of experiment. A typical example of changes of the angle Θ as a function of time is shown on the Fig. 2. In this case one gyration cycle lasted from 3 to 8 min.

Besides the gyration of the body around the vertical, one could observe the torsion of the body around its own longitudinal axis. The torsion of the body is clearly seen in amoebae with lateral pseudopodia which

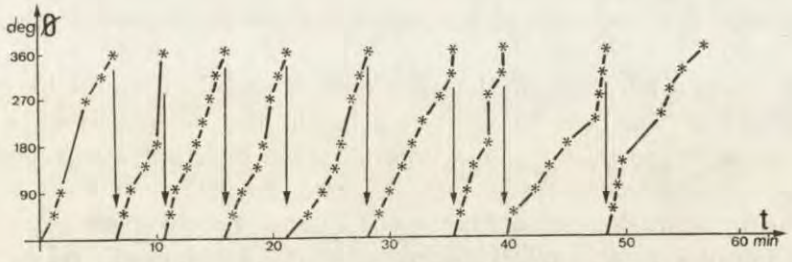

Fig. 2. The time dependence of the angle (Θ) between the projection of the longitudinal body axis upon the horizontal plane at the successive stages of gyration

serve as markers facilitating the observations. These pseudopodia (besides their flowing upwards) changed their position in respect to the longitudinal body axis. These ones, which initialy were seen on the right side of the body, after certain period of time were observed on its left side (and vice-versa).

No evident correlation between the direction and period of gyration and of torsion was found.

Discussion

There exist in the literature some mentions concerning the rotational component in the movement of amoebae, appearing in some special situations. The rotation of amoebae under conditions of cell flattening between two slides was observed by Goldacre (1956) and by Czarska and Grębecki (1965). In this case cell rotation arises when amoeba may establish the contact with the substrate as well by its lower as by the upper surface, i. e., to attach to both slides.

But twisting may appear in a quite different situation: Stockem et al. (1969) mention, that the free frontal part of monotactic *A. proteus*, when the animal is attached only by the uroid, may rotate. This observation has been confirmed in this laboratory (Pl. I). Probably, another expression of the same tendency of monotactic amoebae is the fact that during migration they describe loops, as demonstrated by Grębecki and Grębecka (1978) by photomacrographic recording of their paths. The rotation of the anterior body part when the rear end is attached to the substrate, as well as rotation of the tail when the anterior end is attached, was observed in normal body position in small amoeba *Vahlkampfia* by Jarosch (1971).

In the present study it is demonstrated that in the majority of monotactic specimens of *A. proteus* hanging vertically, the free end of the body gyrates in constant direction because of the body bendings proceeding in a definite order. It is seen on the Pl. II that the bendings in question are active, i. e., they result from the lateral contractions, because the body curvature is opposite to the direction of motion (as in the case of lateral movements of contracting pseudopodia analysed by Grębecki 1977).

The endless gyration of the free end of amoebae would be easy to understand in the case of existence inside the ectoplasm of a spiral structure able to contract. This type of space distribution of contractile or supporting elements is known in some organelles of *Protozoa*. For example in *Spirostomum abiguum* the lateral ectomyonemes are oriented in parallel to the spiral course of cortical ridges (Finley et al. 1964), what may be related to the screw-like body contraction of this ciliate. But the most beautiful example of the relation between the space distribution of contractile and/or supporting elements and the motion, is dependence of the rotational component in the beating of cilia and flagella on the spiral pattern of microtubules in them, described first by Gibbons and Grimstone (1960).

However, there is no evidence that in the cell of amoeba contractile elements are arranged in such an order at the supramolecular level, and

the only hypothesis known from the literature (J a r o s c h 1971) relates the rotational components of movement in *Rhizopoda* directly to the helicoidal structure of contractile proteins.

A little more is known about space organization of the contractile apparatus in the protoplasmic thread of the slime mold *Physarum polycephalum*. W o h l f a r t h - B o t t e r m a n n (1975) showed that, according to the arrangement and direction of fibrils in respect to the long axis of the strand, three different systems of fibrils are present in movement of the slime mold thread is not well understood. The torsion movement of the slime mold thread is not well understod. The torsion was observed in hanging strains of plasmodium, first by S e i f r i z (1946) and then investigated by K a m i y a and S e i f r i z (1954). To explain this phenomenon as well as some other effects, T e p l o v (1976) introduced the idea of "the spiral field of forces" in respect to the slime mold thread. The material basis of this field is not clear.

The other possibility to explain the regular gyration of monotactic amoebae hanging vertically, would be following: If, because of unknown reasons, the wave of excitation in propagated in one direction circularly along the perimeter of the body in the zone of bendings, the contraction of the successive parts of ectoplasmic tube would take place in the same order. The resultant effect should be the gyration. But this explanation also remains as yet a speculative one.

Further study of this problem would be interesting, because the capacity of amoeba to twist certainly reflects some basic properties of its contractile apparatus. The solution of this question might give a contribution to the knowledge of the geometrical pattern of acto-myosin network and/or of space organization of the excitation-contraction processes in amoebae.

ACKNOWLEDGEMENTS

The author thanks dr. A. Grębecki for many helpful suggestions.

RÉSUMÉ

On étudiait le comportement des individus monotactiques de *l'Amoeba proteus* qui pendaient librement vers le bas étant attachés à la paroi supérieure de la cuvette expérimentale seulement par l'uroïde. On a enrégistré dans ces conditions l'existence d'un mouvement rotatoire des amibes, ainsi que de ses deux composantes: la rotation du corps autour de la verticale et sa torsion par rapport à son propre axe longitudinal.

REFERENCES

Czarska L. and Grębecki A. 1965: Rotary movement in *Amoeba proteus*. In: Progress in Protozoology, Second int. Conf. Protozool., London 1965, Abstr. 327.

Dellinger O. P. 1906: Locomotion of *Amoeba* and allied forms. J. Exp. Zool., 3, 337–356.

Finley H. E., Brown C. A. and Daniel W. A. 1964: Electron microscopy of the ectoplasm and infraciliature of *Spirostomum ambiguum*. J. Protozool., 11, 246–280.

Gibbons I. R. and Grimstone A. V. 1960: On flagellar structure in certain flagellates. J. Biophys. Biochem. Cytol., 7, 697–715.

Goldacre R. 1956: The regulation movement and polar organization in *Amoeba* by intracellular feedback. In: Abstracts from the Proceedings of the Ist international Congress on Cybernetics. Namur., 715–725.

Grębecki A. 1977: Non-axial cell frame movements and the locomotion of *Amoeba proteus*. Acta Protozool., 16, 53–85.

Grębecki A. and Grębecka L. 1978: Morphodynamic types of *Amoeba proteus*: a terminological proposal. Protistologica, (in press).

Jarosch R. 1971: Vergleichende Studien zur amöboiden Beweglichkeit. Protoplasma, 72, 79–100.

Kamiya N. and Seifriz W. 1954: Torsion in a protoplasmic thread. Exp. Cell Res., 6, 1–16.

Seifriz W. 1946: Torsion in protoplasm. J. Colloid Sci., 1, 27.

Stockem W., Wohlfarth-Bottermann K. E. und Haberey M. 1969: Pinocytose und Bewegung von Amöben. V. Mitteilung Konturveränderungen und Faltungsgrad der Zelloberfläche von *Amoeba proteus*. Cytobiologie, 1, 37–57.

Teplov V. A. 1976: Mehanika protoplasmatičeskih tjažéj plasmodija miksomiceta. In: Nemyšečnyje formy podvižnosti. Puščino, 37–46.

Wohlfarth-Bottermann K. E. 1975: Weitreichende fibrillaere protoplasmadifferenzierungen und ihre bedeutung fuer die protoplasmastroemung. X. Die anordung der actomyosinfibrillen in experimentell unbeeinflussten protoplasmadern von *Physarum in situ*. Protistologica, 11, 19–30.

Received on 23 October 1977

EXPLANATION OF PLATES I–II

1: Monotactic specimen of *A. proteus* standing up on its uroid
2: Screw-like twisting of the uroid region of monotactic *A. proteus*
3–8: Upside-view of monotactic *A. proteus* hanging vertically down. Successive positions of body projection upon the horizontal plane at 0, 80, 185, 310, 360, 410 s

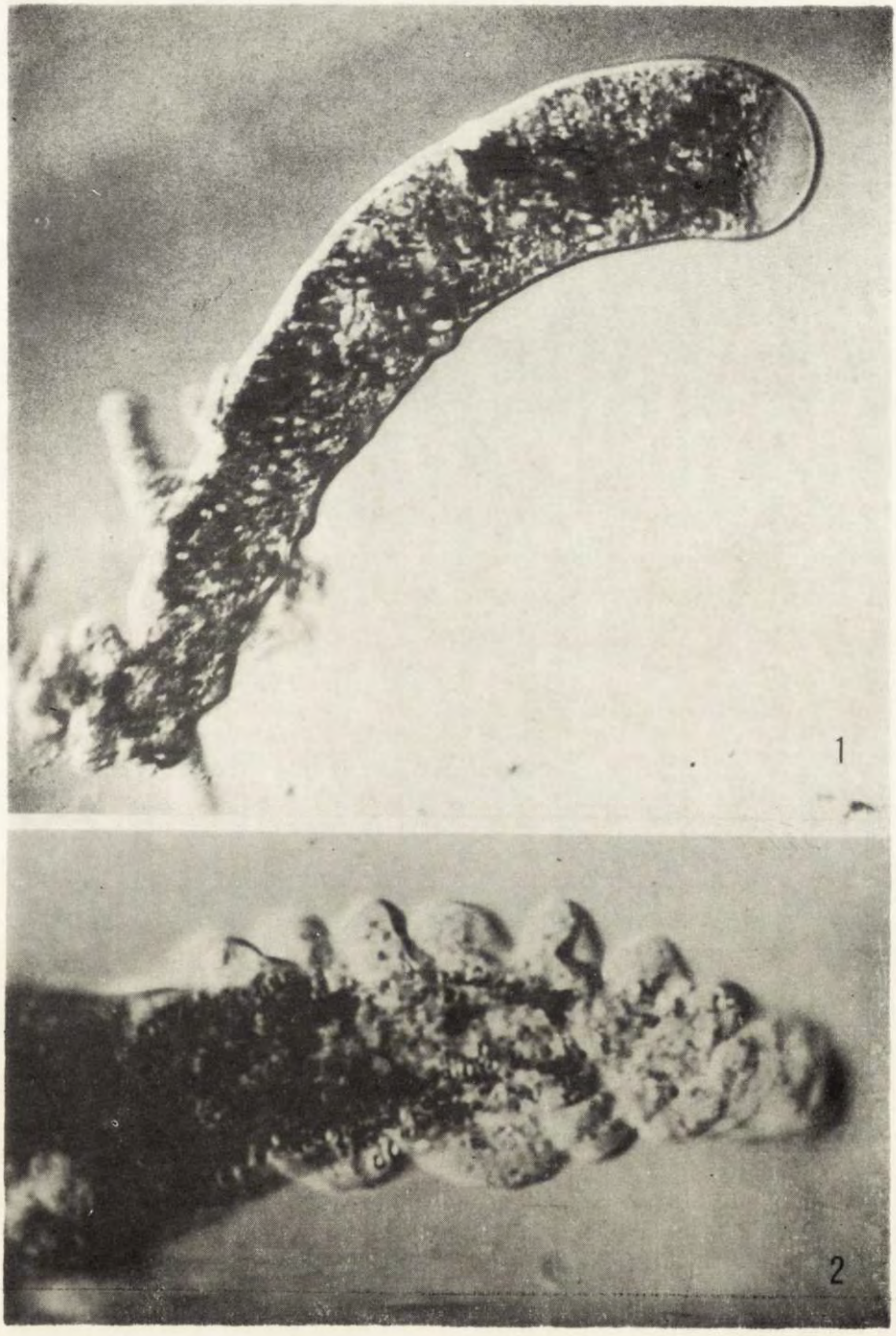

G. Nowakowska A. Grębecki phot.

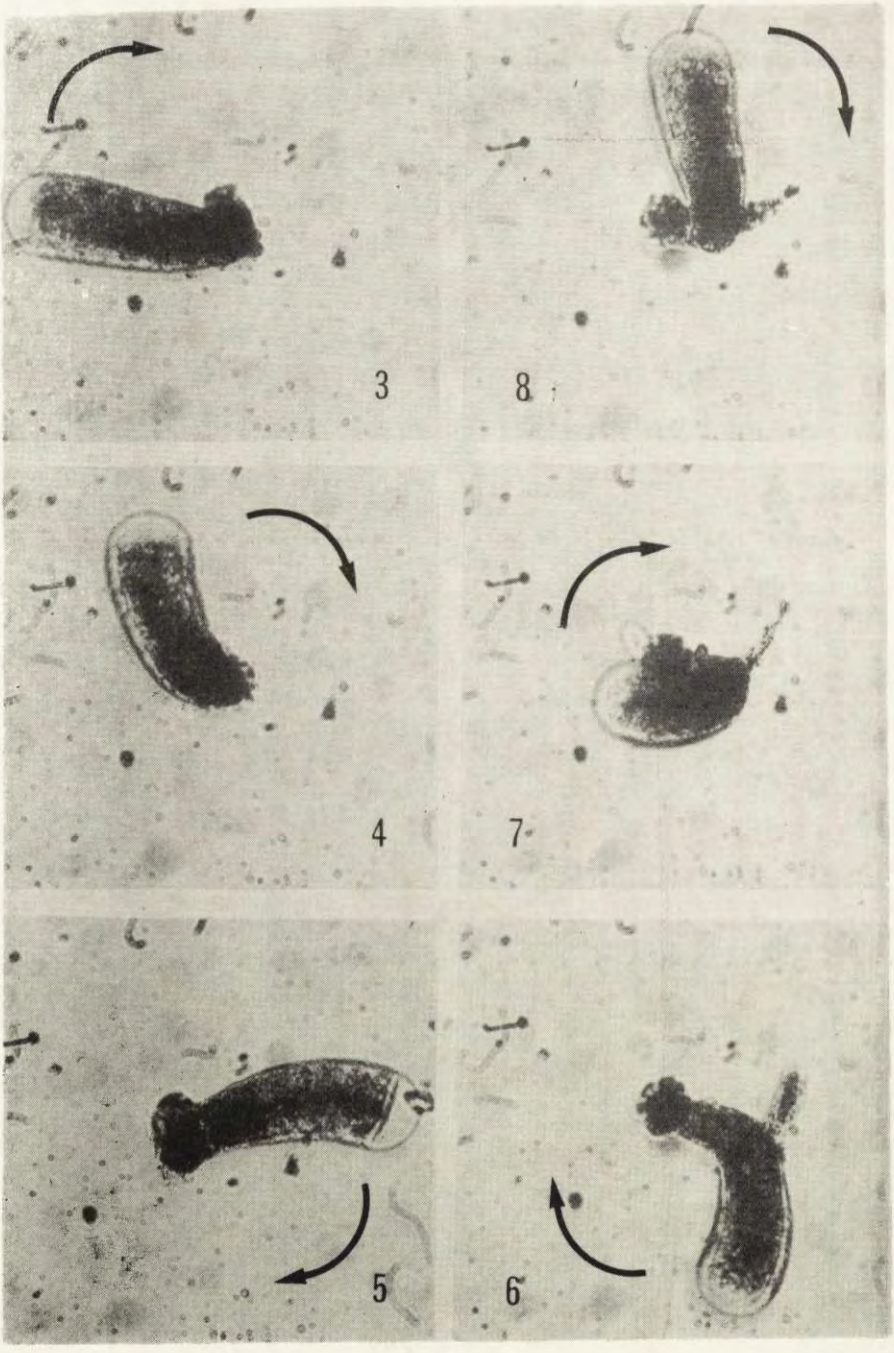

G. Nowakowska auctor phot.

ACTA PROTOZOOLOGICA
VOL. 17 (No. 2) WARSZAWA, 30 VI 1978 pp. 353–358

Department of Cell Biology, M. Nencki Institute of Experimental Biology, Pasteura 3, 02-093 Warszawa, Poland

Grażyna Nowakowska and Andrzej GRĘBECKI

Attachment of *Amoeba proteus* to the Substrate during Upside-down Crawling

Synopsis. In polytactic and orthotactic amoebae attached to the lower surface of a glass shelf and crawling in the upside-down position, the frontal advancing pseudopodia bend upwards in the direction of the substrate. This means that their bending is performed against gravitation, and it should be considered as an active motory phenomenon. The proximity of the substrate is the factor orienting the direction of bending, probably because other existing attachment sites contribute either to the asymmetrical extension or to asymmetrical contraction of new pseudopodia.

In surprisingly few studies of amoeboid movement the side view pictures of migrating amoebae were recorded and analysed, although the first observations of this type were made over 70 years ago by Dellinger (1906). After him only Bell and Jeon (1963), Haberey (1971), and one of the present authors (Grębecki 1976, 1977, and Grębecki and Grębecka 1978), followed this way of investigating the locomotion of amoebae. All these authors utilized the Dellinger's vertical chambers, differently modified, in which amoeba is observed through the microscope mounted in horizontal position. In addition, Bell and Jeon (1963) designed a viewing chamber with a prism, and Grębecki (1976) a chamber with one or two mirrors, both systems allowing to record the lateral view of moving amoeba with the microscope mounted in the usual manner.

The side-view technique has been used by the authors quoted above to clarify the manner of locomotion of *A. proteus*, in particular the succession of leading pseudopodia as depending on their attachment to the substrate and their extension-contraction cycle. All the authors without exception emphasize that a new pseudopodium is initially

Supported by grant MR II. 1.3.1.1.

unattached and extends freely in any direction, and usually it has to bend toward the substrate until it may contact it and attach. The role of gravitation force in this process was discussed but in a speculative way: Bell and Jeon (1963) write that "... pseudopods become extended and large and fall toward the substratum, perhaps by their own weight...", whereas Grębecki (1977) supposes that "the role of gravity in the vertical downward bending of free pseudopodia is still possible but not obviously necessary".

It was the intention of the present authors to clarify this point in the experimental way by checking whether the free new pseudopodia may bend toward the substrate in the inverted position of amoeba, when such a bending should be necessarily performed against the force of gravitation. It is notorious that amoebae may crawl upside down being attached to the lower side of the cover-glass, but nobody after Dellinger (1906) observed this phenomenon in the side view, and nothing is known about the manner of locomotion under such conditions.

Material and Methods

The cultures of *Amoeba proteus* were grown in Pringsheim medium and fed on *Colpidium* sp. All the morphodynamic types (c. f. Grębecki and Grębecka 1978 for their classification) were used in the experiments, but only the behaviour of polytactic, orthotactic and heterotactic specimens is described in this paper, whereas that of the monotactic ones is the subject of a separate article (Nowakowska 1978).

The double reflexion system (used first by Grębecki 1976, and here slightly modified) was adopted for viewing amoebae from the side. In this method, as well the glass shelf made of a piece of cover-glass and serving as substrate for the migration of amoebae, as the mirror reflecting their image, are immersed in a rectangular glass container ($9 \times 6 \times 2.5$ cm) filled with the Pringsheim solution. Amoebae are put on the horizontal shelf, and after allowing them to attach to the substrate, the shelf is carefully inversed upside down. Close to the glass shelf, inside the container, a front surface mirror is mounted, inclined in respect to the shelf at the angle slightly inferior to 45°. The microscope is centered and focussed upon the image reflected by the mirror. The whole system is illuminated by a lateral light beam of the incandescent lamp. The image seen in the microscope is composed of the side-view of amoeba and of its reflection in the glass substrate. The major inconvenience of this method is the low resolution and poor contrasting of the images, because the illumination by lateral beam and reflexion of image in the mirror allow the employment of low power lenses only and exclude the use of any perfectioned contrast optics. On the other hand, the important advantage, essential for the present research, is the possibility of easy identification of points at which amoeba touches the substrate, because at these sites both reflected images come into contact.

The observations were recorded with the 16 mm Bolex movie camera, at the frequency of 4 frames per second, and the records analysed frame by frame.

Results

No distinction will be made here between the polytactic and orthotactic forms, because in the case of polytactic amoebae the microscope was focussed on their leading pseudopodia which behave and look in the side view like orthotactic ones.

As it may be seen from two time-lapse sequences reproduced in the Pl. I 1–6 and 7–11, and two others redrawn in the Fig. 1 A and B, the leading pseudopodium of amoeba which crawls on the ceiling behaves in the same manner as in the individuals migrating in the usual body po-

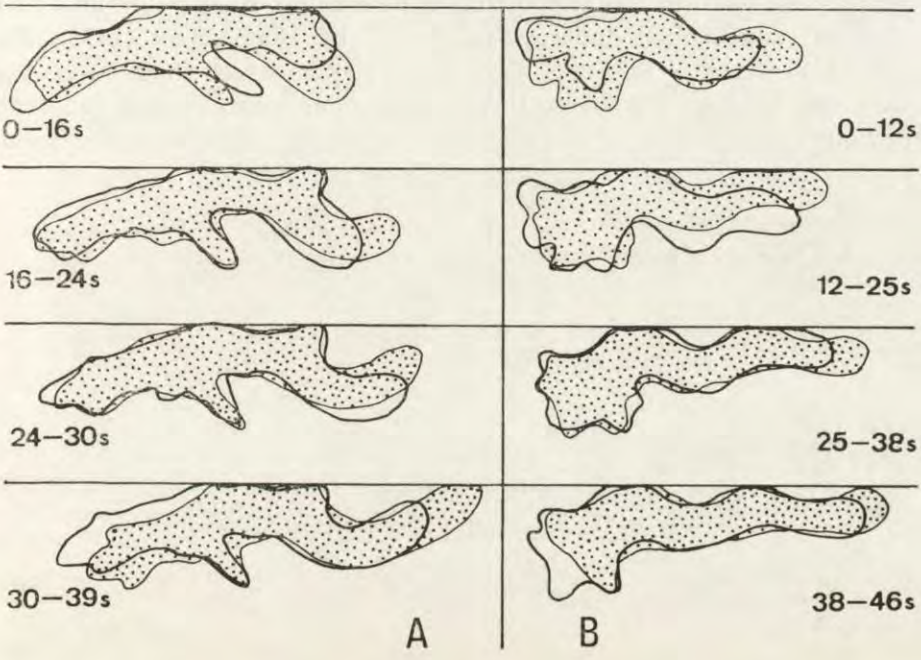

Fig. 1. Two examples of the behaviour of frontal leading pseudopodium in amoebae crawling on the lower surface of the glass shelf. Note the phases of extension of the unattached pseudopodium, its bending upward in the direction of the substrate, and its attachment. Contours of amoebae are redrawn from the 16 mm time-lapse film record. Time in seconds is indicated on the pictures

sition. It is initially extended forwards being unattached at its frontal part and at this stage it usually deviates from the substrate plane. Then, it bends toward the substrate (i.e., upwards), establishes the contact with it, and attaches by the lateral surface of its tip. This sequence of events may be repeated in the cyclic manner, many times by the same pseudopodium (Pl. I 1–6), and this is the common rule in the case of orthotactic

amoebae. In the polytactic ones, the next cycle of free extension, bending upwards directed to the substrate and attachment, is usually performed by a new pseudopodium. The pseudopodium may sometimes bend downwards, probably by a passive falling down during its initial free extension phase, but even in such cases it eventually bends toward the substrate at the next stage (Pl. I 2–3). It should be stressed that the bending of pseudopodia upwards in the direction of the substrate, is not a phenomenon seen occasionally, but the regular common component of the mechanism of locomotion of amoebae in the inverted position.

Under the conditions created in the present experiments one can very well see thin pseudopodia sticking to the glass surface at the uroid region, which were described as "supporting pseudopodia" by Bell and Jeon (1963) and were called "micropseudopodia" by Haberey (1971). The Pl. II 12-15 and the Fig. 2 B show some sequences of their successive detachment. In the Fig. 2 A three phenomena characteristic of their behaviour are seen as separate stages of the same uroidal adherent pseu-

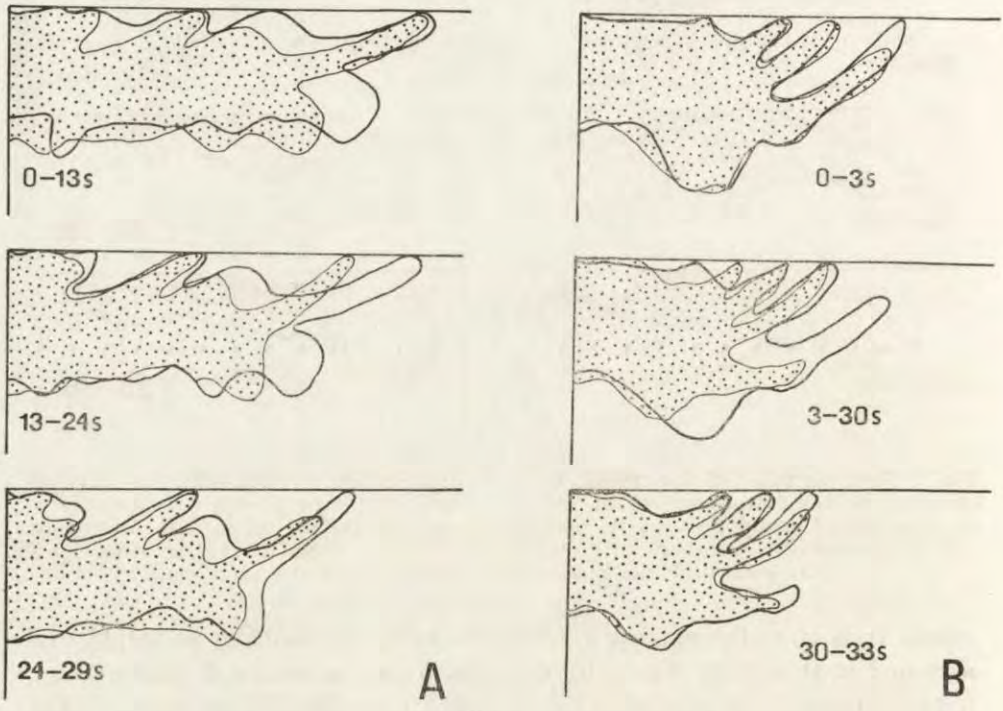

Fig. 2. Two examples of the behaviour of the posterior part of amoeba crawling in the upside-down position. Note the stretching, gliding, and detachment as seen in a single one uroidal pseudopodium (A), and the successive detachment of several such pseudopodia (B). Other explanations as in the Fig. 1

doopodium: it is elastically stretched (stage 0–13 s) as described by Bell and Jeon (1963), it glides over the substrate (stage 13–24 s) as described by Grębecki (1976), and eventually it detaches (stage 24–29 s). Of course, all the three phenomena contribute to the same effect: enabling the posterior body regions to be pulled forwards during cell locomotion.

Also in the case of heterotactic amoebae the type of movements performed in the upside-down position does not differ from that observed under usual conditions. It should be noted in this respect that the generally weaker attachment of heterotactic individuals to the substrate, is however sufficient to maintain them at the ceiling and to allow the changes of shape and alternation of the attachment sites. The Pl. II 16–18 shows the example of heterotactic amoeba which, with a single one attachment point, was able to wind its whole body up and to establish a new contact with the substrate.

Discussion

It is demonstrated by the present research that the advancing pseudopodia of polytactic and orthotactic amoebae bend toward the substrate in the inverted position as well as they do it during normal locomotion. It means that the phenomenon cannot be explained by a passive falling down due to the pseudopodium weight, because it may be perfectly well produced against the force of gravitation. Two conclusions should be drawn from this fact: (1) the bending of pseudopodium which precedes its attachment is an active motory phenomenon, and (2) the proximity of the substrate plays the role of decisive orienting factor.

Of course, a possibility of any kind of perception of the substrate by amoeba before touching it, should be discarded as highly improbable. Two other explanations seem to be plausible:

(1) The asymmetrical extension mechanism, suggested by Grębecki (1977), according to which an advancing pseudopodium should bend laterally if the cortical material may be freely extended on its one side but not on another. As a matter of fact, the extension of the cell cortex of a leading pseudopodium may be relatively free on its dorsal side, whereas on its ventral surface it is restricted by the older sites of attachment to the substrate. This possibility is also supported by the observation of Haberey (1971), that the forward sliding of the cell membrane is slower on the ventral side of advancing pseudopodium than on its dorsal side.

(2) It may be postulated alternatively that the active bending of pseudopodia toward the substrate is due to their asymmetrical contraction or, in other words, that the contractile activity of amoeba is generally asymmetrical, being higher at the substrate side. But this explanation would imply the existence of some contractile activity of the cell cortex even in the expanding frontal regions of amoeba.

The common point of both these hypotheses is the primary role attributed to the existing sites of attachment which were established earlier and are supposed to be responsible either for hampering the extension of the ventral body side or for promoting its stronger contraction. It seems impossible to choose between both hypotheses without further experimental approach.

RÉSUMÉ

Chez les amibes polytactiques et orthotactiques qui se tiennent attachées à la surface inférieure d'une lamelle de verre et rampent dans la position inverse, les pseudopodes produits par le front de la céllule se courbent dans la direction du substratum, c'est-à-dire vers le haut. Ceci signifie que la courbature s'effectue contre la force de gravitation, et elle doit donc être considérée comme un phénomène motorique actif. La proximité du substratum joue le rôle du facteur qui oriente la direction de la courbature, ce qui s'explique probablement par l'influence d'autres points d'attachement, établis antérieurement, qui contribuent à une asymétrie soit de l'extension soit de la contraction des nouveaux pseudopodes.

REFERENCES

Bell L. G. E. and Jeon K. W. 1963: Locomotion of *Amoeba proteus*. Nature, 198, 675–676.

Dellinger O. P. 1906: Locomotion of amoebae and allied forms. J. Exp. Zool., 3, 337–358.

Grębecki A. 1976: Co-axial motion of the semi-rigid cell frame in *Amoeba proteus*. Acta Protozool., 15, 221–248.

Grębecki A. 1977: Non-axial cell frame movements and the locomotion of *Amoeba proteus*. Acta Protozool., 16, 53–85.

Grębecki A. and Grębecka L. 1978: Morphodynamic types of *Amoeba proteus*: a terminological proposal. Protistologica, 14, (in press).

Haberey M. 1971: Bewegungsverhalten und Untergrundkontakt von *Amoeba proteus*. Mikroskopie, 27, 226–234.

Nowakowska G. 1978: Twisting of suspended monotactic specimens of *Amoeba proteus*. Acta Protozool., 17, 347–352.

Received on 23 October 1977

EXPLANATION OF PLATES I–II

1–6: Sequence of selected frames from 16 mm cinematographic record showing two successive cycles of extension, bending and attachment of the same leading pseudopodium (locomotion stages corresponding to 0, 7, 14, 27, 39, and 86 s)
7–11: Selected stages of locomotion of another amoeba crawling in the upside-down position. One full cycle of pseudopodium extension, bending and attachment is shown (at the time 0, 12, 21, 28, and 37 s)
12–15: Selected frames (corresponding to 0, 7, 30, and 44 s) from a film record of movement of the posterior body part of an amoeba migrating in the inverted position. Note the successive detachment of small pseudopodia sticking to the substrate at the uroid region
16–18: Heterotactic amoeba attached to the ceiling initially by one single pseudopodium. Note its ability to pull the body up and to attach by another pseudopodium (frames corresponding to 0, 80, and 120 s)

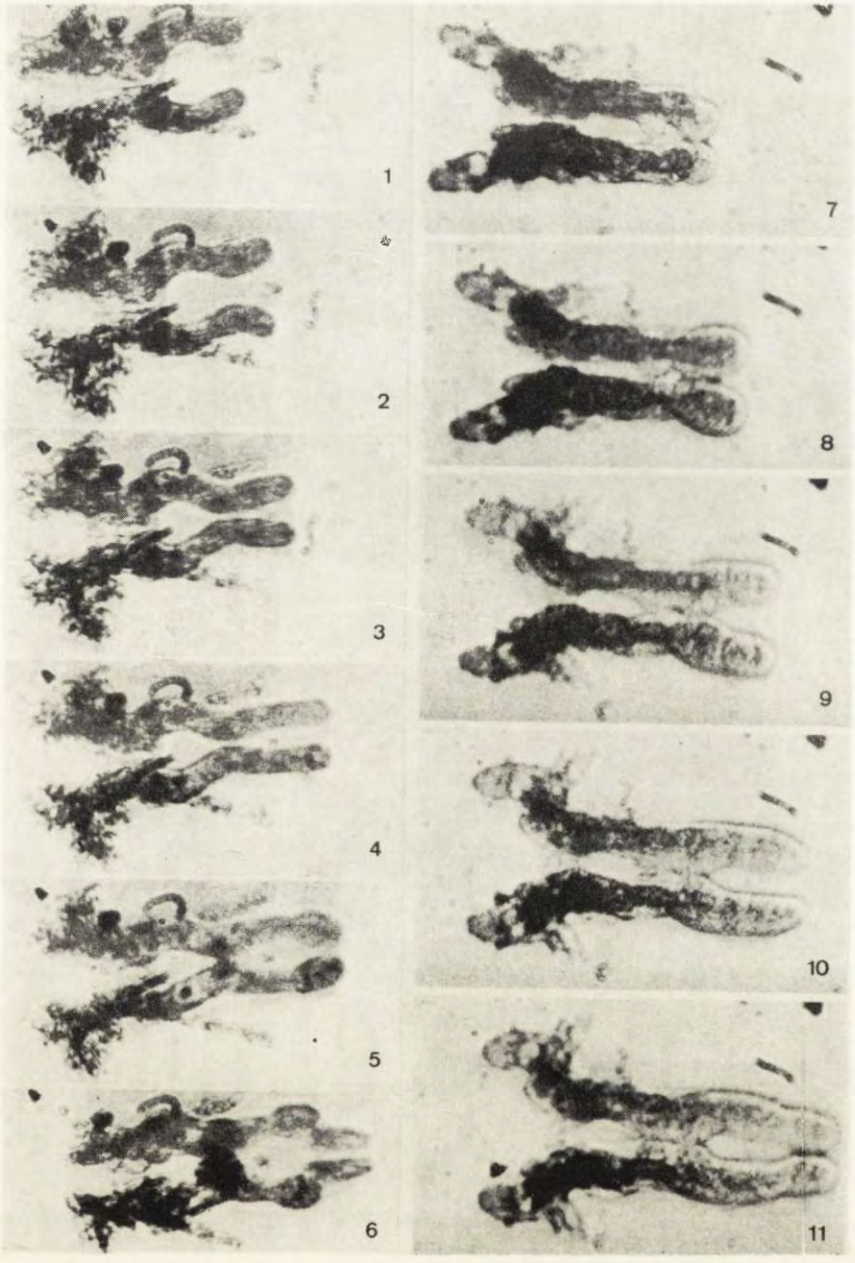

G. Nowakowska et A. Grębecki auctores phot.

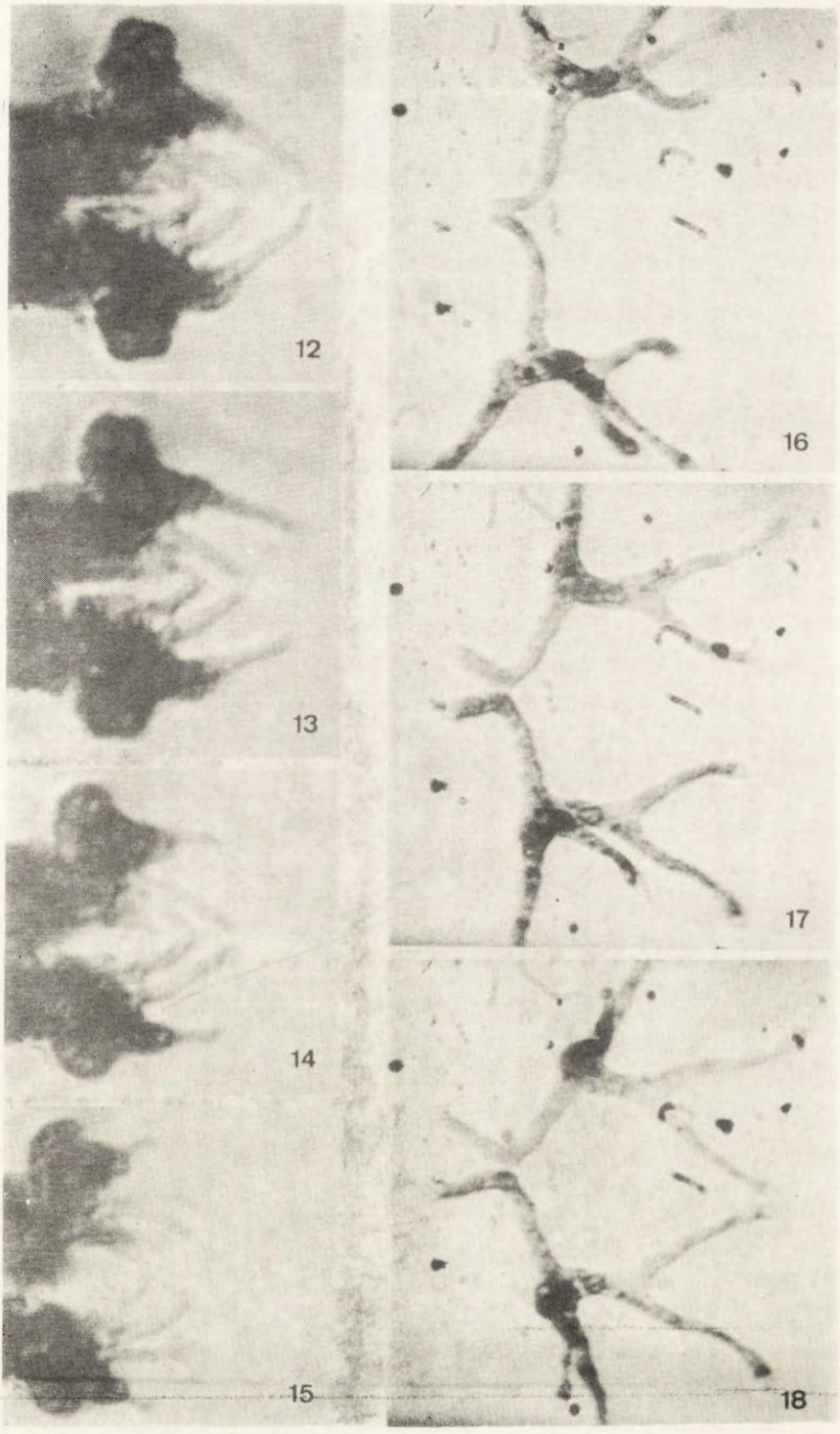

G. Nowakowska et A. Grębecki auctores phot.

ACTA PROTOZOOLOGICA
VOL. 17 (No. 2) WARSZAWA, 30 VI 1978 pp. 361–368

Department of Physiology and Cell Biology, Division of Biological Sciences, University of Kansas, Lawrence, Ks. 66045, U.S.A.

Eugene C. BOVEE[1], Roger A. LINDBERG[2] and Ronald E. GODDARD[3]

The Swimming Velocity of *Paramecium caudatum*

Synopsis. A model for assessing the swimming rate of *Paramecium caudatum* has been developed by computer-programmed analysis of data taken by measuring the swimming rates of two strains of that ciliate and clonal populations derived from them. The analysis indicated that: (1) Clonal populations in logarithmic growth are the more reliable for testing, (2) organisms are in the best condition for testing for 1.5 h following removal from the clone to the testing conditions, (3) under the restraints of (1) and (2), variation in swimming rate is over 99% dependent upon the length of time the organism is in the testing-solution, (4) in the testing conditions, the swimming rate of *Paramecium caudatum* declines steadily from a mean of 2.28 mm/s at onset of testing to 1.83 mm/s after 1.5 h. The model is being successfully used to test effects of various chemicals and various concentrations of them on the rate of swimming.

Few, intermittent reports in the past 50 years deal with the speed of forward swimming of *Paramecium*, either normally (Bullington 1930) or as affected by chemical or physical agents in the environment (cf. references in reviews by Jahn and Bovee 1964, 1967). In none of these has the mean, normal velocity been statistically determined for adequately fed organisms. Usually the organisms were starved 24 h (Lee 1956, Dryl 1959) thereby abnormally stressing them; and Dryl (loc. cit.) further stressed them by "adapting" them in a phosphate-buffered solution. Tawada and Oosawa (1972) grew their strain of *P. caudatum* in a lettuce infusion buffered to pH 7.0 with 2.5 mM Tris-maleate, but

Research supported by NSF Research Grant GB-16616.

[1] To whom reprint requests should be sent.

[2] Present Address: Biophysics Research Laboratories, University of Arizona, Tucson Arizona.

[3] Present Address: Department of Biology, Ottumwa Heights College, Ottumwa, Iowa.

they failed to give accurate data for the mean, normal swimming rate, saying, only, that "... average swimming velocity of paramecia was about 1–2 mm/s..." They gave, thereby, a range of velocity for most organisms, but neither the mean velocity nor a statistically-determined range.

Only Bullington (1930) has cited a presumed, mean, normal velocity for *P. caudatum*, giving 2.647 mm/s at 25°C for some collected near Wood's Hole, Massachusetts, grown in hay infusion at unknown pH. He measured the velocity of 13 organisms, once each, and calculated an average rate. This calculation is inadequate statistically and cannot be accepted on face value.

So that we might assess the effects of chemicals on the speed of forward swimming of *P. caudatum*, we had, first, to determine a statistically valid, mean, normal, swimming speed for healthy, unstarved organisms, with as little alteration of the growth medium as possible.

Material and Methods

Paramecium caudatum was taken from Potter's Pond, a small, artificial lake adjoining the life-science building on the campus of the University of Kansas at Lawrence, Kansas, U.S.A. Populations were fed on bacteria of unknown varieties from the same source, grown with the paramecia in an alfalfa-tea (Mote 1968) prepared in Chalkley's solution (Chalkley 1930) buffered to pH 6.8 with tris (hydroxymethyl) aminomethane, held at a room temperature of 23±0.5°C. Clones derived from those populations were similarly grown. So, also, were populations and clones derived from *P. caudatum* purchased from the General Biological Supply House (TURTOX), Chicago, Illinois, U.S.A.

Each *Paramecium* to be tested was pipetted from the top center of the culture and was isolated in a drop of tris-buffered Chalkley's solution of pH 6.8, to wash it, then was transferred by pipette to another clean drop of the same solution, then a third. The third drop, in a depression slide, was covered by a 25 mm-square coverslip sealed in place with petroleum jelly to prevent evaporation.

This slide was placed on the stage of a micro-projector and the image of the swimming *Paramecium* was projected on a large, white piece of paper. Projection was always done at the same distance from the paper and at the same magnification, which was calibrated so that 1 cm on the paper was equivalent to a real distance of 257 μm. As each *Paramecium* swam, its linear progress was traced across the field with a colored pencil. Time was recorded by an electric timer for the delineated path. Tracing and timing were always done by the same person to eliminate individual differences in reaction time of the investigator.

Computer-evaluation of data from samples run at different times of the day indicated a potential source of experimental error related to the growth cycle and predivisional reduction of swimming rate. All experiments were therefore done between 8 : 30 and 9 : 30 A.M. when few, if any organisms were dividing.

Heat and ultraviolet light from the light source were filtered out by a series of water-filled glass cells before the light reached the substage condenser of the microscope.

Five records were made within one minute at each of the following times for each organism tested: At zero time (immediately after the slide was placed on the microscope); at 15 min, 30 min, 45 min, 60 min, 75 min, 90 min, 120 min, 150 min, 180 min, 240 min, 300 min, and 360 min. Recordings were made for a group of 35 organisms for each group studied. This procedure was followed for heterogeneous and clonal groups in: (A) lag-phase growth; (B) logarithmic growth; (C) asymptotic growth; (D) declining growth; and (E) older, stationary growth.

The data obtained were processed by computer (Honeywell 635, at the University of Kansas) using formulas for parametric analyses of variance (Sokal and Rohlf 1969) and by the non-parametric tests for significance (Wilcoxon 1945) as outlined by Sokal and Rohlf (1969). Data were fed into the computer over a remote-terminal connection from the life-science building or by coded IBM cards. Fortran IV was the computer language used.

A second group of 35 organisms from the same clone were later photographed stroboscopically (see method of Bergquist and Bovee 1976) with 5–6 exposures sec and the distances between photographs of 5 or more organisms measured at each test interval. Swimming rates (means) measured by this method did not differ significantly from those measured by hand tracing, the rates being 2.28 mm/s at zero time and 1.79 mm/s at 75 min.

No statistically significant differences were found between the swimming rates of the clones of locally derived and commercially obtained strains of *Paramecium caudatum*.

Results

Heterogeneous Populations

The computer-analyses of swimming rates for randomly-selected, non-clonal individuals from the gross population of either strain showed that over 32% of the variation in swimming rates was due to individual differences amongst the organisms. Less than 10% was due to the methods. The remainder was due to other factors.

Analyses then made taking into account the age of the culture showed that variances due to individual differences were greater in cultures in lag-phase, asymptotic, declining and stationary growth phases and less in cultures during the logarithmic phase of growth.

Clonal Populations

Analyses of data on swimming speed of clonal paramecia also showed the least individual variation in swimming velocity among the logarithmically growing organisms. Analyses of variance showed that for those, time in the test medium was the principal factor which altered the swimming rate. Over 99% of the individual variation in rate for clonal organisms in logarithmic growth during the first 90 min is a function of

Table 1

A summary of the analysis of variance (ANOVA) of the swimming rate of *Paramecium caudatum* related to time in the resting solution

Source of variation	df	SS	MS	F_s
Among timings	5	93.058826	18.611765	13.087319*
Linear regression	1	92.202081	92. 202091	430.893129*
Deviations from regression	4	0.855919	0.213979	$< 1^{ns}$
Within group	258	366.907500	1.422122	
	263	459.96		

* highly significant ^{ns}not significant

$$R^2 = \frac{\text{Explained variation}}{\text{Total variation}} = \frac{\text{Linear regression}}{\text{Linear regression} + \text{deviations from regression}}$$

$$= \frac{92.202081}{92.202081 + 0.855919} = 0.990802$$

a linear regression related to time (Table 1). This regression establishes an accurate range of swimming rate and an accurate average swimming rate at any time during those first 90 min. After 90 min and during the 6 h thereafter, there was no common, steady rate of swimming amongst the organisms that could be deemed statistically reliable.

For a group of 44 organisms taken randomly from near the central surface of the Potter's Pond clone, the mean swimming speeds as computer-calculated are shown in Table. 2. At zero time, mean rate was

Table 2

Mean swimming rates ($\bar{Y}$) computer-derived, for *Paramecium caudatum*, with standard error

Time	$\bar{Y}$	SE
0 min	2.260 mm/s	0.67 mm/s
15	2.185	0.62
30	2.133	0.36
45	1.953	0.51
60	1.901	0.28
75	1.825	0.36

2.26 mm/s standard error 0.67 mm/s, followed by a steady regression in speed to a mean rate at 75 min of 1.83 mm/s with a standard error of 0.36 mm/s.

Confidence limits on r a n g e of speed at the given times, to the

99.9% confidence level are, 2.07 mm/s to 2.49 mm/s at zero time, regressing steadily to 1.71 to 1.96 mm/s at 75 min (Fig. 1).

Histograms (Fig. 2) prepared for the Potter's Pond clonal sample show that after exposure of 45 min (mid-point in the tests) to this-buffered Chalkley's solution, velocity was more often recorded as faster than 2.1 mm/s but less than 2.2 mm/s.

Swimming rates measured between 90 min and 6 h varied more among clonal organisms than did the swimming rates of organisms during the first 75 min, only a few organisms continuing to swim at a slower, steady rate. Some soon stopped, by 115 min, others cycled, changing speed, others pivoted. Those that continued to swim at a steady rate, more slowly, therefore were a select group, therefore not statistically representative of the group.

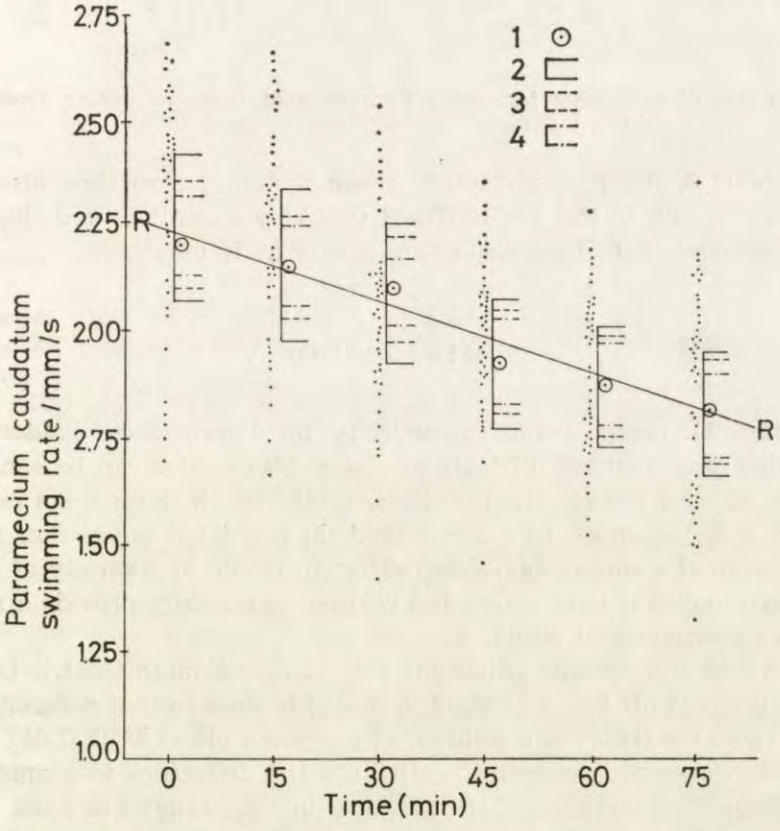

Fig. 1. R–R — Statistically Predicted Regression. *1* — Mean swimming rate; from data. *2* — 95% confidence range, *3* — 97% confidence range, *4* — 99% confidence range. Each dot represents average of 5 measurements of the swimming speed of one organism

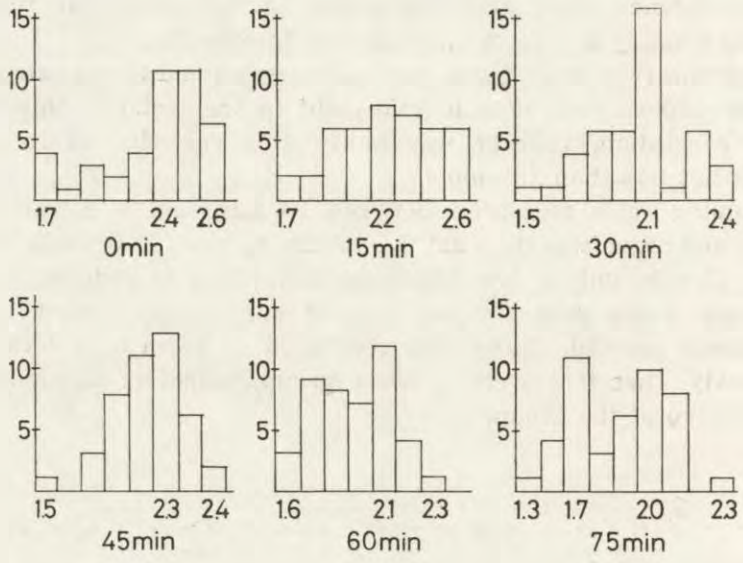

Fig. 2. Rates of swimming for tested Paramecia at times of testing. Ordinate — number of organisms. Abscissa — speed (mm/s)

In general, the paramecia that swam faster at zero time also swam faster at 75 min in the tris-buffered Chalkley's solution, and those that swam slower at zero time also swam slower at 75 min.

Discussion

A normal, mean, swimming velocity for *Paramecium caudatum*, or any other protozoan, is difficult to assess. Mean rates can be considered normal only for the specific conditions under which those mean rates are determined. The mean rate for a random, nonclonal population reflects the average of a sum of individual differences due to a variety of genetic and environmental parameters and will not necessarily provide a reliable base for experimental study.

Although the average swimming rate at zero-time in the tris-buffered test-solution at pH 6.8 at 23°C. (2.26 mm/s) is close to that determined by Bullington (1930) in a solution of unknown pH at 25°C (2.647 mm/s), it is not necessarily accurate to attribute the difference to temperature, even though an increase of temperature in that range has been said to cause altered swimming velocity (Tawada and Oosawa 1972). There are too many unkown parameters in Bullington's (1930) study, as well as in those of Tawada and Oosawa (1972).

While we cannot contend that we have found "the normal" swimming rate for *Paramecium caudatum,* although we may be close to such an expression, we have developed an experimental model with fewer variables and more nearly predictable swimming rates, over a useful period of time. This provides a better basis for the experimental study of altered parameters in the environment than has previously been achieved. We can now ascertain with accuracy the effect of almost any chemical or physical alteration of this model on the swimming rate of *Paramecium caudatum.* Similar models can also be developed for other protozoa or other organisms.

We have already used the model successfully to test the effects of certain chemicals on the swimming rate of *Paramecium caudatum.* Those results will be reported elsewhere.

ZUSMMENFASSUNG

Messungen der Bewegungsgeschwindigkeit in zwei Stämmen von *Paramecium caudatum* wurden mit dem Elektronenrechner analysiert und für die Erstellung eines Modells zur Bestimmung der Bewegungsgeschwindigkeit verwendet. Die Analyse ergab: (1) Die besten Messbedingungen sind während der logarithmischen Wachstumphase einer Kultur gegeben. (2) Die besten Ergebnisse werden der ersten 1.5 Stunden nach Überführing des Organismus in die Testlösung erzielt. (3) Unter die in (1) und (2) gegeben Bedingungen ist die Bewegungsgeschwindigkeit des Organismus zu 99% von der Dauer des Aufenhalts im Testmedium bestimmt. (4) Unter die Testbedingungen nimmt die Bewegungsgeschwindigkeit von *Paramecium caudatum* stetig von 2.28 mm/s zu Testbeginn auf 1.83 mm/s nach 1.5 Stunden ab. Mit Hilfe des Modells kann die Wirkung verscheidenen Chemikalien (in verscheidenen Konzentrationen) auf die Bewegungsgeschwindigkeit bestimmt werden.

REFERENCES

Bullington W. E. 1930: A further study of the spiralling of the ciliate, *Paramecium,* with a note on morphology and taxonomy. J. Exp. Zool., 56, 423–449.

Chalkley H. W. 1930: Stock cultures of *Amoeba proteus.* Science, 71, 442.

Dryl S. 1959: The velocity of forward movement of *Paramecium caudatum* in relation to pH of the medium. Bull. Acad. Sci. Pol. Ser. Sci. Biol., 9, 71–74.

Jahn T. L. and Bovee E. C. 1964: Protoplasmic movements and locomotion of protozoa. In: Physiology and Biochemistry of Protozoa (ed. S. H. Hutner), Vol. 3, 62–129. Academic Press, New York.

Jahn T. L. and Bovee E. C. 1967: Motile behavior of protozoa. In: Research in Protozoology (ed. T. T. Chen), Vol. 1, 41–200. Academic Press, New York.

Lee J. W. 1956: Effect of pH on velocity of ciliary movement in *Paramecium.* J. Protozool., 3 (suppl.), 9.

Mote R. F. 1968: A method of culturing air bacteria for protozoa cultures. Proc. Iowa Acad. Sci., 73, 387–390.

Sokal R. R. and Rohlf F. J. 1969: Biometry. W. H. Freeman and Co. San Francisco.
Tawada K. and Oosawa F. 1972: Responses of *Paramecium* to temperature. J. Protozool., 19, 53–57.
Wilcoxon F. 1945: Individual comparisons by ranking methods. Biom. Bull., 1, 80–83.

Received on 16 November 1977

ACTA PROTOZOOLOGICA
VOL. 17 (No. 2) WARSZAWA, 30 VI 1978 pp. 369–374

Department of Cell Biology, M. Nencki Institute of Experimental Biology, Polish Academy of Sciences, Pasteura 3, 02-093 Warszawa, Poland

Michał OPAS, Barbara HREBENDA
and Barbara TOŁŁOCZKO

Contractility of Glycerol-extracted Nuclei of *Amoeba proteus*

Synopsis. Observations of contractile activity of glycerol-extracted *Amoeba proteus* nuclei led us to the assumption that in the size changes of nuclei two mechanisms may be involved. One of them is based on the dependence of spatial configuration of nucleus components upon ionic properties of a medium; the second one is based on the sensibility of nuclear contractile proteins to ATP. A possible involvement of several nuclear constituents in the size changes is discussed.

Size changes of isolated nuclei of *Amoeba proteus* induced by the treatment with several chemical agents have been described by Korohoda et al. (1968). These authors interpretated the observed size changes as resulting from conformational changes in the nuclear membranes, caused by alterations in their surface charge. Since nuclei of glycerinated *A. proteus* models usually change their size during the contraction of the model, it was of an interest to determine whether the glycerol-extracted nuclei changed their size actively or were collapsed by the contracting environment.

Material and Methods

Amoebae were glycerinated according to Rinaldi et al. (1975) for 6–8 h. The models of amoebae were disrupted and the intact nuclei were released to the washing solution. Then the models of nuclei were placed on a slide and covered with a cover glass with enough space to permit irrigation and to avoid supressing of the nuclei.

Solution used:

Extraction solution: glycerol 50% (v/v), 0.05 M KCl, 0.005 M EDTA, 0.01 M Tris; I ≈ 0.05, pH ≈ 7,0 (adjusted by 0.01 M MES).

Supported by grant MR II. 1.3.2.

Washing solution: 0.05 M KCl, 0.01 M Tris; I ≈ 0.05, pH ≈ 7.0 (adjusted by 0.01 M MES).

Washing solutions of a different ionic strength were obtained by changing KCl concentration in the basic solution.

Contraction solution: 0.005 M ATP, 0.005 M $CaCl_2$, 0.005 M $MgCl_2$, 0.02 M KCl; I ≈ 0.05, pH ≈ 7.0 (adjusted by 0.01 M Tris). ATP, $CaCl_2$, $MgCl_2$ solutions (0.005 M each) were prepared on a basis of the washing solution.

Small spherical fragments (50–120 μm in diameter) obtained by a centrifugation (10000–12000 g) of amoebae were used as a comparative material.

Nuclei were observed in a dark field and differential interference contrast microscopy and were photographed using Polaroid P/N 55 and ORWO NP 20 negatives.

For electron microscopy the cells were fixed in 2% glutaraldehyde followed by 2% OsO_4 in 0.04 M cacodylate buffer pH 7.4 and then dehydrated in increasing ethanol series and two changes of propylene oxide. The material was embedded in Epon and sectioned with LKB ultramicrotome. Sections contrasted with uranyl acetate and lead citrate were examined in JEM 100B electron microscope.

Results

The size of isolated nuclei as well as of their glycerinated models is strongly dependent on pH and on ionic strength of the medium. As pH of the medium increases up to 10.5, isolated nuclei (Pl. I) and the glycerinated models (Pl. II) expand; above pH 10.5 the nuclei as well as their models dissolve.

The effect of ionic strength on the size of nuclei models is not so dramatic as that of pH. When ionic strength of the medium increases from 0.001 to 0.05, slight contraction with concomitant chromatin condensation (Pl. III a–d) occurs in the models; further increment in ionic strength has no influence on the size and chromatin structure (as seen in light microscopy) of nuclei models (Pl. III d–f).

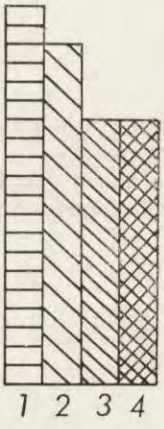

Fig. 1. Sequential effects of ATP, Ca++, and Mg++ on the size of the glycerinated model of *A. proteus* nucleus. The nucleus was placed sequentially in: 1 — washing solution; 2 — ATP solution; 3 — Ca++ solution; 4 — Mg++ solution. The size change of the nucleus in the solutions in presented as a change in the nucleus optical cross-section area. The area of optical cross-section of the nucleus in the washing solution was taken as 100%

Perfusion of the glycerinated models of amoeba nuclei with the contraction solution results in contraction of the models. The extent of size changes during this contraction is very variable. Extremely strong contraction (reduction of optical cross-section area to 44% of initial value) is shown in Pl IV. If the model of a nucleus is passed through the solution of ATP followed by $CaCl_2$ and $MgCl_2$ solutions, a gradual contraction occurs as shown in Fig. 1.

It was found that, unlike nuclei and their models, spherical fragments and their glycerinated models are not sensitive — with respect to their size — to pH changes of a medium (Pl. V and VI). On the other hand, upon application of the contraction solution the glycerinated models of the fragments contract vigorously (Pl. VII).

Discussion

Since the size changes of nuclei observed in contracting glycerinated models of amoebae are observed also in the isolated glycerinated models of *A. proteus* nuclei, therefore we can conclude that amoebic nuclei are able to contract and expand autonomously. In the models of nuclei there are several structures which might play a role in the observed size changes. These are:

Chromatin. Chromatin is thought to be the main nuclear structure responsible for size changes of nuclei under influence of external factors such as pH, ionic strength etc. in many types of nuclei (Anderson and Wilbur 1952, Philpot and Stanier 1956, Olins and Olins 1972, Badr 1974). Although we have been observing chromatin expanding and contracting in concert with the size changes of the nuclei models, our preliminary experiments on glycerinated models of empty nuclear envelopes showed that they react on external factors in essentially the same way as intact nuclei or their models. Therefore, the chromatin, though being undoubtly involved in the size changes of the nuclei models, does not constitute the only and main structure responsible for them.

Perinuclear cisternae. It may be assumed, that amoebic cell membranes can not actively and autonomously change their surface area to a large extent (Wolpert and Gingell 1968). Membranes of perinuclear cisternae, although distinct from plasmalemma (Franke 1974), do not differ from other membranes so profoundly to be thought responsible for the size changes of nuclei. Our experiments on the spherical fragments of amoebae suggest that plasmalemma and, analogically, membranes of perinuclear cisternae are not recognizably sensitive to external factors with respect to the size changes.

Honeycomb layer. A complex fibrous lattice — closely apposed to the inner aspect of perinuclear cisternae — which might be responsible for the nuclear size changes dependent on pH or ionic strength of a mediu is shown in Pl. VIII and IX. The cylindrical elements of the lattice are built of thin fibrils lying parallel to the perinuclear cisternae. In sections parallel to the nucleus surface the fibrils surround the cylinders of the lattice. Due to the tight and ordered arrangement of the cylinders, they are frequently deformed into hexagonal configuration, giving a honeycomb appearance (Greider et al. 1956, Pappas 1956, Mercer 1959, Leeson and Bhatnagar 1975a).

The model of a nucleus behaves like an anionic polyelectrolite in a solution, collapsing as it overall surface charge density is reduced by acidification or increment in ionic strength of the medium (Katchalsky 1964). Our presumption is, that fibrillar elements packed parallely to the perinuclear cisternae act as flexible polyelectrolyte molecules, changing their spatial arrangement upon altered ionic state of an environment. In this way the size of nuclei would be dependent on conformational state of molecules packed in the honeycomb layer (Katchalsky 1964, Scheraga 1967).

ATP-sensitive contractile elements. With respect to the contractile response upon application of the contraction solution, the models of nuclei behave essentially in the same way as the models of sperical fragments. In essence, the glycerinated models of isolated *A. proteus* nuclei contract upon application of ATP-Ca^{2+}-Mg^{2+} exactly like the glycerinated models of whole amoebae (Rinaldi et al. 1975). Since the contraction of the amoeba model depends upon activity of a model cortex (Opas 1976, Rinaldi and Opas 1976) with ordered arrays of filaments (Rinaldi and Hrebenda 1975), it is quite possible that a similiar system might be operating in the models of isolated nuclei.

The possibility exists that cytoplasmic filaments closely applied to the nuclear envelope (Pl. X, Leeson and Bhatnagar 1975 b) might be responsible for ATP-induced contraction of the nuclei. Having no electronmicrographs of isloated nuclei we can not exclude this possibility completely, however, in our opinion, the glycerination with subsequent isolation is drastic enough to clean the model from any outer remnants of cytoplasm.

Much more attractive is the possibility that ATP-sensitive contractile proteins are present in the nuclei. Since the first report on the occurrence of contractile proteins of a nuclear origin (Zbarski and Pierewoz-czikowa 1951), the evidence has accumulated that muscle-like contractile proteins are present in various types of nuclei (Ohnishi et al.

1964, Jockusch et al. 1971, 1973, Hauser et al. 1975, Lestourgeon et al. 1975). Contractile proteins are thought to be involved in the mitotic processes and in the structural interconversions of chromatin (Jockusch et al. 1971, Lestourgeon et al. 1975). Myosin-like filaments were observed in *Physarum polycephalum nuclei* (Jockusch et. al. 1973), whereas inside *Amoeba proteus* nuclei thick arrays of filaments ordered parallel to the nuclear envelope were described. (Leeson and Bhatnagar 1975 b). Whether or not these filaments are structural basis for ATP-induced contractions of the nuclei models is not known.

The above discussed data suggest that in *Amoeba proteus* two mechanisms are operating during the size changes of nuclei. One of them is based on the change of spatial arrangement of charged constituents of the nuclear envelope under the influence of altered net surface charge; the second one is based on the sensibility of nuclear contractile proteins to ATP. Both the mechanisms need further investigations.

RÉSUMÉ

L'observation des conctractions des noyaux de l'*Amoeba proteus* aprés leur glycérination indique que deux mécanismes différents peuvent contribuer aux changements de dimensions des noyaux. Le prémier est basé sur la dépendence de la configuration géométrique des composants du noyau de la composition ionique du milieu, et le second sur la sensibilité des protéines nucléaires contractiles à l'ATP. On discute l'engagement possible des différents composants du noyau dans les changements de ses dimensions.

REFERENCES

Anderson N. G. and Wilbur K. M. 1952: Studies on isolated cell components. IV. The effect of various solutions on the isolated rat liver nucleus. J. Gen. Physiol., 35, 781–796.

Badr G. G. 1974: In vitro response of nuclei isolated from rat brain to pH changes, enzymes and heparin treatment: Cytochemical characteristics and incorporation of ^{3}H-uridine and ^{14}C-valine. Cytobiologie, 8, 257–268.

Franke W. W. 1974: Nuclear envelopes. Structure and biochemistry of the nuclear envelope. Phil. Trans. R. Soc. Lond. B., 268, 67–93.

Greider M. H., Kostir W. J. and Frajola W. J. 1956: Electron microscopy of the nuclear membrane of *Amoeba proteus*. J. Bioph. Biochem. Cytol., 2, 445–447.

Hauser M., Beinbrech G., Gröschel-Stewart U. and Jockusch B. M. 1975: Localisation by immunological techniques of myosin in nuclei of lower eucariotes. Expl. Cell Res., 95, 127–135.

Jockusch B. M., Brown D. F. and Rusch H. P. 1971: Synthesis and some properties of an actin-like protein in the slime mold *Physarum polycephalum*. J. Bacteriol., 108, 705–714.

Jockusch B. M., Ryser U. and Behnke O. 1973: Myosin-like protein in *Physarum* nuclei. Expl. Cell Res., 76, 464–466.
Katchalsky A. 1964: Polyelectrolytes and their biological interactions. Biophys. J., 4, 9–41.
Korohoda W., Forrester J. A., Moreman K. G. and Ambrose E. J. 1968: Size changes in isolated nuclei of *Amoeba proteus* on treatment with polyionic substances. Nature, 217, 615–617.
Leeson T. S. and Bhatnagar R. 1975 a: *Amoeba proteus*: The nuclear periphery. Cell Differentiation, 4, 79–86.
Leeson T. S. and Bhatnagar R. 1975 b: Microfibrillar structures in the nucleus and cytoplasm of *Amoeba proteus*. J. Exp. Zool., 192, 265–270.
Lestourgeon W. M., Forer A., Yang-Z., Bertram J. S. and Rusch H. P. 1975: Contractile proteins. Major components of nuclear and chromosome non-histone proteins. Biochim. Biophys. Acta, 379, 529–552.
Mercer E. H. 1959: An electron microscopic study of *Amoeba proteus*. Proc. Roy. Soc. B., 150, 216–232.
Ohnishi T., Kawamura H. and Tanaka Y. 1964: Die Aktin und Myosin ähnliche Proteine im Kalbsthymuszellkern. J. Biochem., 56, 6–15.
Olins D. E. and Olins A. L. 1972: Physical studies of isolated eucariotic nuclei. J. Cell Biol., 53, 715–736.
Opas M. 1976: Course of glycerination of *Amoeba proteus* and contraction of glycerinated models. Acta Protozool., 15, 485–499.
Pappas G. D. 1956: The fine structure of the nuclear envelope of *Amoeba proteus*. J. Bioph. Biochem. Cytol., 2, 431–434.
Philpot J. S. and Stanier J. S. 1956: The choice of the suspension medium for rat-liver-cell nuclei. Biochem. J., 63, 214–223.
Rinaldi R. A. and Hrebenda B. 1975: Oriented thick and thin filaments in *Amoeba proteus*. J. Cell Biol., 66, 193–198.
Rinaldi R., Opas M. and Hrebenda B. 1975: Contractility of glycerinated *Amoeba proteus* and *Chaos chaos*. J. Protozool., 22, 286–292.
Rinaldi R. and Opas M. 1976: Graphs of contracting glycerinated *Amoeba proteus*. Nature, 260, 525–526.
Scheraga H. A. 1967: Contractility and conformation. J. Gen. Physiol., 50, 5–24.
Wolpert L. and Gingell D. 1968: Cell surface membrane and amoeboid movement. In: Aspects of Cell Motility. Symp. Soc. Exp. Biol., 22, 169–198.
Zbarski I. B. and Pierewozczikowa K. A. 1951: Sokratitielnyje swoistwa biełkow kletocznogo jadra. Biokhimia, 16, 112–127.

Received on 26 October 1977

EXPLANATIONS OF PLATES I–X

Plate I: Nucleus in the washing solution, a — pH 8.0; b — pH 4.0. Magnification: 2700 ×

II: Glycerinated model of a nucleus in the washing solution. a — pH 6.5; b — pH 4.0. Magnification: 1900 ×

III: Effect of ionic strength (I) of the medium on the size of the glycerinated model of a nucleus. a — I = 0.001; b — I = 0.01; c — I = 0.03; d — I = 0.05; e — I = 0.1; f — I = 0.2. Magnification: 1000 ×

IV: Effect of ATP-Ca^{++}–Mg^{++} on the size of the glycerinated model of a nucleus. a — before; b — after addition of ATP-Ca^{++}–Mg^{++} solution. Magnification: 1200 ×

V: Lack of effect of pH on the living spherical amoeba fragment. a — pH 5.1; b — pH 9.6. Magnification: 500 ×

VI: Lack of effect of pH on the glycerinated model of a spherical amoeba fragment. a — pH 4.0; b — pH 9.4. Magnification: 500 ×

VII: Effect of ATP-Ca^{++}–Mg^{++} on the size of the glycerinated model of a spherical amoeba fragment. a — before; b — after addition of ATP-Ca^{++}–Mg^{++} solution. Magnification: 800 ×

VIII: a — low power electron micrograph of nucleus. f — cytoplasmic filaments; tr — honeycomb layer cut transversly; tn — honeycomb layer cut tangentially. Magnification: 9600 ×.

b — tangential section of honeycomb layer. Magnification: 54 000 ×

IX: Transverse sections of honeycomb layer. a — magn. 27 600 ×; b — magn. 144 000 ×

X: Thick and thin filaments associated with a nucleus. a — magn. 16 800 ×; b — 27 000 ×

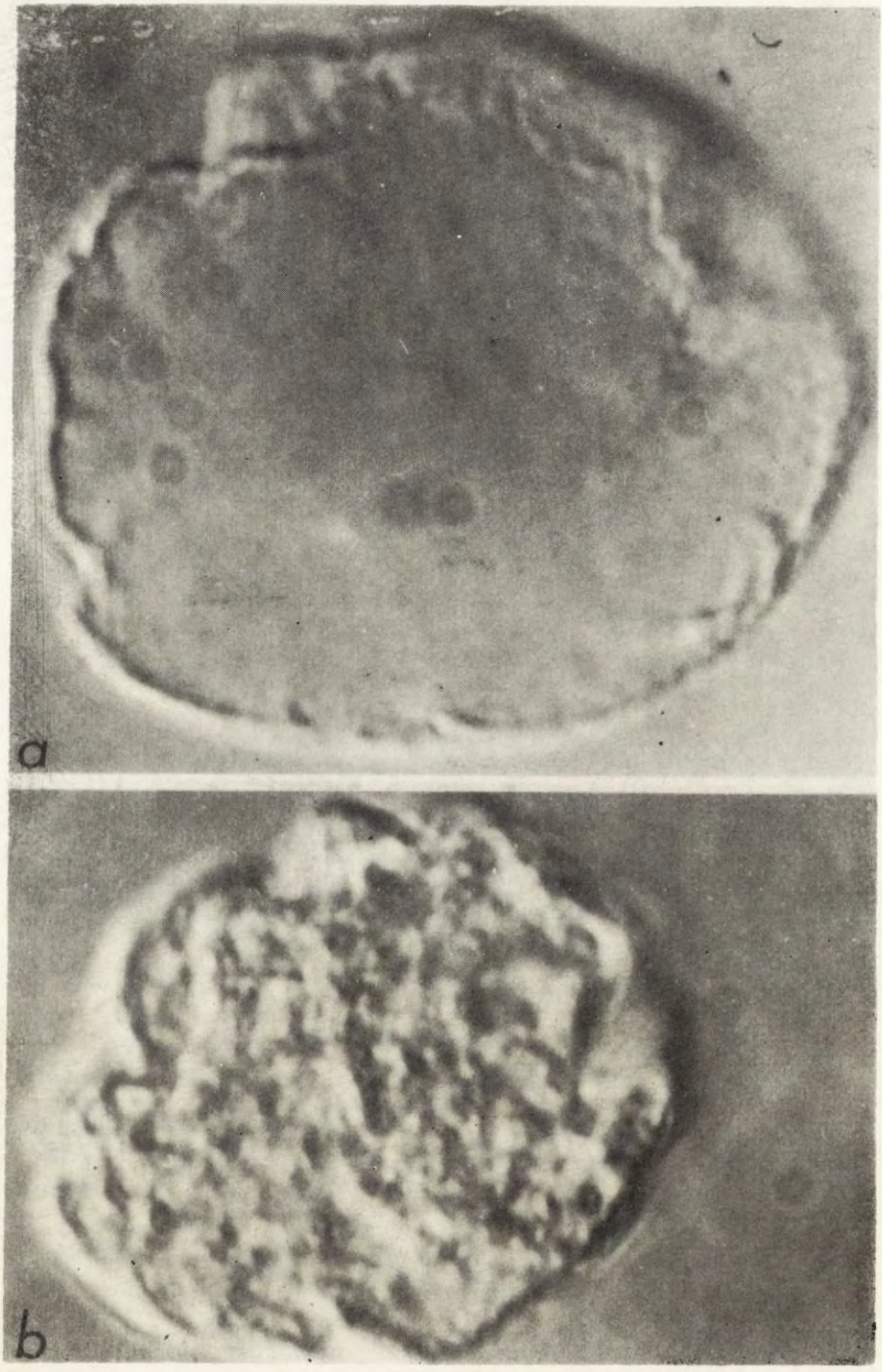

M. Opas et al. auctores phot.

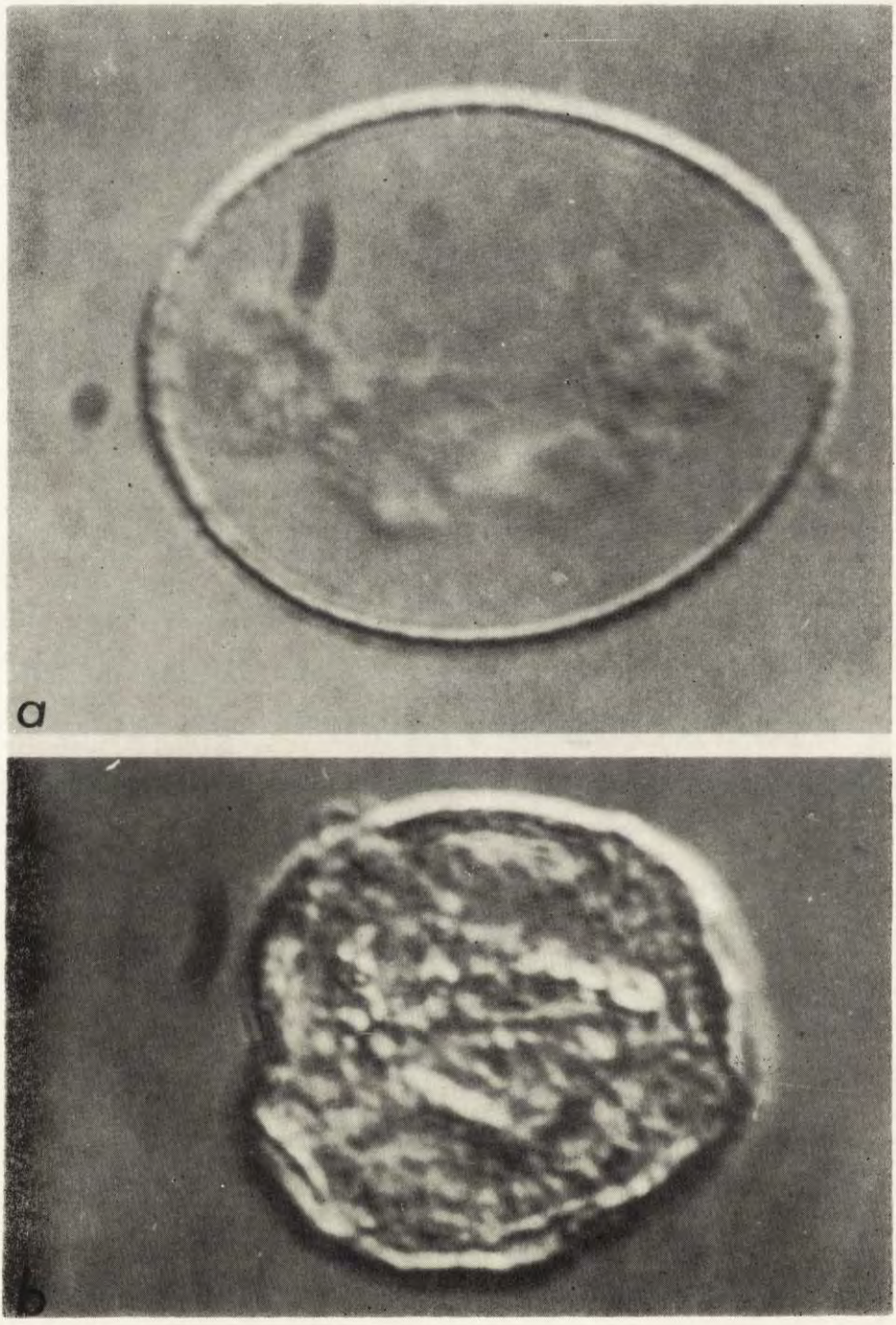

M. Opas et al. auctores phot.

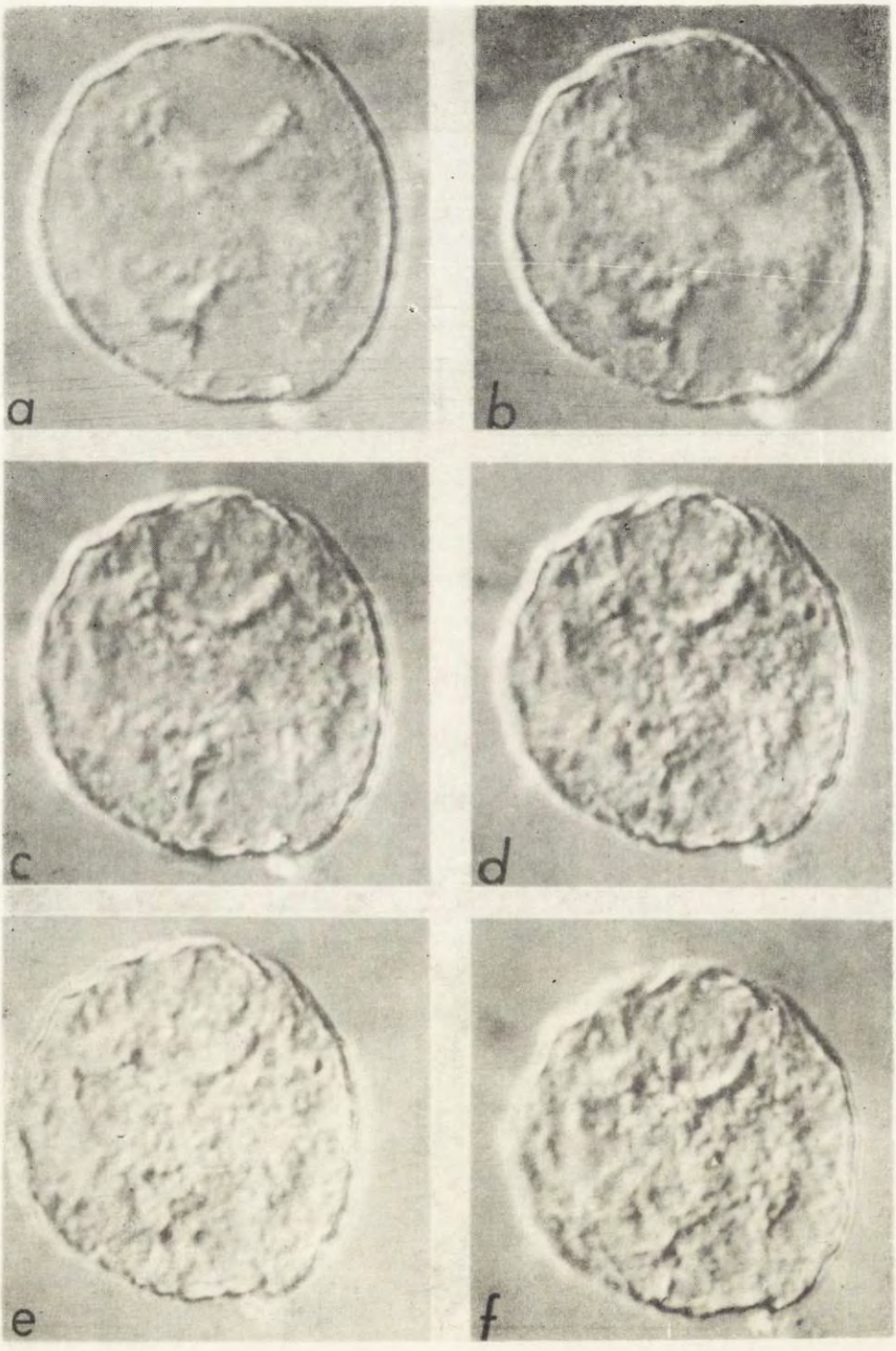

M. Opas et al. auctores phot.

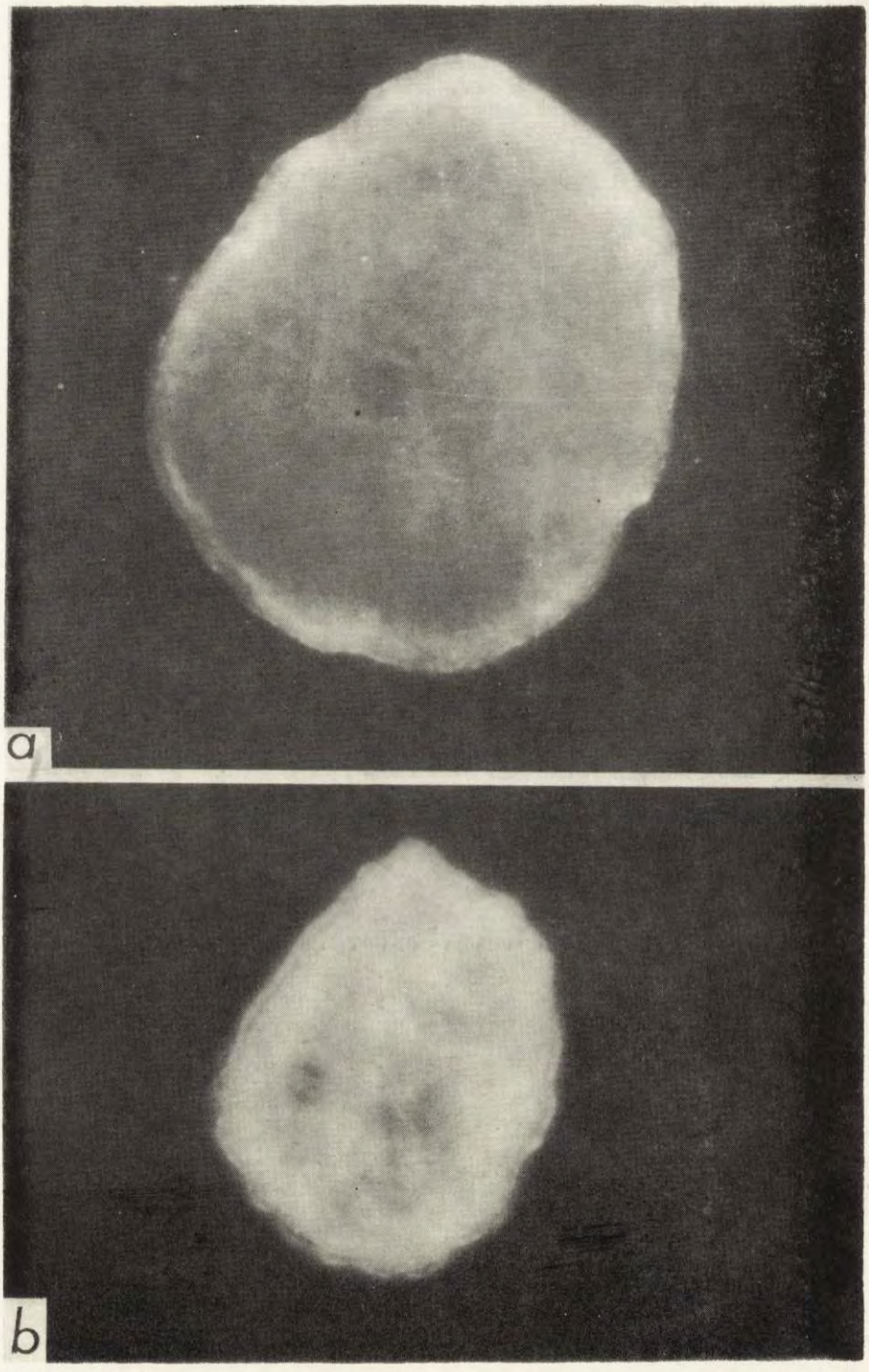

M. Opas et al. auctores phot.

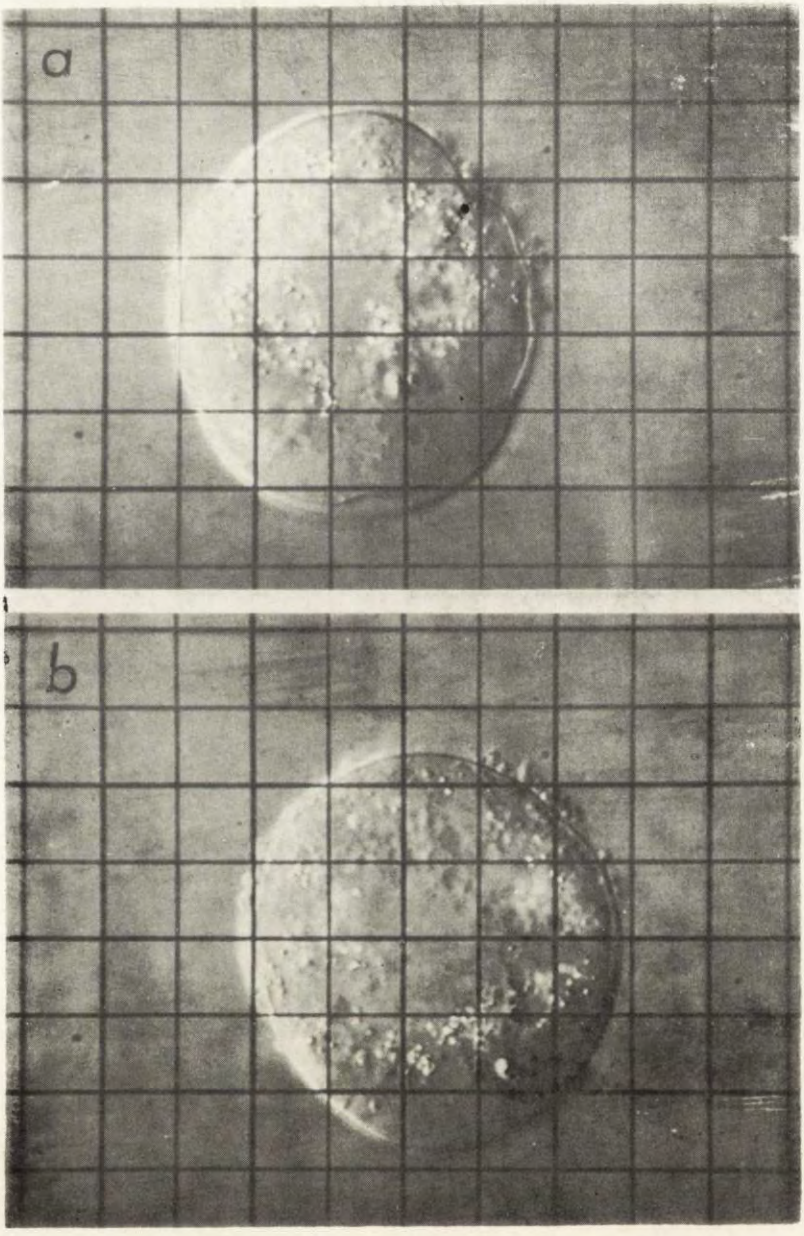

M. Opas et al. auctores phot.

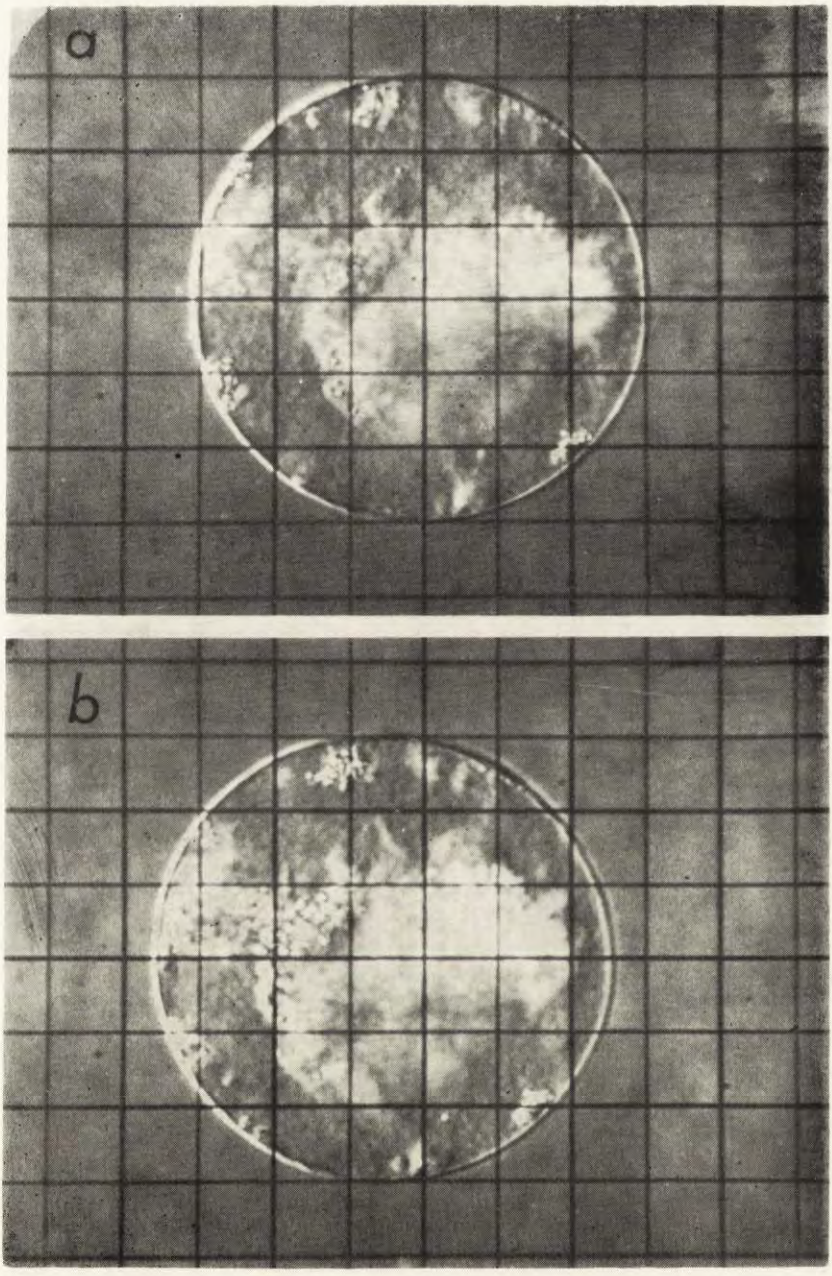

M. Opas et al. auctores phot.

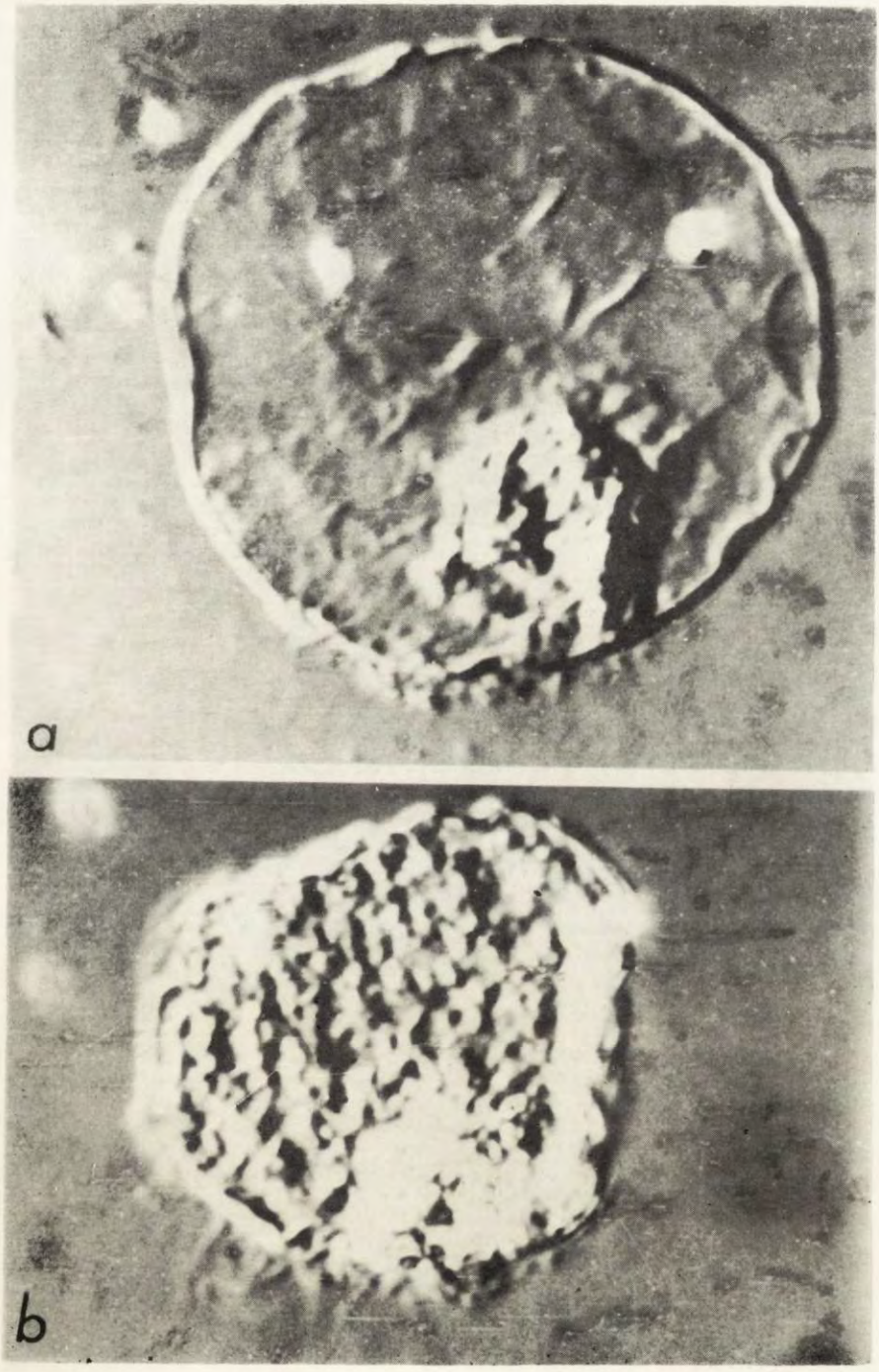

M. Opas et al. auctores phot.

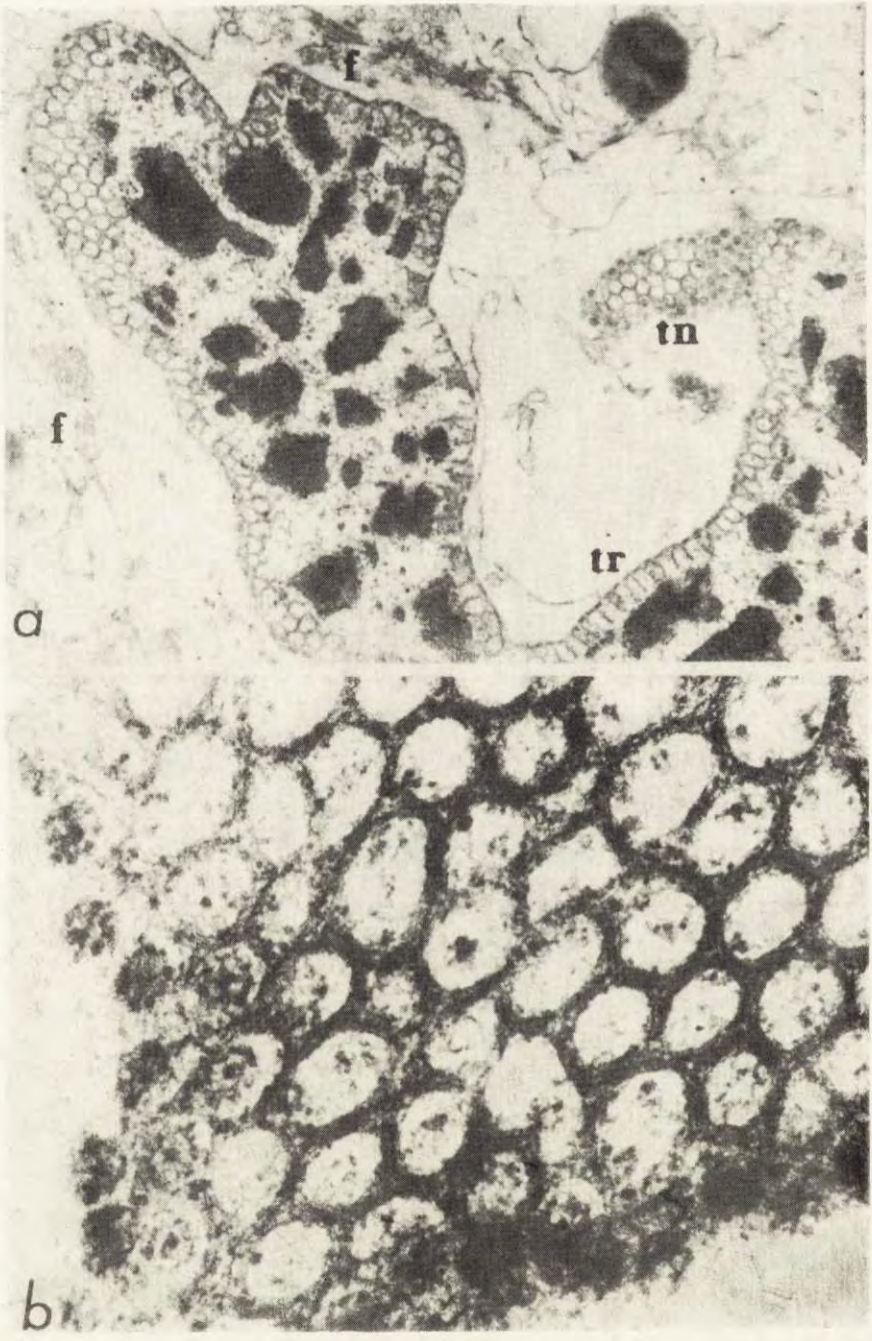

M. Opas et al. auctores phot.

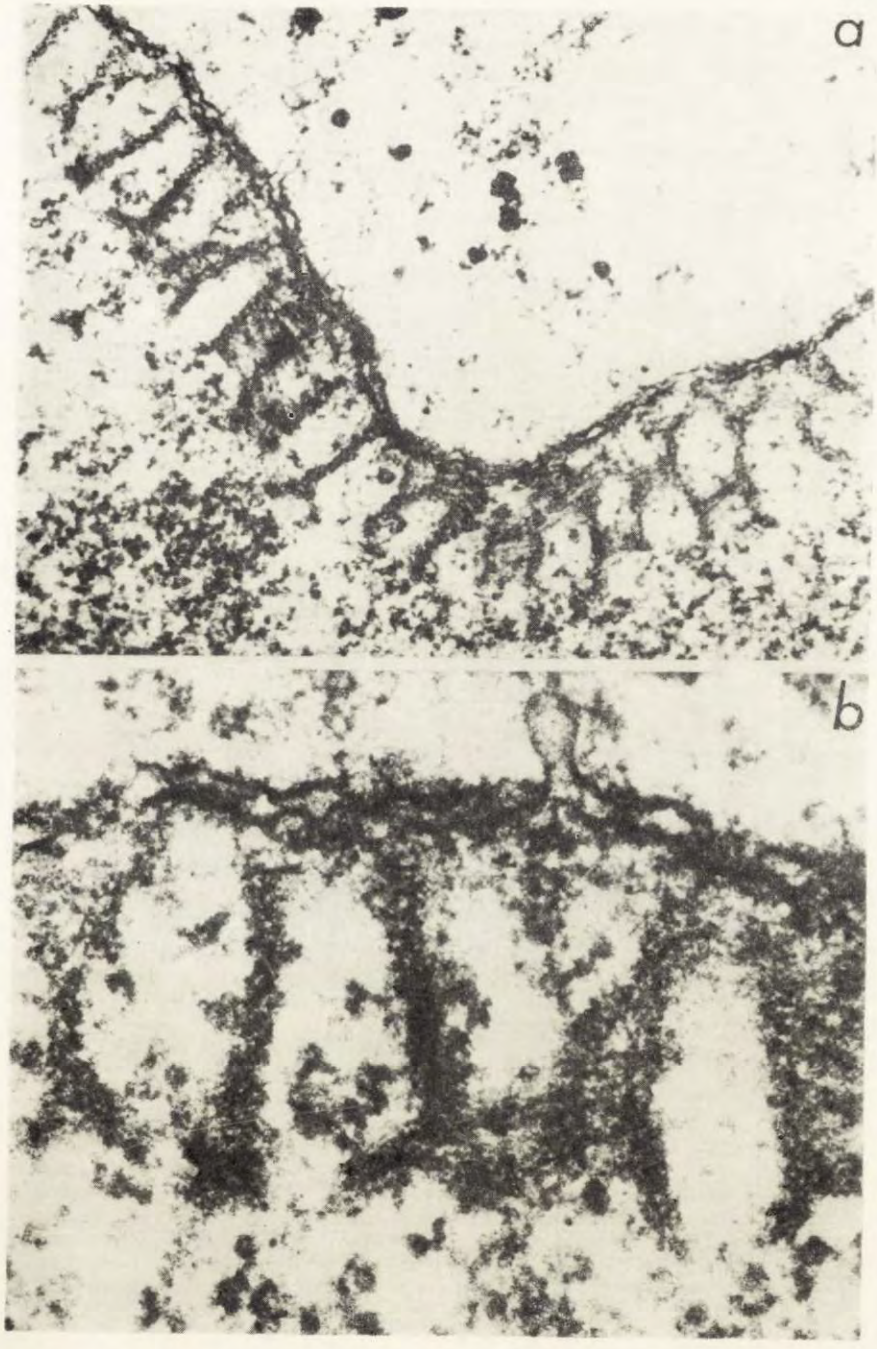

M. Opas et al. auctores phot.

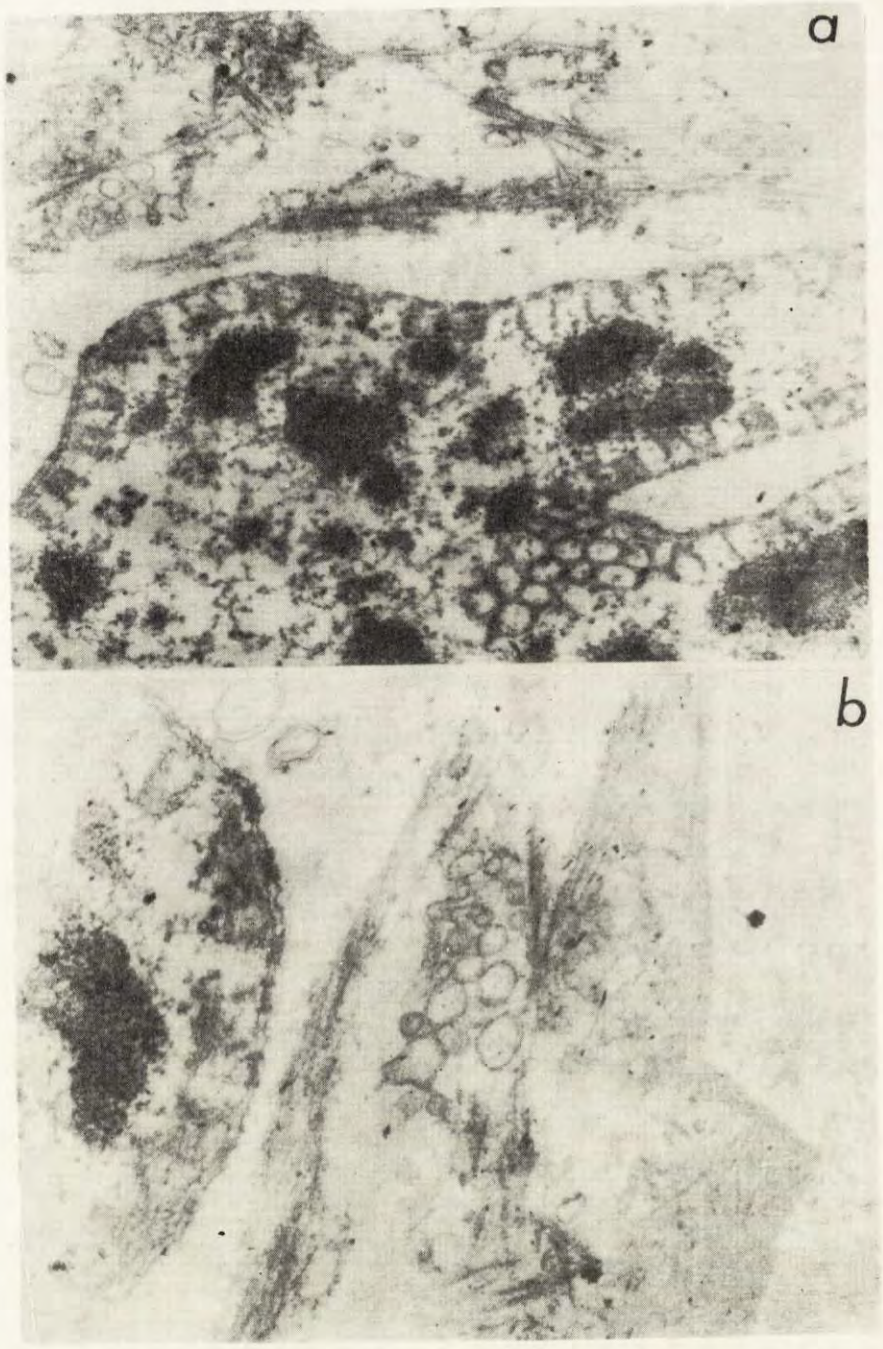

M. Opas et al. auctores phot.

ACTA PROTOZOOLOGICA
VOL. 17 (No. 2) WARSZAWA, 30 VI 1978 pp. 377–388

Department of Biology, Nencki Institute of Experimental Biology, Pasteura 3, 02-093 Warszawa, Poland

Zbigniew BARANOWSKI

The Contraction-relaxation Waves in *Physarum polycephalum* Plasmodia

Synopsis. Migration of *Physarum polycephalum* plasmodia on an agar surface was registrated by use of a 16 mm camera (15 fr/min; transmitted light). On the films, the changes of thickness of the plasmodium are seen as an alternately occurring light and dark areas. These changes are interpretated as contraction–relaxation waves. The waves may appear as ordered (advancing waves) or random (flickering waves) changes of the plasmodium thickness, as shown on phase-graphs obtained by microdensitometry scanning technique. The qualitative and quantitative relationships between the propagation of synchronic contraction–relaxation waves and migration of the organism are discussed.

Plasmodia of *Physarum polycephalum* show a characteristic protoplasmic streaming (shuttle streaming) within plasmodial strands. It is generally accepted that the flow of endoplasm in plasmodium is passive and takes place as a result of small preasure differences between the neighbouring areas of the plasmodium. The preasure changes within the protoplasmic channels, filled with the solificated endoplasm are effected by contraction activity of cytoplasmic actomyosin. Migration of *Physarum polycephalum* plasmodium is caused by the polarity of protoplasm transport (see reviews: Kamiya 1959, Komnick et al. 1973).

A way of arranging the fibrils (Wohlfarth-Bottermann 1975 a) suggests the radial (in relation to the channel) character of action of the actomyosin network, which was confirmed experimentally (Wohlfarth-Bottermann 1975 b, Baranowski 1976 a). Attempts to relate the contraction of the channel to the phenomenon of the endoplasm flow within it met a lot of interpretative difficulies. Both the processes have the same duration of periodic changes, however there is a difference of phase between them (Kamiya 1950, Sachsenmaier et al. 1973,

Supported by grant MR II. 1.3.2.

Baranowski 1976 a). This brought the necessity of introducing of parameter "A" (Baranowski 1976 a). Parameter "A" is an integral in which subintegral function is the process of changes of the area of the channel cross section, limits of integration are defined by the moments of time corresponding with the changes in the direction of endoplasm flow through the investigated cross section. The polarization of this parameter indicated the possibility that the larger mass of the endoplasm can be carried through the given cross section of the channel in one of the two possible directions. However, it does not explain the behaviour of plasmodium as an integrated system. On the other hand, the integration of the contractile processes is indispensable to cause the migration of plasmodium. At the same time the organization of these processes must be labile enough to let the organism react quickly to the changes in its external environment.

This work is an attempt of qualitative and quantitative presenting of wave phenomena taking place in the plasmodium of *Physarum polycephalum*. Part of the work was published previously (Baranowski 1976 b, Baranowski and Kuźnicki 1977).

Material and Methods

Physarum polycephalum was cultured on a wet filter paper with tap water in a dark place and fed with oat meal, according to Camp's method (1936). The pieces of the filter paper with a thick front of actively growing plasmodium were placed on the surface 2% agar on a Petri dish without food supply. After about one hour plasmodium left the filter paper and reached the characteristic migration pattern. The migrating plasmodium on the agar surface was filmed in transmitted light with the frequency of 15 frames/min. The light was turned on automatically 0.1 s before each exposure. The observation was made while the film was projected with the speed of 16 frames/s.

The quantitative data were obtained by means of double-beam recording microdensitometer MK III C.S. (Joyce, Loebel and Co. Ltd.). The microdensitometer possesses a built-in set for 16 mm film fasten. Densitometric cross sections obtained for the same line but from different chosen frames allowed to follow the changes of the plasmodium thickness in time.

Results

Appearance and disappearance of dark fields in the area occupied by the plasmodium were seen in all cases when the film was projected with the speed of 16 frames/s. The propagation of the dark and light areas of plasmodium is further referred to as the propagation of thickness or contraction-relaxation waves.

The Advancing and Flickering Waves

The pictures 1–6 shown in Pl. I present the migration of the plasmodium *Physarum polycephalum*. At the time 800–2000 s, which correspond to the interval between 3, 4, 5 and 6 photographs the organization of appearance and displacement of the dark fields of the plasmodium occured.

The photographs reflect only partly the character of the wave phenomena observed during the projection of the film. The synchronization of the plasmodium thickness changes in the areas lying close to each other takes place in such a manner that it causes the creation of the uniform wave front perpendicular to the main channels of the plasmodium (Pl. II). The sense of the propagation vector is perpendicular to the frontal edge of plasmodium. In the period of time preceding the appearance of the advancing wave a very complicated picture resembling "flickering" is observed. At that time, in the different parts of the plasmodium, waves propagating themselves in the different directions over the limited areas originated. There are no definite place of generation, so, rather unstable in time and space centers of generation occur. Probably every area of the frontal zone of plasmodium is equally capable to create the center of wave generation. On the photographs presented in Pl. I the rectangular test grid was drawn. In rectangles of this grid, where it was possible to estimate, there are the arrows showing the vectors of propagation of the waves observed in these areas in the time intervals between the subsequent photographs. The phase of "flickering" lasts from 0 to about 800 s (Pl. I 1–3). Advancing waves (Pl. I 4–6) appeared afterwards.

The Qualitative Relationship between Migration of Plasmodium and the Direction of Waves Propagation

Plate I presents the migration of *Physarum polycephalum* plasmodium. It is distinctly visible while comparing photographs 3, 4, 5 and 6. At that time, as it was mentioned above, propagation of the uniform front of the synchronic waves in the direction of plasmodium edge has appeared (Pl. II).

Plate III presents the photographs of the plasmodium front which did not migrate. Projecting the film from which those photographs were extracted showed that during the entire observation time the plasmodium was in the phase of flickering or partial synchronization, visible in the front zone only. In the zone of channels the recording and observation of waves was immposible. The arrows, just like in Pl. I show the vectors

of the propagation of locally occurring waves. It is probable that the plasmodium presented in Pl. III was resteering the direction of waves propagation in order to withdraw the protoplasm to the zone being out of the observation area. The decreasing thickness of the plasmodium seems also to point out this possibility.

The change of migration direction and, connected with it, the change of the direction of wave propagation is presented in Pl. IV. It shows the migration of plasmodium and the change in its direction. At the begining the plasmodium was moving downwards of the photographs. After about 26 min there could be seen the process of thickening of the channels in the zone following the front. The migration downwards was stopped after about 80 min. At that time there begun the creation of the wave front propagating itself upwards occurred.

The presented observations seem to be sufficient to draw a conclusion that the dark areas of plasmodium represent the resultant transport of the endoplasm in the direction of the plasmodium migration.

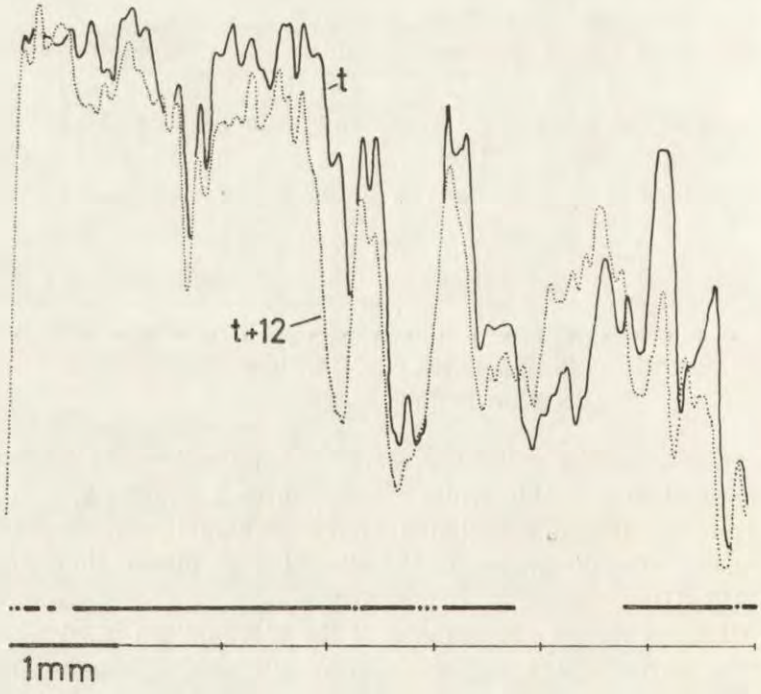

Fig. 1. Densitometric cross sections of plasmodium *Physarum polycephalum* (Pl. I). Time interval between curves — 12 s. The changes of plasmodium thickness are schematically marked on the line under the curves. The continuous line means the contraction of the plasmodium, the dotted line — the lack of thickness changes, the gap — relaxation and increment of plasmodium thickness

The Phase-graphs

In order to follow the wave phenomena in the plasmodium *Physarum polycephalum* phase-graphs were drawn. On the phase-graphs lines perpendicular to the time axis were drawn in the manner explained in Fig. 1.

Figure 2 presents the phase-graph of the advancing wave which was shown in Pl. II. There is clearly seen a streaky order of gaps and continuous lines. Assuming that the increment and decrement of the plasmodium thickness results from its relaxation and contraction, we can interpret these streaks as the protoplasmic contraction–relaxation waves. The phase-graph of the propagation of the contraction–relaxation wave (Fig. 2) demonstrates a break-down of streaks at the distance of 3 mm from the edge of the plasmodium. Horizontal line 3 mm far from the edge of the plasmodium divides the phase-graph into two zones. The frontal zone, where the propagation of the contraction–relaxation wave is clearly seen and the zone where the wave character of phenomenon is not found.

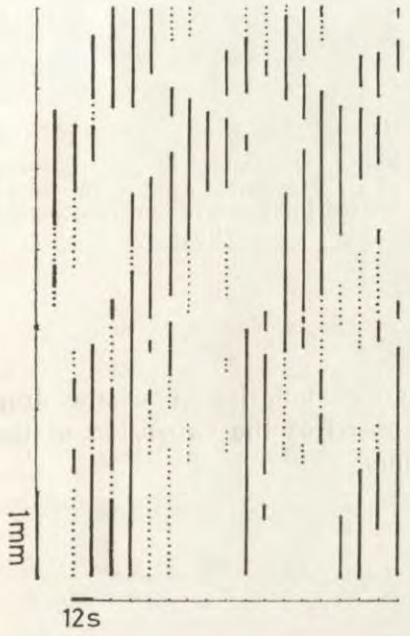

Fig. 2. Phase-graph of the synchronic contraction-relaxation wave in the plasmodium which was shown in Pl. II. The top edge of the phase-graph shows the front of the plasmodium

Fig. 3. Phase-graph of the flickering waves in the plasmodium which was shown in Pl. I. The top edge of the phase-graph shows the front of the plasmodium

On the basis of tangent of the angle between the time axis and the streaks in the frontal zone a speed of the propagation of these waves was estimated as about 35 μm/s. The length of the wave is equal to a width of the frontal zone ($\lambda \simeq 3$ mm).

The period of appearance of the flickering waves in the same plasmodium is shown in Fig. 3. A "random order" of gaps and continuous lines when compared with the previous phase-graph is seen.

Figure 4 presents densitometric cross sections of a protoplasmic drop at the beginning and after about 70 min of observation. The drop was

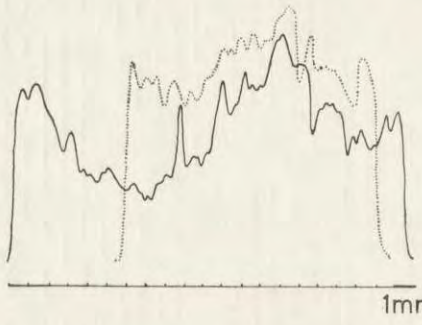

Fig. 4. Densitometric cross sections of a protoplasmic drop at the time 0 (dotted line) and 70 min (continuous line)

obtained by puncturing a plasmodial channel. Polarization of the drop expansion direction is clearly seen. The speed of the expansion of the left edge of the drop equals about 1.3 μm/s.

Fig. 5. Phase-graph of the protoplasmic drop which was shown in Fig. 4. The top edge of the phase-graph shows the left edge of the drop

Figure 5 demonstrates the phase-graph of this protoplasmic drop. The top edge of the phase-graph shows the left edge of the drop. The 3 mm wide frontal zone, where propagation of the contraction-relaxation wave is seen can be distinguished on the top of the phase-graph. The parameter values of this wave as well as of that, which is shown in Fig. 2 are the same. From the top to the bottom of phase-graph, behind the frontal zone, synchronic contraction, random contraction, synchronic contraction and frontal zones can be distinguished in sequence. In the latter, the propagation of the contraction- relaxation wave is not seen.

The occurrence of the contraction-relaxation wave only in the left frontal zone of the drop (see Fig. 4 and 5) indicates once again the possibility that the contraction–relaxation waves are involved in producing the resultant transport of protoplasm and are responsible for migration of the organism.

Discussion

The presented results show the wave character of changes of plasmodium thickness. Whether the changes of thickness may be referred to the contractile activity of the plasmodium, or to the passive effects of the endoplasmic flow, it is hard to judge. Some of results obtained so far seem to indicate that channels and continuous layers in the plasmodium change their dimensions actively. The direct proof for active character of the channel thickness changes are given by tensiometric measurements (the "contact method") performed by Wohlfarth-Bottermann (1975 b). The second method for visualization of the changes of plasmodial thickness in time, is a kind of densitometry performed with a photocell placed in the plane on a screen on which the frame pictures were projected (Baranowski 1976 b). The results of the "contact method" (Wohlfarth-Bottermann 1975 b) measurements, film densitometric (Baranowski 1976 b) measurements as well as of the presented phase-graphs have shown, that durations of the plasmodial thickness changes are within the range of values obtained by Wohlfarth-Bottermann (1977) for the radial contractions of channels. Hence, it seems that there is no evidence to assume the passive character of the changes of channel diameter due to the inflow and outflow of the endoplasm, and therefore the terms "thickness wave" and "contraction–relaxation wave" are used exchangeably in this paper.

The time-lapse cinematographic technique of the registration of wave phenomena in macro-areas ($S \geqslant 70$ mm^2) of plasmodium seems to be

the simplest method of investigation of the organization of contractile processes in plasmodium *Physarum polycephalum*. This method was used by Stewart (1964), who described the propagation of "expansion wave" in the plasmodium. The speed of propagation was estimated as 10 μm/s. According to Stewart's considerations "expansion waves" are connected with efferent and afferent changes of the endoplasmic flow. The frequency of filming used in the presented work, does not allow to follow the changes of flow direction. Therefore, the parameter "A" (Baranowski 1976 a) used to work out the data obtained by the holographic microinterferometry can not be directly introduced. Despite this, the connections between the plasmodium migration and the direction of the synchronic waves propagation, which are shown in the presented photographs suggest that in any point of the plasmodium there should be the conformity between the polarization of the parameter "A" and the direction of the contraction–relaxation wave propagation because they both are involved the resultant transport of the endoplasm.

Assuming, that the connection between the parameter "A" and protoplasmic mass transported through the caudal channels, exist also in the case of frontal zone, a relationship between the speed of propagation of contraction–relaxation wave and the speed of expansion of the plasmodium edge can be easily obtained (see appendix) as follows:

$$V_{exp} = \frac{1}{2} \frac{\overline{\Delta A}}{A} V_w \qquad \text{where:}$$

V_{exp} — average speed of expansion of plasmodium edge,
$\overline{\Delta A}$ — average polarization of the parameter "A",
$\bar{A}$ — average value of the parameter "A",
V_w — average speed of contraction–relaxation wave propagation.

The values of of $\overline{\Delta A}/\bar{A}$ obtained for caudal channels are equal to about 0.15 (Baranowski 1976 a). Assuming, according to phase-graph (Fig. 5) of the protoplasmic drop, the speed of contraction–relaxation wave propagation as about 35 μm/s, on the basis of the above equation we obtained V_{exp} = 2,6 μm/s. This value in respect to the one obtained on the basis of densitometric cross sections of the drop (V_{exp} = 1,3 μm/s) indicates estimative character of the above equation. On the other hand the decrement of the mean value of the expansion speed of the protoplasmic drop edge obtained experimentally can be caused by the flickering waves, which also appeared in the frontal zone. The flickering waves are the indication of the temporary dissynchronization of the contractile processes in the plasmodium which may or must not be connected with the change of the migration direction.

The observation of the wave prenomena occurring in the plasmodium

which is forced to directed migration by external stimuli may result in a complementation or modification of the conclusions presented in this work.

Appendix

The parameter A is defined as follows:

$$A_{\pm} = \int_{t_{\pm}} d^2(t)\, dt, \tag{1}$$

$d(t)$ — thickness of channel measured along optical axis,
$t_{\pm}$ — duration of protoplasmic flow in direction (+) and (−) respectively.

The connection between protoplasmic mass transported through the channel and parameter A is as follows:

$$m_{\pm} = kqv_{\pm}A_{\pm}. \tag{2}$$

k — channel geometry factor,
q — density of protoplasm,
$v_{\pm}$ — flow velocity in direction (+) and (−) respectively.

Average value of the parameter A is defined:

$$\overline{A} = \frac{1}{2n}\left(\sum_{i=1}^{n} A_{+} + \sum_{i=1}^{n} A_{-}\right). \tag{3}$$

n — investigated number of t_+ or t_- periods.

The equation (4) defines the mass of endoplasm (m) in a fragment of frontal zone (λ — length, S — cross section)

$$m = q\ S\ \lambda. \tag{4}$$

From equation (3) for $n = 1$ we obtain

$$\overline{A} = \frac{1}{2}(A_{+} + A_{-}). \tag{5}$$

Coupling eguations (2), (4) and (5), we obtain

$$\lambda = \frac{1}{S} 2k\,|v|\,\overline{A}. \tag{6}$$

The increment of protoplasm mass (Δm) in the fragment under investigation during time T is:

$$\Delta m = k\,q\,|\,v\,|\,\overline{\Delta A}. \tag{7}$$

$\overline{\Delta A}$ — polarization of the parameter A.

It will cause the expansion of the fragment

$$\Delta\lambda = \frac{\Delta m}{Sq} = \frac{kq\,|v|\,\overline{\Delta A}}{Sq} \tag{8}$$

and the relative increase of the length

$$\frac{\Delta\lambda}{\lambda} = \frac{1}{2}\frac{\overline{\Delta A}}{\overline{A}}, \tag{9}$$

in time T, so the speed of expansion (V_{exp}) of plasmodium edge is:

$$V_{exp} = \frac{\Delta\lambda}{T} = \frac{1}{2}\frac{\overline{\Delta A}}{\overline{A}}\frac{\lambda}{T} = \frac{1}{2}\frac{\overline{\Delta A}}{\overline{A}}V_w, \tag{10}$$

V_w — average speed of contraction–relaxation wave propagation.

ACKNOWLEDGEMENT

I am grateful to Dr. V. A. Teplov from Institute of Biological Physics Academy of Sciences USSR in Puschino for microdensitometry scanning analysis.

RÉSUMÉ

La migration du plasmodium de *Physarum polycephalum* sur la surface du gel d'agar était enregistrée avec une caméra de 16 mm à la fréguence de 15 cadres par minute, avec l'éclairage passant à travers le plasmodium. Les changements de l'épaisseur du plasmodium se reproduisent sur la péllicule en forme d'une altérnation des régions plus claires et plus sombres. Ils sont interprétés comme correspondant aux ondes de la contraction et de la rélaxation. Les ondes peuvent apparaitre comme un système ordonné (les ondes synchronisées) ou désordonné (les ondes vacillantes) des changements de l'épaisseur du plasmodium, ce qui était analysé par la microdensitométrie à balayage et mis en évidence sur les diagrammes de décalage de phase. Les relations qualitatives et quantitatives entre la propagation des ondes synchronisées de contraction et de rélaxation et la migration de l'organisme sont l'objet de la discussion.

REFERENCES

Baranowski Z. 1976 a: Three-dimensional analysis of movement in *Physarum polycephalum* plasmodia. Cytobiologie, 13, 118–131.

Baranowski Z. 1976 b: Svjaz volnovych javlenii s migracjej plasmodia miksomiceta. In: Niemysechnyje formy podviznosti (ed. G. M. Frank), Akad. Nauk USSR, Puschino, 47–50.

Baranowski Z. and Kuźnicki L. 1977: The organization of expansion of *Physarum polycephalum* plasmodium. The Fifth International Congress of Protozoology, New York, 61.

Camp W. G. 1936: A method of cultivating myxomycete plasmodia. Bull. Torrey Bot. Club, 63, 205–210.

Kamiya N. 1950: The rate of the protoplasmic flow in the myxomycete plasmodium. II. Cytobiologia, 15, 194–204.

Kamiya N. 1959: Protoplasmic streaming. In: Protoplasmatologia. (eds. L. V. Heilbrunn and F. Weber), Springer, Wien, 1–199.

Komnick H., Stockem W. and Wohlfarth-Bottermann K. E. 1973: Cell motility: mechanisms of protoplasmic streaming and ameboid movement. Int. Rev. Cytol., 34, 169–249.

Sachsenmaier W., Blessing J., Brauser B. and Hansen K. 1973: Protoplasmic streaming in *Physarum polycephalum.* Observation of spontaneous and induced changes of the oscillatory pattern by photometric and fluorometric techniques. Protoplasma, 77, 381–396.

Stewart P. A. 1964: The organization of movement of slime mold plasmodia. In: Primitive Motile Systems in Cell Biology (eds. R. D. Allen and N. Kamiya) Academic Press, New York, 69–78.

Wohlfarth-Bottermann K. E. 1975 a: Weitreichende fibrillare Protoplasmadifferenzierungen und ihre Bedeutung für die Protoplasmastromung. X. Die Anordnung der Actomyosin-Fibrillen in experimentell unbeeinflussten Protoplasmaadern von *Physarum in situ.* Protistologica, XI, 1, 19–30.

Wohlfarth-Bottermann K. E. 1975 b: Tensiometric demonstration of endogenous, oscillating contractions in plasmodia of *Physarum polycephalum.* Z. Pflanzenphysiol., 76, 14–27.

Wohlfarth-Bottermann K. E. 1977: Oscillating contractions in protoplasmic strands of *Physarum*: simultaneous tensiometry of longitudinal and radial rhythms, periodicity analysis and temperature dependence. J. exp. Biol. 67, 49–59.

Received on 7 November 1977

EXPLANATION OF PLATES I–IV

I: Frontal zone of migrating plasmodium of *Physarum polycephalum*. 1–6 frames extracted from 16 mm motion pictures taken at 15 fr/min. Interval between frames — 400 s. The arrows, in rectangles of the grid, show the vectors of propagation of waves observed in these areas in the time intervals between the subsequent photographs. Dashed line (1) marks the path of densiometric scanning

II: Propagation of the contraction-relaxation wave in *Physarum polycephalum* plasmodium. 1–16 frames extracted from 16 mm motion pictures. Intervals between frames — 16 s. The first photograph shows plasmodium (see Pl. I) in 1628th s of observation

III: Frontal zone of non-migrating plasmodium of *Physarum polycephalum*. 1–9 frames extracted from 16 mm motion pictures taken at 15 fr/min. Intervals between frames — 400 s. The arrows in rectangles of the grid show the vectors of propagation of waves observed in these areas in the time intervals between the subsequent photographs

IV: Plasmodium of *Physarum polycephalum* changing the direction of migration. Intervals between frames — 400 s. The arrows show the vectors of propagation of waves observed in the time intervals between the subsequent photographs

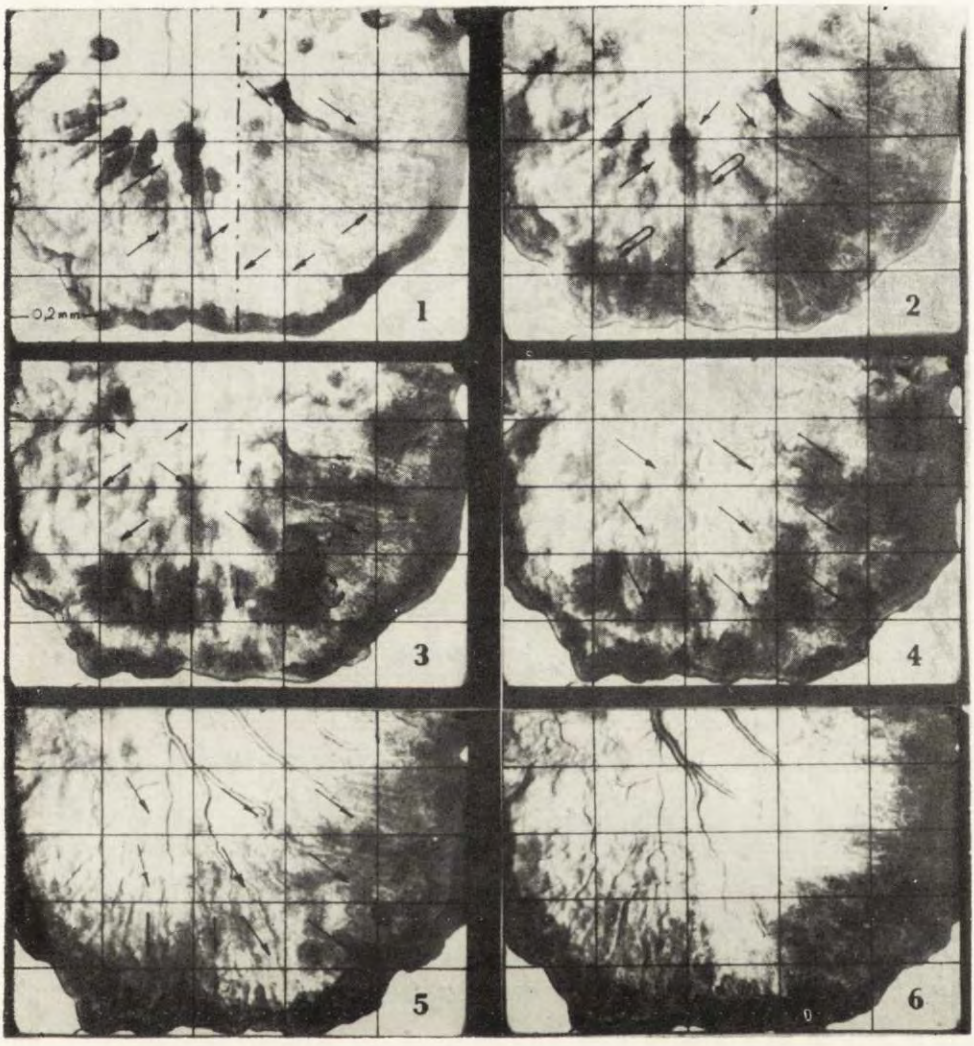

Z. Baranowski auctor phot.

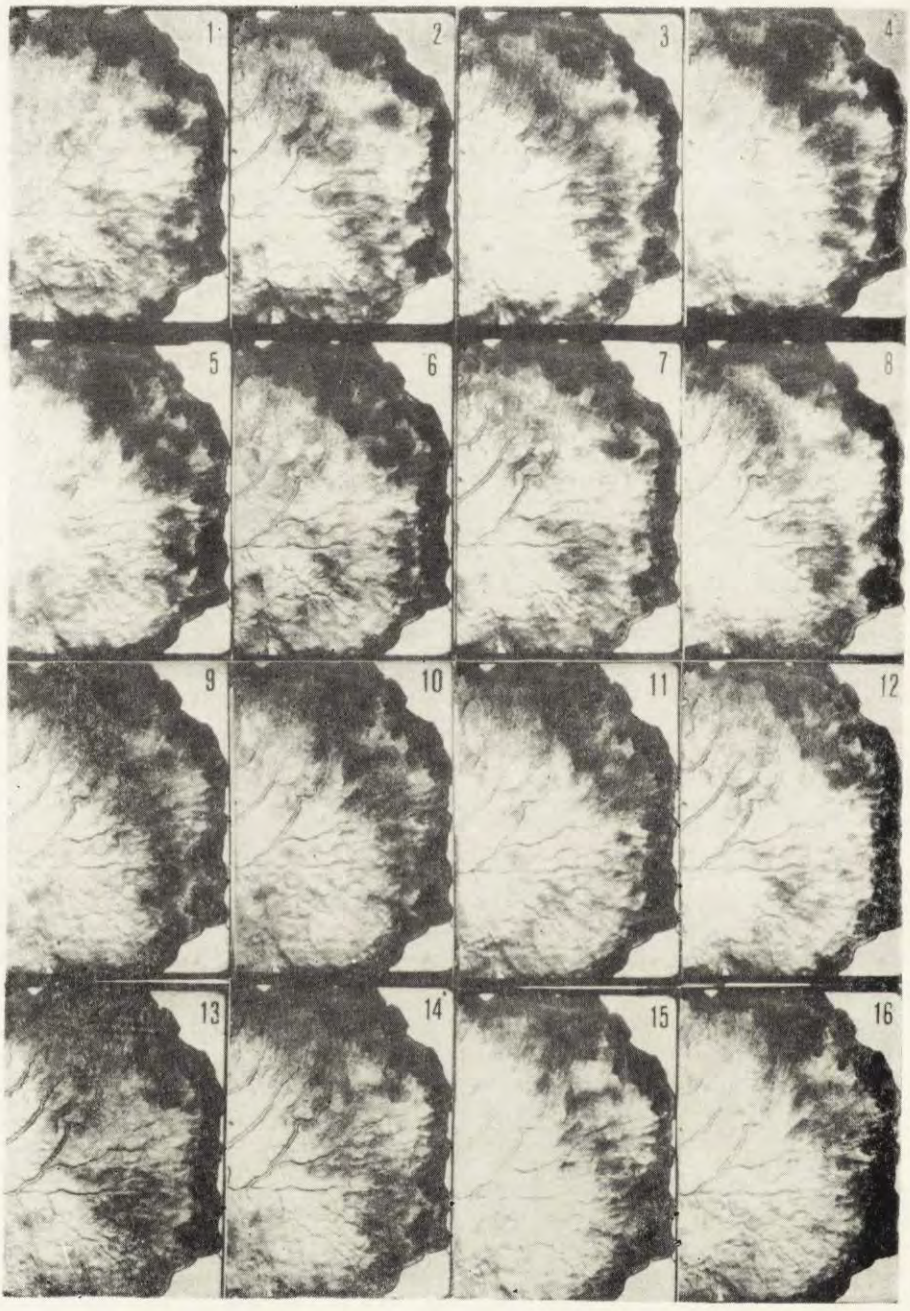

Z. Baranowski auctor phot.

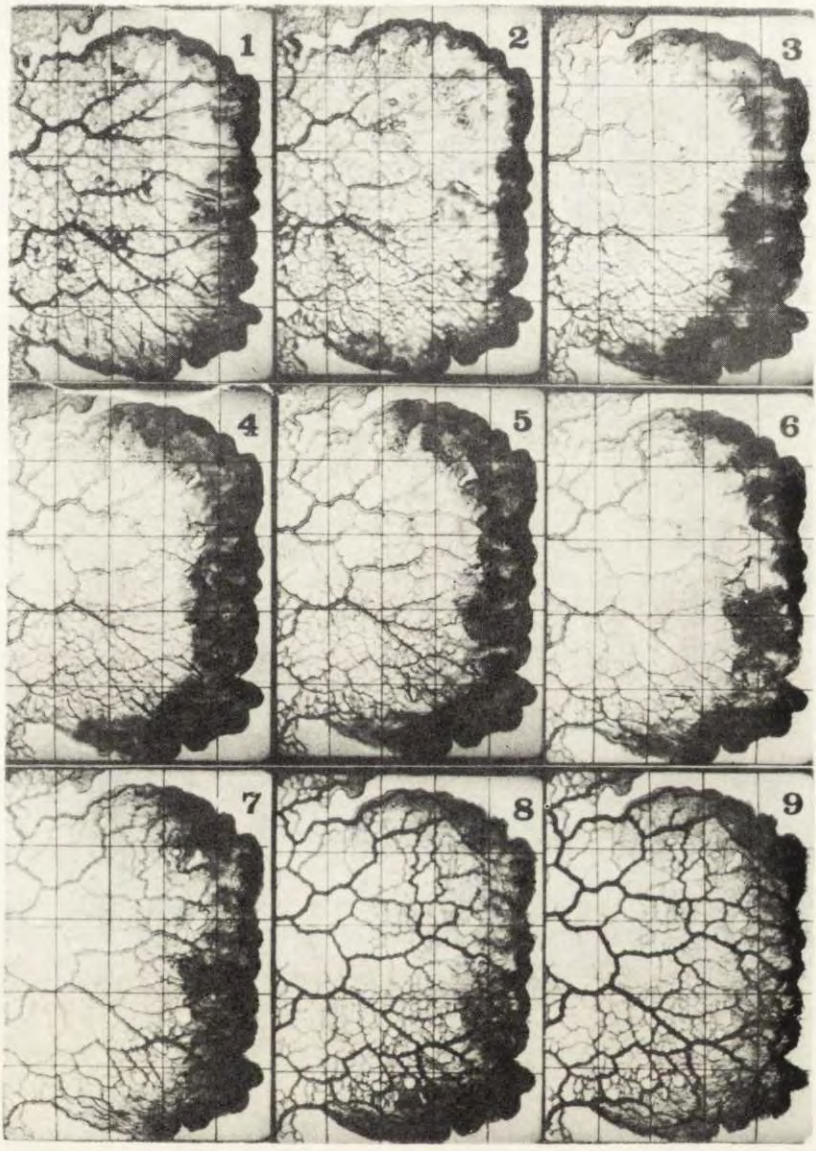

Z. Baranowski auctor phot.

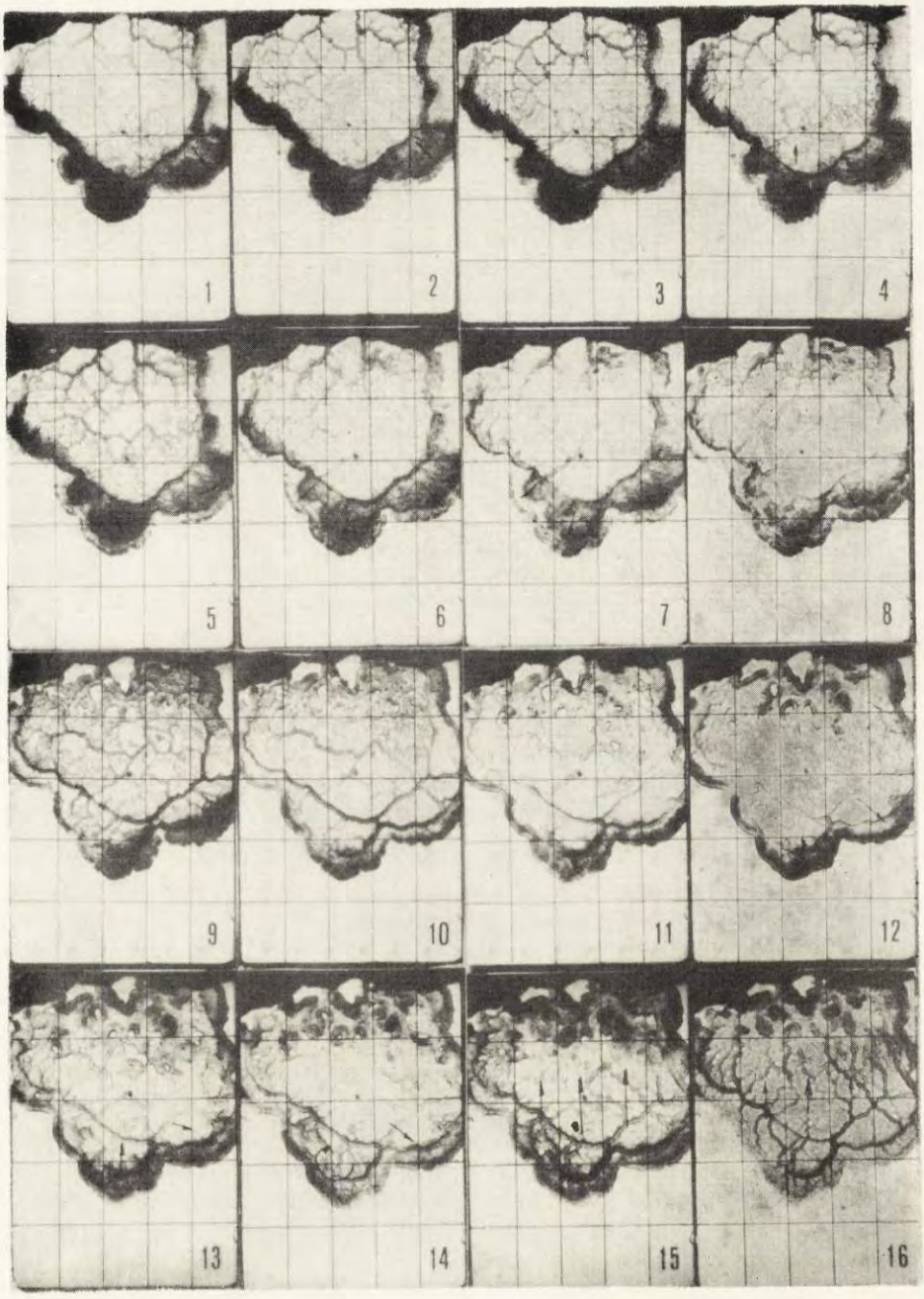

Z. Baranowski auctor phot.

ACTA PROTOZOOLOGICA
VOL. 17 (No. 2) WARSZAWA, 30 VI 1978 pp. 389–397

Department of Cell Biology, M. Nencki Institute of Experimental Biology, Pasteura Str. 3, 02-093 Warszawa, Poland

Jerzy SIKORA and Anna WASIK

Cytoplasmic Streaming Within Ni^{2+} Immobilized *Paramecium aurelia*

Synopsis. The purpose of the study was to examine what conditions have to be fulfilled to obtain the nickel immobilized *Paramecium aurelia* showing cytoplasmic streaming. Observations taken one by one have revealed, that 0.25–0.5 mM $NiCl_2$ in Tris-HCl buffer pH 7.2 containing $CaCl_2$ and KCl of 1mM each seem to fulfill the task well. In the above mentioned medium the completely immobilized paramecia show cytoplasmic streaming.

Low concentrations of nickel chloride or sulphate solutions have been succesfuly used for cessation of locomotive activity of Ciliates (Gelei 1935, Tchakhotine 1938, Tartar 1950, 1961, Thomas 1953, Bovee 1958, Seravin 1961, 1962 a, b, Parducz 1962, Pitelka and Parducz 1962, Puytorac et al. 1962, 1963, Kuźnicki 1963, 1968, Grębecki et al. 1967, Grębecki and Mikołajczyk 1968, Andrivon 1970, 1972, 1974). The peculiarity of an Ni^{2+} immobilization mechanism is that primarily the propulsive function of cilia is affected while the steering function of cilia (ability to change of beating direction) remains in some extent not disturbed in *Paramecium* (Kuźnicki 1963, 1970, Naitoh 1966, Grębecki et al. 1967, Grębecki and Mikołajczyk 1968, Kuźnicki et al. 1968, 1969, Andrivon 1974).

Preliminary observations of *Paramecium aurelia* treated by $NiCl_2$ solutions, used for quiting of *Paramecium caudatum* by Kuźnicki (1963), Naitoh (1966) and Andrivon (1970) have shown that frequently cytoplasmic streaming is ceased within immobilized specimens, although some of them exhibit cytoplasmic streaming as well. Therefore the question arose, whether and what conditions should be fulfilled to obtain an Ni^{2+} immobilized *Paramecium aurelia* with cytoplasmic streaming intact or ceased.

Supported by grant MR II. 1.3.2.

Material and Methods

Paramecium aurelia (= *tetraurelia* Sonneborn, 1974) stock 51 was grown at 27°C in lettuce infusion inoculated with *Aerobacter aerogenes* (Sonneborn 1950, Kuźnicki and Sikora 1971). The cells were collected by centrifugation (up to 300 × G), washed in appriopriate buffer solution three times and left overnight. The pattern of experiments was following. About 200–300 cells with a minute amount of solution (about 25–40 µl) were pipetted into relativly large amount (about 0.6 ml) of experimental solution consisting of $NiCl_2$ and buffer solution in deppresion slide and stirred gently by a blunt glass needle. The buffer solution used consisted of Tris-HCl buffer of pH 7.2–7.8 and constant ionic strength of I = 0.05 with addition of different concentrations of $CaCl_2$ or $CaCl_2$ and KCl, depending on experiment. All the experimental procedure was done at 19 ± 2°C.

After 20 min of treatment of paramecia in experimental solution, immobilized specimens were rinsed in the same buffer solution devoid of $NiCl_2$ and mounted in microscopic preparation. Observations of paramecia under bright and polarized light microscope were taken one by one up to 1 h at 10 min intervals. Concomitantly the control preparations were examined.

Among immobilized paramecia, those with normal and abnormal body shape was counted with the special regard on activity of cytoplasm within cell (Kuźnicki and Sikora 1971). Four types of cells were taken into consideration when preparations were examined: paramecia of normal body shape with a cytoplasmic streaming intact, paramecia with normal body shape with cytoplasmic streaming inhibited, those with abnormal body shape with a cytoplasmic streaming and paramecia of abnormal body shape without cytoplasmic streaming.

Tentative experiments has shown that Ni^{2+} immobilized paramecia if pass through the physiological immobilization and reach the traumatic stage (Grębecki et al. 1967) — usually exhibit more or less visible changes in the body shape. On the other hand in some cases, paramecia in traumatic stage are hard to recognize from dead ones, therefore the type described as abnormal body shape (to avoid misunderstanding) consist of either slightly deformed or even dead specimens.

The markers of cytoplasmic streaming flow was birefringent crystals easely seen under polarized microscope.

Only experiments with almost 100% of specimens immobilized, have been taken into consideration; otherwise cytoplasmic streaming could not be distinguished beyond doubt in swimming paramecia. Therefore the scope of experiments was limited to the extent range of Ni^{2+} ions concentrations evoking complete immobilization of paramecia.

Results

The purpose of the present study was determination of the concentration of $NiCl_2$ in Tris-HCl buffer containing Ca^{2+} and K^+ ions where almost 100% of specimens will be immobilized and most of them will exhibit cytoplasmic straeming. The major part of immobilized specimens should not be affected by Ni^{2+} ions in such extent that premortal signs will occur, defined as abnormal body shape.

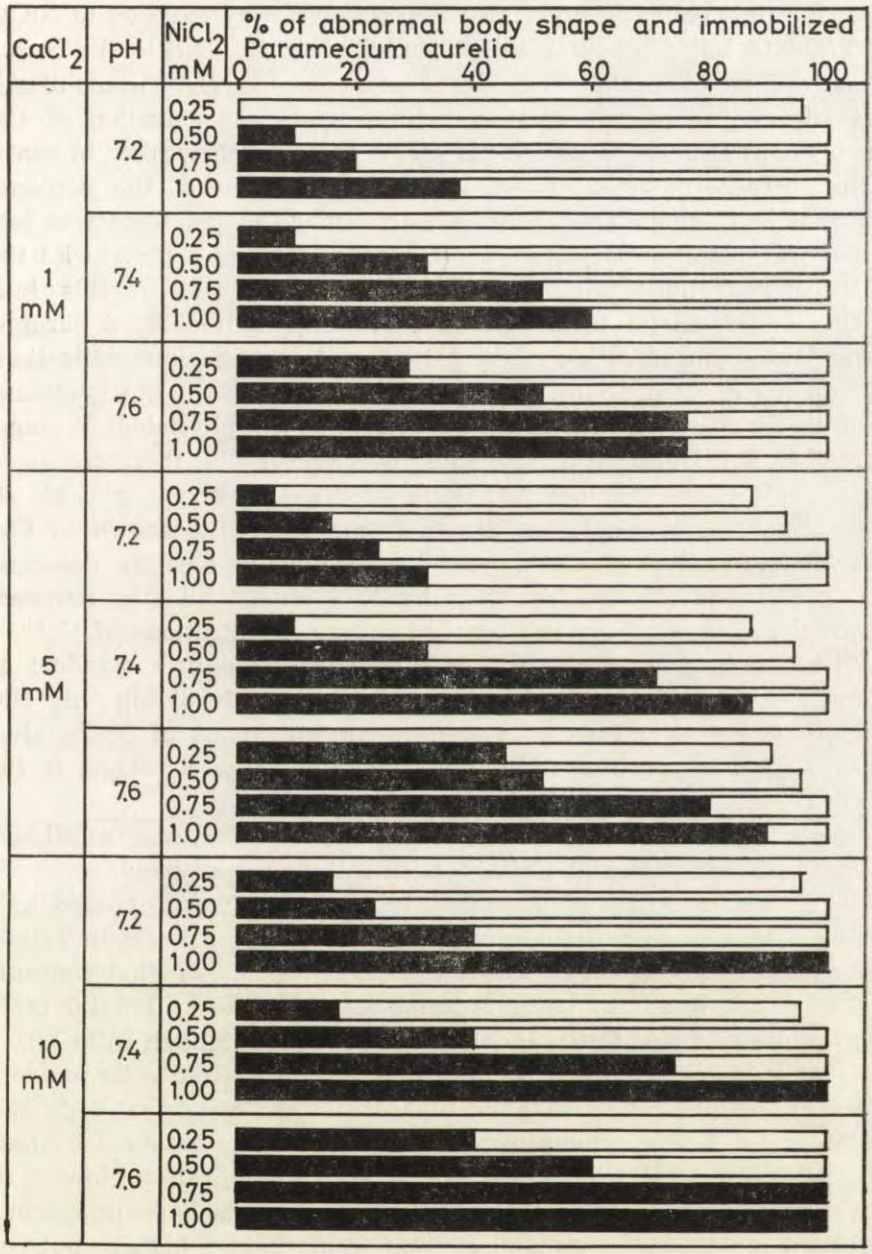

Fig. 1. *Paramecium aurelia* treated by different concentrations of $NiCl_2$ in the buffer of different pH containing different concentrations of $CaCl_2$. Darken area of diagram means the percent of abnormal specimens fraction among immobilized paramecia after 20 min incubation

In the first series of experiments paramecia were exposed to $NiCl_2$ in the Tris-HCl buffer of different pH from 7.2 to 7.8, and to the constant concentrations of $CaCl_2$. The Fig. 1 presents the Ni^{2+} immobilization effect depending on pH of the medium while concentration of $CaCl_2$ remains constant. The effect of pH seems to be much weaker in contrast to the increase of lethal effect expressed in terms of the percent of abnormal body shape specimens. An acid range of pH scale was tested by means of modified Dryl's buffer (G r ę b e c k i and K u ź n i c k i 1963). $NiCl_2$ concentration ranging from 0.062 to 4.0 mM in this buffer solution (pH from 5.1 to 7.1) produce either nonimmobilized paramecia at the lower concentration of Ni^{2+} ions or traumatic immobilization at the higher concentrations. As it will be shown later the cytoplasmic streaming appears mainly within paramecia at the physiological stage of immobilization. Duration of this stage was very short, therefore an acid range of pH of the medium was useless for studies on cytoplasmic streaming. The second conclusion drawn from the results shown in Fig. 1 is that concentration of $CaCl_2$ in the experimental medium determines slightly the rate of immobilization by Ni^{2+} ions, while the percent of abnormal specimens rises apparently in low concentrations of Ca^{2+}.

Within population of *Paramecium aurelia* grown in a standart conditions and adopted to the experimental solutions devoiding only $NiCl_2$, after treatment by means of even low concentrations of $NiCl_2$, always some fraction of specimens was abnormal (in traumatic stage) if 100% of specimens were immobilized.

In control medium, specimens were incubated in the solutions of different pH and different $CaCl_2$ concentrations respectively.

In the second series of experiments paramecia were exposed to the various concentrations of $NiCl_2$ ranging from 0.31 to 4.0 mM in Tris-HCl buffer of pH 7.2, containing $CaCl_2$ + KCl. It was shown that concentrations of $NiCl_2$ worth to be considered were between 0.125–1.0 mM in the presence of 1 mM $CaCl_2$ and 1 mM KCl (Gibbs-Donnan ratio 1.0).

Careful examination one by one of Ni^{2+} immobilized cells under polarized microscope reveal that the highest percent of normal body shape specimens exhibiting cytoplasmic streaming could be obtained by means of 0.25–0.5 mM solution of $NiCl_2$ (Table 1). Although at the lowest concentration of $NiCl_2$ (0.125 mM) the percent of normal body shape specimens exhibiting cytoplasmic streaming was remarkably higher but only 50–60% of specimens of initial sample were immobilized and could be examined due to presence of cytoplasmic streaming. An increase of $NiCl_2$ concentration causes distinct decrease of the percent of normal body shape paramecia with cytoplasmic streaming. Percent of cells lacking cytoplasmic streaming seems to be apparently independent of the

Table 1

Effect of $NiCl_2$ in Tris-HCl buffer of pH 7.2 containing 1 mM $CaCl_2$ and 1 mM KCl, expressed in percent of *Paramecium aurelia* with normal and abnormal body shape, with and without cytoplasmic streaming

Concentration of $NiCl_2$ in mM	Total number of animals tested	Paramecia of normal body shape			Paramecia of abnormal body shape		
		Total in %	Cytoplasmic streaming in %		Total in %	Cytoplasmic streaming in %	
			intact	ceased		intact	ceased
0.125	259	84.2*	72.6	11.6	15.8*	8.9	6.9
0.25	1194	60.3	45.9	14.4	39.7	11.1	28.6
0.5	391	53.5	41.5	12.0	46,5	7.2	39.3
1.0	307	20.5	6.8	13.7	79.5	11.4	68.1

* Data of 0.125 mM $NiCl_2$ concern only 50—60% of *Paramecium aurelia* immobilized fraction used in each sample.

concentration of Ni^{2+} ions used. Among the cells defined as abnormal body shape, the percent of specimens devoid of cytoplasmic streaming also does not change very much. Decrease of the percent of normal body shape specimens along side with an increase of concentration of Ni^{2+} ions used for immobilization and seems to be obvious in respect to the results shown in the first series of experiments.

Tentative evidence shows that an increase of external temperature causes apparently higher frequency of lethal effect among immobilized paramecia, what seems to be in agreement with the rules revieved by Bělehrádek (1957). Therefore all the experiments were taken at temperature 19 ± 2°C.

Discussion

The aim of the present study was to find what conditions have to be fulfilled to apply the nickel immobilization method for *Paramecium aurelia*, which would allow besides the cytoplasmic streaming analysis.

Antiserum immobilization method for *Paramecium aurelia* described by Kuźnicki and Sikora (1971) seems to be less harmful, but is limited to antisera in possesion. Difficulties rise in case of unstabile serotypes used. Also foggy clumps covering outher surface of antiserum immobilized paramecia makes them hard to follow under high power resolution microscopy. The advantage of nickel immobilized paramecia in these aspect is obvious.

The rough observation have shown that within population of *Paramecium aurelia* treated by $NiCl_2$ solution, within immobilized specimens the cytoplasmic streaming may occur or not. To find out, whether, and in what extent the Ni^{2+} ions may interfere or inhibit the cytoplasmic streaming, the method for Ni^{2+} immobilization of *Paramecium caudatum* (Kuźnicki 1963, Naitoh 1966, Andrivon 1970) has been adopted. Some modifications of the nickel method were necessary in order to establish the ionic composition of the medium containing Ni^{2+} ions which would immobilize *Paramecium aurelia* but will not result in traumatic changes (Grębecki et al. 1967). Also the aim was to minimalize the number of additional ions in the medium to reduce the number of interacting factors.

The results show that *Paramecium aurelia* exposed to the Ni^{2+} ions in the presence of Ca^{2+} and K^{+} buffered to pH 7.2 are immobilized and cytoplasmic streaming within cell occur. This motile activity in terms of "presence" (what means that it might be recognized visually under microscope) depends mainly on nickel ions concentration applied. Also

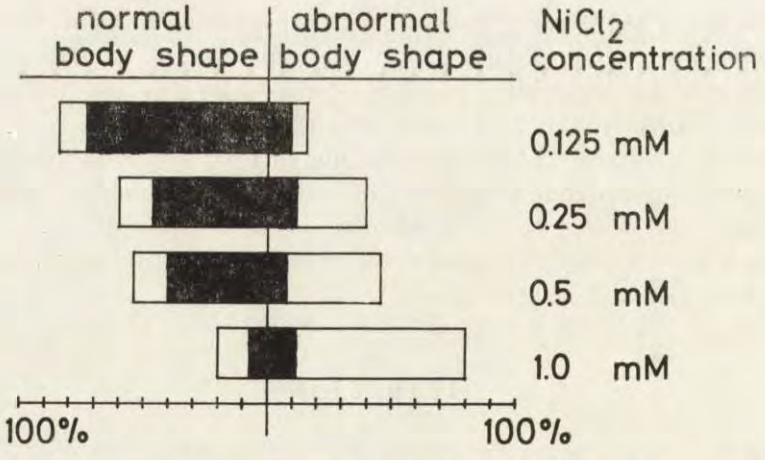

Fig. 2. Diagram expressing different effects evoked by $NiCl_2$ on *Paramecium aurelia* depending on concentration. Dark area means contribution of specimens exhibiting cytoplasmic streaming within normal and abnormal body shape specimens respectively

the percent of abnormal (see Methods and Material) body shape paramecia depends apparently on the concentration of these ion.

The effects of $NiCl_2$ at the different concentrations analysed have been visualized on diagram (Fig. 2). The relations between Ni^{2+} concentrations and the level of survival and appearance of cytoplasmic streaming seem to be apparently clear. Lack of cytoplasmic streaming among about 10% of specimen tested are probably due to spontaneous cessation (Sikora 1976) and cessation at the autogamy (Sikora and Kuźnicki 1976). Unpublished results have shown that approximately 10% of antiserum immobilized *Paramecium aurelia* 51A are devoid of cytoplasmic streaming, what seems to support above mentioned supposition.

In contrary to the opinion of Kuźnicki (1963) concerning survival of *Paramecium caudatum* treated by Ni^{2+} in the present study it have been stated that if 100% nickel treated *Paramecium aurelia* are immobilized, always the traumatic stage (Grębecki et al. 1967) of immobilization will occur.

Almost constant level of the cytoplasmic streaming appearance among abnormal body shape paramecia is obscure.

However, the fundamental mechanism underlying Ni^{2+} ion direct action remains unclear, there is strong evidences that nickel ions does not affect (in certain extent) at least irreversibly motile systems of *Paramecium*. Kuźnicki (1963) has described the conditions which allow to renormalize the locomotive activity of nickel immobilized *Paramecium caudatum*. Naitoh (1966) has shown that steering mechanism remain unaffected by Ni^{2+} ions while Grębecki et al. (1967) has demonstrated the resumption of ciliary beating of Ni^{2+} immobilized *Paramecium caudatum* by means of chelating agents. Furthermore Naitoch (1966) has shown that within nickel immobilized *Paramecium caudatum* intracellular potentials have a similar nature and level as were recorded from normal specimens. Therefore it seems to be resonable to use Ni^{2+} immobilized *Paramecium aurelia* being in physiological immobilization stage (Grębecki et al. 1967) for cytoplasmic streaming studies.

RÉSUMÉ

L'objectif de l'étude présente était d'établir dans quelles conditions le courant cytoplasmique peut être préservé chez *Paramecium aurelia* immobilisé par Ni^{2+}. Les observations des ciliés démontrent que ces conditions sont satisfaites dans le milieu contenant 0.25–0.5 mM $NiCl_2$ dans les tampons Tris-HCl pH 7.2, avec 1 mM $CaCl_2$ et 1 mM KCl. Dans cette solution les paramécies sont parfaitement immobilisées tout en gardant leur courant cytoplasmique actif.

REFERENCES

Andrivon C. 1970: Complément a l'étude de l'action des inhibiteurs du métabolisme sur la résistance aux sels de nickel chez *Paramecium caudatum* et chez quelques autres protozaires ciliés. Protistologica, 6, 199–206.

Andrivon C. 1972: The stopping of ciliary movements by nickel salts in *Paramecium caudatum*: the antagonism of K+ and Ca++ ions. Acta Protozool., 11, 373–386.

Andrivon C. 1974: Inhibition of ciliary movements by Ni^{2+} ions in triton-extracted models of *Paramecium caudatum*. Archs int. Physiol. Biochim., 82, 843–852.

Bělehrádek J. 1957: A unified theory of cellular rate based upon an analysis of temperature action. Protoplasma, 48, 53–71.

Bovee E. 1958: Nickel sulfate as an anesthetic for protozoa. Turtox News., 36, 78.

Gelei J. 1935: Ni-Infusorien im Dienste der Forschung und des Unterrichtes. Biol. Zbl., 55, 57–74.

Grębecki A. and Kuźnicki L. 1963: The influence of external pH on the toxicity of inorganic ions for *Paramecium caudatum*. Acta Protozool., 1, 157–164.

Grębecki A., Kuźnicki L. and Mikołajczyk E. 1967: Right spiralling in *Paramecium* by Ni ions and the hydrodynamics of the spiral movement. Acta Protozool., 4, 389–408.

Grębecki A. and Mikołajczyk E. 1968: Ciliary reversal and re-normalization in *Paramecium caudatum* immobilized by Ni ions. Acta Protozool., 5, 297–303.

Kuźnicki L. 1963: Reversible immobilization of *Paramecium caudatum* evoked by nickel ions. Acta Protozool., 1, 301–312.

Kuźnicki L. 1968: Behavior of *Paramecium* in gravity fields. I, Sinking of immobilized specimens. Acta Protozool., 6, 109–117.

Kuźnicki L. 1970: Mechanisms of the motor responses of *Paramecium*. Acta Protozool., 8, 83–118.

Kuźnicki L., Jahn T. L. and Fonseca J. R. 1968: The helical nature of the ciliary beat of *Paramecium*. Am. Zool., 8, 164 (abstr.).

Kuźnicki L., Jahn T. L. and Fonseca J. R. 1969: Cinematographic analysis of ciliary reversal in *Paramecium*. Progress in Protozoology, Third int. Congr. Protozool., Leningrad 1969, 171 (abstr.).

Kuźnicki L. and Sikora J. 1971: Cytoplasmic streaming within *Paramecium aurelia*. I. Movements of crystals after immobilization by antiserum. Acta Protozool., 8, 439–446.

Naitoh Y. 1966: Reversal response elicited in nonbeating cilia of *Paramecium* by membrane depolarization. Science, 154, 660–662.

Párducz B. 1962: Studies on reactions in Ciliates. IX. Ciliary coordination of right spiralling Paramecia. Annals. Mus. Nat. Hung., Pars Zool., 54, 221–229.

Pitelka D. R. and Párducz B. 1962: Electron-microscope observations on paralysed *Paramecium*. J. Protozool., 9 (Suppl.) 2 (abstr.).

Puytorac P. de, Andrivon C. et Serre F. 1962: Sur l'action cytonarcotique des sels de nickel chez *Paramecium caudatum* Ehrb. J. Protozool., 9, (Suppl.) 23 (abstr.).

Puytorac P. de, Andrivon C. et Serre F. 1963: Sur l'action cytonarcotique des sels de nickel chez *Paramecium caudatum* Ehrb. J. Protozool. 10, 10–19.

Seravin L. N. 1961: Rol adenozintrofosfata v bienii resniček infuzorij. Biohimija, 26, 160–164.

Seravin L. N. 1962 a: Osobiennosti razvitija obščego narkoza u *Spirostonum ambiguum*. Citologija, 4, 52–58.

Seravin L. N. 1962 b: Fizjologičeskie gradienty infuzorii *Spirostomum anbiguum*. Citologija 4, 545–554.

Sikora J. 1976: Cytoplasmic streaming in *Paramecium*. J. Cell Biol., 70, 2, 2, 399 a.

Sikora J. and Kuźnicki L. 1976: Cytoplasmic streaming within *Paramecium aurelia*. IV. Cyclosis during binary fission and conjugation. Acta Protozool., 15, 173–178.

Sonneborn T. M. 1950: Methods in the general biology and genetics of *P. aurelia*. J. exp. Zool., 113, 87–143.

Sonneborn T. M. 1974: *Paramecium aurelia*. In: Handbook of Genetics, (ed. R. C. King), New York (Plenum Press), 469–593.

Tartar V. 1950: Methods for the study and cultivation of Protozoa. In: Studies Honoring Trevor Kincaid, (ed. M. E. Hath), Univ. Wash. Press, Seatle.

Tartar V. 1961: The Biology of *Stentor*. Pergamon Press, Oxford, London, New York, Paris.

Tchakhotine S. 1938: Études physiologiques et embriologiques au moyen de la methode des microgouttes. Trav. Str. Zool. Vimereux, 13, 647–663.

Thomas R. 1953: Action anesthésique du sulfate de nickel sur *Paramecium caudatum*. Bull. Microsc. Appl. 2e, série, 3, 73–76.

Received on 20 October 1977

NOTICE TO AUTHORS

Acta Protozoologica is intended as a journal serving for the publication of original papers embodying the results of experiments or theoretical research in all fields of protozoology with the exception of faunistic notices of the local character and purely clinical reports. The papers should be concise and will not be accepted if they have been previously published elsewhere. After acceptance by the Editors, papers will be printed in the possibly shortest time.

Papers are accepted in English, French, German and Russian. Every paper should begin with the name and postal address of the laboratory, name and the surname of the author and title in the language of the text. The titles in German and French should be translated into English according to the demands of "Current Contents". The paper should be accompanied by synopsis in the language of the text not exceeding 100 words and by short summary in one of 4 languages accepted in the Journal. In the Russian text also the name and the postal address of the laboratory, legends of tables, plates and text-illustrations must be translated, the translation of the summary may be somewhat more extensive, and the name of the author should be given additionally also in the Latin characters.

Manuscript should be doublespaced typescript (30 lines on one side of a sheet) with a normal margin. No elements of the text should be fully typed in capitals nor in spaced set (only underlining with pencil is addmittable). In decimal fractions points not commas should be used. The generally accepted abbreviations and symbols are recommended. Nomenclature must agree with the International Code of Zoological Nomenclature, London 1961. The original and one carbon copy of the whole text material should be supplied. References must be cited in the text indicating only the author and year, thus: "K i n o s i t a (1954) found that, etc."

Only all references cited in the text should be listed. The list must be arranged as follows: E h r e t C. F. and P o w e r s E. L. 1959: The cell surface of *Paramecium* Int. Rev. Cytol., 8, 97–133.
G e l e i J. von 1939: Das äussere Stützgerüstsystem des Parameciumkörpers. Arch. Protistenk., 92, 245–272.

Titles of references are given in their original language (not translated). In papers written in English, French or German, the Cyrillic type of the Russian references is transliterated according to the international system (ISO Recommendation R 9 September). This regulation is not applied to names if there exists their traditional spelling. Also author may freely choose the transliteration of his own name. In Russian papers, the Russian references are cited in Cyrillic, the others in the Latin characters, but they must be listed all together in the Latin alphabetical order.

The following material should be supplied on separate sheets: 1. the running title for the page headlines, 2. tables, 3. legends for text figures, 4. legends for plates. Line-drawings will be published in the text, photographs and raster-figures on separate plates. No coloured photographs can be published presently. Lettering on photographs and drawings should be marked in pencil. With no regard to the language of the text, only the Latin lettering, arabic numerals or generally accepted symbols are admittable for marking on illustrations. Numbering of text-figures, plates and tables must be also marked in pencil, as well in the legends as in the text.

Galley proofs are sent to the authors. Authors receive 75 reprints without covers.

In preparation:

L. N. Seravin and Z. P. Gerassimova: A New Macrosystem of Ciliates – F. G. Agamaliev: Morphology of Some Free-living Ciliates of the Caspian Sea – M. Wolska: *Triadinium caudatum* Fiorent. Electron Microscope Examinations – C. Kalavati and C. C. Narasimhamurti: A New Microsporidian, *Octosporea porcellioi* sp. n. from *Porcellio laevus* Latr. (*Oniscidae, Isopoda, Crustacea*) – A. A. Narasimhamurti and C. Kalavati: A New Microsporidian, *Pleistophora blatellae* sp. n. from the Malphigian Tubules of *Blatella germanica* – B. Kalisz-Nowak: Experimental Study on Locomotion of *Amoeba proteus*. II. Reactions to Some External Stimuli in *Amoeba proteus* and its Fragments from which a Part of the Cytoplasm has been Removed – S. Dryl and J. Kurdybacha: Galvanotactic Response in *Paramecium caudatum* at various Levels of External Calcium Ions

Warunki prenumeraty

Cena prenumeraty krajowej: rocznie zł 200,— półrocznie zł 100,—

Prenumeratę przyjmują Oddziały RSW „Prasa-Książka-Ruch" oraz urzędy pocztowe i doręczyciele w terminach:

— do dnia 25 listopada na styczeń, I kwartał, I półrocze i cały rok następny.

— do dnia 10 każdego miesiąca (z wyjątkiem grudnia) poprzedzającego okres prenumeraty.

Jednostki gospodarki uspołecznionej, instytucje i organizacje społeczno-polityczne oraz wszelkiego rodzaju inne zakłady pracy, składają zamówienia w miejscowych Oddziałach RSW „Prasa-Książka-Ruch".

Zakłady pracy w miejscowościach, w których nie ma Oddziałów RSW, oraz prenumeratorzy indywidualni zamawiają prenumeratę w urzędach pocztowych lub u doręczycieli.

Prenumeratę ze zleceniem wysyłki zagranicę, która jest o 50% droższa od prenumeraty krajowej, przyjmuje Biuro Kolportażu Wydawnictw Zagranicznych RSW „Prasa-Książka-Ruch", ul. Wronia 23, 00-958 Warszawa.

Bieżące i archiwalne numery można nabyć lub zamówić we Wzorcowni Wydawnictw Naukowych PAN-Ossolineum-PWN, Pałac Kultury i Nauki (wysoki parter), 00-901 Warszawa, oraz w księgarniach naukowych „Domu Książki".

Cena zł 50.—

CONTENTS

Państwowe Wydawnictwo Naukowe — Oddział we Wrocławiu

Nakład 487 + 103 egz. Ark. wyd. 16; ark. druk. 11½ + wkl. kred. Pap. druk. sat. kl. III, 70 × 100, 80 g. Oddano do składania 19 XII 1977 r. Podpisano do druku w lipcu 1978. Zamówienie nr 16/78. Cena zł 50,—

Wrocławska Drukarnia Naukowa

Indeks 35133